

**Development and validation of stem cell-based test
methods contributing to a human *in vitro* battery
for regulatory developmental neurotoxicity
evaluation**

Dissertation to obtain the degree

Doctor rerum naturalium (Dr. rer. nat.)

at the Heinrich-Heine-University Düsseldorf

submitted by

Kristina Eva Bartmann

from

Düsseldorf

Düsseldorf, July 2022

**Entwicklung und Validierung von Stammzell-
basierten Testmethoden im Rahmen einer
humanen *in vitro*-Batterie zur regulatorischen
Testung auf Entwicklungsneurotoxizität**

Inaugural-Dissertation

Zur Erlangung des Doktorgrades
der Mathematisch-Naturwissenschaftlichen Fakultät
der Heinrich-Heine-Universität Düsseldorf

vorgelegt von

Kristina Eva Bartmann

aus

Düsseldorf

Düsseldorf, Juli 2022

Angefertigt am IUF – Leibniz-Institut für umweltmedizinische Forschung GmbH
an der Heinrich-Heine-Universität Düsseldorf

Gedruckt mit der Genehmigung der
Mathematisch-Naturwissenschaftlichen Fakultät der
Heinrich-Heine-Universität Düsseldorf

Berichtersteller:

1. Prof. Dr. Ellen Fritsche
2. Prof. Dr. Rüdiger Simon

Tag der mündlichen Prüfung: 14.11.2022

***„The difficulty lies not so much in developing new ideas
as in escaping from old ones“***

(John M. Keynes)

Table of Contents

1	Introduction.....	1
1.1	Brain development.....	1
1.2	Developmental Neurotoxicity (DNT).....	2
1.2.1	DNT testing.....	4
1.3	Alternative toxicity testing.....	5
1.3.1	<i>In vitro</i> DNT testing – the DNT-IVB.....	6
1.3.2	The ‘Neurosphere Assay’ as a new approach model for DNT testing.....	8
1.3.3	Gaps of the DNT-IVB.....	10
1.4	Neural networks on microelectrode arrays (MEA).....	12
1.5	Aim of this thesis.....	15
2	Manuscripts.....	17
2.1	Scientific validation of human neurosphere assays for developmental neurotoxicity evaluation.....	19
2.2	Neurodevelopmental toxicity assessment of flame retardants using a human DNT <i>in vitro</i> testing battery.....	48
2.3	Establishment of a human cell-based <i>in vitro</i> battery to assess developmental neurotoxicity hazard of chemicals.....	78
2.4	Measurement of electrical activity of differentiated human iPSC-derived neurospheres recorded by microelectrode arrays (MEA).....	147
2.5	A human iPSC-based <i>in vitro</i> neural network formation assay to investigate neurodevelopmental toxicity of pesticides.....	165
3	Discussion.....	205
3.1	The DNT-IVB and its regulatory applications.....	206
3.2	Closure of identified gaps in the DNT-IVB.....	209
3.2.1	Establishment of a novel method for neural network formation and function...	210
3.3	Validation of new approach methods for regulatory application.....	214
3.4	From screen hit to DNT toxicant.....	216
4	Abstract.....	221

5 Zusammenfassung	222
Abbreviations	223
References	231
Danksagung.....	248
Eidesstattliche Erklärung/Declaration	251

1 Introduction

1.1 Brain development

The human brain is the most complex organ of the human body. In its developing state, the brain consists of about 100 billion neurons, which form networks of approximately 60 trillion neuronal connections responsible for our thoughts, feelings, actions, and sensations (Stiles and Jernigan, 2010). At the beginning of the third week of gestation (GW), the development of the brain commences and exceeds until the mid-20s, controlled by a variety of cellular key neurodevelopmental processes (KNDP; Figure 1).

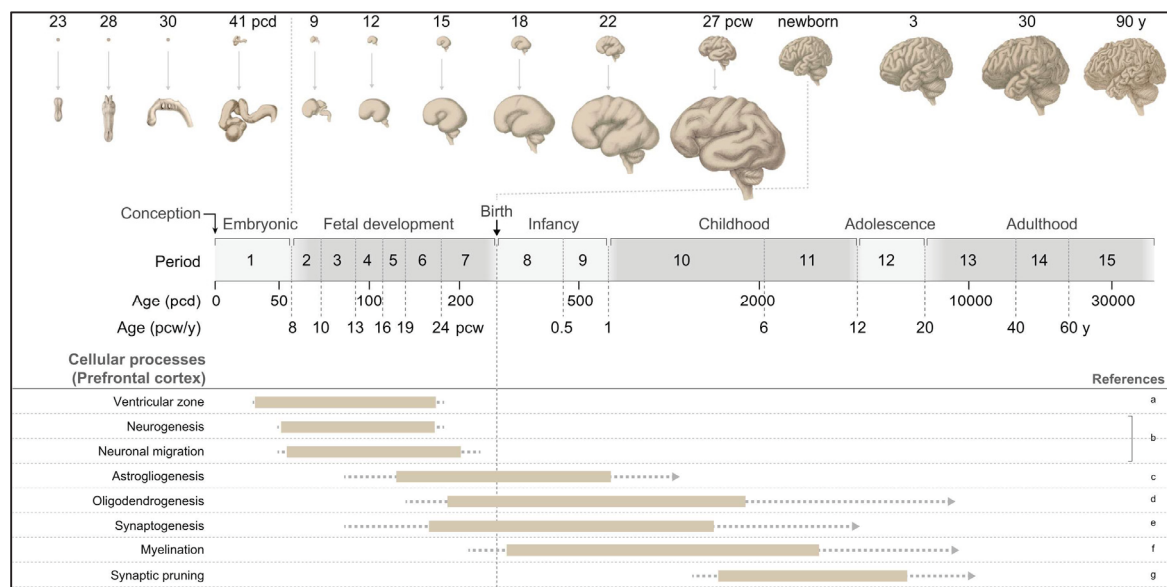


Figure 1: Human brain development. Several processes during human brain development are illustrated in a time-dependent manner from the early embryonic phase to adulthood. pcd: postconceptional days; pcw: postconceptional weeks; postnatal years (y) (adapted from Silbereis et al., 2016).

The initiation of processes is described by the formation and proliferation of neural progenitor cells (NPCs), which are capable of differentiating into the different cell types of the central nervous system (CNS; Stiles and Jernigan, 2010). During neurulation, the first stage of development, the neural tube is formed from the ectoderm, which is a precursor of the brain and the spinal cord (Copp et al., 2003). The next stage, neurogenesis, describes the formation of neurons. At the beginning of this process, the population of NPCs is enlarged, allowing them to differentiate into radial glial cells and neurons (gliogenesis and neurogenesis). As neurons migrate from the center of the brain, the ventricular zone, out to the developing neocortex, radial glial cells form a scaffold for migrating neurons (Borrell and Götz, 2014; Fernández et al., 2016). Once they have reached

their target region in the cortex, they differentiate and further mature into multiple subtypes of inhibitory and excitatory neurons. Finally, the neurons start forming neuronal extensions, called axons and dendrites and, connect to other neurons through synapses. The completion of these processes creates a neuronal network, which enables the transmission of electrochemical information and ensures communication within the brain (Stiles and Jernigan, 2010). Synaptogenesis begins during fetal development and continues into adulthood (Fig. 1). Before birth, about 50% of all neurons are eliminated by programmed cell death or apoptosis. However, also during adulthood, half of the synapses are disabled with the aim of increasing the efficiency of synaptic transmission, a process called synaptic pruning (Purves and Lichtman, 1980; Stiles and Jernigan, 2010; Tau and Peterson, 2010). Shortly after the beginning of neurogenesis, oligodendrocytes and astrocytes are generated from radial glial cells (Howard et al., 2008; Kriegstein and Alvarez-Buylla, 2009). Oligodendrocytes form myelin sheaths around adjacent axons to insulate them and provide higher saltatory conduction of action potentials (Jakovcevski et al., 2009). This process, called myelination begins at the natal age and in concert with synaptic pruning, elaborates the functional network structures of the brain through adolescence (Fields, 2008; Spear, 2013; de Hoz and Simons, 2015).

Taken together, the spatiotemporal orchestration of the above-mentioned processes in combination with a plethora of molecular events drives human brain development, beginning in the third GW and extending through late adolescence (Stiles and Jernigan, 2010).

1.2 Developmental Neurotoxicity (DNT)

Disruption of one of the mentioned processes by a chemical or physical agent, leading to structural and in the end, functional impairment is called developmental neurotoxicity (DNT; Giordano and Costa, 2012). Many environmental substances, e.g. lead, mercury, and polychlorinated bisphenyls are known to interfere with neurodevelopmental processes, causing neurodevelopmental disorders, such as autism, mental retardation, attention deficit disorder, or other subclinical brain dysfunctions. As the developing brain is much more vulnerable compared to the adult brain, even exposure at low doses can affect proper brain function (Grandjean and Landrigan, 2006). In 1988, Bernard Weiss emphasized the impact of a 5-point IQ loss in a hypothetical population of 100 million people with an average IQ of 100 (Fig. 2). Thus, the number of people scoring below 70 and classified as “intellectual disabled” would increase by 57% and be paralleled by a 60% decrease of individuals counted as gifted (IQ>130; Weiss, 1988; Schmidt, 2013). An average 5-point IQ loss may not have a major impact on each individual, but socioeconomic consequences

can be enormous, like diminished economic productivity or an increased number of people needing special education (Grandjean and Landrigan, 2006). For example, the annual cost of prenatal methylmercury (MeHg) exposure is estimated at \$8.7 billion (Trasande et al., 2005). Furthermore, Bellanger and colleagues emphasize the importance of prevention of MeHg exposures, which can benefit 600,000 IQ points per year, resulting in an annual economic benefit of up to €9,000 million within the EU (Bellanger et al., 2013).

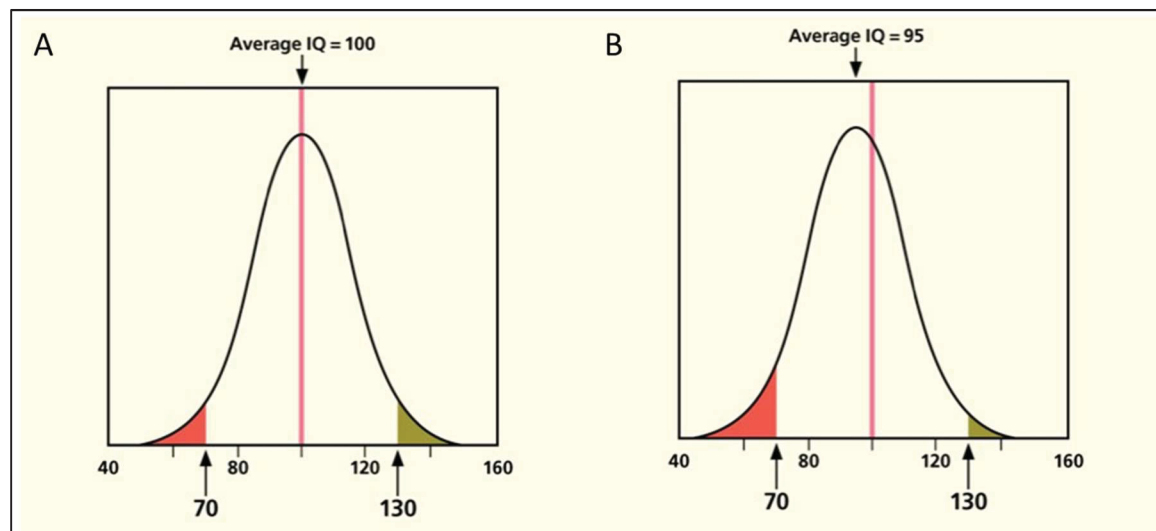


Figure 2: Relevance of an average IQ loss in a hypothetical population. An average loss of 5 IQ points (B) in a hypothetical population of 100 million people increases the number of people with IQs below 70, thus categorized as “intellectual disabled” and at the same time decreases the population of the “very gifted” with IQs above 130. Figure adapted from Schmidt, 2013.

Besides lead, MeHg, polychlorinated biphenyls, arsenic, toluene, and ethanol, unambiguously identified by epidemiological approaches (Grandjean and Landrigan, 2006), Grandjean and Landrigan documented six additional developmental neurotoxicants since 2006: manganese, fluoride, chlorpyrifos, dichlorodiphenyltrichloroethane, tetrachloroethylene, and the polybrominated diphenyl ethers (Grandjean and Landrigan, 2014). Along with valproic acid, for which clinical evidence exists (Balmer et al., 2012; Kadereit et al., 2012; Aschner et al., 2017), the total number of chemicals that have been identified as disruptors of neurodevelopment in humans is relatively small in comparison to the worldwide chemical landscape of around 350,000 chemicals, registered for production and use (Wang et al., 2020) and which DNT potential is still unknown.

In comparison to the adult brain, the developing brain is more susceptible to environmental toxicants (Rice and Barone, 2000), which may be explained by the long developmental period, the high plasticity of the developing brain, the multiple neurodevelopmental processes involving

many different cell types that offer a large number of chemical targets and the limited protection of the blood-brain barrier until early infancy (Zheng et al., 2003). Exposure to environmental chemicals originates prenatally from the maternal circulation via the placenta (Needham et al., 2011; Grandjean and Landrigan, 2014) or postnatally through breast milk (Needham et al., 2011). Compared to the low number of known DNT positive substances, more than 200 chemicals are known to be neurotoxic in humans. In addition, for most of the substances in the chemical universe, DNT effects have not been studied indicating a great data gap in the testing of chemicals for DNT (Grandjean and Landrigan, 2006).

1.2.1 DNT testing

DNT testing is currently performed according to *in vivo* testing guidelines: the OECD 426 (OECD, 2007), EPA 870.6300 (U.S. EPA, 1998), or OECD 443 (OECD, 2018), an extended one-generation reproductive toxicity study. These studies are not mandatory and are only performed upon specific trigger factors. OECD 426 or 443 are only requested when there is evidence for neurotoxicity in standard adult and/or reproductive toxicity studies (Bal-Price et al., 2015; Pistollato et al., 2021). Preferably, these are conducted in rats and include several structural and functional tests, characterizing physical development, the assessment of brain weights, neuropathology, behavioral ontogeny, motor activity, motor and sensory function, learning and memory restricted to a period from early gestation until the end of lactation. Due to their high resource intensity regarding time, money, and animals, only between 110 (OECD, 2008) and 140 chemicals have been assessed for their DNT potential (Makris et al., 2009; Sachana et al., 2019; Crofton and Mundy, 2021). To be precise, the testing of one compound requires 1 year, costs up to 1-1.4 million US\$ (Crofton et al., 2012; Smirnova et al., 2014), and raises ethical concerns with an animal consumption of around 1000 rat pups (Smirnova et al., 2014), resulting in a huge DNT data gap. Furthermore, the limitations of these studies extend to their substantial variability and the resulting lack of reproducibility, which culminates in the uncertainty of extrapolation from rodents to humans (Tsuji and Crofton, 2012; Terron and Bennekou, 2018; Sachana et al., 2019; Paparella et al., 2020). The previously described social, societal, and economic impacts that DNT entails and the resulting lack of testing data, stresses the importance of an alternative strategy, allowing a more efficient assessment of DNT and thereby closure of the data gap. In the last years, academia, industry, and regulatory authorities from across the world agreed on the need for alternative, so-called new approach methods (NAMs; Kavlock et al., 2018) for DNT testing *in vitro*, designed to allow a cheaper and faster assessment of DNT hazard (Lein et al., 2007; Crofton et al.,

2011, 2014; Bal-Price et al., 2012, 2015; EFSA, 2013; Fritsche et al., 2017; Bal-Price et al., 2018; Fritsche, Grandjean, et al., 2018).

1.3 Alternative toxicity testing

The need for alternative testing strategies expands to the entire field of toxicological risk assessment, and initial efforts to drive this paradigm shift can be traced back to the early 2000s. In 2005, the U.S. Environmental Protection Agency (EPA) and the U.S. National Toxicology Program (NTP) started to develop a long-dated roadmap for toxicity testing, to meet evolving regulatory needs. Within this funded project at the National Research Council (NRC), two reports had been published, emphasizing the current key issues of toxicity testing, and developed a strategy to create a paradigm shift in chemical hazard and risk assessment (National Research Council, 2006, 2007). This paradigm shift should move toxicology away from the apical endpoint assessments of resource-intense *in vivo* testing with limited human relevance, to a next-generation risk assessment, based on high-throughput *in vitro* screening assays and computational toxicology. The agencies demanded, that more focus should be placed on the efforts of toxicology of the 21st century, which includes biochemical- and cell-based *in vitro* assays, alternative animal models (*Danio rerio* (zebrafish), *drosophila melanogaster*, *caenorhabditis elegans*), as well as computational *in silico* models. Compared to the standard rodent toxicological tests, which allow a testing of 10-100 substances per year, the alternative models enable a greater cost efficiency and a higher throughput of 100-10,000 substances per year, up to 10,000 chemicals per day (Collins et al., 2008; Gibb, 2008; Krewski et al., 2019). In summary, these NAMs support the paradigm shift by moving the current hazard and risk assessment towards a mechanistic understanding of generated data and enabling access to human-relevant approaches (Collins et al., 2008). Nevertheless, results from new approach test methods are not yet widely accepted for their use in a regulatory context. Therefore, the OECD developed an integrated approach to testing and assessment (IATA) framework, which is “based on multiple information sources used for hazard identification, hazard characterization and/or safety assessment of chemicals” (OECD, 2016) and can be built on results of various methods (QSAR (quantitative structure-activity relationship), RASAR (read-across structure-activity relationship), *in silico*, *in chemico*, *in vitro*, *ex vivo*, *in vivo*, ‘-omic’ technologies). Each IATA is designed with the goal of combining and weighing all relevant existing information to allow efficient decision-making with regard to potential hazard and/or risk of a substance (OECD, 2020).

1.3.1 *In vitro* DNT testing – the DNT-IVB

A plethora of KNDPs is involved in the development of a functional human brain; e.g. proliferation and migration, as well as the differentiation of progenitors into the effector cells of the brain. These processes culminate in the generation of an operational neural network (Fig. 3). To assess developmental neurotoxicity, evoked by the disturbance of at least one KNDP by a chemical or physical agent, in a cost- and time-efficient manner, new approach methods have been developed (Kavlock et al., 2018). Since a single *in vitro* method is not capable of capturing the complexity of human brain development, there was an urgent need for the design of a battery of different test methods, covering the majority of these KNDPs (Paparella et al., 2020). For this effort, one or more KNDP is mimicked by a neurodevelopmental test system, i.e. cells that represent a developing brain cell and are capable of performing a function crucial for brain development (EFSA, 2013; Crofton et al., 2014; Bal-Price et al., 2015; Fritsche et al., 2017; Bal-Price et al., 2018; Fritsche, Grandjean, et al., 2018).

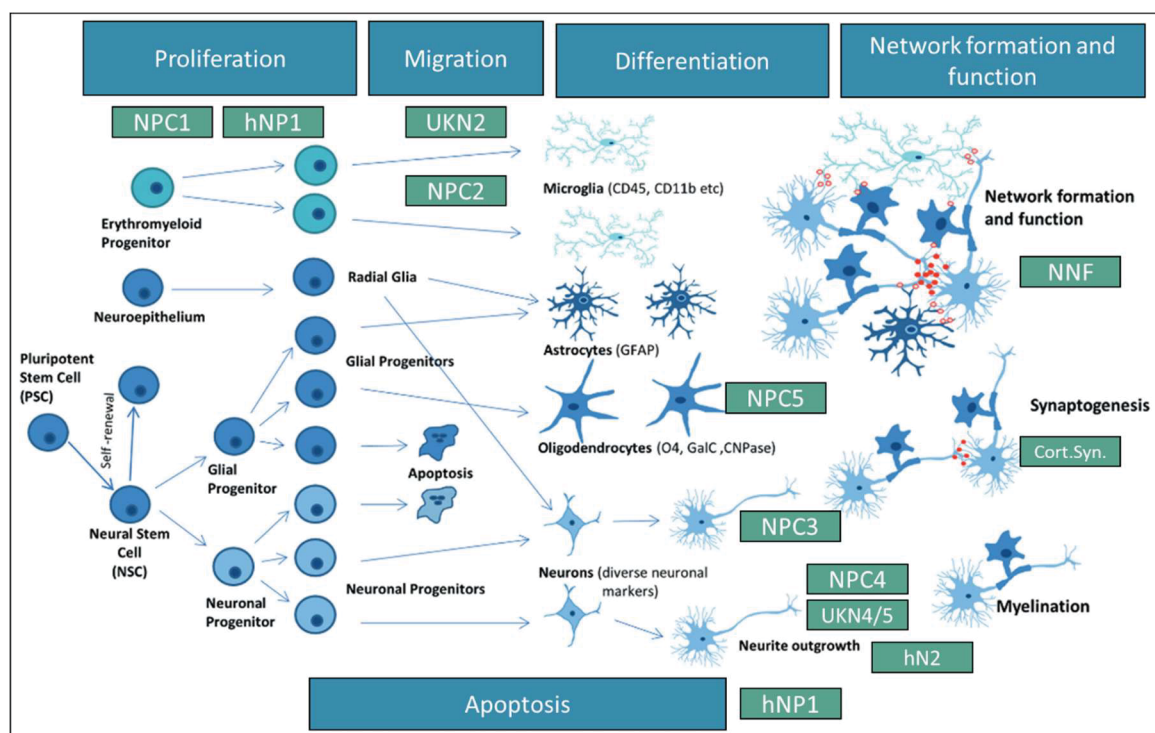


Figure 3: Key neurodevelopmental processes during brain development with relevance for DNT and their respective assays in the DNT-IVB. Neural stem cells proliferate and migrate into neuronal and glial progenitor cells, which can differentiate into different effector cell types of the human brain. These cells mature, connect via synapses and build a neural network. Microglia migrate into the brain from GW4 to 24 and are of mesodermal origin. The DNT-IVB covers these KNDPs through multiple test methods (green boxes). Adapted from Bal-Price et al. (2018).

Under the umbrella of the OECD and funded by the European Food Safety Authority (EFSA), a DNT-IVB was assembled, including 17 *in vitro* assays developed by the U.S. EPA and two research groups from Düsseldorf (IUF) and Konstanz (UKN), modelling the following KNDPs (Fig. 3): proliferation, differentiation, apoptosis, migration, neurite outgrowth, synaptogenesis, and neural network formation. The test systems are based on six different cell models: human NPCs grown as proliferating 3D neurospheres (NPC1-5), human NPCs (hNP1), human neural stem cell (NSC)-derived neural crest cells (UKN2), a v-myc transformed human NSC-line (UKN4), human iPSC-derived peripheral (sensory) neurons (UKN5), human NPC-derived neurons (hN2/igluta) and 3 assays based on rat primary neocortical cells (cortical initiation and maturation, cortical MEA). Some KNDPs modeled by the DNT-IVB assays are described by multiple assays (Figure 5). For example, proliferation is assessed by two different methods, migration by four, and neurite outgrowth even by four human, and one rat-based assay. At first glance, the assays might appear redundant, but Masjosthusmann et al. (2020) showed by extensive analyses of all assays, the non-redundancy of the DNT-IVB test methods, and a clear need for multiple assays modelling the same endpoint. For example, the four migration assays mainly differ in the cell types used for the endpoint analyses: human induced pluripotent stem cell (hiPSC)-derived neural crest cells (UKN2), as well as primary human NPCs differentiated into radial glia (NPC2a), neurons (NPC2b) or oligodendrocytes (NPC2c) in a mixed culture. Because every cell type has a different timing of occurrence (migration of neural crest cells occurs during embryogenesis, thus earlier than, for example, migration of oligodendrocytes, which occurs at a later period to improve neuronal function) and also needs different stimuli for migration, a large overlap of migration effect was not expected. Furthermore, these methods vary in their dimensionality (secondary 3D or 2D), as well as in assay duration and their exposure scheme (120h or 24h; Masjosthusmann et al., 2020).

One crucial requirement for an OECD application of test methods and their use for hazard identification and risk assessment is validation, to ensure that these methods are able to produce data that can help address regulatory requirements (Coecke et al., 2007; Griesinger et al., 2016). Classic validation, as recommended by the OECD, is very time-consuming, as it includes the transferability of the test method between laboratories and relies on animal data. Instead of this classic technical validation, as conducted for e.g. skin sensitization NAMs (OECD, 2021; Strickland et al., 2022), the idea of a more scientific biological validation for NAMs has been suggested (Leist et al., 2014). The validation of NAMs is centered on a mechanistic rationale approach, with regard to active or inactive pathways of toxicity, different modes of action, as well as adverse outcome pathways, to ensure the representability of the respective KNDP by the test method. The time-consuming lab-to-lab comparison is not part of the procedure, but the assay consistency, e.g.

reproducibility of endpoint measures is an important criterion for scientific validation (Hartung, 2007; Leist et al., 2012, 2014; Hartung et al., 2013). Scientific validation has been performed by all of the 17 DNT IVB assays and is available in the ToxTemps attached to Crofton and Mundy (2021). Scientific validation of the neurosphere assay is also part of this thesis work (Koch et al. 2022 - Manuscript 2.1). As the lab-to-lab validation of test methods increases confidence of its use, this process is currently being initiated by the EFSA for all 17 assays of the DNT-IVB and will bring the DNT field one step closer towards reduction of animal experiments for DNT with the long-term goal of replacing DNT *in vivo* test guidelines.

Taken together, the DNT-IVB is currently ready to be used in three major regulatory fields: (i) for the use in screening approaches for the prioritization of substances, for which data on DNT is lacking or limited, (ii) for follow-up screenings, whenever a substance was positively identified by QSAR or other computational models for DNT, and (iii) for single chemical hazard assessment, with the goal of more target-aimed *in vivo* DNT guideline studies or to inform on the weight of evidence (WoE) for DNT if existing *in vivo* DNT data is equivocal (Crofton and Mundy, 2021).

1.3.2 The 'Neurosphere Assay' as a new approach model for DNT testing

An *in vitro* new approach model that has been successfully used for DNT testing and is also included in the DNT-IVB, is the 'Neurosphere Assay', which has been thoroughly characterized and standardized in the last 15 years (Moors et al., 2007, 2009; Baumann et al., 2014, 2015, 2016; Masjosthusmann et al., 2018; Koch et al., 2022 - Manuscript 2.1). The 'Neurosphere Assay' is based on primary human neural progenitor cells (hNPCs), which mimic basic processes of brain development, e.g. NPC proliferation, migration, and differentiation into the major cell types of the brain: radial glial cells, neurons, oligodendrocytes, and astrocytes. hNPCs are obtained from

human fetal cortices of both sexes at GW 16 to 19 and cultured as free-floating three-dimensional cell aggregates, so-called neurospheres (Fig. 4).

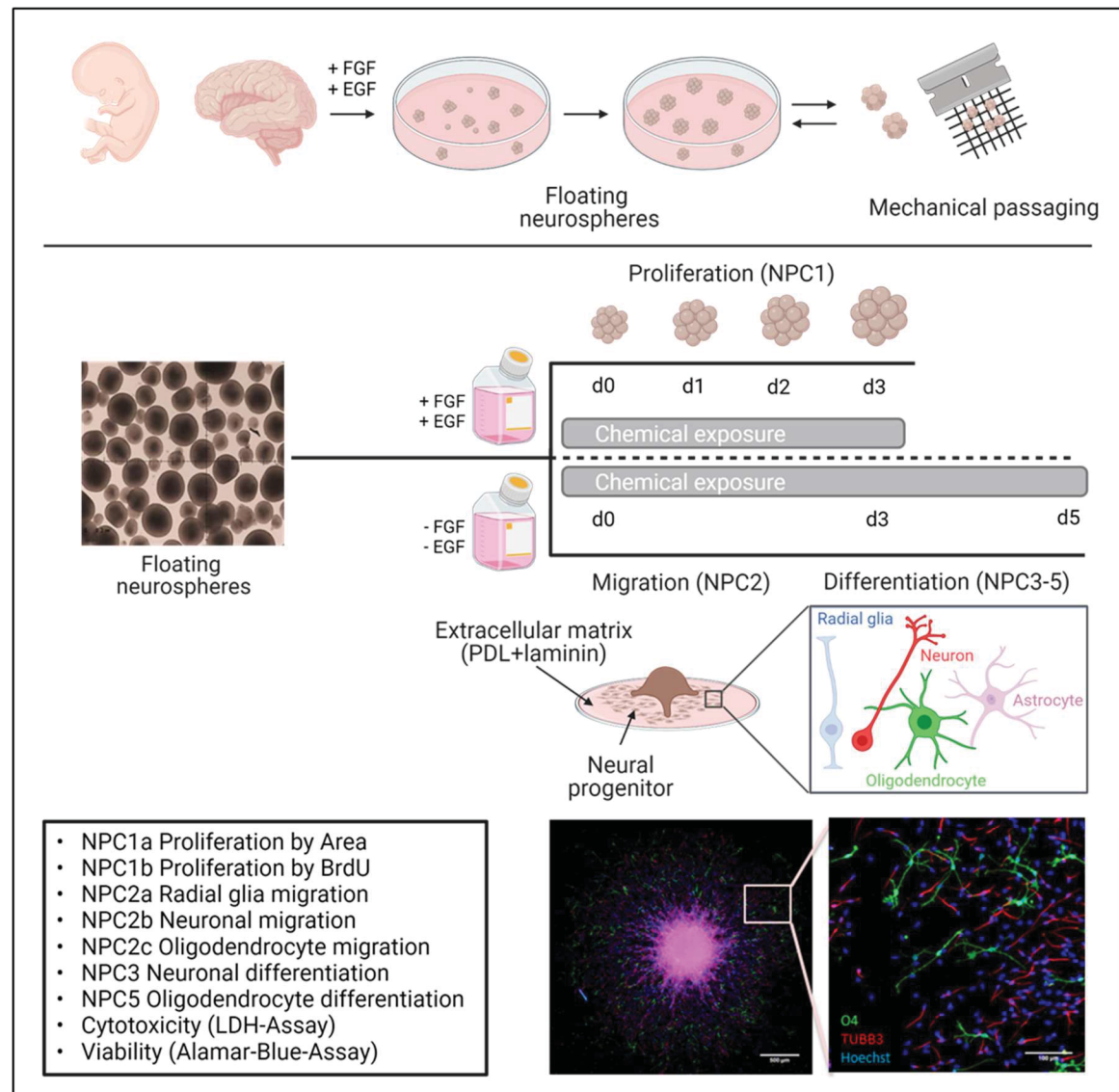


Figure 4: hNPC culture and experimental setup of the 'Neurosphere Assay'. hNPCs are generated from GW16-19 brain cortices (purchased from Lonza, Belgium) and cultivated as three-dimensional cell aggregates, so-called neurospheres. Two days prior to the experiment neurospheres are mechanically passaged and cultivated in suspension, supplemented with EGF and FGF. Proliferation is assessed by measuring the increase in sphere diameter (NPC1a) and by quantification of BrdU incorporation into the DNA (NPC1b). In the absence of growth factors and plated on an extracellular matrix (poly-D-lysine (PDL) and laminin), neurospheres radially migrate out of the sphere core and differentiate into the main effector cells of the brain, astrocytes (not shown), neurons (red) and oligodendrocytes (green). Nuclei are stained with Hoechst 33258 (blue). These processes are represented in six individual assays of the 'Neurosphere Assay': NPC proliferation (NPC1ab), migration of radial glia cells (NPC2a), neurons (NPC2b) and oligodendrocytes (NPC2c), neuronal differentiation (NPC3) and morphology (NPC4), as well as

oligodendrocyte differentiation (NPC5). Cells are exposed to the respective chemical during the entire assay period (NPC1ab: 3 days; NPC2-5: 5 days). Figure created with biorender.com.

Proliferative properties are maintained over several months by weekly mechanical passaging and cultivation in serum-free medium supplemented with epidermal growth factor (EGF) and fibroblast growth factor (FGF; Reynolds et al., 1992; Buc-Caron, 1995; Svendsen et al., 1995). Under growth factor deprived conditions and plated on a poly-D-lysine (PDL)/laminin matrix, NPCs are able to radially migrate out of the sphere core and differentiate into β -III-tubulin⁺ neurons, O4⁺ oligodendrocytes and GFAP⁺ astrocytes (Piper et al., 2001; Reubinoff et al., 2001; Moors et al., 2009). These three cell types can be immunocytochemically stained and quantified. In the present thesis, only the quantification of neurons and oligodendrocytes is considered (Schmuck et al., 2017; Förster et al., 2021).

In total, the 'Neurosphere Assay' models eight human fetal neurodevelopmental key events (KEs) which are associated with toxicity of the developing brain (Fig. 4). These KEs are divided into the endpoints NPC1-6. The NPC2-5 endpoints can be quantified using a high-content image analysis tool (Omnisphero) in conjunction with two implemented convolutional neural networks (CNN). Free of human bias, this tool is capable of quantifying neurons and oligodendrocytes, assessing the migration distance and neuronal morphology, allowing a standardized and reproducible assessment of each endpoint (Schmuck et al., 2017; Förster et al., 2021). The quantification of astrocytes is currently under development and not considered in this study.

Another endpoint assessed within the neurosphere assay is NPC6 (not shown in Fig. 4), which models the TH-dependent oligodendrocytes maturation, by quantification of myelin basic protein (*MBP*) mRNA expression, divided by the total percentage of oligodendrocytes (NPC5) in the migration area of the respective neurosphere (Dach et al., 2017; Klose et al., 2021). Additionally, all endpoints can be multiplexed with cytotoxicity and viability assessment, to discriminate specific from unspecific effects of the administered compound.

1.3.3 Gaps of the DNT-IVB

The current DNT-IVB models a variety of KNDPs of human brain development from the fetal and postnatal phase, represented by 17 individual assays, based on neural stem cells, neural progenitor cells, neurospheres, and primary cells (Masjosthusmann et al., 2020; Crofton and Mundy, 2021).

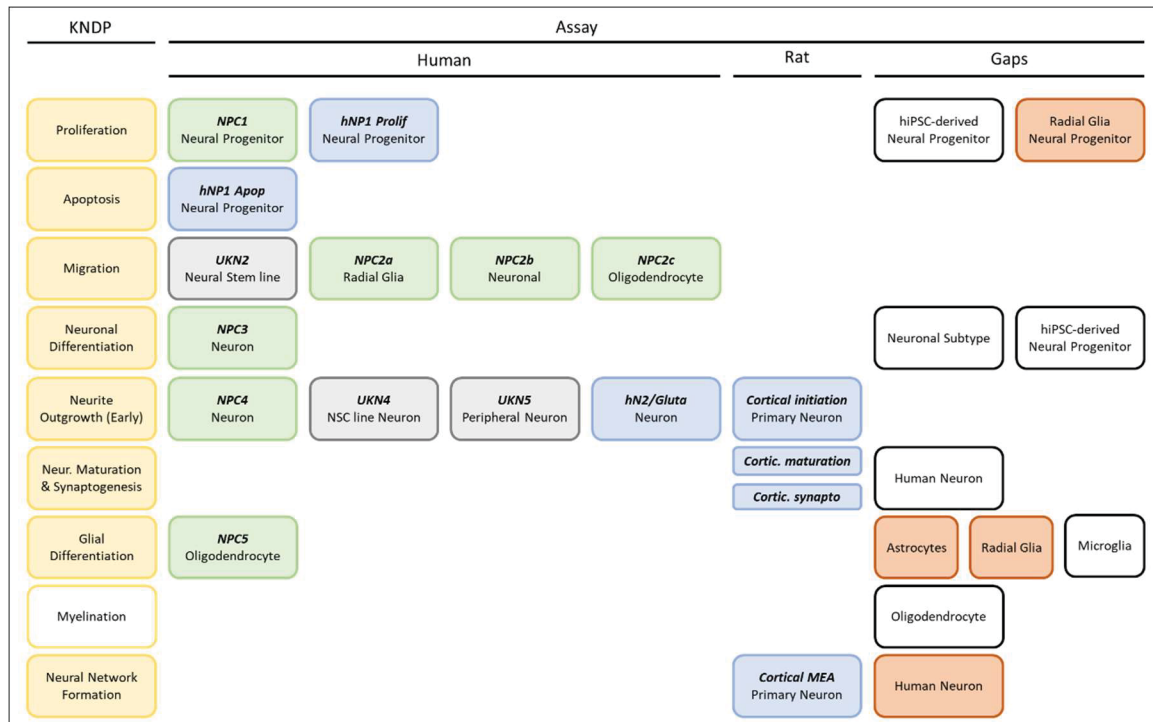


Figure 5: Assays and gaps of the DNT-IVB modelling a variety of key neurodevelopmental processes (KNDP). The DNT-IVB models different KNDPs (yellow boxes) and is comprised of a variety of test systems established at the Leibniz Research Institute for Environmental Medicine Düsseldorf (IUF; green boxes), University of Konstanz (UKN; grey boxes) and the US Environmental Protection Agency (U.S. EPA; blue boxes). Assays that are currently under development at the IUF to fill the gap, are marked in orange. Modified from Crofton and Mundy, 2021.

The assessed endpoints mainly focus on neurons and oligodendrocytes, but the battery fails to cover some important key events, such as radial glia (RG), astrocyte (AC) and microglia (MG) processes, which are essential for a proper brain development and function (Allen, 2014; Borrell and Götz, 2014; Knuesel et al., 2014). To address these issues, the two laboratories in Düsseldorf (IUF) and Konstanz (UKN) have initiated a Cefic-LRI funded research project aimed at extending the DNT-IVB by RG-, AC- and MG-based test systems by 2023.

Besides different cell types, also hormones are key players during brain development (Adhya et al., 2018; Bernal, 2022). The disruption of, for example maternal TH levels *in vivo* may trigger DNT (Miller et al., 2009) and a systematic testing for DNT is currently not included in the evaluation of potential endocrine disrupting chemicals (EDC). ENDpoiNTs is a Horizon 2020 project composed of 16 international partners, that focuses on the development of new testing and screening methods to identify potential EDCs that may induce human DNT. To also capture a broad variety of neurodevelopmental key events, an ED-DNT-IVB will be assembled for regulatory application (Lupu et al., 2020).

As previously described, the DNT-IVB is based on human- and rat-derived neural cell cultures and comes along with many advantages, but also disadvantages. The developing rat brain exhibits substantial distinctions *in vivo* compared to human brain development, such as the absence of gyrification, a process that ensures the complexity of the human brain (Dubois et al., 2008). Furthermore, these two species differ with regard to their qualitative and quantitative molecular composition, which may trigger species-specific cellular responses and underlines the importance of taking these differences into consideration for DNT assessment (Masjosthusmann et al., 2018). To minimize this uncertainty of interspecies extrapolation, the use of human-based cell systems is preferred, but currently not ensured for three of the DNT-IVB assays, including the assessment of neural network formation (Brown et al., 2016; Frank et al., 2017). Despite advances in the field of stem cell biology and the resulting accessibility to human-based models, culturing human neural cells can also have drawbacks, e.g. the prolonged developmental timeline of human cells compared to rodent neural cells (Odawara et al., 2016; Hyvärinen et al., 2019; Nimtz et al., 2020; Saavedra et al., 2021). Furthermore, hiPSC-derived neural networks face the problem that each differentiated neural network consists of a variable number of neuronal subtypes and features a diverse neuron/glia ratio. This fact is accompanied by a high plate-to-plate variability and makes standardized assessment of network formation and function challenging (Fritsche et al., 2018; Nimtz et al., 2020; Bartmann et al., 2021 - Manuscript 2.4). In a research project funded by the Danish EPA, a human-based neural network formation assay was established, that uses commercially available hiPSC-derived neurons and primary human astrocytes in a defined ratio to overcome the afore-mentioned issues and facilitates the closure of one important identified gap (Bartmann et al. submitted - Manuscript 2.5). It is expected that covering the gaps will increase the predictive ability of the DNT-IVB.

1.4 Neural networks on microelectrode arrays (MEA)

During brain development synapses form points of connection between axons and the target neurons, to allow the transmission of electrochemical signals and the construction of information processing networks (Stiles and Jernigan, 2010). The communication between synaptically connected neurons is based on all-or-none action potentials, defined by a change in the membrane potential of neurons across a certain threshold (Bean, 2007). Synapses can be divided into two types: electrical synapses, which transmit simple electrical signals by direct current flow at gap junctions and chemical synapses, which release chemical signals, so-called neurotransmitters, to transport excitatory, inhibitory and complex biochemical information (Hyman, 2005). The two most important neurotransmitters in the mammalian brain are

glutamate, the main excitatory, and γ -aminobutyric acid (GABA), the main inhibitory neurotransmitter (Roberts and Frankel, 1950; Fonnum, 1984), based on their ability to either activate cation (e.g. Na^+ or Ca^{2+}) or anion (Cl^-) channels (Hyman, 2005).

In the last years, *in vitro* models have been developed to capture the complexity of human brain development. These methods are often based on multiple types of neurons (excitatory and inhibitory) and also supportive cells, such as astrocytes, which form neural networks and therefore mimic the *in vivo* situation as precisely as possible (Tukker et al., 2016). Important tools to study the electrophysiological activity of these networks are microelectrode arrays (MEA). Compared to other techniques, such as the so-called patch clamp method, MEAs provide a platform to measure the electrical transmission of not only individual neurons, but of an entire neural network. These integrated arrays consist of multiple electrodes, photoetched into a glass slide or a “chip” and coated with a conductive material, allowing the simultaneous recording of extracellular action potentials (Johnstone et al., 2010). These electrodes can record the neuronal activity resulting from transmembrane currents, even over distances of hundreds of micrometers (Egert and Hämmerle, 2002).

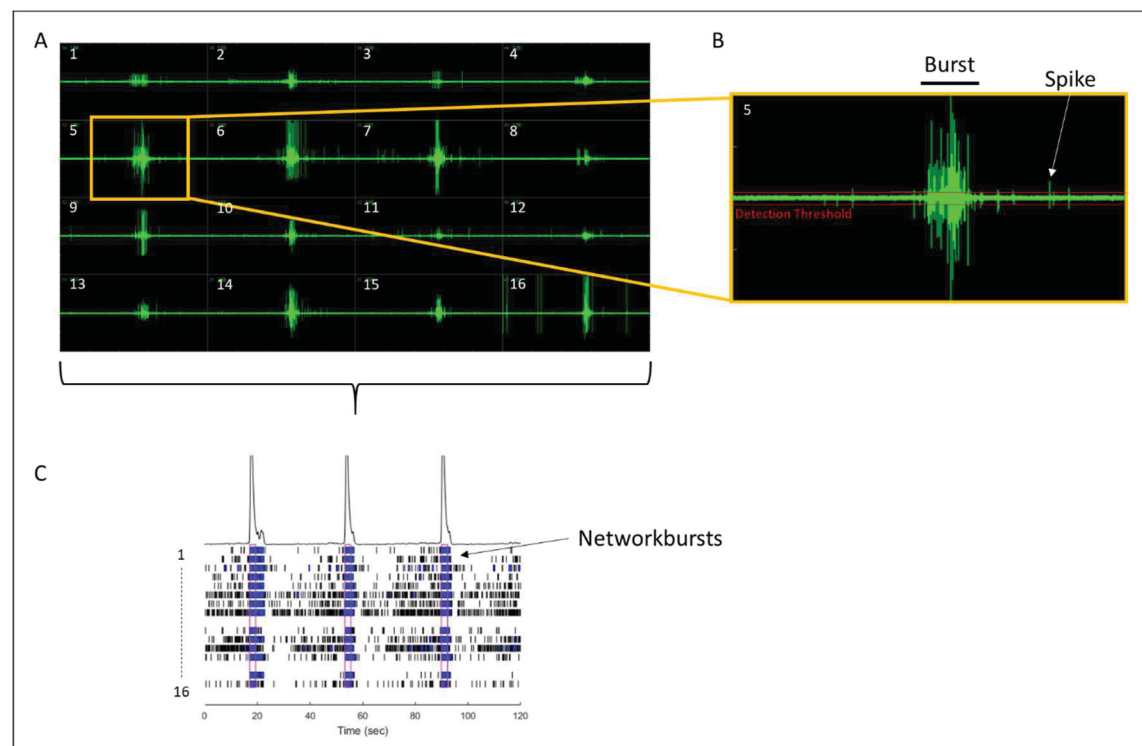


Figure 6: Spike and bursting activity of neural cells detected by microelectrode arrays (MEA). (A) Example recording of differentiated neural networks, consisting of excitatory and inhibitory neurons and astrocytes, exhibiting spontaneous electrical activity on 16 electrodes per well of a 48-well MEA plate. (B) Single electrode activity reveals detection of a single action potential (“spike”) and grouped activity, so-called “bursts”, crossing a defined detection threshold (red line). (C) Plotting of single electrode activity of one

MEA well in a time-dependent manner shows synchronized bursting activity of networks (“networkbursts” in blue).

Extracellular action potentials (“spikes”) can be assessed in their native form and result from the intracellular influx of Na⁺ ions, and the subsequent outflow of K⁺ ions, giving rise to extracellular recorded signals (Buzsáki et al., 2012). But also groups of spikes (“bursts”) and the more organized and synchronized type of activity, so-called “networkbursts” can be recorded on each electrode, whenever they cross a specific detection threshold (Fig. 5; Johnstone et al., 2010). Depending on the type of platform, each MEA recording can provide information on more than 70 parameters, including spike and burst rates, as well as specific patterns of spontaneous electrical firing, based on specified algorithms (Kapucu et al., 2012).

In the last years, research showed that MEAs are a valuable tool to assess alterations of chemicals on network formation and function in a variety of rodent and human neural cell cultures (Brown et al., 2016; Frank et al., 2017; Nimtz et al., 2020; Tukker, Bouwman, et al., 2020). Such networks can be characterized by their neuronal subtype and receptor constitution as well as by pharmacological modulation with specific agonists and antagonists, e.g. GABA, bicuculline, glutamate, and CNQX (Odawara et al., 2016; Hyvärinen et al., 2019; Nimtz et al., 2020). So far, only neural networks generated with rat primary cortical cultures were applied for screening purposes. As there are species differences between rat and human cultures, establishment of neural networks of human origin is desired.

1.5 Aim of this thesis

It is well known that the developing human brain is more vulnerable to chemical exposure than the adult brain, but the chemical landscape has not been adequately studied regarding its DNT potential. This large data gap can be explained by the current *in vivo* DNT testing guidelines, which obstruct a time- and cost-efficient testing of a large number of chemicals and additionally creates the problem of extrapolation to humans. To address this data gap, researchers and regulatory authorities agreed on the need for a paradigm shift and the development of a human-relevant DNT-IVB, based on a variety of alternative methods, modelling several key events of brain development. This DNT-IVB can already be used for mechanism-based hazard assessment and prioritization of substances for further testing. Nevertheless, the 17 DNT-IVB methods are not capable of representing all key neurodevelopmental processes, thus different gaps have been analyzed that need to be filled by newly developed human-based *in vitro* assays.

To contribute to this task and to enhance the acceptance and readiness of the current DNT-IVB for a regulatory application, the following aims were pursued in this thesis:

1. Enhancing the validity of the 'Neurosphere Assay' for DNT evaluation by scientific validation.
2. DNT hazard assessment of 135 compounds using a DNT *in vitro* testing battery for future use in a regulatory context.
3. Establishment of a human-based *in vitro* assay for the assessment of neural network formation and function (hNNF) and testing of 27 pesticides using the hNNF assay to evaluate its use in a regulatory context.

2 Manuscripts

The present thesis consists of the following five manuscripts:

The first manuscript 2.1, 'Scientific Validation of Human Neurosphere Assays for Developmental Neurotoxicity Evaluation' (Koch et al., 2022) is about the scientific validation of the 'Neurosphere Assay' (NPC1-6), as well as two additional assays, based on hiPSCs (iNPC1-2a). This five-tiered validation of each assay, confirms the 'Neurosphere Assay' as an integral part of the current DNT-IVB.

The second manuscript 2.2, 'Neurodevelopmental toxicity assessment of flame retardants using a human DNT *in vitro* testing battery' (Klose et al., 2021) investigates the DNT potential of selected flame retardants, based on eight assays of the DNT-IVB, the 'Neurosphere Assay' (NPC1-5), as well as three assays established at the University of Konstanz (UKN2, UKN4, UKN5). This study supports the use of eight human-based *in vitro* assays as part of the DNT-IVB for hazard assessment and prioritization of compounds.

The third manuscript 2.3, 'Establishment of a human cell-based *in vitro* battery to assess developmental neurotoxicity hazard of chemicals' (Blum et al. under review) explores the feasibility of DNT hazard assessment based on a DNT-IVB, that models different KNDPs. The study provides alerts for the majority of the tested known DNT toxicants with a specificity of >94% and provides strategies on the use of the data in a regulatory context.

The fourth manuscript 2.4, 'Measurement of Electrical Activity of Differentiated Human iPSC-Derived Neurospheres Recorded by Microelectrode Arrays (MEA)' (Bartmann et al., 2021) is a book chapter describing a protocol for the neural induction of hiPSCs to human neural progenitor cells (hiNPC) in the form of free-floating spheres and their differentiation into functional neural networks on MEAs. The chapter further explains the measurement of electrical network activity, as well as the evaluation of the generated data.

The fifth manuscript 2.5, 'A human iPSC-based *in vitro* neural network formation assay to investigate neurodevelopmental toxicity of pesticides' (Bartmann et al. under review) provides

novel insight into the establishment of a human-based *in vitro* method, modelling the formation and function of neural networks on MEA plates. In addition to a pharmacological modulation and the establishment of an assay positive control, the test method was challenged with 28 substances, mainly pesticides. This study suggests that the hNNF assay is a valuable addition to the current DNT *in vitro* testing battery.

2.1 Scientific validation of human neurosphere assays for developmental neurotoxicity evaluation

Katharina Koch, **Kristina Bartmann**, Julia Hartmann, Julia Kapr, Jördis Klose, Eliška Kuchovská, Melanie Pahl, Kevin Schlüppmann, Etta Zühr and Ellen Fritsche

Frontiers in Toxicology

Es wird ein Paradigmenwechsel in der Bewertung von Entwicklungsneurotoxizität (DNT) gefordert, welcher die Implementierung schnellerer, kosteneffizienterer und für den Menschen relevanter Testsysteme als die derzeitigen *in vivo* Richtlinienstudien einschließt. Unter der Federführung der Organisation für wirtschaftliche Zusammenarbeit und Entwicklung (OECD) wird derzeit ein Leitdokument finalisiert, das Anweisungen für den Nutzen einer DNT *in vitro* Batterie (DNT-IVB) für regulatorische Anwendungen enthält. Ein entscheidender Punkt bei der Anwendung von OECD-Methoden ist die (mechanistische) Validierung, die bei sogenannten *new approach methods* (NAMs) innovative Ansätze erfordert. Hier sind mechanistische Informationen, die zuvor *in vivo* identifiziert wurden sowie bekannte neurologische Entwicklungsstörungen als Reaktion auf Störungen auf Zell- und Gewebeebene von zentraler Bedeutung. In dieser Studie validieren wir wissenschaftlich den Neurosphären Assay, welcher auf menschlichen primären neuronalen Vorläuferzellen (hNPCs) basiert und ein integraler Bestandteil der DNT-IVB ist. Er modelliert Schlüsselereignisse (*key events*, KEs) der neuronalen Entwicklung wie beispielsweise die Proliferation von NPCs (NPC1ab), die Migration radialer Gliazellen (NPC2a), die neuronale Differenzierung (NPC3), den Auswuchs von Neuriten (NPC4), die Differenzierung von Oligodendrozyten (NPC5) und die schilddrüsenhormonabhängige Reifung von Oligodendrozyten (NPC6). Darüber hinaus erweitern wir unsere Arbeit von den hNPCs auf NPCs, die aus human-induzierte pluripotente Stammzellen gewonnen wurden (hiNPCs) für die NPC-Proliferation (iNPC1ab) und die radiale Glia-Migration (iNPC2a). Der Validierungsprozess basiert auf 1) einer Beschreibung der Relevanz der jeweiligen Endpunkte für die Entwicklung des Gehirns, 2) einer Bestätigung der *in vitro* beobachteten zelltypspezifischen Morphologie, 3) der Expression von zelltypspezifischen Markern, die mit diesen Morphologien übereinstimmen, 4) den angemessenen antizipierten Reaktionen auf physiologisch relevante Signalstimuli und 5) den Veränderungen spezifischer *in vitro* Endpunkte bei Exposition der Zellen mit bekannten DNT-Substanzen. Angesichts dieser

starken mechanistischen Grundlagen gehen wir davon aus, dass der Neurosphären Assay als integraler Bestandteil der DNT-IVB gut für die DNT-Bewertung im Rahmen einer regulatorischen Anwendung geeignet ist.



Scientific Validation of Human Neurosphere Assays for Developmental Neurotoxicity Evaluation

Katharina Koch¹, Kristina Bartmann¹, Julia Hartmann¹, Julia Kapr¹, Jödis Klose¹, Eliška Kuchovská¹, Melanie Pahl¹, Kevin Schlüppmann¹, Etta Zühr¹ and Ellen Fritsche^{1,2*}

¹IUF—Leibniz Research Institute for Environmental Medicine, Duesseldorf, Germany, ²Medical Faculty, Heinrich-Heine-University, Duesseldorf, Germany

OPEN ACCESS

Edited by:

Andrea Terron,
European Food Safety Authority, Italy

Reviewed by:

Mary E. Gilbert,
United States Environmental
Protection Agency (EPA),
United States
Joshua Harrill,
United States Environmental
Protection Agency (EPA),
United States

*Correspondence:

Ellen Fritsche
Ellen.Fritsche@iuf-duesseldorf.de

Specialty section:

This article was submitted to
Neurotoxicology,
a section of the journal
Frontiers in Toxicology

Received: 16 November 2021

Accepted: 21 January 2022

Published: 02 March 2022

Citation:

Koch K, Bartmann K, Hartmann J,
Kapr J, Klose J, Kuchovská E, Pahl M,
Schlüppmann K, Zühr E and Fritsche E
(2022) Scientific Validation of Human
Neurosphere Assays for
Developmental
Neurotoxicity Evaluation.
Front. Toxicol. 4:816370.
doi: 10.3389/ftox.2022.816370

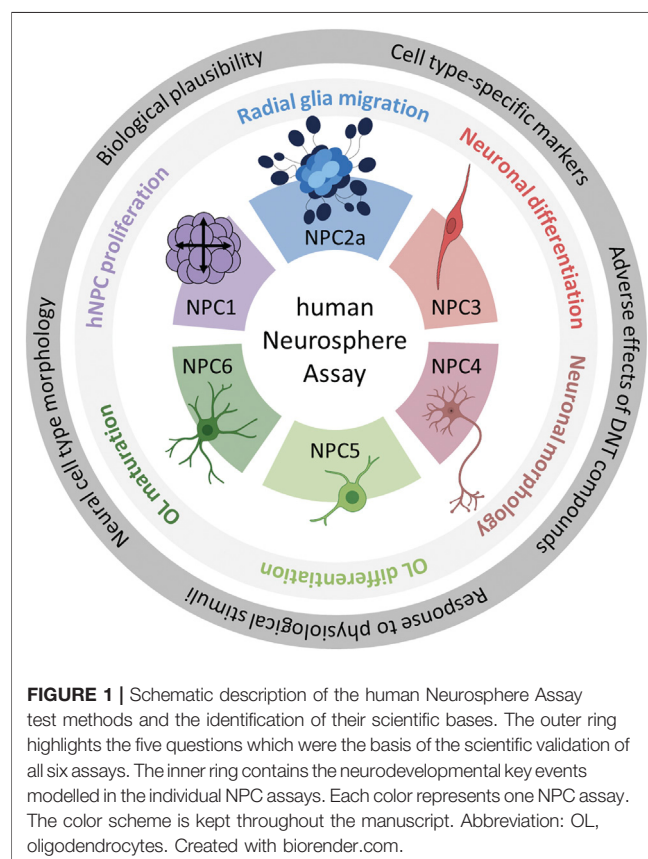
There is a call for a paradigm shift in developmental neurotoxicity (DNT) evaluation, which demands the implementation of faster, more cost-efficient, and human-relevant test systems than current *in vivo* guideline studies. Under the umbrella of the Organisation for Economic Co-operation and Development (OECD), a guidance document is currently being prepared that instructs on the regulatory use of a DNT *in vitro* battery (DNT IVB) for fit-for-purpose applications. One crucial issue for OECD application of methods is validation, which for new approach methods (NAMs) requires novel approaches. Here, mechanistic information previously identified *in vivo*, as well as reported neurodevelopmental adversities in response to disturbances on the cellular and tissue level, are of central importance. In this study, we scientifically validate the Neurosphere Assay, which is based on human primary neural progenitor cells (hNPCs) and an integral part of the DNT IVB. It assesses neurodevelopmental key events (KEs) like NPC proliferation (NPC1ab), radial glia cell migration (NPC2a), neuronal differentiation (NPC3), neurite outgrowth (NPC4), oligodendrocyte differentiation (NPC5), and thyroid hormone-dependent oligodendrocyte maturation (NPC6). In addition, we extend our work from the hNPCs to human induced pluripotent stem cell-derived NPCs (hiNPCs) for the NPC proliferation (iNPC1ab) and radial glia assays (iNPC2a). The validation process we report for the endpoints studied with the Neurosphere Assays is based on 1) describing the relevance of the respective endpoints for brain development, 2) the confirmation of the cell type-specific morphologies observed *in vitro*, 3) expressions of cell type-specific markers consistent with those morphologies, 4) appropriate anticipated responses to physiological pertinent signaling stimuli and 5) alterations in specific *in vitro* endpoints upon challenges with confirmed DNT compounds. With these strong mechanistic underpinnings, we posit that the Neurosphere Assay as an integral part of the DNT *in vitro* screening battery is well poised for DNT evaluation for regulatory purposes.

Keywords: developmental neurotoxicity, neural progenitor cells, neurons, oligodendrocytes, new approach methodologies, 3D *in vitro* models, human induced pluripotent stem cells, radial glia cells

1 INTRODUCTION

During the last years, enormous scientific and regulatory efforts have been focusing on the establishment of a novel procedure for developmental neurotoxicity (DNT) evaluation (Sachana et al., 2019). The two main drivers for these efforts were the extremely high costs that current DNT guideline studies demand and the resulting overall lack of data, including mechanistic information, that exists for chemicals concerning their influence on brain development. In addition, unique features of the human brain and its development (Rice and Barone Jr., 2000; Dehay and Kennedy, 2007, 2009; Somel et al., 2011; Florio and Huttner, 2014; Pollen et al., 2015; Borrell, 2019) strongly support the general endeavor to use human-derived models for risk decisions in 21st-century toxicity evaluation (National Research Council, 2007). There is a vast amount of data on different compound classes including metals, pesticides, and drugs linking compound exposure to adverse neurodevelopmental outcomes in children, like a drop in IQ or memory and attention deficits (Vorhees et al., 2018). Nevertheless, so far only 110–140 chemicals have been evaluated using *in vivo* DNT guideline studies (Makris et al., 2009; Paparella et al., 2020), while for the majority of the human exposome this data is lacking (Sachana et al., 2021a). Moreover, the contribution of chemical exposure to human neurodevelopmental diseases like autism spectrum or attention deficit hyperactivity disorder has so far only been heavily discussed on an associative basis but not finally mechanistically substantiated (Grandjean and Landrigan, 2006; Abbasi, 2016; Bennett et al., 2016; Gould et al., 2018; Moosa et al., 2018; Cheroni et al., 2020; Masini et al., 2020). Considering the social, societal and economic consequences that DNT entails (Bellinger, 2012; Grandjean and Landrigan, 2014), it is obvious that strategies are needed that allow a faster, more cost-efficient and human-relevant assessment of DNT for closing this obvious data gap.

Efforts for the implementation of DNT *in vitro* alternative methods for hazard identification and risk assessment have been evolving over more than 15 years (Coecke et al., 2007; Lein et al., 2007; Crofton et al., 2011; Bal-Price et al., 2012; Bal-Price et al., 2015a; Fritsche, 2017; Fritsche et al., 2017). According to the proposed paradigm shift in DNT testing (Sachana et al., 2019), a DNT *in vitro* battery (IVB) was assembled based on neurodevelopmental key events (KE; Fritsche et al., 2018b) and assay readiness (Bal-Price et al., 2018). DNT test methods have been assembled (Harrill et al., 2018; Masjosthusmann et al., 2020) and are the basis for a currently prepared guidance document of the Organisation for Economic Co-operation and Development (OECD) with the purpose to shape a framework facilitating the regulatory use of DNT *in vitro* data with fit-for-purpose applications (Crofton and Mundy, 2021). The guidance document rests on two pillars, i.e. 1) the data generated through the experimental work (Masjosthusmann et al., 2020) and 2) the development of a variety of case studies including integrated approaches to testing and assessment (IATA) for screening and prioritization. The OECD guidance document is planned to be published in the first quarter of 2022.



One crucial issue for OECD application of methods is validation (Coecke et al., 2007; Gourmelon and Delrue, 2016; Griesinger et al., 2016). While the traditional practice for assay validation is lengthy and relies on animal data, new approach methods (NAMs) need novel validation approaches. Here, mechanistic information previously identified *in vivo*, as well as reported neurodevelopmental adversities in response to disturbances on the cellular and tissue level, are of central importance (Hartung et al., 2013; Leist and Hartung, 2013). Here the scientific basis of a test method provides the mechanistic rationale for the predictive capacity of the assay. In addition, reliability, defined by the quality of the test method, is a crucial parameter. The scientifically sound, reliable test method also has to be fit-for-purpose implying that the regulatory question is known (Leist et al., 2010, 2014). Lab-to-lab transferability of assays has always been one crucial aspect of assay reliability. However, when e.g. certain robotics equipment is available only in one place, ring trials cannot be performed (Judson et al., 2013).

In this study, we validate the Neurosphere Assay, a high content assay for DNT evaluation, which is part of the DNT IVB (Masjosthusmann et al., 2020), using a mechanistic rationale approach. The Neurosphere Assay is based on human fetal neural progenitor cells (hNPCs) which are cultivated as proliferative neurospheres that have the potential to differentiate into brain effector cells including neurons, astrocytes and oligodendrocytes. Six early human fetal neurodevelopment key events (KEs) which

are associated with DNT, are assessed in assays termed NPC1-6. Human NPC proliferation (NPC1ab) is a prerequisite for brain formation, with disturbances causing alterations in brain morphology and microcephaly (de Groot et al., 2005). Radial glia cell migration (NPC2a) generates a scaffold for migrating neurons during the course of corticogenesis and ensures normal brain structure and function. Alterations in this KE cause developmental brain disorders such as heterotopia and lissencephaly (Barkovich et al., 2005). Neuronal differentiation (NPC3) and neurite outgrowth (NPC4) are key cellular features associated with the functional maturation of the CNS. Disturbances in both directions (promotion or inhibition) are considered as adverse and are associated with depressive mood disorders and intellectual disabilities (Song and Wang, 2011; Guidi et al., 2018). Oligodendrocyte differentiation (NPC5) and thyroid hormone-dependent oligodendrocyte maturation (NPC6) are indispensable for the insulation of neuronal axons with disturbances causing demyelination diseases like leukomalacia that severely affect neuronal functioning (Baumann and Pham-Dinh, 2001; Volpe et al., 2011). Besides these DNT-relevant neurodevelopmental KEs, the Neurosphere Assay assesses the mitochondrial function and detects cytotoxicity upon chemical exposure to discriminate specific from unspecific effects (Figure 1).

All individual test method evaluations are automated, and concerning the experimental procedures, i.e. most pipetting steps are performed by a liquid handling system. The NPC2-5 assays are multiplexed. Quantification of differentiated neurons and oligodendrocytes is achieved by automated image analyses of immunostained cells that migrate out of the spheres in 96-well plates using convolutional neuronal networks (CNN; Förster et al., 2021). All endpoints are then analyzed using the Omnisphero software (Schmuck et al., 2017). This automated endpoint evaluation system allows an investigator bias-free, objective and low hands-on-effort identification of specific brain cells that used to be only possible by manual counting. In addition to cell identification, sphere-related endpoints like radial migration can be assessed. We further add data on the novel human induced pluripotent stem cell (hiPSC)-derived NPC (hiNPC) assays (hiNPC1/2) investigating similar endpoints. This hiPSC-based test system provides an unlimited cell source that is thoroughly characterized in a quality-controlled banking process (Tigges et al., 2021) that contributes to increasing the reproducibility of the test results. Furthermore, since iPSCs are reprogrammed from somatic cells (e.g. fibroblasts), the cell source raises fewer ethical concerns regarding its derivation process than primary cell material. However, hiNPCs represent a more immature developmental stage than fetal NPCs, hence they also have distinct applicability domains concerning neurodevelopmental timing.

Here we present the scientific basis for the individual NPC test methods. That the endpoints tested with the Neurosphere Assay are biologically indispensable for normal brain development (biological plausibility) was described in detail earlier (Fritsche et al., 2018b). Therefore, we now focus on the morphology of the different neural cell types, the expression of cell type-specific markers, the responses of the neurodevelopmental processes to

physiological stimuli by using signaling pathway modulators and the predictive power to identify adverse effects of known DNT compounds. Together with the biological relevance of the endpoint, these five aspects build the scientific basis of the Neurosphere Assay.

2 MATERIALS AND METHODS

2.1 Reagents

Test compounds applied for the validation process are summarized in Table 1. Details for each specific assay are described below.

2.2 Basic hNPC and hiNPC Cell Culture

Primary human NPCs (hNPCs) were isolated from cortices of gestational week 16–19 fetuses and purchased from Lonza Verviers SPRL, Belgium (#PT-2599). The hiPSCs were purchased from Alstem (iPS11) and WiCell (IMR-90, Clone-4). The neural induction of hiPSCs into human-induced neural progenitor cells (hiNPCs) was performed in our laboratory as described in detail in Nimtz et al. (2020). The hNPCs and hiNPCs were cultured as free-floating neurospheres in proliferation medium consisting of DMEM (#31966-021, Thermo Fisher, United States) and Hams F12 (#31765-027, Thermo Fisher, United States) in a 2:1 ratio (v:v) supplemented with 2% B27 (#17504044, Thermo Fisher, United States), 20 ng/ml EGF (#PHG0313, Thermo Fisher, United States), 20 ng/ml FGF basic (#233-FB, R&D Systems, United States), and 100 U/ml penicillin and 100 µg/ml streptomycin (#P06-07100, Pan-Biotech, Germany). Neurospheres were cultured under standard cell culture conditions at 37°C and 5% CO₂ in 10 cm diameter cell culture dishes coated with poly-2-hydroxyethyl methacrylate (poly-Hema; #P3932, Merck, United States). For cell passaging, once per week, neurospheres were mechanically dissociated into cubicles of 0.2 mm edge length using a McIlwain tissue chopper (#TC752, Campden Instruments, United Kingdom). Neurospheres were supplied with fresh culture medium three times per week, by replacing half of the culture medium.

2.3 The Neurosphere Assay (NPC1-6)

2.3.1 Proliferation (NPC1ab)

hNPC and hiNPC proliferation (NPC1ab assay) was scientifically validated by assessing the incorporation of bromodeoxyuridine (BrdU, NPC1b, #11669915001, Roche, Switzerland) into the DNA and by measuring the increase in sphere size (NPC1a; 0, 24, 48, and 72 h) using the Cellomics ArrayScan and the provided HCS Studio Cellomics software (version 6.6.0; Thermo Fisher Scientific). In brief, proliferating NPCs of 300 µm diameter were cultivated for 3 days in 100 µl proliferation medium containing EGF and FGF basic (detailed composition described in the basic cell culture section). One NPC neurosphere was cultivated in 100 µl medium in a well of a poly-Hema-coated 96-well plate and 4–5 technical replicates were prepared for each experimental condition. Proliferating NPCs were further exposed to the EGF receptor inhibitor PD153035 (0.01, 0.16 and 0.64 µM), known

TABLE 1 | List of chemicals used in the experimental part, including their sources, catalog numbers, stock concentrations, and solvents.

Reagents	Source	Catalog Number	Solvent	Stock
Ascorbic acid	Merck	A92902	H ₂ O	100 mM
Bisindolylmaleimide 1 (Bis-I)	Merck	203290	DMSO	20 mM
Cadmium chloride	Toxcast library	DTXSID6020226	DMSO	20 mM
N-[N-(3,5-Difluorophenacetyl)-L-alanyl]-S-phenylglycine t-butyl ester (DAPT)	Merck	D5942	DMSO	40 mM
Deltamethrin	Merck	45423	DMSO	20 mM
Epidermal growth factor (EGF)	Thermo Fisher	PHG0313	DPBS +/-	10 µg/ml
Fibroblast growth factor (FGF) basic	R&D Systems	233-FB	0.1% BSA, 1 mM DTT in DPBS +/-	10 µg/ml
Methylmercury(II) chloride	Merck	33368	H ₂ O	20 mM
Narciclasine	Cayman Chemicals	20361	DMSO	20 mM
NH-3	Nguyen et al. (2002) Singh et al. (2016)	-	DMSO	1 mM
PD153035	Merck	SML0564	DMSO	5 mM
PP2	Merck	P0042	DMSO	10 mM
Rotenone	Santa Cruz Biotechnology	203242	DMSO	100 mM
L-3,3',5 triiodothyronine (T3)	Merck	T2877	1:1 (v/v) 96% EtOH : 1 M HCl	0.3 mM
Tetrabromobisphenol A (TBBPA)	Merck	330396	DMSO	50 mM

DNT-positive chemicals with known modes of action, i.e. cadmium chloride (0.03–20 µM) and rotenone (0.01–2.22 µM), or the respective solvent (solvent control) over the whole 3 days. As an endpoint-specific positive control, confirming that the assay detects reductions in NPC proliferation, NPCs were cultivated in medium without growth factors (w/o growth factors). For the assessment of the sphere size, images of neurospheres were taken daily using an inverted microscope CKX41 (Olympus) with a ×100 magnification. Detailed descriptions of the NPC1ab and iNPC1ab assays can be found in the DNT *in vitro* testing battery report (Masjosthusmann et al., 2020) and in (Hofrichter et al., 2017), respectively. Besides proliferation, cell viability (CellTiter-Blue Assay (CTB), #G8081, Promega, Madison, United States) and cytotoxicity (CytoTox-ONE Homogeneous Membrane Integrity Assay; #G7891, Promega, Madison, United States) were assessed simultaneously.

Flow cytometry analyses were performed to confirm the cell type-specific marker expression in proliferating hNPC and hiNPC neurospheres. Neurospheres (hNPCs in passage 4, hiNPCs in passage 5) were singularized with accutase (Stemcell Technologies, Canada) for 20 min at 37°C on an orbital shaker (800 rpm) and stained with viability stain 510 (#564406, BD Bioscience, Germany), anti-Nestin-Alexa647 antibody (#560341, BD Bioscience, Germany) and anti-Sox2-PerCP-Cy5.5 antibody (#561506, BD Bioscience, Germany). The antibodies were all diluted 1:20 in BD Pharmingen stain buffer (BD Bioscience, Germany) except for the viability stain (1:1000 in DPBS -/-, #14190144, Thermo Fisher, United States). Samples were analyzed using a BD FACSCanto II (BD Bioscience, Germany) and FlowJo software (10.8.0). Debris, doublets, and dead cells were discarded during the gating process. 20000 cells were analyzed per sample.

2.3.2 hNPC Differentiation and Immunocytochemical Staining (NPC2-5)

For the initiation of cell differentiation into neurons, oligodendrocytes, and astrocytes (Moors et al., 2009; Breier et al., 2010), 0.3 mm hNPC neurospheres were transferred into 96-well plates coated with 0.1 mg/ml poly-D-lysine (#P0899-50MG, Merck, United States) and 12.5 µg/ml laminin (#L2020-1MG, Merck, United States). The following differentiation medium was prepared and used for neurosphere cultivation: DMEM (#31966-021, Thermo Fisher, United States) and Ham's F12 (#31765-027, Thermo Fisher, United States) in a 2:1 ratio (v:v) supplemented with 1% N2 (#17502-048, Thermo Fisher, United States) and 100U/mL penicillin and 100 µg/ml streptomycin (#P06-07100, Pan-Biotech, Germany). After 5 days of differentiation, migrated cells were fixed with 4% paraformaldehyde for 30 min at 37°C and stained with antibodies against β(III)tubulin (neurons) and O4 (oligodendrocytes) as previously described in detail by (Klose et al., 2021b; 2021a). In brief, unspecific binding sites on the fixated cells were blocked with 10% goat serum (GS, #G9023-10ml, Merck, United States) in PBS for 30 min at 37°C. Primary antibodies against β(III)tubulin (1:400, rabbit anti-β(III)tubulin monoclonal antibody [EP1569Y]-Alexa Fluor® 647, #ab190575, Abcam, United Kingdom) and O4 (1:400, mouse anti-O4 IgM, #MAB1326, R&D systems, United States) were incubated overnight in PBS containing 0.01% Triton-X and 2% GS at 4°C. After three washing steps with PBS, the cells were incubated with the secondary antibody for the O4-staining (1:400, goat anti-mouse IgM-Alexa Fluor® 488, #A-21042, Thermo Fisher, United States) and Hoechst33258 (1:100, #94403-1ML, Merck, United States) in PBS containing 2% GS for 60 min at 37°C. For the staining of radial glia, fixated cells were blocked with 10% GS in PBS for 30 min at 37°C and stained with antibodies against nestin (1:200, Alexa Fluor® 647 mouse anti-nestin,

#560393, BD Biosciences, United States), Ki67 (1:500, Ki67 (8D5) mouse mAb, #9449, Cell Signaling Technologies, United States) or GFAP (1:200, anti-GFAP mouse (GA5) antibody, #G9269, Merck, United States) overnight in PBS containing 0.01% Triton-X and 2% GS at 4°C. After three washing steps with PBS, the cells were incubated with the secondary antibodies for Ki67 (1:400, goat anti-mouse IgG 488, #A-11001, Thermo Fisher, United States) and GFAP (1:400, goat anti-rabbit IgG 488, #A-11008, Thermo Fisher, United States) and Hoechst33258 (1:100, #94403-1ML, Merck, United States) in PBS containing 2% GS for 60 min at 37°C. All pictures of immunocytochemical stainings were acquired with the High Content Analysis (HCA) platform Cellomics ArrayScan using a 200-fold magnification, a resolution of 552×552 pixel and the provided HCS Studio Cellomics software (version 6.6.0; Thermo Fisher Scientific).

2.3.3 hiNPC Differentiation and Migration (hiNPC2a+3)

Differentiation of hiNPCs was performed as described above for primary hNPCs, with the exception that hiNPCs were cultivated in CINDA medium containing DMEM (#31966-021, Thermo Fisher, United States) and Ham's F12 (#31765-027, Thermo Fisher, United States) in a 2:1 ratio (v:v) supplemented with 1% N2 (#17502-048, Thermo Fisher, United States), 2% B27 (#17504044, Thermo Fisher, United States), 100 U/ml penicillin and 100 µg/ml streptomycin (#P06-07100, Pan-Biotech, Germany), 5 mM creatine monohydrate (#C3630, Merck, United States), 100 U/ml Interferon-γ (#300-02, PeproTech, Germany), 20 ng/ml neurotrophin-3 (#450-03, PeproTech, Germany), 300 µM dibutyryl-cAMP (#D0260, Merck, United States) and 20 µM ascorbic acid (#A5960, Merck, United States). The neural induction of human induced pluripotent stem cells (hiPSCs) into human induced neural progenitor cells (hiNPCs) is described in detail in Bartmann et al. (2021) and Nimtz et al. (2020). After 3 days of differentiation, cells were fixed with 4% paraformaldehyde for 30 min at 37°C, washed four times with PBS, and stained with S100β antibody (1:500, rabbit anti-S100 beta antibody [EP1576Y], #ab52642, Abcam, United Kingdom) in 0.05% PBS-T with 3% GS overnight at 4°C, followed by five PBS washing steps, before incubation with the secondary antibody (1:500, goat anti-rabbit IgG 488, #A-11008, Thermo Fisher, United States) in PBS with 2% GS and 1% Hoechst 33258 (1:100, #94403-1ML, Merck, United States) for 60 min at room temperature. After 5 washing steps with PBS, cells were stained with the conjugated β(III)tubulin antibody (1:400, rabbit anti-β(III)tubulin monoclonal antibody [EP1569Y]-Alexa Fluor® 647, #ab190575, Abcam, United Kingdom) in PBS with 2% GS. After 5 washing steps with PBS, images of immunocytochemical stainings were acquired as described for primary hNPCs.

For the scientific validation of the hiNPC migration assay, hiNPCs were exposed to either EGF (0.5–1 ng/ml) alone or in combination with the EGFR-inhibitor PD153035 (1–2 µM), the SRC-kinase inhibitor PP2 (10 µM), narciclasine (0.0001–0.1 µM) or the respective solvent (solvent control). The migration distance was assessed after 24, 48 or 72 h as described for hNPC migration below.

2.3.4 hNPC Migration (NPC2)

Upon plating of hNPC neurospheres on PDL-laminin matrices, NPCs radially migrate out of the sphere core, thereby adapting a radial glia-like morphology and forming a circular migration area. The migration distance of radial glia cells (RG, NPC2a) is assessed manually after 72 h using bright-field microscopy and automated after 120 h by analyzing the ICC stainings with the software Omnisphero as previously described by Schmuck et al. (2017). In brief, RG migration is assessed manually on bright-field pictures, taken with the Cellomics ArrayScan using a 50-fold magnification, by measuring the radial distance of the furthest migrated cells to the sphere core as number of pixels following conversion into µm using Fiji Image J software (Schneider et al., 2012). After 120 h, RG migration is evaluated automatically by defining the area of Hoechst33258-stained nuclei as the migration area of this particular sphere using the Omnisphero software. Additionally, the migratory capacity of neurons (NPC2b) and oligodendrocytes (NPC2c), defined as the mean distance of all neurons/oligodendrocytes within the migration area divided by the RG migration distance, is automatically assessed after 120 h. The validation of the NPC2b and NPC2c assay is not included in this manuscript.

For the scientific validation of the NPC2a assay, hNPCs were exposed to human-relevant pathway modulators as well as known DNT-positives during the 5 days of differentiation. Neurospheres were differentiated in presence of 1) epidermal growth factor (EGF, 0.5–1 ng/ml) alone or in combination with the EGF receptor-inhibitor PD153035 (1–2 µM), 2) the Src-kinase inhibitor PP2 (10 µM), 3) increasing concentrations of methylmercury (MeHg, 0.003–2.22 µM) or 4) the respective solvent (solvent control). Besides RG migration analysis, cytotoxicity was assessed.

2.3.5 Neuronal and Oligodendrocyte Differentiation and Neuronal Morphology (NPC3-5)

Multiplexed with the assessment of RG migration after 120 h (NPC2a), further endpoints can be assessed in an automated way using different software tools. The endpoints NPC3-5 model neuronal differentiation (NPC3) and morphology (NPC4), as well as oligodendrocyte differentiation (NPC5) after 120 h of differentiation.

After staining of the differentiated cells with the above-mentioned antibodies and subsequent image acquisition with the Cellomics ArrayScan (see section “hNPC Differentiation and Immunocytochemical staining”), a series of separate images were edited together to create one image per well, including all three channels (nuclei (Hoechst33258), neurons (Alexa647[®]), oligodendrocytes (Alexa488[®])). For this step, the high-content analysis (HCA) tool Omnisphero was used (Schmuck et al., 2017). Based on the cells with Hoechst-positive nuclei migrating out of the sphere core and the formed circular migration area, RG migration was calculated for each sphere after 120 h. Neuronal (NPC3) and oligodendrocyte (NPC5) differentiation is defined by the number of cells stained for β(III)tubulin and O4, respectively, as a percentage of the total nuclei count within the migration area. The stained neurons and oligodendrocytes are identified using two convolutional neural

networks (CNN) based on the Keras architecture implemented in Python 3, which were trained by historical handpicked data (Förster et al., 2021). The number of nuclei was determined using the SpotDetector (V4.1) bio-application of the HCS Studio Cellomics software (version 6.6.0, Thermo Fisher Scientific). All neurons identified by the CNN were additionally analyzed regarding their morphology by assessing their neurite length and area (NPC4).

For the scientific validation of the NPC3 assay, neurospheres were differentiated in presence of DAPT (0.01 μM –10 μM), narciclasine (0.00014 μM –0.1 μM), or the respective solvent (solvent control). For the scientific validation of the NPC4 assay, neurospheres were differentiated in presence of narciclasine (0.00014 μM –0.1 μM), bisindolylmaleimide 1 (0.027–20 μM) or the respective solvent (solvent control). For the scientific validation of the NPC5 assay, neurospheres were differentiated in presence of DAPT (0.01 μM –10 μM), 100 μM ascorbic acid, deltamethrin (0.027–20 μM), tetrabromobisphenol A (0.027–20 μM) or the respective solvent (solvent control).

2.3.6 Oligodendrocyte Maturation Assay (NPC6)

The methodology is described in detail in (Dach et al., 2017; Klose et al., 2021b). In brief, hNPCs were plated on 8-chamber slides (five spheres per chamber) and 24-well plates (10 spheres per well) in differentiation medium containing either solvent or 3 nM triiodothyronine (T3) and incubated for 5 days on PDL-laminin matrices. To test for thyroid hormone disruption, hNPCs were additionally differentiated in presence of T3 with or without increasing concentrations of the thyroid hormone receptor antagonist NH-3 (4–400 nM) or the flame retardant TBBPA (0.01–1 μM). After 5 days, immunocytochemical stainings for oligodendrocytes (O4) and cell nuclei (Hoechst33258) were performed in the 8-chamber slides as described above. Imaging of stained 8-chamber slides was performed using the Cellomics ArrayScan VTI instrument (Thermo Fisher Scientific) and the software Omnisphero (Schmuck et al., 2017). For two defined areas (1098 mm x 823 mm size) within the migration area, the oligodendrocyte number was calculated and expressed as a percentage of the total number of nuclei. Oligodendrocyte percentages were averaged per sphere and the mean and standard deviation were calculated for the five spheres per chamber.

From the spheres plated within the 24-well plate, total RNA was extracted and 150 ng were transcribed into cDNA using the RNeasy Mini Kit (#74106, Qiagen, Germany) and the Quantitect Reverse Transcription Kit (#205313, Qiagen, Germany) according to the manufacturer's instructions. Quantitative real-time polymerase chain reactions (qRT-PCR) were performed with the QuantiFast SYBR Green PCR Kit (#204054, Qiagen, Germany) and the Rotor-Gene Q Cycler (Qiagen, Germany) using primers for ACTB (fw: CAGGAAGTCCCTTGCCATCC, rev: ACCAAAAGCCTTCATACATCTCA), MBP (fw: CAGAGC GTCCGACTATAAATCG, rev: GGTGGGTTTTTCAGCGTCT A). Gene expression was quantified with the copy number method and MBP expression was normalized to 10.000 ACTB copy numbers (Dach et al., 2017; Klose et al., 2021b).

The maturation quotient (Q_M) is then calculated as MBP copy numbers divided by the percentage of oligodendrocytes within the

hNPC differentiated culture. Therefore, an increase in the Q_M represents an increase in oligodendrocyte maturation.

2.3.7 Mitochondrial Activity and Cytotoxicity Assays

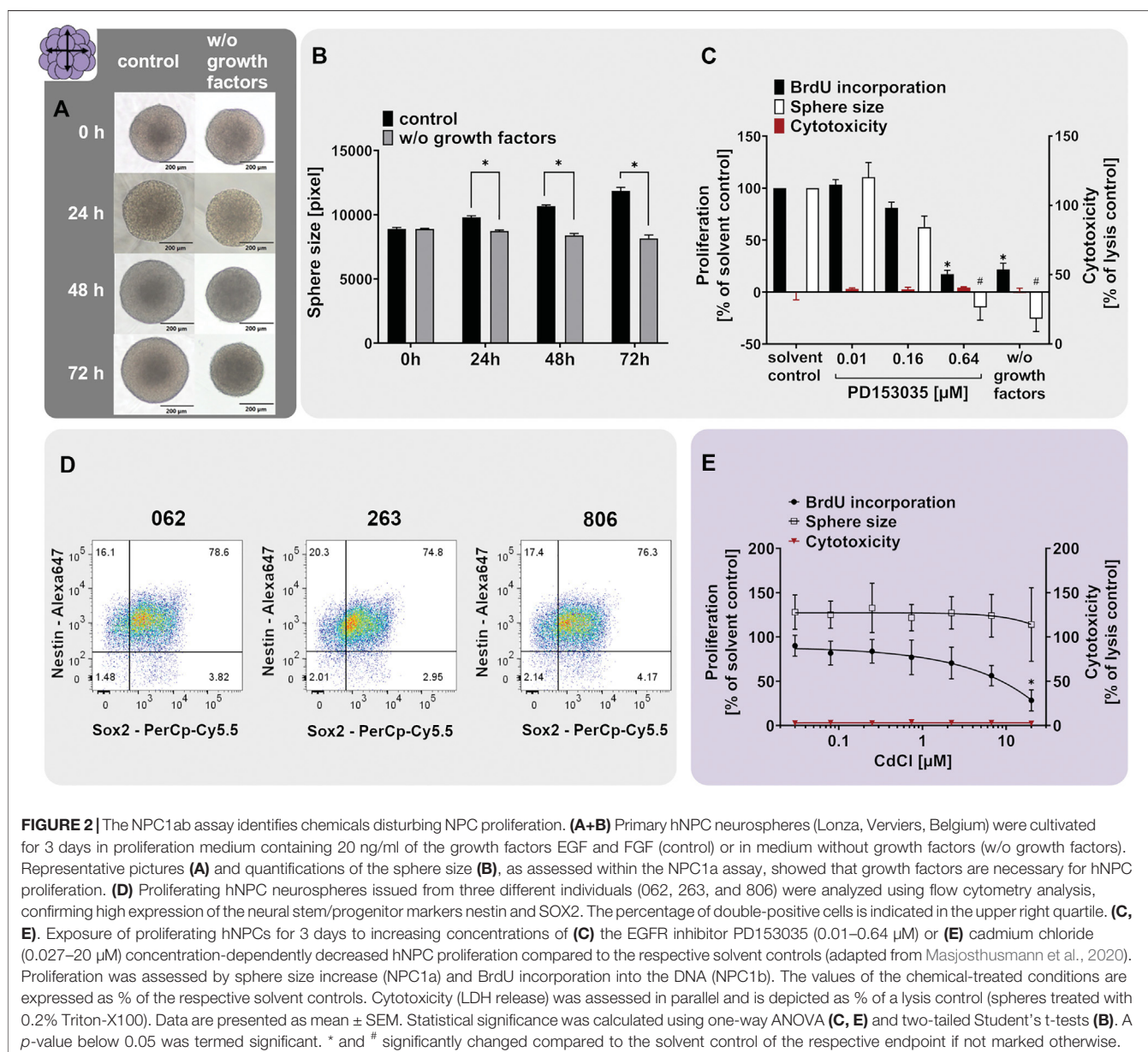
Mitochondrial activity and cytotoxicity were assessed in parallel to the specific endpoints of the Neurosphere Assay to discriminate specific compound effects from unspecific effects originating from necrosis or reduced cell viability. After the respective days of chemical exposure, mitochondrial activity was assessed using the Alamar blue assay (CellTiter-Blue Assay (CTB), #G8081, Promega, United States). In parallel, cytotoxicity was determined by measuring the release of lactate dehydrogenase (LDH) from cells with damaged membranes (CytoTox-ONE Homogeneous Membrane Integrity Assay; #G7891, Promega, United States). As lysis control for the LDH assay, neurospheres were incubated for 45 min with 0.2% Triton X-100. Fluorescence was measured with a Tecan infinite M200 Pro reader (ex: 540 nm; em: 590 nm). The relative fluorescence unit (RFU) values of the replicates were averaged and medium without cells was used to correct for background fluorescence. Of note, impaired radial glia migration and reduced nuclei count correlate with a reduced CTB value as a consequence of the diminished cell number within the migration area (Fritsche et al., 2018a; Klose et al., 2021a). Therefore, in the case of a compound inhibiting radial glia migration or reducing the nuclei count, the CTB assay is an inadequate measure of viability and thus the LDH assay alone should be used as the reference to identify DNT-specific effects (Klose et al., 2021a). In the figures, except for **Figures 5F+G** and **Figure 7F**, only cytotoxicity is displayed.

2.3.8 Statistics

For all hNPC experiments, at least two different individuals (hNPC donors) were used and for all hNPC and hiNPC experiments, at least three independent biological replicates with at least three technical replicates each were performed. Experiments were defined as independent if they were generated with hNPCs from different individuals or a different passage number. Results are presented as mean \pm SEM unless otherwise indicated. For calculating dose-response curves, a sigmoidal curve fit was applied using GraphPadPrism software. Statistical significance was calculated using one-way ANOVA with Bonferroni's post hoc tests or two-tailed Student's t-tests ($p \leq 0.05$ was termed significant).

3 RESULTS AND DISCUSSION

In the next paragraphs, we will guide through the endpoints of the Neurosphere Assays, starting with the human NPC assays that are based on primary human fetal NPCs. Succeeding, we present endpoints of a novel iNeurosphere Assay, which is based on human induced pluripotent stem cells. During method development, we proceeded according to the Guidance Document on Good *In Vitro* Method Practices (GIVIMP) principles, to ensure predictivity and reproducibility of the test methods (OECD, 2018; Pamies et al., 2022). The description of each



Neurosphere Assay endpoint follows the same rationale. First, the relevance of the respective endpoint for brain development is described. Second, *in vitro* morphologies and expressions of respective markers corresponding to the individual cell types and test methods are shown. Third, endpoint responses to a selection of physiologically pertinent signaling stimuli during neurodevelopmental processes are demonstrated. These data underscore the biological relevance of the individual endpoints. Fourth, examples of adverse effects of DNT compounds on neurosphere endpoints are displayed. These data are important building blocks for scientific validation of DNT test methods since they contribute to the scientific basis and applicability domains of the studied neurodevelopmental processes and hence increase confidence in their usage.

3.1 NPC Proliferation (NPC1)

Proliferation is one of the essential neurodevelopmental processes during brain development and comprises the increase in cell number through cell growth and division (Homem et al., 2015). Disturbances in both directions (decrease and increase of proliferation) may result in neurodevelopmental disorders such as microcephaly or megalencephaly, respectively. Microcephaly is manifested by a severe reduction in brain size and was linked to prenatal exposure of human fetuses to the Zika virus (Devakumar et al., 2018). Megalencephaly, on the other hand, is defined as increased growth of cerebral structures during development and is associated with metabolic disorders such as L-2-hydroxyglutaric aciduria (Pavone et al., 2017). Both microcephaly and megalencephaly may result in severe neurological disabilities such as global

developmental delay, seizures, deficits in language development and social interactions (Guerrini and Dobyns, 2014).

Neurospheres are valuable 3D test systems to study NPC proliferation since they are highly proliferative in suspension culture in the presence of growth factors (Reynolds et al., 1992). For our specific neurosphere test system (Lonza, Verviers, Belgium), expression of the cell type-specific CNS neural stem and progenitor cell markers nestin and SRY-box 2 (SOX2) in proliferating hNPCs was confirmed (**Figure 2D**). Nestin is an intermediate filament protein type IV (Lendahl et al., 1990) used as a molecular marker for neuroepithelial stem cells and CNS progenitors. When human multipotent CNS progenitors differentiate into neurons and glial cells, nestin expression is rapidly downregulated *in vivo* (Dahlstrand et al., 1995) confirming its usefulness as a neural progenitor cell marker. SOX proteins comprise a group of transcription factors conserved throughout evolution. SOX2 is a marker for proliferating CNS progenitors and its overexpression inhibits neuronal differentiation (Pevny and Placzek, 2005). The primary hNPCs used in this study were double-positive for nestin and SOX2 as shown in **Figure 2D**. In total, 76.6, 74.8, and 76.3% of cells issued from the three different individuals, respectively, were double-positive for the two markers, and only 1.48, 2.01, and 2.14% of cells expressed none of them, hence confirming their resemblance to neural progenitors *in vivo*. The expression of nestin and SOX2 was assessed in primary hNPCs previously (Hofrichter et al., 2017). Although the percentage of cells expressing neither of the two markers was comparable in these two studies, the average percentage of double-positive cells was lower in the present study (75.9% in the present study versus 96.3% (Hofrichter et al., 2017)). This might be explained by a higher passage number (4) of hNPCs used in this study (i.e. the highest passage usually used within the Neurosphere Assay) in comparison with passage 0 used in the study of (Hofrichter et al., 2017). In addition to their expected marker expression, hNPCs exert the expected morphology (**Figure 2A**). Neurospheres of a few hundred μm in diameter consist of individual cells (e.g. one neurosphere with 300 μm in diameter contains 2.6×10^3 cells; (Moors et al., 2009)) and display a perfectly round shape with no disintegrated borders.

The proliferative capacity of hNPCs was assessed by cultivating them in either medium supplemented with (control) or deprived of (w/o growth factors) the human growth factors EGF and FGF basic (20 ng/ml each). Human NPCs cultivated for 3 days in control medium increased their size on average by 33%, whereas hNPCs cultivated in growth factor-deprived medium (w/o growth factors) did not proliferate and even slightly shrunk in size by 8.2% (**Figures 2A,B**). Direct measurements of proliferation by BrdU incorporation indicated a 78.1% decrease in BrdU incorporation in spheres growing in the absence (w/o growth factors) compared to the presence (solvent control) of growth factors (**Figure 2C**). The proliferative capacity of Lonza hNPCs was reported previously (Moors et al., 2009; Baumann et al., 2015; Klose et al., 2021a).

The neurodevelopmental process of proliferation is guided by various signaling pathways including the epidermal growth factor receptor (EGFR) signaling (Ayuso-Sacido et al., 2010).

To elucidate if EGFR mediates this proliferative cell response in hNPC, we assessed hNPC proliferation in presence of the EGFR inhibitor quinazoline PD153035. PD153035 antagonized the EGF-induced hNPC proliferation, as assessed via BrdU incorporation and sphere size increase, without inducing cytotoxicity. This confirms that EGFR signaling regulates hNPC proliferation *in vitro* (**Figure 2C**). EGFR signaling generally regulates cell proliferation, growth, differentiation and cell survival (Oda et al., 2005). In the developing brain, the EGFR is increasingly expressed over time (Romano and Bucci, 2020) and is mainly found in proliferating and migratory brain regions (Kornblum et al., 1997; Caric et al., 2001). The EGFR is therefore indispensable for proper rodent brain development (Romano and Bucci, 2020). Specifically, the proliferation of murine neural stem cells and nestin⁺ progenitor cells was previously increased by EGFR signaling *in vitro* (Sun et al., 2005; Ayuso-Sacido et al., 2010). *In vivo*, EGF induced proliferation of stem cells and progenitors in the murine fourth ventricle and central canal of the spinal cord (Martens et al., 2002) and ependymal precursor cells of the adult rat spinal cord (Kojima and Tator, 2000). Moreover, PD153035 reportedly suppressed proliferation of murine neural stem cells *in vitro* (Tropepe et al., 1999). These data—especially from the *in vivo* studies—support the importance of the EGFR pathway for NPC proliferation.

As a chemical exerting adverse effects on hNPC proliferation, we selected cadmium chloride. Prenatal exposure to cadmium chloride is associated with a lower child intelligence score (Kippler et al., 2012b), memory deficits, and learning disabilities in children (Tian et al., 2009). In rodents, cadmium causes behavioral and neurotoxicological changes (Dési et al., 1998). Hence, it is listed amongst the compounds triggering DNT (Mundy et al., 2015; Aschner et al., 2017). Cadmium is acting via the induction of oxidative stress, thus causing cell death and affecting mTOR, Erk1/2, and JNK signaling pathway activity (Kippler et al., 2012a; Leal et al., 2012). In mouse neural stem/progenitor cells, cadmium remarkably influenced the expression of genes related to cell growth, proliferation, cell cycle, and survival (Deng et al., 2020). In the present study, concentration-dependent inhibition of hNPC proliferation was observed following exposure to cadmium chloride compared to the solvent control without any observed cytotoxicity (**Figure 2E** adapted from Masjosthusmann et al. (2020)). Of note, the effects on NPC1b (BrdU incorporation) were much more pronounced compared to NPC1a (sphere size), highlighting that NPC1b is the more sensitive endpoint since differences in DNA replication by far precede the microscopic changes. The hNPC proliferation assay previously identified numerous compounds eliciting adverse effects on the proliferation process e.g. MeHgCl, arsenic, methylazoxy methanol acetate, NaAsO₂ (Baumann et al., 2016), the flame retardants EHDPHP and TCP (Klose et al., 2021a) and a variety of compounds in a large screening study (Masjosthusmann et al., 2020). These studies support the usefulness of the 3D hNPC test system for assessing the effects of compounds on NPC proliferation.

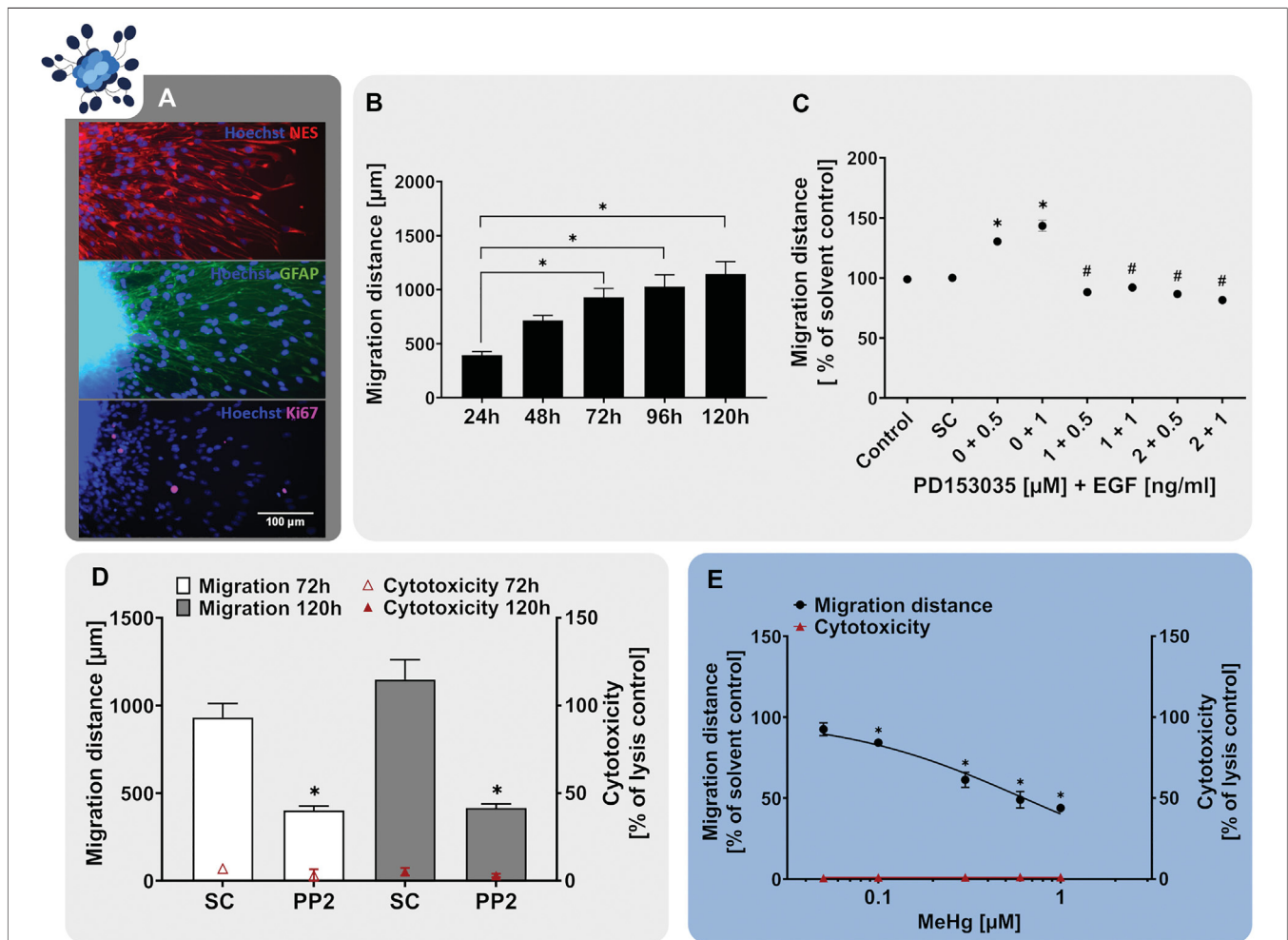


FIGURE 3 | The NPC2a assay identifies chemicals disturbing radial glia migration. Primary hNPCs were differentiated on PDL-laminin-coated 96-well plates in the absence of growth factors. **(A)** After 24 h, immunocytochemical stainings for nestin, GFAP and Ki-67 were performed confirming radial glia-typic marker expression and morphology. Nuclei were counterstained with Hoechst33258. **(B)** Over the 5 days of differentiation, cells radially migrate out of the sphere core and form a circular migration area. The migration distance of hNPCs increased gradually over time, as assessed by determining the distance from the sphere core to the furthest migrated cells at four opposite positions in brightfield images every 24 h **(C)** hNPC migration over 5 days was assessed in presence of EGF (0.5–1 ng/ml) alone, in combination with the EGFR inhibitor PD153035 (1–2 μM), or the respective solvent. While EGF increased hNPC migration compared to the solvent control, PD153035 inhibited the EGF-induced effect. **(D)** A negative effect of the SRC-family kinase inhibitor PP2 on hNPC migration was confirmed by differentiating hNPCs for 3 and 5 days in presence of 10 μM PP2 or the respective solvent (SC). **(E)** hNPCs differentiation in presence of increasing concentrations of methyl-mercury (MeHg, 0.005–1 μM) for 3 days concentration-dependently reduced the migration distance (adapted from Fritsche et al., 2018a). For **(D,E)**, cytotoxicity (LDH release) was assessed in parallel and is depicted as % of a lysis control (differentiated hNPCs treated with 0.2% Triton-X100). Data are presented as mean ± SEM. Statistical significance was calculated using one-way ANOVA **(B, E)** and two-tailed Student's t-tests **(C, D)**. A *p*-value below 0.05 was termed significant. *significantly changed compared to the respective solvent control. #significantly changed compared to the respective EGF concentration.

3.2 Radial Glia Migration (NPC2a)

Fetal cortex development is characterized by different migratory processes mainly involving radial glia cells (RG) and neurons (Borrell and Götz, 2014; Falk and Götz, 2017). Human RG exhibit two distinct functions, which are prerequisites for cortex development, especially the higher organization of the human brain: 1) due to their self-renewing capacity, RG increase the cortical cell pool before terminally differentiating into neurons and glial cells. This leads to cortical expansion, increases neurogenesis and causes the characteristic folded cerebral cortex architecture in gyrencephalic species like humans. 2)

due to their migratory capacity, RG form scaffolds for migrating neurons and hence represent the pillars of cortex formation (Borrell and Götz, 2014; Falk and Götz, 2017). As a consequence of disturbance of RG function during human brain development, neurodevelopmental disorders such as heterotopia and lissencephaly can develop (Barkovich et al., 2005; Matsumoto et al., 2017; Ferent et al., 2020).

Neurospheres are well-suited cell systems for studying neural cell migration since without any additional cues the cells start wandering out of the spheres once they are plated on a suitable matrix (Zhou and Chiang, 1998; Kukekov et al., 1999). In our

human neurosphere test system, we established a RG migration test method (NPC2a assay) that specifically measures the migration distance travelled by RG cells (Moors et al., 2007, 2009; Baumann et al., 2015). In our studies, plating of hNPC neurospheres on poly-D-lysine/laminin-coated matrices initiates cell migration in radial trajectories, forming a circular migration area around the sphere core. After 24 h, the migrated cells exhibit the characteristic elongated RG-like morphology and express the RG-markers nestin and GFAP as well as the proliferation marker Ki-67 (**Figure 3A**). *In vivo*, RG are highly polarized and have a particular elongated morphology since they form processes extending from the apical to the basal side of the cortex (Ferent et al., 2020). In accordance with that, the nestin- and GFAP-positive cells migrating out of the hNPC sphere core display an active growth cone protrusion which diverges from the cell body to explore the vicinal environment (**Figure 3A**; Baumann et al. (2015)). The migratory potential of the hNPC-derived RG is preserved *in vitro* over the time-course of at least 120 h (**Figure 3B**). However, a decrease in migration speed can be observed after the first 24 h. Since the specific RG architecture provides a scaffold supporting neuronal migration during cortex development, the correct formation and maintenance of the RG scaffold is crucial for the organization of neuronal networks and disturbances correlate with cortical malformations such as human lissencephaly, polymicrogyria and heterotopia (Ferent et al., 2020). Therefore, RG migration (NPC2) is a fundamental neurodevelopmental key event, which is indispensable in a predictive testing battery identifying chemical-induced DNT.

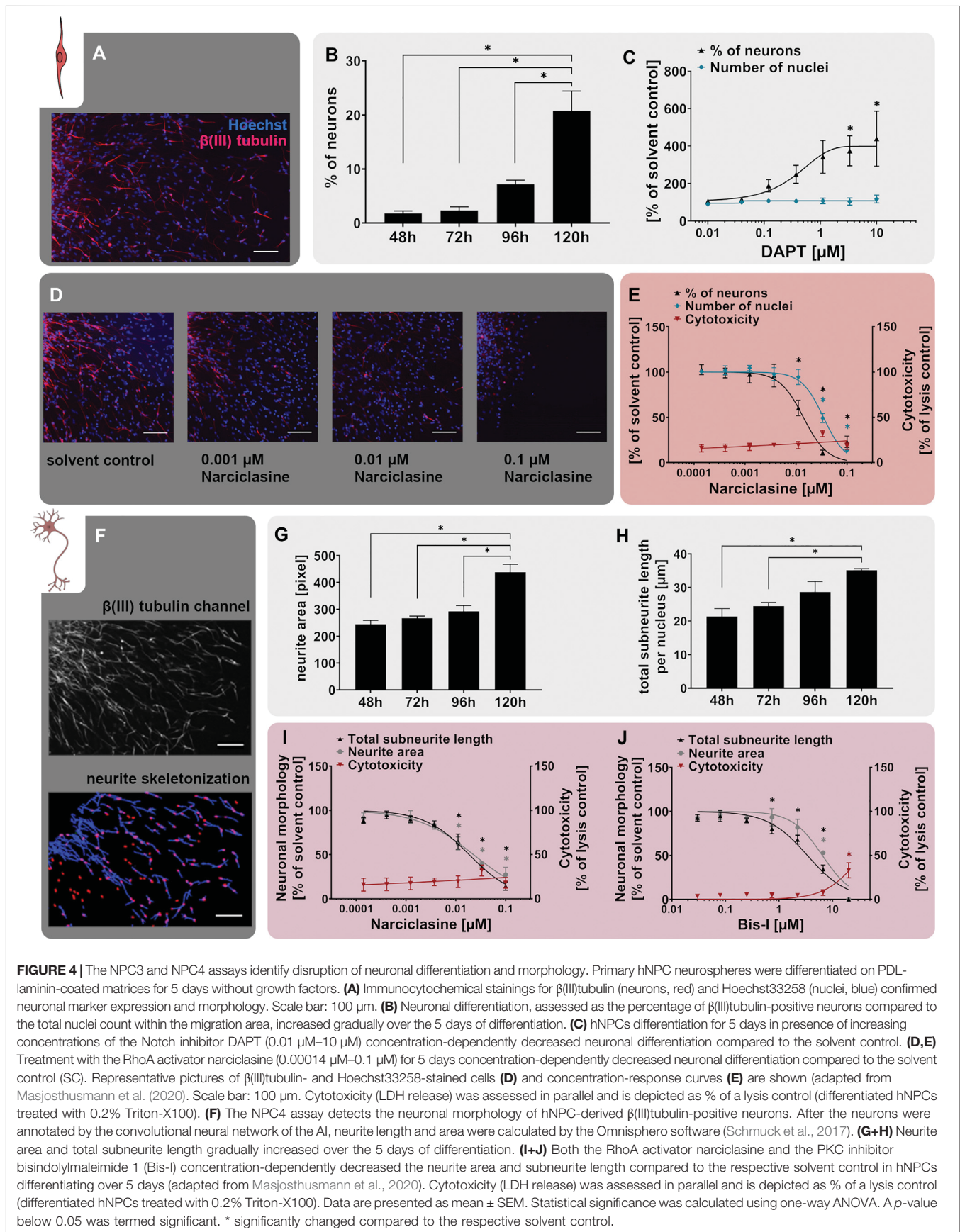
During human brain development, migratory processes are regulated by various signaling pathways, whose activity should be preserved within a predictive *in vitro* model. Similar to NPC proliferation, migration of neural stem cells is regulated by EGF, exerting its actions through the EGFR (Ayuso-Sacido et al., 2010). The EGFR is expressed not only in proliferating but also in differentiating hNPC and was identified as a human-relevant key regulator in a gene-gene interaction network involved in hNPC migration together with SRC-kinase (Masjosthusmann et al., 2018). Studies on EGFR knockout mice reported a decrease in brain size, supporting the involvement of the EGFR in migratory processes during cortical development (Kornblum et al., 1998). Moreover, intraventricular administration of EGF caused migration of subependymal NPCs from the lateral ventricle into the adjacent neural tissue in the adult mouse brain (Craig et al., 1996). Similarly, exposure to EGF (0.5–1 ng/ml) after neurosphere plating enhanced hNPC migration compared to the solvent control (**Figure 3C**). In addition, co-administration of the EGFR-inhibitor PD153035 (1–2 μ M) antagonized the EGF-induced migratory stimulating effect demonstrating EGF action on NPC migration via the EGFR. As a second human-relevant key regulator of migration, which is expressed in hNPCs (Masjosthusmann et al., 2018), we assessed the effects of SRC-family kinase inhibition on RG migration. SRC-family kinases are fundamental for brain development and disruption of their activity correlates with defects in radial migration and reeler-like malformations of cortical development (Jossin et al., 2003; Kuo, 2005; Wang et al., 2015). Exposure of migrating hNPCs to

the SRC-family kinase inhibitor PP2 reduced hNPC migration to 40% of the solvent control without causing any signs of cytotoxicity (**Figure 3D**; Moors et al., 2007). Our results indicate that human-relevant signaling pathways involved in neurodevelopmental migratory processes *in vivo* (EGFR and SRC) are preserved in the hNPC-derived cells *in vitro* supporting the applicability of the NPC2a assay to study cell migration during development.

In addition to studying signaling pathways, the NPC2a assay is also able to identify chemicals evidently disturbing migratory processes upon chemical exposure. Prenatal exposure to MeHg causes severe neurological symptoms including intellectual disabilities and cerebral palsy in children (Harada, 1978). Investigations of brain autopsy samples confirmed that exposure to MeHg perturbed cell migration and disorganized neocortical layering (Choi et al., 1978), which was verified in animal models (Kakita et al., 2002). Dysplasia and abnormal cortical cytoarchitecture have been attributed to a MeHg-mediated genetic reprogramming of signaling pathways regulating neural development. Hence disrupting the cerebral cortical organization, disturbing migratory processes and causing heterotopia (Choi et al., 1978; Rand et al., 2009; Faustman et al., 2012). One signaling pathway affected by MeHg exposure is the Notch receptor pathway, which controls cell fate decisions, proliferation, migration and neurite outgrowth during neural development (Bland and Rand, 2006). Moreover, MeHg disturbs the cytoskeletal organization involved in cell migration by disrupting the assembly and polymerization of microtubules (Choi, 1991). Exposure of differentiating hNPCs to MeHg resulted in a concentration-dependent reduction of RG migration at *in vivo* relevant concentrations (**Figure 3E** adapted from Fritsche et al. (2018a), Moors et al. (2009), Baumann et al. (2016)). No cytotoxicity was observed in the tested concentration range, indicating a specific effect of MeHg on hNPC migration. As demonstrated with MeHg, the NPC2a assay is able to detect specific alterations in cell migration and therefore allows for the detection of chemically-induced disruption of migration in the context of brain development. Besides RG migration (NPC2a) the Neurosphere Assay covers the endpoints neuronal (NPC2b) and oligodendrocyte migration (NPC2c). However, for these endpoints, the identification of signaling pathways and model substances is still ongoing, which is the reason why they are not included in this study.

3.3 Neuronal Differentiation and Morphology (NPC3+4)

During cortex development, NPCs including RG cells eventually lose their proliferative capacity and terminally differentiate into neural effector cells, i.e. neurons and glia cells (oligodendrocytes and astrocytes). Neurons then migrate alongside the scaffold of RG to their final destinations, to generate the different cortical layers (Rakic, 1972; Gilmore and Herrup, 1997). The generation of sufficient numbers of neurons is a prerequisite for the functionality of neuronal networks and associated learning and memory functions (Berdugo-Vega et al., 2020). Therefore, disturbed neurogenesis manifests in several behavioral



disorders such as depression (Song and Wang, 2011) or the intellectual disabilities of patients with Down Syndrome (Guidi et al., 2018; Stagni et al., 2018). In addition, an elevation in neurogenesis is a major driver of epileptogenesis (Jessberger and Parent, 2015). Hence, the correct balance of neurogenesis is crucial for normal brain development.

As a very simplified model, the Neurosphere Assay mimics cortex development *in vitro* since during the time-course of hNPC differentiation, neurons arise and migrate along the scaffold of RG cells (Fritsche et al., 2018b). Such young neurons are typically bipolar in shape and display neurites that show very limited branching (Figures 4A,E,F and Budday et al., 2015). Using high content imaging (HCI) and a subsequent artificial intelligence (AI; developed in collaboration with Prof. Dr. Axel Mosig (Ruhr University Bochum), Förster et al., 2021) we define neuronal identity in the mixed-culture neurosphere migration area due to immunocytochemical stainings with β (III)tubulin (Figure 4A). Over time, neurons progressively appear in the migration zone representing approximately 20% of the mixed culture after 5 days (Figure 4B), which is the time point of endpoint analysis in the NPC3 test method.

Neurogenesis during brain development is primarily regulated by the Notch signaling pathway, which is evolutionarily highly conserved and operates at many stages of human brain development (Yoon and Gaiano, 2005; Louvi and Artavanis-Tsakonas, 2006; Pierfelice et al., 2011). Stimulation of the Notch pathway could be correlated with impaired neuronal differentiation *in vivo* (Zhou W. et al., 2016; Zhang et al., 2018). In contrast, inhibited Notch signaling is known to accelerate neuronal differentiation *in vitro* and *in vivo* (Borghese et al., 2010). This can be pharmacologically excited by the Notch receptor inhibitor N-[N-(3,5-Difluorophenacetyl)-L-alanyl]-S-phenylglycine t-butyl ester (DAPT) through blockage of the presenilin- γ -secretase complex (Dovey et al., 2001). Moreover, the Notch pathway is involved in the formation of long-term memory and is thus a putative actuator of developmental disorders (Costa et al., 2005). According to our comprehensive transcriptomic analysis, differentiating hNPCs express Notch receptors 1-3 (Masjosthusmann et al., 2018). Here we show that similar to our previously published work after 72 h of differentiation (Masjosthusmann et al., 2018), DAPT increases neuronal numbers to 187% and 439% of the respective solvent control at 0.12 and 10 μ M DAPT, respectively, after 5 days of differentiation. Of note, the total cell number was not affected, indicating that the increase in neuronal numbers is at the expense of another cell type within the mixed culture (Figure 4C). The higher sensitivity of hNPC towards DAPT in this study is possibly due to the longer experimental time. Moreover, here we use different individuals compared to the previous study. These results indicate that the human-relevant Notch signaling pathway, which is one of the main drivers of neuronal differentiation *in vivo*, is also active in the hNPCs *in vitro*.

The positive effect of Notch inhibition on neuronal differentiation is thought to be - at least in part - attributed to suppression of the Rho GTPase RhoA (Peng et al., 2019).

Consistent with this notion, narciclasine, an activator of RhoA, reduced neuronal differentiation of primary hNPCs cultured for 5 days in a concentration-dependent manner, together with a less sensitive reduction of the nuclei number (Figures 4D,E adapted from Masjosthusmann et al. (2020)). Increased RhoA activity correlated with reduced neuronal differentiation of murine neural stem cells and human iPSCs (Yang et al., 2016; Bogetofte et al., 2019). In contrast, inactivated RhoA signaling was sufficient to stimulate axon regeneration and recovery of hindlimb function after spinal cord injury in mice (Dergham et al., 2002) supporting the concept of RhoA activity as an inhibitory driver of neurogenesis.

Besides the generation of adequate neuronal numbers during neurogenesis, neuronal maturation, especially neurite outgrowth, and branching are equally important for the functional maturation of the CNS. Perturbations of which are assumed to be linked to neurodevelopmental disorders like autism spectrum disorder in humans (Zikopoulos and Barbas, 2010). The NPC4 assay measuring neurite outgrowth builds upon the neuronal differentiation assay (NPC3) and evaluates the neurite morphology within the multicellular differentiated neurosphere culture. After AI-based identification of β (III)tubulin⁺ neurons, their morphological features, e.g. neurite length and neurite area, are evaluated (Figure 4F) using the Omnisphero software (Schmuck et al., 2017). During the 5 days of hNPC differentiation, neurite maturation is characterized by an elongation of neurites and an increase in neurite area (Figures 4G+H).

Consistent with the above-mentioned effect of RhoA activation on neuronal differentiation (NPC3), narciclasine also reduced both neurite area and neurite length (Figure 4I adapted from Masjosthusmann et al. (2020)) within the NPC4 assay. This is in line with previous studies, reporting that narciclasine reduced neurite outgrowth via the Rho-associated protein kinase (ROCK) pathway in neurons differentiated from LUHMES human neuronal precursor cells (Krug et al., 2013). Moreover, a contactin-1 knock-down-dependent increase in RhoA activity caused morphological alterations in rat cortical neurons *in vivo* (Chen et al., 2018). Neurite outgrowth is further regulated by protein kinase C (PKC), a serine/threonine kinase, which controls various cellular responses by phosphorylation of substrate molecules and alteration of gene transcription (Nishizuka, 1986; Newton, 1995). While PKC activation induced neurite outgrowth in rat pheochromocytoma (PC-12) cells and primary rat spinal cord neurons from embryonic day 14 (Hundle et al., 1995; Yang et al., 2010), inhibition of PKC with the PKC inhibitor bisindolylmaleimide 1 (Bis-I) reduced neurite growth in PC-12 cells (Das et al., 2004), rat cortical neurons and human iPSC-derived neurons (Druwe et al., 2016). Similar effects were identified in the NPC4 assay upon exposure of hNPCs to Bis-I, which reduced neurite length and area compared to the solvent control (Figure 4J adapted from Masjosthusmann et al. (2020)).

Neuronal differentiation and maturation are tightly regulated processes, which are controlled by a variety of different signaling pathways, whose perturbation can cause severe adverse

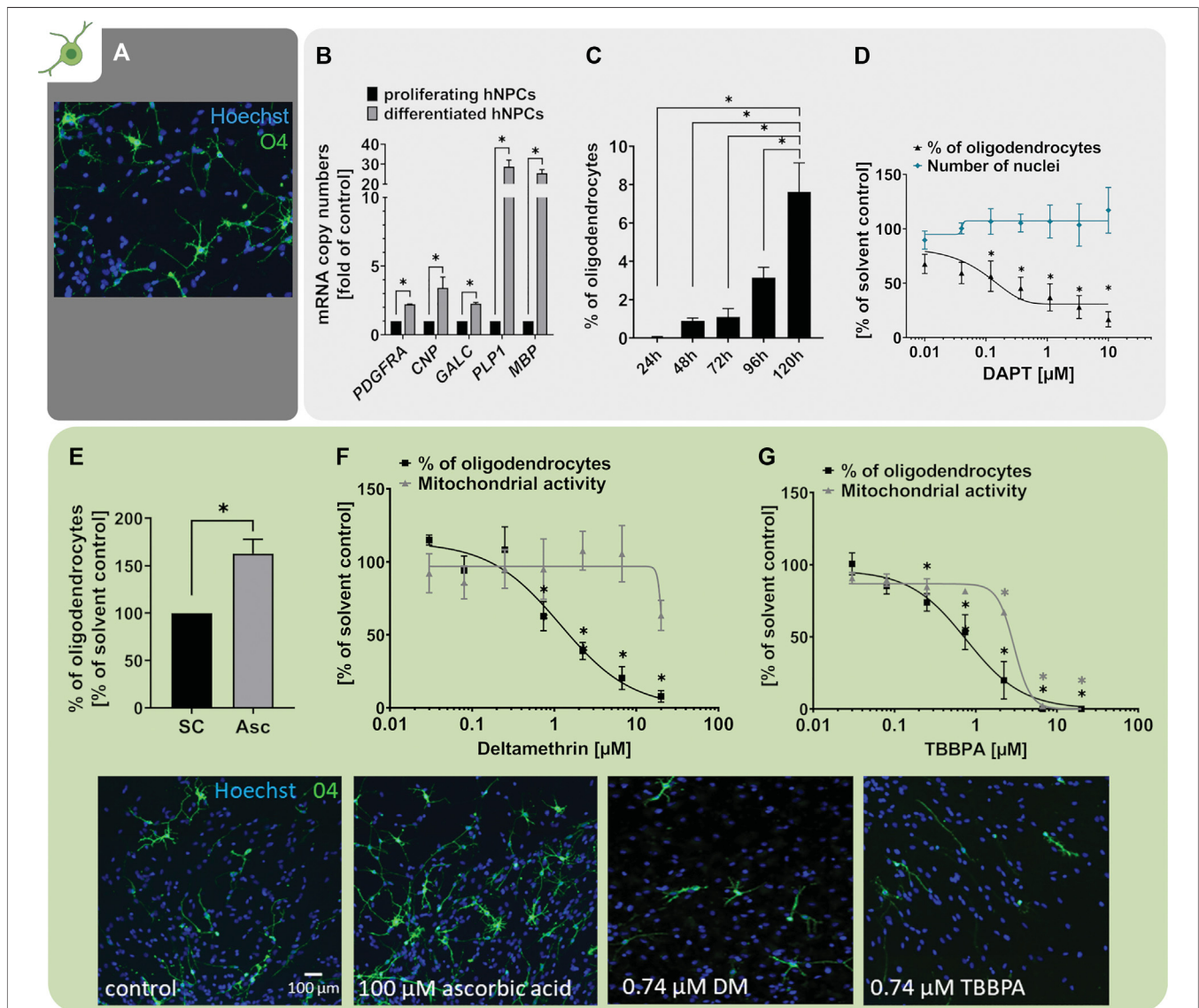


FIGURE 5 | Oligodendrocyte differentiation is assessed with the NPC5 assay. **(A)** Primary hNPCs were differentiated for 5 days in differentiation medium without growth factors on PDL-laminin-coated plates. Immunocytochemical stainings were performed to identify cells of the OL lineage (O4) and cell nuclei (Hoechst33258). **(B)** mRNA expression of OL lineage markers *PDGFRA*, *CNP*, *GALC*, *PLP1* and *MBP* was assessed in proliferating hNPCs and hNPC differentiated for 60 h using quantitative real-time PCR. Expression was calculated as copy numbers (CN) per CN of the reference gene *ACTB* multiplied by 10,000. The expression in differentiated hNPCs is displayed as fold of expression in proliferating hNPCs. Expression of all markers increased during hNPC differentiation (adapted from Klose et al. (2021a)). **(C)** Oligodendrocyte differentiation, assessed as the percentage of O4-positive OLs compared to the total nuclei count within the migration area, increased gradually over the 5 days of differentiation. **(D)** hNPCs differentiation for 5 days in presence of increasing concentrations of the Notch inhibitor DAPT (0.01 μM –10 μM) concentration-dependently decreased OL differentiation compared to the solvent control. **(E)** hNPCs differentiation in presence of 100 μM ascorbic acid (Asc) increased the percentage of OLs in the differentiated culture. **(F+G)** Both exposure to the insecticide deltamethrin (DM, 0.027–20 μM , adapted from Masjosthusmann et al., 2020) and the flame retardant tetrabromobisphenol A (TBBPA, 0.027–20 μM , adapted from Klose et al., 2021a) during the 5 days of differentiation concentration-dependently decreased OL differentiation compared to the respective solvent controls. For deltamethrin and TBBPA the mitochondrial activity was assessed in parallel and is depicted as % of solvent control. For **(E–G)**, representative pictures of O4⁺ OLs exposed to solvent control or the respective treatments are shown. Data are presented as mean \pm SEM. Statistical significance was calculated using one-way ANOVA **(C,D,F,G)** and two-tailed Student's t-tests **(B,E)**. A *p*-value below 0.05 was termed significant. *significant compared to the respective solvent control.

neurodevelopmental effects. The NPC3 (neuronal differentiation) and NPC4 (neuronal morphology) assays respond to known pathway modulators regulating neurogenesis and neurite outgrowth *in vivo* and are therefore predictive assays to identify chemicals disturbing neuronal development.

3.4 Oligodendrocyte Differentiation (NPC5)

Myelinating oligodendrocytes (OLs) are responsible for the formation of insulating myelin sheaths, thus accelerating the conduction of electrical impulses along axons and preserving axonal integrity during neurodevelopment and beyond. OLs derive from NPCs and RG cells differentiating into

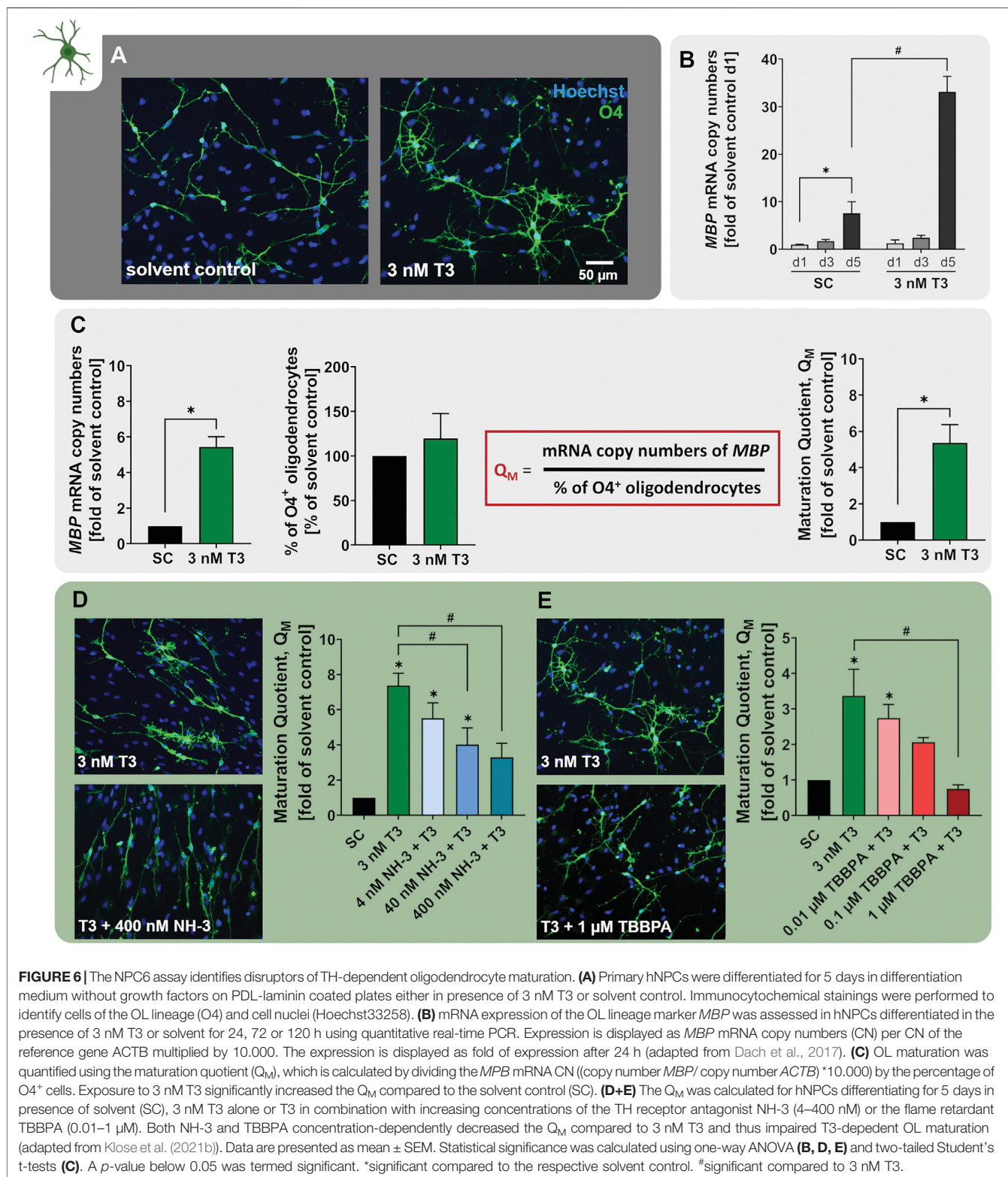
oligodendrocyte precursor cells (OPCs) and terminally into pre-myelinating OLs (pre-OLs) and myelin-producing mature OLs (Emery, 2010; van Tilborg et al., 2018). The OL-derived myelin ensheathing neuronal axons is indispensable for the development and function of the human brain (reviewed in Barateiro et al. (2016)). However, both pre-OLs and myelinating OLs are susceptible to various stressors including oxidative stress, astrogliosis, excitotoxicity and inflammation (reviewed in van Tilborg et al. (2016)) rendering them susceptible to a variety of exogenous stressors. Disturbances in oligodendrogenesis during neurodevelopment are associated with hypomyelination and white-matter deficits manifesting in clinical pathologies including the Allan-Herndon-Dudley Syndrome (Sarret et al., 2010) and periventricular leukomalacia (PVL; Back et al., 2001). Since the pool of OLs in humans remains stable after childhood, especially interference in OL development during the neurodevelopmental period is crucial (Yeung et al., 2014). The generation of pre-myelinating OLs can be modelled in hNPCs *in vitro* (NPC5). Differentiation of hNPCs over 5 days generated cells expressing the OL-marker O4, which exhibit the typical OL morphology with multiple branched processes necessary to ensheath neuronal axons (**Figure 5A**). Compared to undifferentiated hNPC neurospheres, differentiating hNPCs significantly increased mRNA expression of the OL markers *PDGFRA* (platelet-derived growth factor alpha, *PDGFRα*), *CNP* (*CNPase*), *GALC* (Galactosylceramidase), *PLP1* (proteolipid protein 1), and *MBP* (myelin basic protein) already after 60 h (**Figure 5B** adapted from Klose et al. (2021a)). While *PDGFRA* is predominantly a marker of immature OPCs, especially *MBP* is a myelin-associated gene increasingly expressed during oligodendrocyte maturation (Barateiro and Fernandes, 2014; Marinelli et al., 2016). Based on the marker expression and the highly branched morphology (**Figures 5A,B**), we conclude that our pre-OLs exhibit a certain degree of maturity. Similar to the neuronal differentiation described above, also the percentage of OLs within the multicellular hNPC-derived migration area increased over the differentiation time resulting in approximately 8% OLs after 5 days (**Figure 5C**; Moors et al., 2009).

It is well studied that several signaling pathways, including the Notch pathway, regulate NPC differentiation into OPCs (reviewed by He and Lu, 2013). A study on zebrafish embryos revealed that Notch is responsible for increased production of OPCs from ventral spinal cord precursors and that the increased OPC number is not due to increased OPC proliferation (Snyder et al., 2012). Moreover, contactin/F3-dependent Notch signaling promoted OPC differentiation from the rat oligodendroglial OLN-93 cell line and further increased the expression of myelin-associated glycoprotein (*MAG*; Hu et al., 2003). In line with that, differentiation of hNPCs in presence of the Notch inhibitor DAPT concentration-dependently decreased the percentage of O4⁺ cells compared to the solvent control, indicating that Notch signaling is a prerequisite for hNPC differentiation into the OL lineage (**Figure 5D**). In addition, OL differentiation is negatively influenced by bone morphogenic protein (BMP) 7 (Baumann et al., 2015) and BMP2 (Masjosthusmann et al., 2018), proteins of the transforming

growth factor β family. BMP 2 and 7 also negatively regulated oligodendrocyte differentiation of primary rat NPC generated from E17 and PND2 brains (Zhu et al., 1999) and reduced myelin gene expression in Schwann cells (Liu et al., 2016). These data demonstrate that two major developmental pathways, i.e. Notch and BMP, are functional in these hNPCs.

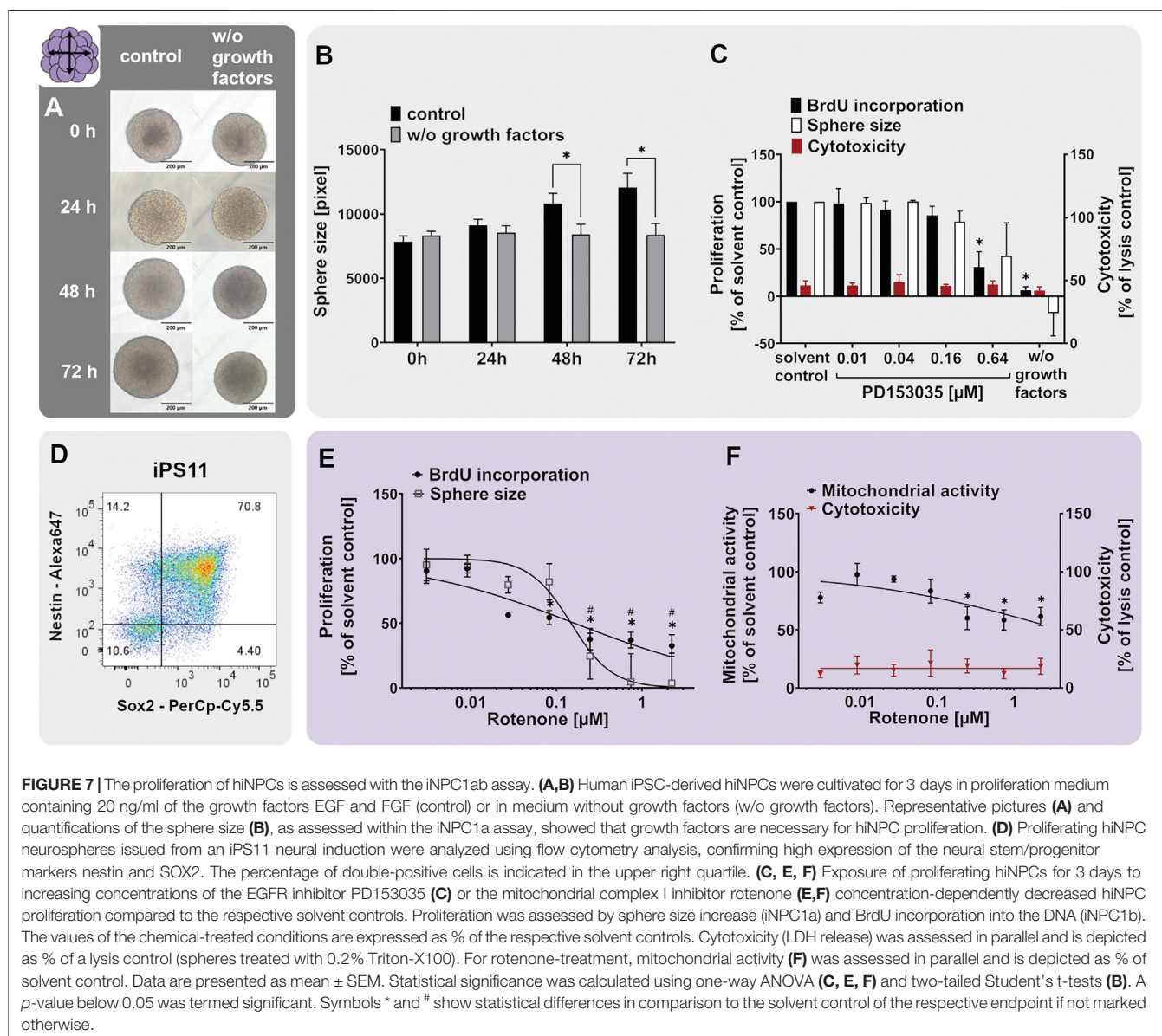
Several studies — including observations in humans — confirmed that pre-OLs are especially susceptible to oxidative stress and that pre-OL damage by reactive oxygen species (ROS) is a potential underlying factor for the emergence of the cerebral white matter injury termed periventricular leukomalacia (PVL) (reviewed in Volpe et al. (2011)). In accordance, Guo et al. (2018) reported that the ROS scavenger vitamin C (ascorbic acid, Asc, 150 μ M) enhanced the differentiation of primary mouse NPC-derived OPCs into OLs and further promoted expression of OL lineage markers O4, *CNPase* and *MBP* concentration-dependently (Guo et al., 2018). We also observed that ascorbic acid enhanced hNPC-derived OL maturation (Dach et al., 2017). However, in contrast to Guo et al. (2018), we did not observe this enhanced maturation in OLs derived from PND1 mouse neurospheres. This might be due to different developmental stages of animals as Guo et al. (2018) used cortices of E14.5 mouse embryos for NPC generation. Likewise, differentiation of hNPCs in presence of 100 μ M ascorbic acid increased the percentage of O4⁺ oligodendrocytes within the NPC5 assay by approximately 60% (**Figure 5E**). This is in contrast to our previously published data where ascorbic acid solely induced maturity but not the number of OLs (Dach et al., 2017), which might be explained by inter-individual differences of the one individual used in the Dach et al. (2017) compared to the three individuals in this study.

Due to the particular sensitivity of OPCs and pre-OLs towards multiple stressors including ROS, excitotoxic damage, thyroid hormone disruption, or inflammatory cues (Volpe et al., 2011; Barateiro et al., 2016; Chesnut et al., 2021a), it is hypothesized that they might also be highly sensitive towards a variety of chemical noxae (Chesnut et al., 2021a). Within the NPC5 assay, we here show as two examples that both the insecticide deltamethrin (DM, **Figure 5F** adapted from Masjosthusmann et al. (2020)) and the organophosphate flame retardant tetrabromobisphenol A (TBBPA, **Figure 5G** adapted from Klose et al. (2021a)) diminished the number of O4⁺ oligodendrocytes concentration-dependently. Childhood exposure to pyrethroids like DM correlates with neurodevelopmental disorders including autism, attention deficit hyperactivity disorder (ADHD) and developmental delays reviewed in Pitzer et al. (2021). Likewise, developmental and early-life exposure to DM in rodents is associated with ADHD-like and anxiety-like behavior as well as deficits in working memory and spatial learning, often depending on the developmental stage of exposure (reviewed in Pitzer et al. (2019), (2021); Richardson et al. (2015)). The primary mode-of-action (MoA) of DM for its anti-pest action in mature neurons is the prolonged opening of voltage-gated sodium channels (VGSC). OPCs express active VGSC rendering this MoA highly likely for DM action on this immature OL state (comprehensively summarized in Hernández-Jerez et al. (2021)). In addition, DM induces oxidative stress and lipid peroxidation, which most likely also



contribute to its neurotoxicity (reviewed in Pitzer et al. (2021)). The flame retardant (FR) TBBPA interferes with brain development in rodents (Hendriks et al., 2015; Rock et al., 2019) and its DNT-relevance for humans is supported by

studies reporting bioaccumulation in maternal serum, cord blood and breast milk (Cariou et al., 2008; Kim and Oh, 2014). The adverse effects of TBBPA on OL differentiation in the NPC5 assay were accompanied by deregulation of a gene

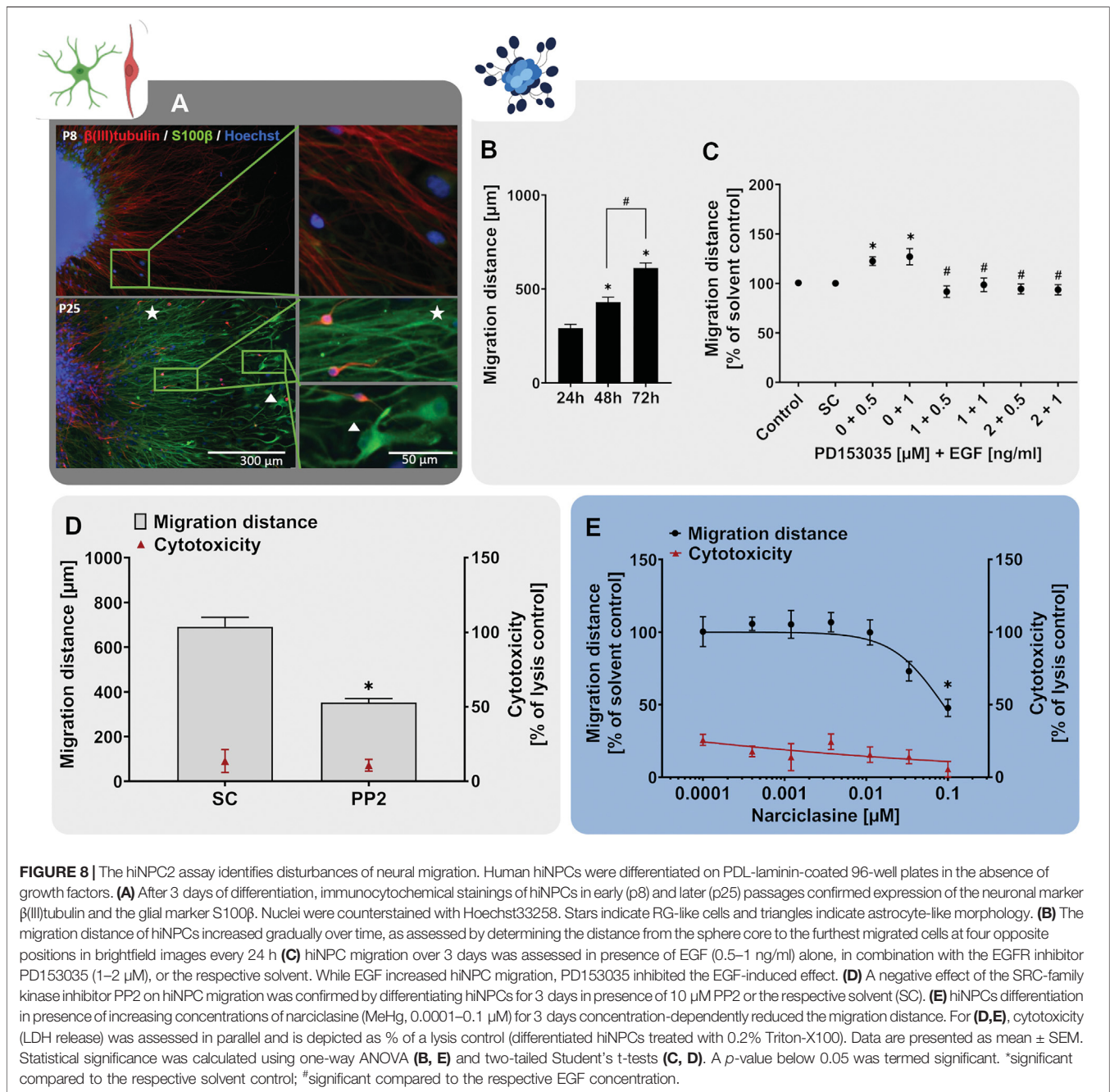


cluster involved in cholesterol metabolism suggesting lipotoxicity as TBBPA's MoA (Klose et al., 2021b). Since myelinating OLs exhibit an exceptionally high rate of cholesterol metabolism, disturbances are particularly problematic in this cell type (Haq et al., 2003; Bezine et al., 2017).

In the past, the NPC5 assay has been identifying compounds of various substance classes as disruptors of OL differentiation including brominated as well as alternative organophosphate FRs (Dach et al., 2017; Klose et al., 2021a), sodium arsenite (Masjosthusmann et al., 2019), and a variety of substances within a recent screening project where the NPC5 assay was the most frequently positive assay across the Neurosphere Assay battery (Masjosthusmann et al., 2020). In neurotoxicological studies, oligodendrocytes are an understudied, yet highly relevant cell type that just recently received more attention (Chesnut et al., 2021a).

3.5 Thyroid Hormone (TH)-dependent Oligodendrocyte Maturation (NPC6)

In order to develop into myelinating OLs, OPCs and pre-OLs have to mature and express myelin-associated genes including myelin basic protein (MBP) and myelin proteolipid protein (PLP1). This maturation processes and the proper development of white matter tracts in humans depend on thyroid hormones (TH), such as the thyroxine metabolite triiodothyronine (T₃; Annunziata et al., 1983; Baas et al., 1997; Murray and Dubois-Dalq, 1997). In line with that, *in vivo* studies on hypothyroid rats reported reduced numbers of mature OLs and impaired expression of PLP1 and MBP (Ibarrola and Rodríguez-Peña, 1997; Schoonover et al., 2004). The devastating effects of TH disruption for human neurodevelopment are illustrated by clinical pathologies describing hypomyelination as a result of TH insufficiencies, including congenital hypothyroidism, maternal hypothyroidism, or the



Allan-Herndon-Dudley syndrome (AHDS). These conditions feature clinical symptoms ranging from mild cognitive deficits to severe intellectual disabilities (Haddow et al., 1999; Rovet and Daneman, 2003; Sarret et al., 2010). ADHS is caused by inactivating mutations in the monocarboxylate transporter 8 (MCT8), a TH transporter, which is responsible for TH transport into the brain, and thus required for OL maturation (Vatine et al., 2021).

Maturation of pre-OLs can be induced *in vitro* by differentiation of hNPCs in presence of 3 nM T3 (NPC6). Exposure to T3 clearly caused the O4⁺ cells to develop a more mature morphology with

more branched processes (Figure 6A). Moreover, MBP mRNA expression increases over the time-course of differentiation already under control conditions, and even further in the presence of 3 nM T3 (Figure 6B adapted from Dach et al. (2017)). Since MBP is one of the major components of myelin, hNPC-derived pre-OLs differentiating in presence of T3 are on the path to myelinating OLs. In order to quantify the degree of OL maturation within the NPC6 assay, we calculated the maturation quotient (Q_M), which is defined as the mRNA copy numbers of MBP per percentage of O4⁺ cells within the migration area. In line with the multitude of studies reporting that TH favor OL maturation (Baas et al., 1997; Dach

et al., 2017; Klose et al., 2021b), we observed an increase of the Q_M upon exposure to 3 nM T3 (**Figure 6C**). The TH-dependent maturation of hNPC-derived OLs within the NPC6 assay further reacts to the synthetic antagonist NH-3 (Nguyen et al., 2002; Singh et al., 2016) since NH-3 concentration-dependently reduced the Q_M indicating that disruptors of TH receptor signaling can be identified with the NPC6 assay (**Figure 6D** adapted from Klose et al. (2021b), Dach et al. (2017)). A human-relevant disruptor of OL maturation identified within the NPC6 assay is TBBPA. At low concentrations, not yet affecting OL differentiation, TBBPA disturbs TH-dependent OL maturation, hence concentration-dependently reducing the Q_M in hNPCs differentiated in presence of 3 nM T3 (**Figure 6E** adapted from Klose et al. (2021b)). Impaired OL maturation is accompanied by alteration of TH-dependent genes, including *EGR1*, *IGFBP4*, *IL33* and *KLF9* (Klose et al., 2021b). These data provide the scientific basis for studying the disruption of TH-dependent oligodendrocyte maturation in differentiating hNPC. In the past, the NPC6 assay identified both BDE-99 and perfluorooctanoic acid (PFOA) not to be disruptors of human TH-dependent OL maturation, although BDE-99 reduced OL numbers (Dach et al., 2017; Klose et al., 2021b).

3.6 Human iPSC-derived hiNPC proliferation, migration and differentiation (hiNPC1+2a+3)

For 21st-century toxicity evaluation, hiPSCs have been strongly promoted as the basis for diverse test systems since they are of human origin, have unlimited availability and resemble different features of the desired target tissues very well (Wobus and Löser, 2011; Jennings, 2015; Csöbönyeiová et al., 2016; Fritsche et al., 2021). For brain tissues, one can generate hiPSC-derived neural progenitor cell (hiNPC) neurospheres, a relatively simple and easy to generate cell system (Sareen et al., 2014; Hofrichter et al., 2017; Kobolak et al., 2020). The hiNPCs have the ability to differentiate into neurons and astrocytes in secondary 3D (Sareen et al., 2014; Paşca et al., 2015; Zhou S. et al., 2016; Hofrichter et al., 2017; Nimtz et al., 2020; Soubannier et al., 2020) and 3D cultures (Pamies et al., 2017; Sloan et al., 2017; Marton et al., 2019; Chesnut et al., 2021b). For the generation of OLs, however, hiNPC differentiation time takes at least 8 weeks (Pamies et al., 2017) and is therefore not directly comparable to the primary neurospheres which produce OLs within 5 days of differentiation. Here we present data on hiNPC proliferation, migration and the differentiation potential.

When relating hiNPC (**Figure 7A**) to hNPC neurospheres (**Figure 2A**), they display the same neurosphere morphology and cannot be distinguished from each other with the bare eye. Moreover, hiNPCs express the neural stem/progenitor markers nestin and SOX2 (**Figure 7D**). The percentage of Nestin/SOX2 double-positive hiNPCs (70.8%) was in the same ballpark as that of hNPC (76.6%). Human iNPCs contained 10.6% cells not expressing any of the two markers, which is higher compared to the average of 1.9% of the three hNPC individuals (**Figure 2**). The proliferative capacity of hiNPCs was confirmed by measuring the sphere size increase over

3 days (iNPC1a) as shown in **Figure 7B**. hiNPC neurospheres increased their size by 53.6% during the 3 days in a proliferation medium containing EGF and FGF basic (control), whereas hiNPCs cultivated in proliferation media without growth factors (w/o growth factors) did not increase in size. In comparison, primary hNPC spheres only increased by approximately 30% in size over the 3 days (**Figure 2B**). EGF-dependent hiNPC proliferation is also EGFR-dependent since the EGFR inhibitor PD153035 decreased hiNPC proliferation (**Figure 7C**) similar to the primary hNPCs. These data demonstrate that the EGFR, as a crucial molecule for NPC proliferation, is also functioning in proliferating hiNPCs.

The proliferation of hiNPCs was also effectively inhibited by rotenone, an anti-proliferative compound with a known mode of action i.e. inhibition of the mitochondrial complex I of the electron transport chain (Saravanan et al., 2005). Rotenone produced oxidative stress in iPSC-derived neural stem cells (Pistollato et al., 2017) and mitochondrial dysfunction in human neural progenitor cells (Mahajan et al., 2019). In the present study, rotenone inhibited the proliferation of hiNPCs in a concentration-dependent manner with the lowest observed effect concentration of 30 nM (**Figure 7E**). In comparison, the proliferation of primary hNPCs was not affected by rotenone in the same concentration range (Masjosthusmann et al., 2020). Rotenone did not cause cytotoxicity in hiNPCs, however as expected from a mitochondrial complex I inhibitor, significantly reduced the mitochondrial activity (**Figure 7F**). Overall, the iNPC1ab assay behaves similar to the NPC1ab assay, however, hiNPCs proliferate faster.

Plating hiNPC neurospheres onto a PDL-laminin-coated matrix-initiated cell migration out of the sphere core accompanied by neuronal and astrocyte differentiation (**Figure 8A**). Importantly, the migration and neuron-glia cell differentiation patterns, as well as their respective cell morphologies highly depended on the sphere culture passage number. Early passages (P8) first and primarily differentiated into β (III)tubulin-positive neurons with elongated neurites that form dense neuronal networks followed by the appearance of S100 β -positive astrocytes. Differentiation of hiNPCs from higher passages (P25) first led to the emergence of S100 β -positive cells with RG-like morphology and subsequently of β (III)tubulin-positive neurons (**Figure 8A**). Regarding the S100 β -positive cells, one could distinguish between elongated RG-like cells (**Figure 8A**, stars) and more star-shaped astrocytes (**Figure 8A**, triangle), the first being overrepresented in differentiating hiNPCs from higher passages.

Next, we inquired whether hiNPC neurospheres can also be used for studying neural migration. Therefore, we assessed the migratory capacity of hiNPC-derived cells (passages >17). After plating on PDL-laminin-coated matrices, the hiNPC-derived cells formed a circular migration area comparable to the primary hNPCs. Moreover, as observed for the hNPCs (**Figure 3B**), the migration distance of cells emerging from hiNPCs increased over time (**Figure 8B**). After 72 h, hiNPC migration was shorter (~600–750 μ m) than hNPC migration (~950 μ m, **Figure 2**), yet reproducible and fully sufficient for analyses.

As discussed above, EGFR-dependent signaling guides radial migration *in vivo* (Craig et al., 1996; Kornblum et al., 1998). To study migratory responses to EGF in hiNPCs, we measured the migration distances of hiNPC-derived cells in presence and absence of EGF and the EGFR inhibitor PD153035. Similar to hNPCs, the migration of plated hiNPCs was increased by both 0.5 and 1 ng/ml EGF, which was antagonized by co-treatment with PD153035 at concentrations of 1 and 2 μM (Figure 8C). Yet the EGF effects on hiNPC migration were weaker than in primary hNPCs (122% compared to 130% (0.5 ng/ml EGF) and 127% compared to 143% (1 ng/ml EGF)). This might be due to the developmental timing since the density of EGFR increases processivity through brain development (Burrows et al., 1997; Lillien and Raphael, 2000). Hence, the reduced responsiveness of hiNPCs to EGFR signaling could indicate that hiNPCs represent an earlier developmental time point compared to fetal hNPCs. However, since the observed differences were minor, additional studies are needed to thoroughly compare EGF function on hNPC and hiNPC migration. Further important regulators of neurodevelopmental migratory processes are SRC-kinases (Jossin et al., 2003; Kuo, 2005; Moors et al., 2007; Wang et al., 2015). Treatment of differentiating hiNPCs with the SRC-kinase inhibitor PP2 for 72 h reduced the migration distance to 51% of the respective solvent control without inducing any signs of cytotoxicity (Figure 8D). This is comparable to the hNPC response to PP2 exposure (Figure 3D). Last, we studied the effects of the RhoA GTPase activator narciclasine on hiNPC migration. RhoA activation reduced hiNPC migration in a concentration-dependent manner (Figure 8E). Comparing the hiNPC results (Figure 8E) to the response of primary hNPCs to narciclasine exposure (Masjosthusmann et al., 2020), the two cell systems did not differ in sensitivity (BMR_{10} 0.010 and 0.018 μM , respectively). In line with our observations, knockout of RhoA destabilized the actin and tubulin cytoskeleton in neurons and especially in radial glia cells, resulting in accelerated migration *in vitro* and *in vivo* (Cappello et al., 2012). Hence, narciclasine-mediated activation of RhoA could cause a hyperstabilization of the cytoskeleton and thus impair migration. This was observed in PARK2 knockout hiPSC-derived neurons, where migration was reduced by RhoA upregulation and rescued by RhoA inhibition (Bogetofte et al., 2019). Likewise, methylmercury, a metal disturbing neural migration in humans, affected hiNPC and hNPC migration at similar concentrations (Hofrichter et al., 2017).

Taken together, hiNPC proliferation and migration (iNPC1/2) work similarly as in primary hNPCs (NPC1/2). More work is needed to understand if these two test systems have also distinct applicability domains, i.e. concerning developmental timing, or if these are redundant assays. Nevertheless, primary NPCs produce oligodendrocytes within a very short time of 5 days, whereas hiPSCs need several weeks to produce oligodendrocytes. In addition, the convolutional neuronal networks were trained to quantify neuron and oligodendrocyte differentiation in the primary NPC assays. This has not been established for differentiating hiNPC, hence objective quantification methods for cell differentiation

are lacking for this test system. Therefore, the primary neurosphere assay possesses its unique selling points.

3.7 Applications of the Neurosphere Assay

The Neurosphere test methods, which allow studying a large variety of neurodevelopmental KE, are suitable for many different applications ranging from basic scientific to different regulatory questions. The Neurosphere Assay can be applied in low to medium throughput formats by manual pipetting up to larger-scale applications for screening purposes using liquid handling systems. In the past, we studied the contribution of a variety of signaling pathways including interleukin-7 (Moors et al., 2009), the extracellular related kinase Erk1/2 (Moors et al., 2007), NO signaling (Tegenge et al., 2011), BMP2, the EGFR in intrinsic signaling, Notch1 (Masjosthusmann et al., 2018) and TH signaling (Dach et al., 2017) on neurodevelopmental KE using the Neurosphere assay. Moreover, we assessed the effects of a large variety of compounds on the Neurosphere Assay KEs and studied their MoA for some of them (Fritsche et al., 2005; Moors et al., 2007; Schreiber et al., 2010; Gassmann et al., 2010, 2014; Baumann et al., 2016; Barenys et al., 2017; Masjosthusmann et al., 2019, 2020; Klose et al., 2021b, 2021a). In addition, species aspects were investigated using time-matched (Clancy et al., 2007) rat, mouse or rabbit neurospheres (Gassmann et al., 2010; Baumann et al., 2016; Barenys et al., 2017, 2021; Dach et al., 2017; Masjosthusmann et al., 2018, 2019; Ali et al., 2019; Kühne et al., 2019; Klose et al., 2021b). On the regulatory side, data from the Neurosphere Assay was used for hazard characterization of deltamethrin and flufenacet building an IATA (Hernández-Jerez et al., 2021). Also, the application of screening and prioritization was served by the neurospheres studying banned and currently in use flame retardants (Klose et al., 2021a). Last, data from the Neurosphere Assay contributed to the establishment of putative AOPs (Bal-Price et al., 2015b; Barenys et al., 2020; Klose et al., 2021b) demonstrating the usefulness for helping to frame the regulatory landscape.

Currently, we are further expanding the future regulatory application of this promising test system. Firstly, we have been studying the contribution of 14 hormone receptors, i.e. AhR, RAR, RXR, GR, LXR, PPAR α , δ / γ , TH, and the consequences of their disruption to hNPC development (Koch et al., in preparation) within the H2020 ENDpoiNTs project (Lupu et al., 2020). This work shall bring about new test methods for studying endocrine disruption-related DNT (ED-DNT) for regulatory application. Secondly, the Neurosphere Assays are used for feeding and substantiating ontologies for risk assessment purposes concerning cognitive function defects within the H2020 ONTOX project (Vinken et al., 2021). Moreover, more radial and astroglia-related endpoints are currently established with the hNPC test system, since these cell types are not entirely covered in the current assay setup. Besides these applications, we are currently enlarging the data basis for signaling pathways known to be crucial for human brain development (Fritsche, 2017; Sachana et al., 2021b). Altogether

these data will continue to define the biological and toxicological applicability domains of the Neurosphere Assay and hence increase confidence in this valuable assay.

To use the results from the Neurosphere Assay in a risk assessment context, the calculated Point of Departure (PoD) values, in our case a benchmark concentration (BMC), need to be translated to an internal dose within the fetal brain. Therefore, reverse physiology-based kinetic modeling (PBK) and quantitative *in vitro* to *in vivo* extrapolations (qIVIVE) can be applied (Basketter et al., 2012; Proença et al., 2021). One fundamental input to IVIVE is the determination of the free test compound concentration, which is defined as the concentration of the compound not bound to plastics, protein or lipid. If the nominal concentration is used instead, the uncertainty of the data analysis increases. The internal dose, determined by qIVIVE can then be translated into an external dose which highly depends on the exposure scenario (e.g. oral, dermal) and modeling of the barriers relevant for the respective type of exposure (e.g. oral bioavailability, dermal bioavailability). Especially in the DNT-context not only the classical parameters like uptake, distribution, metabolism and excretion are relevant, but additional modeling of the blood-placenta barrier and the developing blood-brain-barrier is of the highest relevance. The calculated external concentration can then be used to determine a toxic threshold dose and define an acceptable daily exposure/intake. As an alternative to the approach, known human exposures can be used as a starting point. As an example, they can be modeled from average food intake, dermal exposure or measured as plasma concentrations in epidemiological studies (Sexton et al., 1995). Moreover, exposure limits from animal studies that evidently caused a DNT phenotype can be used as a starting point for the setup of *in vitro* experiments. Another important point that needs to be considered is the metabolism of the test compound in the human body, which is only partially covered in a human cell-based assay. To some extent enzymes are present in the different cell types which metabolize the test compound, however, the complete liver metabolism is absent. Therefore, the metabolism and distribution of a test compound have to be modeled using PBK and *in vitro* screening of metabolites instead of parent compounds has to be considered depending on the distribution of the parent compound and metabolites *in vivo*. In a neurodevelopmental context, PBK modeling could be used in the future to calculate fetal brain concentrations from plasma concentrations measured *in vivo*. These values can then be compared to the PoD values determined with the Neurosphere Assay.

4 CONCLUSION

The scientific validation of the Neurosphere Assay demonstrates that the neurodevelopmental processes, i.e. NPC proliferation, migration, neuronal differentiation, neurite outgrowth, oligodendrocyte differentiation and maturation, are well represented by the test methods. However, they denote a certain developmental time, the fetal period, and during this

time especially early neurodevelopmental processes, like the switch from proliferation to initial migration and differentiation. However, how the assays are set up at the moment using an *in vitro* time of only 5 days, the developmental KEs are not followed to full cell maturity. Neurons stay in a mostly bipolar state and also oligodendrocytes do not reach the full myelinating condition. For studying earlier time-points during development, i.e. the embryonic period, or more mature endpoints, i.e. neuronal network formation and function or neuronal myelination, other assays are necessary. The current DNT IVB is evolving to close such biological gaps, yet thorough scientific validation has to be a prerequisite for each novel test system/method to proceed from hazard characterization finally to contributing to risk assessment for DNT using NAMs. Our data provide the rationale for the scientific validity of the endpoints depicted with the Neurosphere Assays. Hence, the DNT IVB, with the Neurosphere Assay as an integral part, is on a solid way to regulatory acceptance.

DATA AVAILABILITY STATEMENT

The raw data supporting the conclusions of this article will be made available by the authors upon request.

AUTHOR CONTRIBUTIONS

KK: Validation, formal analysis, investigation, writing—original draft, writing—review and editing, supervision, project administration; KB: Formal analysis, investigation, writing—original draft; JH: Formal analysis, investigation, writing—review and editing; JKa: Writing—review and editing, visualization; JKl: Formal analysis, investigation, writing—original draft; EK: Formal analysis, investigation, writing—original draft, writing—review and editing; MP: Formal analysis, investigation, writing—original draft; KS: Formal analysis, investigation, writing—original draft; EZ: Formal analysis, investigation, writing—original draft; EF: Conceptualization, validation, writing—original draft, writing—review and editing, supervision, project administration, funding acquisition.

FUNDING

This work was supported by the project CERST (Center for Alternatives to Animal Testing) of the Ministry for culture and science of the State of North-Rhine Westphalia, Germany (file number 233-1.08.03.03-121972/131 – 1.08.03.03 – 121972), the Danish Environmental Protection Agency (EPA) under the grant number MST-667-00205, the European Chemical Industry Council Long-Range Research Initiative (Cefic LRI) under the project name AIMT11 and the European Union's Horizon 2020 Research and Innovation Program, under the Grant Agreement number: 825759 of the ENDpoiNTs project

and Grant Agreement number: 963845 of the ONTOX project. This work was further supported by the Deutsche Forschungsgemeinschaft (DFG; Research Training Group (RTG) 417677437/RTG2578; “Impact

of genotoxins on the differentiation efficacy of murine and human stem and progenitor cells and functional competence of thereof derived differentiated progeny”; Sub-project 1c; Dr. Fritsche.

REFERENCES

- Abbasi, J. (2016). Call to Action on Neurotoxin Exposure in Pregnant Women and Children. *JAMA* 316, 1436–1437. doi:10.1001/jama.2016.11576
- Ali, A. A. H., Schwarz-Herzke, B., Mir, S., Sahlender, B., Victor, M., Görg, B., et al. (2019). Deficiency of the Clock Gene *Bmal1* Affects Neural Progenitor Cell Migration. *Brain Struct. Funct.* 224, 373–386. doi:10.1007/s00429-018-1775-1
- Annunziata, P., Federico, A., D’Amore, I., Corona, R. M., and Guazzi, G. C. (1983). Impairment of Human Brain Development: Glycoconjugate and Lipid Changes in Congenital Athyroidism. *Early Hum. Dev.* 8, 269–278. doi:10.1016/0378-3782(83)90009-9
- Aschner, M., Ceccatelli, S., Daneshian, M., Fritsche, E., Hasiwa, N., Hartung, T., et al. (2017). *Reference Compounds for Alternative Test Methods to Indicate Developmental Neurotoxicity (DNT) Potential of Chemicals: Example Lists & Criteria for Their Selection & Use*. Elsevier GmbH. doi:10.14573/altex.1604201
- Ayuso-Sacido, A., Moliterno, J. A., Kratovac, S., Kapoor, G. S., O’Rourke, D. M., Holland, E. C., et al. (2010). Activated EGFR Signaling Increases Proliferation, Survival, and Migration and Blocks Neuronal Differentiation in post-natal Neural Stem Cells. *J. Neurooncol.* 97, 323–337. doi:10.1007/S11060-009-0035-X
- Baas, D., Bourbeau, D., Sarlike, L. L., Ittel, M.-E., Dussault, J. H., and Puymirat, J. (1997). Oligodendrocyte Maturation and Progenitor Cell Proliferation Are Independently Regulated by Thyroid Hormone. *Glia* 19, 324–332. doi:10.1002/(sici)1098-1136(199704)19:4<324::aid-glia5>3.0.co;2-x
- Back, S. A., Luo, N. L., Borenstein, N. S., Levine, J. M., Volpe, J. J., and Kinney, H. C. (2001). Late Oligodendrocyte Progenitors Coincide with the Developmental Window of Vulnerability for Human Perinatal White Matter Injury. *J. Neurosci.* 21, 1302–1312. doi:10.1523/JNEUROSCI.21-04-01302.2001
- Bal-Price, A., Coecke, S., Costa, L., Crofton, K. M., Fritsche, E., Goldberg, A., et al. (2012). Advancing the Science of Developmental Neurotoxicity (DNT): Testing for Better Safety Evaluation. *ALTEX* 29, 202–215. doi:10.14573/altex.2012.2.202
- Bal-Price, A., Crofton, K. M., Leist, M., Allen, S., Arand, M., Buetler, T., et al. (2015a). International Stakeholder Network (ISTNET): Creating a Developmental Neurotoxicity (DNT) Testing Road Map for Regulatory Purposes. *Arch. Toxicol.* 89, 269–287. doi:10.1007/s00204-015-1464-2
- Bal-Price, A., Crofton, K. M., Sachana, M., Shafer, T. J., Behl, M., Forsby, A., et al. (2015b). Putative Adverse Outcome Pathways Relevant to Neurotoxicity. *Crit. Rev. Toxicol.* 45, 83–91. doi:10.3109/10408444.2014.981331
- Bal-Price, A., Hogberg, H. T., Crofton, K. M., Daneshian, M., FitzGerald, R. E., Fritsche, E., et al. (2018). Recommendation on Test Readiness Criteria for New Approach Methods in Toxicology: Exemplified for Developmental Neurotoxicity. *ALTEX* 35, 306–352. doi:10.14573/altex.1712081
- Barateiro, A., Brites, D., and Fernandes, A. (2016). Oligodendrocyte Development and Myelination in Neurodevelopment: Molecular Mechanisms in Health and Disease. *Cpd* 22, 656–679. doi:10.2174/1381612822666151204000636
- Barateiro, A., and Fernandes, A. (2014). Temporal Oligodendrocyte Lineage Progression: *In Vitro* Models of Proliferation, Differentiation and Myelination. *Biochim. Biophys. Acta (Bba) - Mol. Cel Res.* 1843, 1917–1929. doi:10.1016/J.BBAMCR.2014.04.018
- Barenys, M., Illa, M., Hofrichter, M., Loreiro, C., Pla, L., Klose, J., et al. (2021). Rabbit Neurospheres as a Novel *In Vitro* Tool for Studying Neurodevelopmental Effects Induced by Intrauterine Growth Restriction. *Stem Cell Transl. Med.* 10, 209–221. doi:10.1002/SCTM.20-0223
- Barenys, M., Masjosthusmann, S., and Fritsche, E. (2016). Is Intake of Flavonoid-Based Food Supplements during Pregnancy Safe for the Developing Child? A Literature Review. *Cdt* 18, 196–231. doi:10.2174/1389450116666150804110049
- Barenys, M., Reverte, I., Masjosthusmann, S., Gómez-Catalán, J., and Fritsche, E. (2020). Developmental Neurotoxicity of MDMA. A Systematic Literature Review Summarized in a Putative Adverse Outcome Pathway. *Neurotoxicology* 78, 209–241. doi:10.1016/J.NEURO.2019.12.007
- Barkovich, A. J., Kuzniecky, R. I., Jackson, G. D., Guerrini, R., and Dobyns, W. B. (2005). A Developmental and Genetic Classification for Malformations of Cortical Development. *Neurology* 65, 1873–1887. doi:10.1212/01.wnl.0000183747.05269.2d
- Bartmann, K., Hartmann, J., Kapr, J., and Fritsche, E. (2021). “Measurement of Electrical Activity of Differentiated Human iPSC-Derived Neurospheres Recorded by Microelectrode Arrays (MEA),” in *Experimental Neurotoxicology Methods. Neuromethods*. Editors J. Llorens and M. Barenys (New York: Humana, 172, 473–488. doi:10.1007/978-1-0716-1637-6_22
- Basketter, D., Clewell, H., Kimber, I., Rossi, A., Blaauboer, B., Burrier, R., et al. (2012). A Roadmap for the Development of Alternative (Non-animal) Methods for Systemic Toxicity Testing. *ALTEX* 29, 3–91. doi:10.14573/altex.2012.1.003
- Baumann, J., Dach, K., Barenys, M., Giersiefer, S., Goniwiecha, J., Lein, P. J., et al. (2015). “Application of the Neurosphere Assay for DNT Hazard Assessment: Challenges and Limitations,” in *Methods in Pharmacology and Toxicology* (Totowa, NJ: Humana Press), 29. doi:10.1007/7653_2015_49
- Baumann, J., Gassmann, K., Masjosthusmann, S., DeBoer, D., Bendt, F., Giersiefer, S., et al. (2016). Comparative Human and Rat Neurospheres Reveal Species Differences in Chemical Effects on Neurodevelopmental Key Events. *Arch. Toxicol.* 90, 1415–1427. doi:10.1007/S00204-015-1568-8
- Baumann, N., and Pham-Dinh, D. (2001). Biology of Oligodendrocyte and Myelin in the Mammalian Central Nervous System. *Physiol. Rev.* 81 (2), 871–927. doi:10.1152/physrev.2001.81.2.871
- Bellinger, D. C. (2012). Comparing the Population Neurodevelopmental Burdens Associated with Children’s Exposures to Environmental Chemicals and Other Risk Factors. *Neurotoxicology* 33, 641–643. doi:10.1016/J.NEURO.2012.04.003
- Bennett, D., Bellinger, D. C., Birnbaum, L. S., Bradman, A., Chen, A., Cory-Slechta, D. A., et al. (2016). Project TENDR: Targeting Environmental Neurodevelopmental Risks the TENDR Consensus Statement. *Environ. Health Perspect.* 124, A118–A122. doi:10.1289/EHP358
- Berdugo-Vega, G., Arias-Gil, G., López-Fernández, A., Artegiani, B., Wasielewska, J. M., Lee, C.-C., et al. (2020). Increasing Neurogenesis Refines Hippocampal Activity Rejuvenating Navigational Learning Strategies and Contextual Memory throughout Life. *Nat. Commun.* 11, 135. doi:10.1038/s41467-019-14026-z
- Bezine, M., Debbabi, M., Nury, T., Ben-Khalifa, R., Samadi, M., Cherkaoui-Malki, M., et al. (2017). Evidence of K+ Homeostasis Disruption in Cellular Dysfunction Triggered by 7-ketocholesterol, 24S-Hydroxycholesterol, and Tetracosanoic Acid (C24:0) in 158N Murine Oligodendrocytes. *Chem. Phys. Lipids* 207, 135–150. doi:10.1016/J.CHEMPHYSLIP.2017.03.006
- Bland, C., and Rand, M. D. (2006). Methylmercury Induces Activation of Notch Signaling. *Neurotoxicology* 27, 982–991. doi:10.1016/j.neuro.2006.04.005
- Bogetoft, H., Jensen, P., Okarmus, J., Schmidt, S. I., Agger, M., Ryding, M., et al. (2019). Perturbations in RhoA Signalling Cause Altered Migration and Impaired Neurogenesis in Human iPSC-Derived Neural Cells with PARK2 Mutation. *Neurobiol. Dis.* 132, 104581. doi:10.1016/j.nbd.2019.104581
- Borghese, L., Dolezalova, D., Opitz, T., Haupt, S., Leinhaas, A., Steinfarz, B., et al. (2010). Inhibition of Notch Signaling in Human Embryonic Stem Cell-Derived Neural Stem Cells Delays G1/S Phase Transition and Accelerates Neuronal Differentiation *In Vitro* and *In Vivo*. *Stem Cells* 28, 955–964. doi:10.1002/stem.408
- Borrell, V., and Götz, M. (2014). Role of Radial Glial Cells in Cerebral Cortex Folding. *Curr. Opin. Neurobiol.* 27, 39–46. doi:10.1016/j.conb.2014.02.007
- Borrell, V. (2019). Recent Advances in Understanding Neocortical Development. *F1000Res* 8, 1791. doi:10.12688/F1000RESEARCH.20332.1
- Breier, J. M., Gassmann, K., Kayser, R., Stegeman, H., De Groot, D., Fritsche, E., et al. (2010). Neural Progenitor Cells as Models for High-Throughput Screens of Developmental Neurotoxicity: State of the Science. *Neurotoxicol. Teratol.* 32, 4–15. doi:10.1016/j.jnt.2009.06.005
- Budday, S., Steinmann, P., and Kuhl, E. (2015). Physical Biology of Human Brain Development. *Front. Cel. Neurosci.* 9. doi:10.3389/fncel.2015.00257
- Burrows, R. C., Wancio, D., Levitt, P., and Lillien, L. (1997). Response Diversity and the Timing of Progenitor Cell Maturation Are Regulated by Developmental

- Changes in EGFR Expression in the Cortex. *Neuron* 19, 251–267. doi:10.1016/S0896-6273(00)80937-X
- Cappello, S., Böhringer, C. R. J., Bergami, M., Conzelmann, K.-K., Ghanem, A., Tomassy, G. S., et al. (2012). A Radial Glia-specific Role of RhoA in Double Cortex Formation. *Neuron* 73, 911–924. doi:10.1016/j.neuron.2011.12.030
- Caric, D., Raphael, H., Viti, J., Feathers, A., Wancio, D., and Lillien, L. (2001). EGFRs Mediate Chemotactic Migration in the Developing Telencephalon. *Development* 128, 4203–4216. doi:10.1242/dev.128.21.4203
- Cariou, R., Antignac, J.-P., Zalko, D., Berrebi, A., Cravedi, J.-P., Maume, D., et al. (2008). Exposure Assessment of French Women and Their Newborns to Tetrabromobisphenol-A: Occurrence Measurements in Maternal Adipose Tissue, Serum, Breast Milk and Cord Serum. *Chemosphere* 73, 1036–1041. doi:10.1016/J.CHEMOSPHERE.2008.07.084
- Chen, Y.-A., Lu, I.-L., and Tsai, J.-W. (2018). Contactin-1/F3 Regulates Neuronal Migration and Morphogenesis through Modulating RhoA Activity. *Front. Mol. Neurosci.* 11. doi:10.3389/fnmol.2018.00422
- Cheroni, C., Caporale, N., and Testa, G. (2020). Autism Spectrum Disorder at the Crossroad between Genes and Environment: Contributions, Convergences, and Interactions in ASD Developmental Pathophysiology. *Mol. Autism* 11, 1–18. doi:10.1186/S13229-020-00370-1
- Chesnut, M., Hartung, T., Hogberg, H., and Pamies, D. (2021a). Human Oligodendrocytes and Myelin *In Vitro* to Evaluate Developmental Neurotoxicity. *Ijms* 22, 7929. doi:10.3390/IJMS22157929
- Chesnut, M., Paschoud, H., Repond, C., Smirnova, L., Hartung, T., Zurich, M.-G., et al. (2021b). Human iPSC-Derived Model to Study Myelin Disruption. *Ijms* 22, 9473. doi:10.3390/IJMS22179473
- Choi, B. H. (1991). “Effects of Methylmercury on the Developing Brain,” in *Advances in Mercury Toxicology. Rochester Series on Environmental Toxicity*. Editors T. Suzuki, N. Imura, and T. W. Clarkson (Boston, MA: Springer US), 315–337. doi:10.1007/978-1-4757-9071-9_20
- Choi, B. H., Lapham, L. W., Amin-Zaki, L., and Saleem, T. (1978). Abnormal Neuronal Migration, Deranged Cerebral Cortical Organization, and Diffuse White Matter Astrocytosis of Human Fetal Brain. *J. Neuropathol. Exp. Neurol.* 37, 719–733. doi:10.1097/00005072-197811000-00001
- Clancy, B., Kersh, B., Hyde, J., Darlington, R. B., Anand, K. J. S., and Finlay, B. L. (2007). Web-Based Method for Translating Neurodevelopment from Laboratory Species to Humans. *Neuroinform* 5, 79–94. doi:10.1385/NI:5:1:110.1385/ni:5:1:79
- Coecke, S., Goldberg, A. M., Allen, S., Buzanska, L., Calamandrei, G., Crofton, K., et al. (2007). Workgroup Report: Incorporating *In Vitro* Alternative Methods for Developmental Neurotoxicity into International Hazard and Risk Assessment Strategies. *Environ. Health Perspect.* 115, 924–931. doi:10.1289/ehp.9427
- Costa, R., Drew, C., and Silva, A. (2005). Notch to Remember. *Trends Neurosciences* 28, 429–435. doi:10.1016/j.tins.2005.05.003
- Craig, C., Tropepe, V., Morshead, C., Reynolds, B., Weiss, S., and van der Kooy, D. (1996). *In Vivo* growth Factor Expansion of Endogenous Subependymal Neural Precursor Cell Populations in the Adult Mouse Brain. *J. Neurosci.* 16, 2649–2658. doi:10.1523/JNEUROSCI.16-08-02649.1996
- Crofton, K. M., and Mundy, W. R. (2021). External Scientific Report on the Interpretation of Data from the Developmental Neurotoxicity *In Vitro* Testing Assays for Use in Integrated Approaches for Testing and Assessment. *EFSA Supporting Publications* 18. doi:10.2903/sp.efsa.2021.EN-6924
- Crofton, K., Mundy, W. R., Lein, P. J., Bal-Price, A., Coecke, S., Seiler, A. E. M., et al. (2011). Developmental Neurotoxicity Testing: Recommendations for Developing Alternative Methods for the Screening and Prioritization of Chemicals. *ALTEX* 28, 9–15. doi:10.14573/altex.2011.1.009
- Csőbőnyeiová, M., Polák, Š., and Danišovič, L. u. (2016). Toxicity Testing and Drug Screening Using iPSC-Derived Hepatocytes, Cardiomyocytes, and Neural Cells. *Can. J. Physiol. Pharmacol.* 94, 687–694. doi:10.1139/cjpp-2015-0459
- Dach, K., Bendt, F., Huebenthal, U., Giersiefer, S., Lein, P. J., Heuer, H., et al. (2017). BDE-99 Impairs Differentiation of Human and Mouse NPCs into the Oligodendroglial Lineage by Species-specific Modes of Action. *Sci. Rep.* 7. doi:10.1038/srep44861
- Dahlstrand, J., Lardelli, M., and Lendahl, U. (1995). Nestin mRNA Expression Correlates with the central Nervous System Progenitor Cell State in many, but Not All, Regions of Developing central Nervous System. *Dev. Brain Res.* 84, 109–129. doi:10.1016/0165-3806(94)00162-S
- Das, K., Freudenrich, T. M., and Mundy, W. R. (2004). Assessment of PC12 Cell Differentiation and Neurite Growth: a Comparison of Morphological and Neurochemical Measures. *Neurotoxicology and Teratology* 26, 397–406. doi:10.1016/J.NTT.2004.02.006
- de Groot, D. M. G., Hartgring, S., van de Horst, L., Moerkens, M., Otto, M., Bos-Kuijpers, M. H. M., et al. (2005). 2D and 3D Assessment of Neuropathology in Rat Brain after Prenatal Exposure to Methylazoxymethanol, a Model for Developmental Neurotoxicity. *Reprod. Toxicol.* 20 (3), 417–432. doi:10.1016/j.reprotox.2005.04.006
- Dehay, C., and Kennedy, H. (2007). Cell-cycle Control and Cortical Development. *Nat. Rev. Neurosci.* 8, 438–450. doi:10.1038/nrn2097
- Dehay, C., and Kennedy, H. (2009). Transcriptional Regulation and Alternative Splicing Make for Better Brains. *Neuron* 62, 455–457. doi:10.1016/J.NEURON.2009.05.006
- Deng, P., Ma, Q., Xi, Y., Yang, L., Lin, M., Yu, Z., et al. (2020). Transcriptomic Insight into Cadmium-Induced Neurotoxicity in Embryonic Neural Stem/progenitor Cells. *Toxicol. Vitro* 62, 104686. doi:10.1016/J.TIV.2019.104686
- Dergham, P., Ellezam, B., Essagian, C., Avedissian, H., Lubell, W. D., and McKerracher, L. (2002). Rho Signaling Pathway Targeted to Promote Spinal Cord Repair. *J. Neurosci.* 22, 6570–6577. doi:10.1523/JNEUROSCI.22-15-06570.2002
- Dési, I., Nagymajtényi, L., and Schulz, H. (1998). Behavioural and Neurotoxicological Changes Caused by Cadmium Treatment of Rats during Development. *J. Appl. Toxicol.* 18, 63–70. doi:10.1002/(SICI)1099-1263(199801/02)18:1<63::AID-JAT475>3.0.CO;2-Z
- Devakumar, D., Bamford, A., Ferreira, M. U., Broad, J., Rosch, R. E., Groce, N., et al. (2018). Infectious Causes of Microcephaly: Epidemiology, Pathogenesis, Diagnosis, and Management. *Lancet Infect. Dis.* 18, e1–e13. doi:10.1016/S1473-3099(17)30398-5
- Dovey, H. F., John, V., Anderson, J. P., Chen, L. Z., De Saint Andrieu, P., Fang, L. Y., et al. (2001). Functional Gamma-Secretase Inhibitors Reduce Beta-Amyloid Peptide Levels in Brain. *J. Neurochem.* 76, 173–181. doi:10.1046/J.1471-4159.2001.00012.X
- Druwe, I., Freudenrich, T. M., Wallace, K., Shafer, T. J., and Mundy, W. R. (2016). Comparison of Human Induced Pluripotent Stem Cell-Derived Neurons and Rat Primary Cortical Neurons as *In Vitro* Models of Neurite Outgrowth. *Appl. Vitro Toxicol.* 2, 26–36. doi:10.1089/aivt.2015.0025
- Emery, B. (2010). Regulation of Oligodendrocyte Differentiation and Myelination. *Science* 330, 779–782. doi:10.1126/science.1190927
- Falk, S., and Götz, M. (2017). Glial Control of Neurogenesis. *Curr. Opin. Neurobiol.* 47, 188–195. doi:10.1016/j.conb.2017.10.025
- Faustman, E. M., Gohlke, J. M., Ponce, R. A., Lewandowski, T. A., Seeley, M. R., Whittaker, S. G., et al. (2012). “Experimental Approaches to Evaluate Mechanisms of Developmental Toxicity,” in *Developmental and Reproductive Toxicology: A Practical Approach*. Editor R. D. Hood (CRC Press), 15–60.
- Ferent, J., Zaidi, D., and Francis, F. (2020). Extracellular Control of Radial Glia Proliferation and Scaffolding during Cortical Development and Pathology. *Front. Cel Dev. Biol.* 8, 578341. doi:10.3389/fcell.2020.578341
- Florio, M., and Huttner, W. B. (2014). Neural Progenitors, Neurogenesis and the Evolution of the Neocortex. *Development* 141, 2182–2194. doi:10.1242/DEV.090571
- Förster, N., Butke, J., Keßel, H. E., Bendt, F., Pahl, M., Li, L., et al. (2021). Reliable Identification and Quantification of Neural Cells in Microscopic Images of Neurospheres. *Cytometry*. doi:10.1002/cyto.a.24514
- Fritsche, E., Barenys, M., Klose, J., Masjosthusmann, S., Nimtz, L., Schmuck, M., et al. (2018a). Current Availability of Stem Cell-Based *In Vitro* Methods for Developmental Neurotoxicity (DNT) Testing. *Toxicol. Sci.* 165, 21–30. doi:10.1093/toxsci/kfy178
- Fritsche, E., Barenys, M., Klose, J., Masjosthusmann, S., Nimtz, L., Schmuck, M., et al. (2018b). Development of the Concept for Stem Cell-Based Developmental Neurotoxicity Evaluation. *Toxicol. Sci.* 165, 14–20. doi:10.1093/toxsci/kfy175
- Fritsche, E., Cline, J. E., Nguyen, N.-H., Scanlan, T. S., and Abel, J. (2005). Polychlorinated Biphenyls Disturb Differentiation of normal Human Neural Progenitor Cells: Clue for Involvement of Thyroid Hormone Receptors. *Environ. Health Perspect.* 113, 871–876. doi:10.1289/EHP.7793

- Fritsche, E., Crofton, K. M., Hernandez, A. F., Hougaard Bennekou, S., Leist, M., Bal-Price, A., et al. (2017). OECD/EFSA Workshop on Developmental Neurotoxicity (DNT): The Use of Non-animal Test Methods for Regulatory Purposes. *ALTEX* 34, 311–315. doi:10.14573/altex.1701171s
- Fritsche, E., Haarmann-Stemmann, T., Kapr, J., Galanjuk, S., Hartmann, J., Mertens, P. R., et al. (2021). Stem Cells for Next Level Toxicity Testing in the 21st Century. *Small* 17, e2006252. doi:10.1002/sml.202006252
- Fritsche, E. (2017). Report on Integrated Testing Strategies for the Identification and Evaluation of Chemical Hazards Associated with the Developmental Neurotoxicity (DNT), to Facilitate Discussions at the Joint EFSA/OECD Workshop on DNT. ENV/JM/MONO(2017)4/ANN1.
- Gassmann, K., Abel, J., Bothe, H., Haarmann-Stemmann, T., Merk, H. F., Quasthoff, K. N., et al. (2010). Species-Specific Differential AhR Expression Protects Human Neural Progenitor Cells against Developmental Neurotoxicity of PAHs. *Environ. Health Perspect.* 118, 1571–1577. doi:10.1289/EHP.0901545
- Gassmann, K., Schreiber, T., Dingemans, M. M. L., Krause, G., Roderigo, C., Giersiefer, S., et al. (2014). BDE-47 and 6-OH-BDE-47 Modulate Calcium Homeostasis in Primary Fetal Human Neural Progenitor Cells via Ryanodine Receptor-independent Mechanisms. *Arch. Toxicol.* 88, 1537–1548. doi:10.1007/s00204-014-1217-7
- Gilmore, E. C., and Herrup, K. (1997). Cortical Development: Layers of Complexity. *Curr. Biol.* 7, R231–R234. doi:10.1016/S0960-9822(06)00108-4
- Gould, E. R., Tarbox, J., and Coyne, L. (2018). Evaluating the Effects of Acceptance and Commitment Training on the Overt Behavior of Parents of Children with Autism. *J. Contextual Behav. Sci.* 7, 81–88. doi:10.1016/j.jcbs.2017.06.003
- Gourmelon, A., and Delrue, N. (2016). “Validation in Support of Internationally Harmonised OECD Test Guidelines for Assessing the Safety of Chemicals,” in *Validation of Alternative Methods for Toxicity Testing*. Editors C. Eskes and M. Whelan (Springer), 9–32. doi:10.1007/978-3-319-33826-2_2
- Grandjean, P., and Landrigan, P. (2006). Developmental Neurotoxicity of Industrial Chemicals. *The Lancet* 368, 2167–2178. doi:10.1016/S0140-6736(06)69665-7
- Grandjean, P., and Landrigan, P. J. (2014). Neurobehavioural Effects of Developmental Toxicity. *Lancet Neurol.* 13, 330–338. doi:10.1016/S1474-4422(13)70278-3
- Griesinger, C., Desprez, B., Coecke, S., Casey, W., and Zuang, V. (2016). “Validation of Alternative *In Vitro* Methods to Animal Testing: Concepts, Challenges, Processes and Tools,” in *Validation of Alternative Methods for Toxicity Testing*. Editors C. Eskes and M. Whelan (Springer), 65–132. doi:10.1007/978-3-319-33826-210.1007/978-3-319-33826-2_4
- Guerrini, R., and Dobyns, W. B. (2014). Malformations of Cortical Development: Clinical Features and Genetic Causes. *Lancet Neurol.* 13, 710–726. doi:10.1016/S1474-4422(14)70040-7
- Guidi, S., Giacomini, A., Stagni, F., Emili, M., Uguagliati, B., Bonasoni, M. P., et al. (2018). Abnormal Development of the Inferior Temporal Region in Fetuses with Down Syndrome. *Brain Pathol.* 28, 986–998. doi:10.1111/BPA.12605
- Guo, Y.-e., Suo, N., Cui, X., Yuan, Q., and Xie, X. (2018). Vitamin C Promotes Oligodendrocytes Generation and Remyelination. *Glia* 66, 1302–1316. doi:10.1002/GLIA.23306
- Haddow, J. E., Palomaki, G. E., Allan, W. C., Williams, J. R., Knight, G. J., Gagnon, J., et al. (1999). Maternal Thyroid Deficiency during Pregnancy and Subsequent Neuropsychological Development of the Child. *N. Engl. J. Med.* 341, 549–555. doi:10.1056/NEJM199908193410801
- Haq, E., Giri, S., Singh, I., and Singh, A. K. (2003). Molecular Mechanism of Psychosine-Induced Cell Death in Human Oligodendrocyte Cell Line. *J. Neurochem.* 86, 1428–1440. doi:10.1046/J.1471-4159.2003.01941.X
- Harada, M. (1978). Congenital Minamata Disease: Intrauterine Methylmercury Poisoning. *Teratology* 18, 285–288. doi:10.1002/tera.1420180216
- Harrill, J. A., Freudenrich, T., Wallace, K., Ball, K., Shafer, T. J., and Mundy, W. R. (2018). Testing for Developmental Neurotoxicity Using a Battery of *In Vitro* Assays for Key Cellular Events in Neurodevelopment. *Toxicol. Appl. Pharmacol.* 354, 24–39. doi:10.1016/j.TAAP.2018.04.001
- Hartung, T., Hoffmann, S., and Stephens, M. (2013). Food for Thought ... Mechanistic Validation. *ALTEX* 30, 119–130. doi:10.14573/ALTEX.2013.2.119
- He, L., and Lu, Q. R. (2013). Coordinated Control of Oligodendrocyte Development by Extrinsic and Intrinsic Signaling Cues. *Neurosci. Bull.* 29, 129–143. doi:10.1007/s12264-013-1318-y
- Hendriks, H. S., Koolen, L. A. E., Dingemans, M. M. L., Viberg, H., Lee, I., Leonards, P. E. G., et al. (2015). Effects of Neonatal Exposure to the Flame Retardant Tetrabromobisphenol-A, Aluminum Diethylphosphinate or Zinc Stannate on Long-Term Potentiation and Synaptic Protein Levels in Mice. *Arch. Toxicol.* 89, 2345–2354. doi:10.1007/s00204-014-1366-8
- Hernández-Jerez, A., Hernández-Jerez, A., Adriaanse, P., Aldrich, A., Berny, P., Coja, T., et al. (2021). Development of Integrated Approaches to Testing and Assessment (IATA) Case Studies on Developmental Neurotoxicity (DNT) Risk Assessment. *Efsj* 19, 63. doi:10.2903/j.efsa.2021.6599
- Hofrichter, M., Nimtz, L., Tigges, J., Kabiri, Y., Schröter, F., Royer-Pokora, B., et al. (2017). Comparative Performance Analysis of Human iPSC-Derived and Primary Neural Progenitor Cells (NPC) Grown as Neurospheres *In Vitro*. *Stem Cell Res.* 25, 72–82. doi:10.1016/j.SCR.2017.10.013
- Homem, C. C. F., Repic, M., and Knoblich, J. A. (2015). Proliferation Control in Neural Stem and Progenitor Cells. *Nat. Rev. Neurosci.* 16, 647–659. doi:10.1038/NNR4021
- Hu, Q.-D., Ang, B.-T., Karsak, M., Hu, W.-P., Cui, X.-Y., Duka, T., et al. (2003). F3/Contactin Acts as a Functional Ligand for Notch during Oligodendrocyte Maturation. *Cell* 115, 163–175. doi:10.1016/S0092-8674(03)00810-9
- Hundle, B., McMahon, T., Dadgar, J., and Messing, R. O. (1995). Overexpression of ϵ -Protein Kinase C Enhances Nerve Growth Factor-Induced Phosphorylation of Mitogen-Activated Protein Kinases and Neurite Outgrowth. *J. Biol. Chem.* 270, 30134–30140. doi:10.1074/jbc.270.50.30134
- Ibarrola, N., and Rodríguez-Peña, A. (1997). Hypothyroidism Coordinately and Transiently Affects Myelin Protein Gene Expression in Most Rat Brain Regions during Postnatal Development. *Brain Res.* 752, 285–293. doi:10.1016/S0006-8993(96)01480-1
- Jennings, P. (2015). “The Future of *In Vitro* Toxicology”. *Toxicol. Vitro* 29, 1217–1221. doi:10.1016/J.TIV.2014.08.011
- Jessberger, S., and Parent, J. M. (2015). Epilepsy and Adult Neurogenesis. *Cold Spring Harb. Perspect. Biol.* 7, a020677. doi:10.1101/cshperspect.a020677
- Jossin, Y., Ogawa, M., Metin, C., Tissir, F., and Goffinet, A. M. (2003). Inhibition of Src Family Kinases and Non-classical Protein Kinases C Induce a Reeler-like Malformation of Cortical Plate Development. *J. Neurosci.* 23, 9953–9959. doi:10.1523/jneurosci.23-30-09953.2003
- Judson, R., Kavlock, R., Martin, M., Reif, D., Houck, K., Knudsen, T., et al. (2013). Perspectives on Validation of High-Throughput Assays Supporting 21st Century Toxicity Testing. *ALTEX* 30, 51–66. doi:10.14573/ALTEX.2013.1.051
- Kakita, A., Inenaga, C., Sakamoto, M., and Takahashi, H. (2002). Neuronal Migration Disturbance and Consequent Cytoarchitecture in the Cerebral Cortex Following Transplacental Administration of Methylmercury. *Acta Neuropathol.* 104, 409–417. doi:10.1007/s00401-002-0571-3
- Kim, U.-J., and Oh, J.-E. (2014). Tetrabromobisphenol A and Hexabromocyclododecane Flame Retardants in Infant-Mother Paired Serum Samples, and Their Relationships with Thyroid Hormones and Environmental Factors. *Environ. Pollut.* 184, 193–200. doi:10.1016/J.ENVPOL.2013.08.034
- Kippler, M., Bakhtiar Hossain, M., Lindh, C., Moore, S. E., Kabir, I., Vahter, M., et al. (2012a). Early Life Low-Level Cadmium Exposure Is Positively Associated with Increased Oxidative Stress. *Environ. Res.* 112, 164–170. doi:10.1016/j.envres.2011.11.012
- Kippler, M., Tofail, F., Hamadani, J. D., Gardner, R. M., Grantham-McGregor, S. M., Bottai, M., et al. (2012b). Early-life Cadmium Exposure and Child Development in 5-Year-Old Girls and Boys: A Cohort Study in Rural Bangladesh. *Environ. Health Perspect.* 120, 1462–1468. doi:10.1289/EHP.1104431
- Klose, J., Pahl, M., Bartmann, K., Bendt, F., Blum, J., Dolde, X., et al. (2021a). Neurodevelopmental Toxicity Assessment of Flame Retardants Using a Human DNT *In Vitro* Testing Battery. *Cell Biol. Toxicol.* 1–27. doi:10.1007/s10565-021-09603-2
- Klose, J., Tigges, J., Masjosthusmann, S., Schmuck, K., Bendt, F., Hübenal, U., et al. (2021b). TBBPA Targets Converging Key Events of Human Oligodendrocyte Development Resulting in Two Novel AOPs. *ALTEX* 38, 215–234. doi:10.14573/altex.2007201
- Kobolak, J., Teglas, A., Bellak, T., Janstova, Z., Molnar, K., Zana, M., et al. (2020). Human Induced Pluripotent Stem Cell-Derived 3D-Neurospheres Are Suitable for Neurotoxicity Screening. *Cells* 9, 1122. doi:10.3390/CELLS9051122
- Kojima, A., and Tator, C. H. (2000). Epidermal Growth Factor and Fibroblast Growth Factor 2 Cause Proliferation of Ependymal Precursor Cells in the Adult

- Rat Spinal Cord *In Vivo*. *J. Neuropathol. Exp. Neurol.* 59, 687–697. doi:10.1093/JNEN/59.8.687
- Kornblum, H. I., Hussain, R. J., Bronstein, J. M., Gall, C. M., Lee, D. C., and Serogy, K. B. (1997). Prenatal Ontogeny of the Epidermal Growth Factor Receptor and its Ligand, Transforming Growth Factor Alpha, in the Rat Brain. *J. Comp. Neurol.* 380, 243–261. doi:10.1002/(sici)1096-9861(19970407)380:2<243::aid-cne7>3.0.co;2-3
- Kornblum, H. I., Hussain, R., Wiesen, J., Miettinen, P., Zurcher, S. D., Chow, K., et al. (1998). Abnormal Astrocyte Development and Neuronal Death in Mice Lacking the Epidermal Growth Factor Receptor. *J. Neurosci. Res.* 53, 697–717. doi:10.1002/(SICI)1097-4547(19980915)53:6<697::AID-JNR8>3.0.CO;2-0
- Krug, A. K., Balmer, N. V., Matt, F., Schönenberger, F., Merhof, D., and Leist, M. (2013). Evaluation of a Human Neurite Growth Assay as Specific Screen for Developmental Neurotoxicants. *Arch. Toxicol.* 87, 2215–2231. doi:10.1007/s00204-013-1072-y
- Kühne, B. A., Puig, T., Ruiz-Martínez, S., Crous-Masó, J., Planas, M., Feliu, L., et al. (2019). Comparison of Migration Disturbance Potency of Epigallocatechin Gallate (EGCG) Synthetic Analogs and EGCG PEGylated PLGA Nanoparticles in Rat Neurospheres. *Food Chem. Toxicol.* 123, 195–204. doi:10.1016/J.FCT.2018.10.055
- Kukekov, V. G., Laywell, E. D., Suslov, O., Davies, K., Scheffler, B., Thomas, L. B., et al. (1999). Multipotent Stem/Progenitor Cells with Similar Properties Arise from Two Neurogenic Regions of Adult Human Brain. *Exp. Neurol.* 156, 333–344. doi:10.1006/exnr.1999.7028
- Kuo, G. (2005). Absence of Fyn and Src Causes a Reeler-like Phenotype. *J. Neurosci.* 25, 8578–8586. doi:10.1523/JNEUROSCI.1656-05.2005
- Leal, R. B., Rieger, D. K., Peres, T. V., Lopes, M. W., and Gonçalves, C. A. S. (2012). “Cadmium Neurotoxicity and its Role in Brain Disorders,” in *Metal Ion in Stroke*. Editors Y. V. Li and J. H. Zhang (New York: Springer Science+Business Media), 751–766. doi:10.1007/978-1-4419-9663-310.1007/978-1-4419-9663-3_34
- Lein, P., Locke, P., and Goldberg, A. (2007). Meeting Report: Alternatives for Developmental Neurotoxicity Testing. *Environ. Health Perspect.* 115, 764–768. doi:10.1289/ehp.9841
- Leist, M., Efreanova, L., and Karreman, C. (2010). Food for Thought Considerations and Guidelines for Basic Test Method Descriptions in Toxicology. *ALTEX* 27, 309–317. doi:10.14573/altex.2010.4.309
- Leist, M., and Hartung, T. (2013). Inflammatory Findings on Species Extrapolations: Humans Are Definitely No 70-kg Mice. *Arch. Toxicol.* 87, 563–567. doi:10.1007/S00204-013-1038-0
- Leist, M., Hasiwa, N., Rovida, C., Daneshian, M., Basketter, D., Kimber, I., et al. (2014). Consensus Report on the Future of Animal-free Systemic Toxicity Testing. *ALTEX* 31, 341–356. doi:10.14573/altex.1406091
- Lendahl, U., Zimmermann, L. B., and McKay, R. D. G. (1990). CNS Stem Cells Express a New Class of Intermediate Filament Protein. *Cell* 60, 585–595. doi:10.1016/0092-8674(90)90662-X
- Lillien, L., and Raphael, H. (2000). BMP and FGF Regulate the Development of EGF-Responsive Neural Progenitor Cells. *Development* 127, 4993–5005. doi:10.1242/dev.127.22.4993
- Liu, X., Zhao, Y., Peng, S., Zhang, S., Wang, M., Chen, Y., et al. (2016). BMP7 Retards Peripheral Myelination by Activating P38 MAPK in Schwann Cells. *Sci. Rep.* 6, 1–13. doi:10.1038/srep31049
- Louvi, A., and Artavanis-Tsakonas, S. (2006). Notch Signalling in Vertebrate Neural Development. *Nat. Rev. Neurosci.* 7, 93–102. doi:10.1038/nrn1847
- Lupu, D., Andersson, P., Bornehag, C.-G., Demeneix, B., Fritsche, E., Gennings, C., et al. (2020). The ENDpoiNTs Project: Novel Testing Strategies for Endocrine Disruptors Linked to Developmental Neurotoxicity. *Ijms* 21, 3978. doi:10.3390/IJMS21113978
- Mahajan, G., Lee, M.-Y., and Kothapalli, C. (2019). Biophysical and Biomechanical Properties of Neural Progenitor Cells as Indicators of Developmental Neurotoxicity. *Arch. Toxicol.* 93, 2979–2992. doi:10.1007/S00204-019-02549-9
- Makris, S. L., Raffaele, K., Allen, S., Bowers, W. J., Hass, U., Alleva, E., et al. (2009). A Retrospective Performance Assessment of the Developmental Neurotoxicity Study in Support of OECD Test Guideline 426. *Environ. Health Perspect.* 117, 17–25. doi:10.1289/EHP.11447
- Marinelli, C., Bertalot, T., Zusso, M., Skaper, S. D., and Giusti, P. (2016). Systematic Review of Pharmacological Properties of the Oligodendrocyte Lineage. *Front. Cel. Neurosci.* 10. doi:10.3389/FNCEL.2016.00027
- Martens, D. J., Seaberg, R. M., and van der Kooy, D. (2002). In Vivo Infusions of Exogenous Growth Factors into the Fourth Ventricle of the Adult Mouse Brain Increase the Proliferation of Neural Progenitors Around the Fourth Ventricle and the central Canal of the Spinal Cord. *Eur. J. Neurosci.* 16, 1045–1057. doi:10.1046/J.1460-9568.2002.02181.X
- Marton, R. M., Miura, Y., Sloan, S. A., Li, Q., Revah, O., Levy, R. J., et al. (2019). Differentiation and Maturation of Oligodendrocytes in Human Three-Dimensional Neural Cultures. *Nat. Neurosci.* 22, 484–491. doi:10.1038/s41593-018-0316-9
- Masini, E., Loi, E., Vega-Benedetti, A. F., Carta, M., Doneddu, G., Fadda, R., et al. (2020). An Overview of the Main Genetic, Epigenetic and Environmental Factors Involved in Autism Spectrum Disorder Focusing on Synaptic Activity. *Ijms* 21, 8290. doi:10.3390/ijms21218290
- Masjosthusmann, S., Becker, D., Petzuch, B., Klose, J., Siebert, C., Deenen, R., et al. (2018). A Transcriptome Comparison of Time-Matched Developing Human, Mouse and Rat Neural Progenitor Cells Reveals Human Uniqueness. *Toxicol. Appl. Pharmacol.* 354, 40–55. doi:10.1016/j.taap.2018.05.009
- Masjosthusmann, S., Blum, J., Bartmann, K., Dolde, X., Holzer, A. K., Stürzl, L. C., et al. (2020). Establishment of an A Priori Protocol for the Implementation and Interpretation of an In-vitro Testing Battery for the Assessment of Developmental Neurotoxicity. *EFSA Supporting Publications* 17. doi:10.2903/sp.efsa.2020.en-1938
- Masjosthusmann, S., Siebert, C., Hüenthal, U., Bendt, F., Baumann, J., and Fritsche, E. (2019). Arsenite Interrupts Neurodevelopmental Processes of Human and Rat Neural Progenitor Cells: The Role of Reactive Oxygen Species and Species-specific Antioxidative Defense. *Chemosphere* 235, 447–456. doi:10.1016/j.chemosphere.2019.06.123
- Matsumoto, N., Hoshiba, Y., Morita, K., Uda, N., Hirota, M., Minamikawa, M., et al. (2017). Pathophysiological Analyses of Periventricular Nodular Heterotopia Using Gyrencephalic Mammals. *Hum. Mol. Genet.* 26, 1173–1181. doi:10.1093/hmg/ddx038
- Moors, M., Cline, J., Abel, J., and Fritsche, E. (2007). ERK-dependent and -independent Pathways Trigger Human Neural Progenitor Cell Migration. *Toxicol. Appl. Pharmacol.* 221, 57–67. doi:10.1016/j.taap.2007.02.018
- Moors, M., Rockel, T. D., Abel, J., Cline, J. E., Gassmann, K., Schreiber, T., et al. (2009). Human Neurospheres as Three-Dimensional Cellular Systems for Developmental Neurotoxicity Testing. *Environ. Health Perspect.* 117, 1131–1138. doi:10.1289/EHP.0800207
- Moosa, A., Shu, H., Sarachana, T., and Hu, V. W. (2018). Are Endocrine Disrupting Compounds Environmental Risk Factors for Autism Spectrum Disorder? *Horm. Behav.* 101, 13–21. doi:10.1016/J.YHBEH.2017.10.003
- Mundy, W. R., Padilla, S., Breier, J. M., Crofton, K. M., Gilbert, M. E., Herr, D. W., et al. (2015). Expanding the Test Set: Chemicals with Potential to Disrupt Mammalian Brain Development. *Neurotoxicology and Teratology* 52, 25–35. doi:10.1016/j.ntt.2015.10.001
- Murray, K., and Dubois-Dalcq, M. (1997). Emergence of Oligodendrocytes from Human Neural Spheres. *J. Neurosci. Res.* 50, 146–156. doi:10.1002/(sici)1097-4547(19971015)50:2<146::aid-jnr4>3.0.co;2-f
- National Research Council (2007). *Toxicity Testing in the 21st Century*. Washington, D.C: National Academies Press. doi:10.17226/11970
- Newton, A. C. (1995). Protein Kinase C: Structure, Function, and Regulation. *J. Biol. Chem.* 270, 28495–28498. doi:10.1074/jbc.270.48.28495
- Nguyen, N.-H., Apriletti, J. W., Cunha Lima, S. T., Webb, P., Baxter, J. D., and Scanlan, T. S. (2002). Rational Design and Synthesis of a Novel Thyroid Hormone Antagonist that Blocks Coactivator Recruitment. *J. Med. Chem.* 45, 3310–3320. doi:10.1021/jm0201013
- Nimtzt, L., Hartmann, J., Tigges, J., Masjosthusmann, S., Schmuck, M., Keßel, E., et al. (2020). Characterization and Application of Electrically Active Neuronal Networks Established from Human Induced Pluripotent Stem Cell-Derived Neural Progenitor Cells for Neurotoxicity Evaluation. *Stem Cell Res.* 45, 101761. doi:10.1016/J.SCR.2020.101761
- Nishizuka, Y. (1986). Studies and Perspectives of Protein Kinase C. *Science* 233, 305–312. doi:10.1126/science.3014651
- Oda, K., Matsuoka, Y., Funahashi, A., and Kitano, H. (2005). A Comprehensive Pathway Map of Epidermal Growth Factor Receptor Signaling. *Mol. Syst. Biol.* 1, 2005.0010. doi:10.1038/MSB4100014
- OECD (2018). *Guidance Document on Good in Vitro Method Practices (GIVIMP)*. Paris: OECD Publishing. doi:10.1787/9789264304796-en

- Pamies, D., Barrera, P., Block, K., Makri, G., Kumar, A., Wiersma, D., et al. (2017). A Human Brain Microphysiological System Derived from Induced Pluripotent Stem Cells to Study Neurological Diseases and Toxicity. *ALTEX* 34, 362–376. doi:10.14573/ALTEX.1609122
- Pamies, D., Leist, M., Coecke, S., Bowe, G., Allen, D. G., Gstraunthaler, G., et al. (2022). Guidance Document on Good Cell and Tissue Culture Practice 2.0 (GCCP 2.0). *ALTEX* 39, 30–70. doi:10.14573/altex.2111011
- Paparella, M., Bennekou, S. H., and Bal-Price, A. (2020). An Analysis of the Limitations and Uncertainties of *In Vivo* Developmental Neurotoxicity Testing and Assessment to Identify the Potential for Alternative Approaches. *Reprod. Toxicol.* 96, 327–336. doi:10.1016/J.REPROTOX.2020.08.002
- Paşca, A. M., Sloan, S. A., Clarke, L. E., Tian, Y., Makinson, C. D., Huber, N., et al. (2015). Functional Cortical Neurons and Astrocytes from Human Pluripotent Stem Cells in 3D Culture. *Nat. Methods* 12, 671–678. doi:10.1038/NMETH.3415
- Pavone, P., Praticò, A. D., Rizzo, R., Corsello, G., Ruggieri, M., Parano, E., et al. (2017). A Clinical Review on Megalencephaly. *Med. (United States)* 96, e6814. doi:10.1097/MD.00000000000006814
- Peng, Z., Li, X., Fu, M., Zhu, K., Long, L., Zhao, X., et al. (2019). Inhibition of Notch1 Signaling Promotes Neuronal Differentiation and Improves Functional Recovery in Spinal Cord Injury through Suppressing the Activation of Ras Homolog Family Member A. *J. Neurochem.* 150, 709–722. doi:10.1111/jnc.14833
- Pevny, L., and Placzek, M. (2005). SOX Genes and Neural Progenitor Identity. *Curr. Opin. Neurobiol.* 15, 7–13. doi:10.1016/J.CONB.2005.01.016
- Pierfelice, T., Alberi, L., and Gaiano, N. (2011). Notch in the Vertebrate Nervous System: An Old Dog with New Tricks. *Neuron* 69, 840–855. doi:10.1016/j.neuron.2011.02.031
- Pistollato, F., Canovas-Jorda, D., Zagoura, D., and Bal-Price, A. (2017). Nrf2 Pathway Activation upon Rotenone Treatment in Human iPSC-Derived Neural Stem Cells Undergoing Differentiation towards Neurons and Astrocytes. *Neurochem. Int.* 108, 457–471. doi:10.1016/J.NEUINT.2017.06.006
- Pitzer, E. M., Sugimoto, C., Gudelsky, G. A., Huff Adams, C. L., Williams, M. T., and Vorhees, C. V. (2019). Deltamethrin Exposure Daily from Postnatal Day 3–20 in Sprague-Dawley Rats Causes Long-Term Cognitive and Behavioral Deficits. *Toxicol. Sci.* 169, 511–523. doi:10.1093/TOXSCI/KFZ067
- Pitzer, E. M., Williams, M. T., and Vorhees, C. V. (2021). Effects of Pyrethroids on Brain Development and Behavior: Deltamethrin. *Neurotoxicology and Teratology* 87, 106983. doi:10.1016/J.NTT.2021.106983
- Pollen, A. A., Nowakowski, T. J., Chen, J., Retallack, H., Sandoval-Espinosa, C., Nicholas, C. R., et al. (2015). Molecular Identity of Human Outer Radial Glia during Cortical Development. *Cell* 163, 55–67. doi:10.1016/J.CELL.2015.09.004
- Proença, S., Escher, B. I., Fischer, F. C., Fisher, C., Grégoire, S., Hewitt, N. J., et al. (2021). Effective Exposure of Chemicals in *In Vitro* Cell Systems: A Review of Chemical Distribution Models. *Toxicol. Vitro* 73, 105133. doi:10.1016/j.tiv.2021.105133
- Rakic, P. (1972). Mode of Cell Migration to the Superficial Layers of Fetal Monkey Neocortex. *J. Comp. Neurol.* 145, 61–83. doi:10.1002/cne.901450105
- Rand, M. D., Dao, J. C., and Clason, T. A. (2009). Methylmercury Disruption of Embryonic Neural Development in *Drosophila*. *Neurotoxicology* 30, 794–802. doi:10.1016/j.neuro.2009.04.006
- Reynolds, B., Tetzlaff, W., and Weiss, S. (1992). A Multipotent EGF-Responsive Striatal Embryonic Progenitor Cell Produces Neurons and Astrocytes. *J. Neurosci.* 12, 4565–4574. doi:10.1523/JNEUROSCI.12-11-04565.1992
- Rice, D., and Barone, S., Jr. (2000). Critical Periods of Vulnerability for the Developing Nervous System: Evidence from Humans and Animal Models. *Environ. Health Perspect.* 108, 511–533. doi:10.1289/EHP.00108S3511
- Richardson, J. R., Taylor, M. M., Shalat, S. L., Guillot, T. S., Caudle, W. M., Hossain, M. M., et al. (2015). Developmental Pesticide Exposure Reproduces Features of Attention Deficit Hyperactivity Disorder. *FASEB J.* 29, 1960–1972. doi:10.1096/FJ.14-260901
- Rock, K. D., Gillera, S. E. A., Devarasetty, P., Horman, B., Knudsen, G., Birnbaum, L. S., et al. (2019). Sex-specific Behavioral Effects Following Developmental Exposure to Tetrabromobisphenol A (TBBPA) in Wistar Rats. *Neurotoxicology* 75, 136–147. doi:10.1016/j.neuro.2019.09.003
- Romano, R., and Bucci, C. (2020). Role of EGFR in the Nervous System. *Cells* 9, 1887. doi:10.3390/CELLS9081887
- Rovet, J., and Daneman, D. (2003). Congenital Hypothyroidism. *Pediatr. Drugs* 5, 141–149. doi:10.2165/00128072-200305030-00001
- Sachana, M., Bal-Price, A., Crofton, K. M., Bennekou, S. H., Shafer, T. J., Behl, M., et al. (2019). International Regulatory and Scientific Effort for Improved Developmental Neurotoxicity Testing. *Toxicol. Sci.* 167, 45–57. doi:10.1093/toxsci/kfy211
- Sachana, M., Shafer, T. J., and Terron, A. (2021a). Toward a Better Testing Paradigm for Developmental Neurotoxicity: Oecd Efforts and Regulatory Considerations. *Biology* 10, 86. doi:10.3390/biology10020086
- Sachana, M., Willett, C., Pistollato, F., and Bal-Price, A. (2021b). The Potential of Mechanistic Information Organised within the AOP Framework to Increase Regulatory Uptake of the Developmental Neurotoxicity (DNT) *In Vitro* Battery of Assays. *Reprod. Toxicol.* 103, 159–170. doi:10.1016/J.REPROTOX.2021.06.006
- Saravanan, K. S., Sindhu, K. M., and Mohanakumar, K. P. (2005). Acute Intranigral Infusion of Rotenone in Rats Causes Progressive Biochemical Lesions in the Striatum Similar to Parkinson's Disease. *Brain Res.* 1049, 147–155. doi:10.1016/J.BRAINRES.2005.04.051
- Sareen, D., Gowing, G., Sahabian, A., Staggenborg, K., Paradis, R., Avalos, P., et al. (2014). Human Induced Pluripotent Stem Cells Are a Novel Source of Neural Progenitor Cells (iNPCs) that Migrate and Integrate in the Rodent Spinal Cord. *J. Comp. Neurol.* 522, 2707–2728. doi:10.1002/CNE.23578
- Sarret, C., Oliver Petit, I., and Tonduti, D. (2010). Allan-Herndon-Dudley Syndrome. *GeneReviews*®. Available at: <https://www.ncbi.nlm.nih.gov/books/NBK26373/> (Accessed November 3, 2021).
- Schmuck, M. R., Temme, T., Dach, K., de Boer, D., Barenys, M., Bendt, F., et al. (2017). Omnisphero: a High-Content Image Analysis (HCA) Approach for Phenotypic Developmental Neurotoxicity (DNT) Screenings of Organoid Neurosphere Cultures *In Vitro*. *Arch. Toxicol.* 91, 2017–2028. doi:10.1007/s00204-016-1852-2
- Schneider, C. A., Rasband, W. S., and Eliceiri, K. W. (2012). NIH Image to ImageJ: 25 Years of Image Analysis. *Nat. Methods* 9, 671–675. doi:10.1038/nmeth.2089
- Schoonover, C. M., Seibel, M. M., Jolson, D. M., Stack, M. J., Rahman, R. J., Jones, S. A., et al. (2004). Thyroid Hormone Regulates Oligodendrocyte Accumulation in Developing Rat Brain White Matter Tracts. *Endocrinology* 145, 5013–5020. doi:10.1210/EN.2004-0065
- Schreiber, T., Gassmann, K., Götz, C., Hübenthal, U., Moors, M., Krause, G., et al. (2010). Polybrominated Diphenyl Ethers Induce Developmental Neurotoxicity in a Human *In Vitro* Model: Evidence for Endocrine Disruption. *Environ. Health Perspect.* 118, 572–578. doi:10.1289/ehp.0901435
- Sexton, K., Callahan, M. A., and Bryan, E. F. (1995). Estimating Exposure and Dose to Characterize Health Risks: the Role of Human Tissue Monitoring in Exposure Assessment. *Environ. Health Perspect.* 103, 13–29. doi:10.1289/ehp.95103s31310.2307/3432556
- Singh, L., Pressly, B., Mengeling, B. J., Fetting, J. C., Furlow, J. D., Lein, P. J., et al. (2016). Chasing the Elusive Benzofuran Impurity of the THR Antagonist NH-3: Synthesis, Isotope Labeling, and Biological Activity. *J. Org. Chem.* 81, 1870–1876. doi:10.1021/ACS.JOC.5B02665
- Sloan, S. A., Darmanis, S., Huber, N., Khan, T. A., Birey, F., Caneda, C., et al. (2017). Human Astrocyte Maturation Captured in 3D Cerebral Cortical Spheroids Derived from Pluripotent Stem Cells. *Neuron* 95, 779–790. doi:10.1016/J.NEURON.2017.07.035
- Snyder, J. L., Kearns, C. A., and Appel, B. (2012). Fbxw7 Regulates Notch to Control Specification of Neural Precursors for Oligodendrocyte Fate. *Neural Dev.* 7, 1–12. doi:10.1186/1749-8104-7-15
- Somel, M., Liu, X., Tang, L., Yan, Z., Hu, H., Guo, S., et al. (2011). MicroRNA-Driven Developmental Remodeling in the Brain Distinguishes Humans from Other Primates. *PLoS Biol.* 9, e1001214. doi:10.1371/JOURNAL.PBIO.1001214
- Song, C., and Wang, H. (2011). Cytokines Mediated Inflammation and Decreased Neurogenesis in Animal Models of Depression. *Prog. Neuro-Psychopharmacology Biol. Psychiatry* 35, 760–768. doi:10.1016/j.pnpb.2010.06.020
- Soubannier, V., Maussion, G., Chaineau, M., Sigutova, V., Rouleau, G., Durcan, T. M., et al. (2020). Characterization of Human iPSC-Derived Astrocytes with Potential for Disease Modeling and Drug Discovery. *Neurosci. Lett.* 731, 135028. doi:10.1016/J.NEULET.2020.135028
- Stagni, F., Giacomini, A., Emili, M., Guidi, S., and Bartesaghi, R. (2018). Neurogenesis Impairment: An Early Developmental Defect in Down

- Syndrome. *Free Radic. Biol. Med.* 114, 15–32. doi:10.1016/J.FREERADBIOMED.2017.07.026
- Sun, Y., Goderie, S. K., and Temple, S. (2005). Asymmetric Distribution of EGFR Receptor during Mitosis Generates Diverse CNS Progenitor Cells. *Neuron* 45, 873–886. doi:10.1016/J.NEURON.2005.01.045
- Tegenge, M. A., Rockel, T. D., Fritsche, E., and Bicker, G. (2011). Nitric Oxide Stimulates Human Neural Progenitor Cell Migration via cGMP-Mediated Signal Transduction. *Cell. Mol. Life Sci.* 68, 2089–2099. doi:10.1007/S00018-010-0554-9
- Tian, L.-L., Zhao, Y.-C., Wang, X.-C., Gu, J.-L., Sun, Z.-J., Zhang, Y.-L., et al. (2009). Effects of Gestational Cadmium Exposure on Pregnancy Outcome and Development in the Offspring at Age 4.5 Years. *Biol. Trace Elem. Res.* 132, 51–59. doi:10.1007/S12011-009-8391-0
- Tigges, J., Bielec, K., Brockerhoff, G., Hildebrandt, B., Hübenthal, U., Kapr, J., et al. (2021). Academic Application of Good Cell Culture Practice for Induced Pluripotent Stem Cells. *ALTEX*, 1–19. doi:10.14573/altex.2101221
- Tropepe, V., Sibilina, M., Ciruna, B. G., Rossant, J., Wagner, E. F., and Van Der Kooy, D. (1999). Distinct Neural Stem Cells Proliferate in Response to EGF and FGF in the Developing Mouse Telencephalon. *Dev. Biol.* 208, 166–188. doi:10.1006/dbio.1998.9192
- van Tilborg, E., de Theije, C. G. M., van Hal, M., Wagenaar, N., de Vries, L. S., Benders, M. J., et al. (2018). Origin and Dynamics of Oligodendrocytes in the Developing Brain: Implications for Perinatal white Matter Injury. *Glia* 66, 221–238. doi:10.1002/GLIA.23256
- van Tilborg, E., Heijnen, C. J., Benders, M. J., van Bel, F., Fleiss, B., Gressens, P., et al. (2016). Impaired Oligodendrocyte Maturation in Preterm Infants: Potential Therapeutic Targets. *Prog. Neurobiol.* 136, 28–49. doi:10.1016/j.pneurobio.2015.11.002
- Vatine, G. D., Shelest, O., Barriga, B. K., Ofan, R., Rabinski, T., Mattis, V. B., et al. (2021). Oligodendrocyte Progenitor Cell Maturation Is Dependent on Dual Function of MCT8 in the Transport of Thyroid Hormone across Brain Barriers and the Plasma Membrane. *Glia* 69, 2146–2159. doi:10.1002/glia.24014
- Vinken, M., Benfenati, E., Busquet, F., Castell, J., Clevert, D.-A., de Kok, T. M., et al. (2021). Safer Chemicals Using Less Animals: Kick-Off of the European ONTOX Project. *Toxicology* 458, 152846. doi:10.1016/J.TOX.2021.152846
- Volpe, J. J., Kinney, H. C., Jensen-Jensen, F. E., and Rosenberg, P. A. (2011). The Developing Oligodendrocyte: Key Cellular Target in Brain Injury in the Premature Infant. *Int. J. Dev. Neurosci.* 29, 423–440. doi:10.1016/J.IJDEVNEU.2011.02.012
- Vorhees, C. V., Sprowles, J. N., Regan, S. L., and Williams, M. T. (2018). A Better Approach to *In Vivo* Developmental Neurotoxicity Assessment: Alignment of Rodent Testing with Effects Seen in Children after Neurotoxic Exposures. *Toxicol. Appl. Pharmacol.* 354, 176–190. doi:10.1016/J.TAAP.2018.03.012
- Wang, J. T., Song, L. Z., Li, L. L., Zhang, W., Chai, X. J., An, L., et al. (2015). Src Controls Neuronal Migration by Regulating the Activity of FAK and Cofilin. *Neuroscience* 292, 90–100. doi:10.1016/j.neuroscience.2015.02.025
- Wobus, A. M., and Löser, P. (2011). Present State and Future Perspectives of Using Pluripotent Stem Cells in Toxicology Research. *Arch. Toxicol.* 85, 79–117. doi:10.1007/s00204-010-0641-6
- Yang, J., Wu, C., Stefanescu, I., Jakobsson, L., Chervoneva, I., and Horowitz, A. (2016). RhoA Inhibits Neural Differentiation in Murine Stem Cells through Multiple Mechanisms. *Sci. Signal.* 9. doi:10.1126/scisignal.aaf0791
- Yang, P., Li, Z.-Q., Song, L., and Yin, Y.-Q. (2010). Protein Kinase C Regulates Neurite Outgrowth in Spinal Cord Neurons. *Neurosci. Bull.* 26, 117–125. doi:10.1007/s12264-010-1105-y
- Yeung, M. S. Y., Zdunek, S., Bergmann, O., Bernard, S., Salehpour, M., Alkass, K., et al. (2014). Dynamics of Oligodendrocyte Generation and Myelination in the Human Brain. *Cell* 159, 766–774. doi:10.1016/J.CELL.2014.10.011
- Yoon, K., and Gaiano, N. (2005). Notch Signaling in the Mammalian central Nervous System: Insights from Mouse Mutants. *Nat. Neurosci.* 8, 709–715. doi:10.1038/nn1475
- Zhang, R., Engler, A., and Taylor, V. (2018). Notch: an Interactive Player in Neurogenesis and Disease. *Cell Tissue Res* 371, 73–89. doi:10.1007/S00441-017-2641-9
- Zhou, F. C., and Chiang, Y. H. (1998). Long-term Nonpassaged EGF-Responsive Neural Precursor Cells Are Stem Cells. *Wound Repair Regen.* 6, S-337348. doi:10.1046/j.1524-475X.1998.60409.x
- Zhou, S., Szczesna, K., Ochalek, A., Kobilák, J., Varga, E., Nemes, C., et al. (2016a). Neurosphere Based Differentiation of Human iPSC Improves Astrocyte Differentiation. *Stem Cell Int.* 2016, 1–15. doi:10.1155/2016/4937689
- Zhou, W., He, Q., Zhang, C., He, X., Cui, Z., Liu, F., et al. (2016b). BLOS2 Negatively Regulates Notch Signaling during Neural and Hematopoietic Stem and Progenitor Cell Development. *Elife* 5, e18108. doi:10.7554/eLife.18108
- Zhu, G., Mehler, M. F., Zhao, J., Yu Yung, S., and Kessler, J. A. (1999). Sonic Hedgehog and BMP2 Exert Opposing Actions on Proliferation and Differentiation of Embryonic Neural Progenitor Cells. *Dev. Biol.* 215, 118–129. doi:10.1006/dbio.1999.9431
- Zikopoulos, B., and Barbas, H. (2010). Changes in Prefrontal Axons May Disrupt the Network in Autism. *J. Neurosci.* 30, 14595–14609. doi:10.1523/JNEUROSCI.2257-10.2010

Conflict of Interest: The authors declare that the research was conducted in the absence of any commercial or financial relationships that could be construed as a potential conflict of interest.

Publisher's Note: All claims expressed in this article are solely those of the authors and do not necessarily represent those of their affiliated organizations, or those of the publisher, the editors and the reviewers. Any product that may be evaluated in this article, or claim that may be made by its manufacturer, is not guaranteed or endorsed by the publisher.

Copyright © 2022 Koch, Bartmann, Hartmann, Kapr, Klose, Kuchovská, Pahl, Schlüppmann, Zühr and Fritsche. This is an open-access article distributed under the terms of the Creative Commons Attribution License (CC BY). The use, distribution or reproduction in other forums is permitted, provided the original author(s) and the copyright owner(s) are credited and that the original publication in this journal is cited, in accordance with accepted academic practice. No use, distribution or reproduction is permitted which does not comply with these terms.

Scientific validation of human neurosphere assays for developmental neurotoxicity evaluation

Katharina Koch, **Kristina Bartmann**, Julia Hartmann, Julia Kapr, Jördis Klose, Eliška Kuchovská, Melanie Pahl, Kevin Schlüppmann, Etta Zühr and Ellen Fritsche

Journal:	Frontiers in Toxicology
Impact factor:	-
Contribution to the publication:	15%
	Performance and evaluation of NPC3+4 experiments and writing of chapter 3.3 “Neuronal Differentiation and Morphology”
Type of authorship:	co-authorship
Status of publication:	Published 02 March 2022

2.2 Neurodevelopmental toxicity assessment of flame retardants using a human DNT *in vitro* testing battery

Jördis Klose, Melanie Pahl, **Kristina Bartmann**, Farina Bendt, Jonathan Blum, Xenia Dolde, Anna-Katharina Holzer, Ulrike Hübenthal, Hagen Eike Keßel, Katharina Koch, Stefan Masjosthusmann, Sabine Schneider, Lynn-Christin Stürzl, Selina Woeste, Andrea Rossi, Adrian Covaci, Mamta Behl, Marcel Leist, Julia Tigges, Ellen Fritsche

Cell Biology and Toxicology

Aufgrund ihrer Entwicklungsneurotoxizität (*developmental neurotoxicity*, DNT) wurden Flammschutzmittel (*flame retardants*, FR) wie beispielsweise polybromierte Diphenylether vom Markt verbannt und durch alternative Flammschutzmittel wie Organophosphor-Flammschutzmittel ersetzt, deren toxikologisches Profil weitgehend unbekannt ist. Um ihre Entwicklungsneurotoxizität zu untersuchen, haben wir die Gefährlichkeit verschiedener FRs, einschließlich der ausgemusterten polybromierten FRs und Organophosphor-Flammschutzmittel untersucht: 2,2',4,4'-Tetrabromdiphenylether (BDE-47), 2,2',4,4',5-Pentabromdiphenylether (BDE-99), Tetrabromobisphenol A, Triphenylphosphat, Tris(2-butoxyethyl)phosphat und dessen Metabolit Bis-(2-butoxyethyl)phosphat, Isodecyl diphenyl phosphat, Isopropyliertes Triphenylphosphat, Trikresylphosphat, Tris(1,3-Dichlor-2-propyl)phosphat, Tert-Butylphenyl diphenyl phosphat, 2-Ethylhexyldiphenylphosphat, Tris(1-chlorisopropyl)phosphat und Tris(2-chlorethyl)phosphat. Hierfür verwendeten wir eine auf humanen Zellen basierende DNT *in vitro* Testbatterie (DNT-IVB), welche eine Vielzahl von Schlüsselprozessen der Gehirnentwicklung abbildet. Die Potenz basierend auf der jeweils empfindlichsten Benchmark-Konzentration (BMC) in der Batterie lag zwischen <1 µM (5 FRs), 1<10 µM (7 FRs) bis hin zu >10 µM (3FRs). Die Auswertung der Daten mit dem ToxPiTool ergab eine andere Rangfolge (a) als mit den BMC Werten und (b) im Vergleich zu den ToxCast-Daten, was darauf hindeutet, dass das DNT-Potenzial dieser FRs durch ToxCast-Tests nicht so gut vorhergesagt wird. Die Extrapolation der DNT-IVB BMCs auf die menschliche FR-Exposition über die Muttermilch deutet auf ein geringes Risiko für einzelne Substanzen hin. Da der Mensch jedoch nicht einzelnen Verbindungen, sondern Gemischen ausgesetzt ist, kann es dennoch zu einem Risiko führen, insbesondere wenn verschiedene Verbindungen durch unterschiedliche Wirkungsweisen auf gemeinsame Endpunkte

einwirken wie in dieser Studie auf die Differenzierung von Oligodendrozyten. Diese Fallstudie legt nahe, dass die DNT-IVB auf der Basis humaner Zellen ein vielversprechender Ansatz für die Bewertung von entwicklungsneurologische Gefahreinschätzung und die Priorisierung von Substanzen bei der Risikobewertung darstellt.



Neurodevelopmental toxicity assessment of flame retardants using a human DNT in vitro testing battery

Jördis Klose · Melanie Pahl · Kristina Bartmann · Farina Bendt · Jonathan Blum · Xenia Dolde · Nils Förster · Anna-Katharina Holzer · Ulrike Hübenthal · Hagen Eike Keßel · Katharina Koch · Stefan Masjosthusmann · Sabine Schneider · Lynn-Christin Stürzl · Selina Woeste · Andrea Rossi · Adrian Covaci · Mamta Behl · Marcel Leist · Julia Tigges · Ellen Fritsche

Received: 16 November 2020 / Accepted: 11 March 2021
© The Author(s) 2021

Abstract Due to their neurodevelopmental toxicity, flame retardants (FRs) like polybrominated diphenyl ethers are banned from the market and replaced by alternative FRs, like organophosphorus FRs, that have mostly unknown toxicological profiles. To study their neurodevelopmental toxicity, we evaluated the hazard of several FRs including phased-out polybrominated FRs and organophosphorus FRs: 2,2',4,4'-tetrabromodiphenylether

(BDE-47), 2,2',4,4',5-pentabromodiphenylether (BDE-99), tetrabromobisphenol A, triphenyl phosphate, tris(2-butoxyethyl) phosphate and its metabolite bis-(2-butoxyethyl) phosphate, isodecyl diphenyl phosphate, triphenyl isopropylated phosphate, tricresyl phosphate, tris(1,3-dichloro-2-propyl) phosphate, tert-butylphenyl diphenyl phosphate, 2-ethylhexyl diphenyl phosphate, tris(1-chloroisopropyl) phosphate, and tris(2-chloroethyl)

Highlights

- A human DNT in vitro testing battery was applied for assessing hazards of phased-out and alternative flame retardants (FR) for prioritization.
- Oligodendrocyte development was identified as a common key event for FR-induced DNT in vitro.
- Multiple modes-of-action seem to contribute to oligodendrocyte toxicity.
- Prioritization of FRs according to the DNT in vitro battery differs from FRs ranking using ToxCast assays.

J. Klose · M. Pahl · K. Bartmann · F. Bendt · U. Hübenthal · H. E. Keßel · K. Koch · S. Masjosthusmann · S. Schneider · L.-C. Stürzl · S. Woeste · A. Rossi · J. Tigges · E. Fritsche
IUF-Leibniz Research Institute for Environmental Medicine,
Auf'm Hennekamp 50, 40225 Duesseldorf, NRW, Germany

J. Blum · X. Dolde · A.-K. Holzer · M. Leist
Department of Biology, University of Konstanz, Universitätsstraße
10, 78464 Konstanz, BW, Germany

N. Förster
Faculty for Biology and Biotechnology, Bioinformatics Group,
RUB – Ruhr University Bochum, Bochum, Germany

A. Covaci
Toxicological Centre, Department of Pharmaceutical Sciences,
University of Antwerp, Universiteitsplein 1, 2610 Wilrijk, Belgium

M. Behl
Division of the National Toxicology Program, National Institute of
Environmental Health Sciences, Research Triangle Park, Durham,
North Carolina 27709, USA

E. Fritsche (✉)
Medical Faculty, Heinrich-Heine-University, Universitätsstraße 1,
40225 Duesseldorf, NRW, Germany
e-mail: ellen.fritsche@uni-duesseldorf.de

phosphate. Therefore, we used a human cell-based developmental neurotoxicity (DNT) *in vitro* battery covering a large variety of neurodevelopmental endpoints. Potency according to the respective most sensitive benchmark concentration (BMC) across the battery ranked from <1 μM (5 FRs), 1<10 μM (7 FRs) to the >10 μM range (3 FRs). Evaluation of the data with the ToxPi tool revealed a distinct ranking (a) than with the BMC and (b) compared to the ToxCast data, suggesting that DNT hazard of these FRs is not well predicted by ToxCast assays. Extrapolating the DNT *in vitro* battery BMCs to human FR exposure via breast milk suggests low risk for individual compounds. However, it raises a potential concern for real-life mixture exposure, especially when different compounds converge through diverse modes-of-action on common endpoints, like oligodendrocyte differentiation in this study. This case study using FRs suggests that human cell-based DNT *in vitro* battery is a promising approach for neurodevelopmental hazard assessment and compound prioritization in risk assessment.

Keywords Developmental neurotoxicity · Flame retardants · Human cell-based testing battery · 3D *in vitro* model · New approach methodologies · Hazard assessment

Introduction

Flame retardants (FRs) inhibit or delay the spread of fire by suppressing chemical reactions in the flame or by forming a protective layer on the material surface (Damerud et al. 2001). They are used in commercial products, such as electronics, furniture, and textiles. Since the 1970s, polybrominated diphenyl ether (PBDEs) had been in use as FRs. However, due to their accumulation in environmental samples, house dust, food, animal and human tissues (Damerud et al. 2001; De Wit 2002; Law et al. 2014) and their adversity for human health, particularly neurodevelopment (Chao et al. 2007; Roze et al. 2009; Shy et al. 2011; Eskenazi et al. 2013), the European Commission and the U.S. Environmental Protection Agency (US EPA) caused a phase out of PBDEs in 2004 (Blum et al. 2019). Despite their market ban, they are still present in the environment (Yogui and Sericano 2009; Ma et al. 2013; Law et al. 2014). With the phasing out, PBDEs were replaced by presumably safer and less persistent alternative FRs (aFRs), including organophosphorus FRs (OPFRs). Several aFRs were released onto the market,

although their kinetics and toxicities, specifically their neurodevelopmental hazards, have not been sufficiently investigated. Available data on the physico-chemical properties, environmental persistence, bioaccumulation, and toxicity of a subset of aFRs recently displayed large data gaps (van der Veen and de Boer 2012; Bergman et al. 2012; Waaijers et al. 2013). Similar to PBDEs, there has been growing evidence of widespread exposure to aFRs, as they were found in house dust, furniture foam, and baby articles (Stapleton et al. 2009; Sugeng et al. 2017), as well as in hand wipes and urine samples of children (Stapleton et al. 2014; Mizouchi et al. 2015; He et al. 2018a, b; Bastiaensen et al. 2019a). In general, children and especially toddlers are highly exposed towards FRs as they frequently spend their time close to the floor and exercise children-specific mouthing behavior (Fischer et al. 2006; Toms et al. 2009; Sugeng et al. 2017). Due to this high exposure and the fact that the developmental nervous system is a sensitive target organ for many FRs and organophosphorus pesticides (Muñoz-Quezada et al. 2013), which are structurally similar to OPFRs, it is essential to assess the developmental neurotoxicity (DNT) potential of aFRs (Hirsch et al. 2017).

Current DNT testing follows the *in vivo* guideline studies OECD 426 (OECD 2007) or EPA 870.6300 (EPA 1998) performed with rats. These studies are highly demanding with regard to time, money, and animals (Lein et al. 2005; Crofton et al. 2012) and are not suited for large scale DNT testing. Further limitations include their high variability and lack of reproducibility, as well as the uncertainty of extrapolation from animals to humans (Tsuji and Crofton 2012; Terron and Bennekou Hougaard 2018; Sachana et al. 2019). Therefore, regulators, academic, and industrial scientists recently agreed on a need for a new testing strategy to assess the DNT potential of chemicals (Crofton et al. 2014; Bal-Price et al. 2015; Fritsche et al. 2018b). A mechanistically informed, fit-for-purpose, human-relevant *in vitro* DNT test battery was suggested that covers different neurodevelopmental processes and stages (Andersen 2003; Bal-Price et al. 2018) and allows a faster and cheaper evaluation of substances for their DNT potential (EFSA 2013; Bal-Price et al. 2015, 2018; Fritsche et al. 2015, 2017, 2018a).

In this study, human-induced pluripotent stem cell (hiPSC)-derived neural crest cells (NCC), lund human mesencephalic cells (LUHMES), 3D human primary neural progenitor cell (NPC)-based neurospheres, as well as hiPSC-derived peripheral neurons were applied to study distinct neurodevelopmental key events (KEs)

in vitro. These KEs include NPC proliferation (NPC1), NCC (cMINC/UKN2), radial glia (NPC2a), neuronal (NPC2b) and oligodendrocyte (NPC2c) migration, differentiation into neurons (NPC3), neurite morphology (NPC4, NeuriTox/UKN4, PeriTox/UKN5), and oligodendrocyte differentiation (NPC5; Baumann et al. 2016; Barenys et al. 2017; Schmidt et al. 2017; Fritsche et al. 2018a; Masjosthusmann et al. 2018; Nimtz et al. 2019; Krebs et al. 2020b). These assays comprise a current DNT in vitro testing battery that was recently assembled to test 119 compounds (e.g., carbamates, metals, neonicotinoids, organochlorines/fluorines, and organophosphates pyrethroids) for regulatory purposes. Using selected known human DNT positive and negative compounds as benchmark, this battery performed with a sensitivity of 100% and a specificity of 88% (Masjosthusmann et al. 2020).

To study the neurodevelopmental hazard of FRs, we analyzed their adverse effects on the endpoints of this battery of human neurodevelopmental assays. FRs used include a set of phased-out and currently in use compounds. The phased-out FRs are PBDEs 2,2',4,4'-tetrabromodiphenylether (BDE-47) and 2,2',4,4',5-pentabromodiphenylether (BDE-99), while the current-use FRs include the organophosphorus FRs (OPFRs), such as triphenyl phosphate (TPHP), tris (2-butoxyethyl) phosphate (TBOEP) and its metabolite bis-(2-butoxyethyl) phosphate (BBOEP), isodecyl diphenyl phosphate (IDDPHP), triphenyl isopropylated phosphate (IPPHP), tricresyl phosphate (TCP), tris (1,3-dichloro-isopropyl) phosphate (TDCIPP), tert-butylphenyl diphenyl phosphate (t-BPDPHP), tri-O-cresyl phosphate (TOCP), 2-ethylhexyl diphenyl phosphate (EHDPHP), tris (1-chloro-isopropyl) phosphate (TCIPP), and tris (2-chloroethyl) phosphate (TCEP), as well as the brominated FR Tetrabromobisphenol A (TBBPA) (Table S1). The in vitro data were related to hazardous doses by toxicokinetic considerations. Moreover, such data were compared to potential exposure situations. Relating the phenomics of the in vitro methods to molecular signatures, we performed RNA sequencing analyses. This approach represents a case study for a new risk assessment paradigm for DNT by using phenotypic readouts of human cell-based assays that cover a variety of neurodevelopmental endpoints and studying their molecular signatures in response to different FRs.

Material and methods

Chemicals

TBBPA, BDE-99, TCEP, TPHP, TOCP, and TBOEP (for NPC assays) were purchased from Sigma-Aldrich and were dissolved as 50 mM and 20 mM stocks in dimethyl sulfoxide (DMSO; Carl Roth GmbH). The metabolite BBOEP (1500 ng/ μ L in Methanol) was custom synthesized by Dr. Vladimir Belov (Max Planck Institute, Göttingen, Germany) with a purity > 98% as measured by MS and NMR techniques. The FRs TCIPP, t-BPDPHP, and EHDPHP were obtained from ToxCast and are diluted in DMSO with stock concentration of 20 mM. All other flame retardants IDDPHP, IPPHP, TCP, TDCIPP, BDE-47 (for NPC assays) as well as TBBPA, BDE-47, BDE-99, TCEP, TPHP, IDDPHP, IPPHP, EHDPHP, t-BPDPHP, and TCP (for UKN assays) were provided by M. Behl from the National Toxicology Program, and stock solutions of 20 mM in DMSO were prepared. Solvent concentrations were 0.1% DMSO and 0.4% MeOH for BBOEP in dose-response experiments.

Cell culture

Human NPCs (hNPCs) from three different individuals (gestational week 16-19) were purchased from Lonza Verviers SPRL, Belgium. They were thawed and isolated as previously described (Baumann et al. 2016). hNPCs were cultured as free floating neurospheres in proliferation medium consisting of DMEM (Life Technologies) and Hams F12 (Life Technologies) (3:1) supplemented with 2% B27 (Life Technologies), 20 ng/mL EGF (Thermo Fisher), FGF (R&D Systems), and 1% penicillin and streptomycin (Pan-Biotech). Neurospheres were cultivated at 37 °C with 5% CO₂, passaged mechanically with a tissue chopper (McIlwain) once a week and thrice a week half of the medium was replaced.

For the cMINC assay (UKN2), NCCs are differentiated from the hiPSC line IMR90_clone #4 (WiCell, Wisconsin) by plating cells on Matrigel-coated 6-well plates (Falcon) at a density of 50000 cells/cm². One day prior differentiation, cells are cultivated in essential 8 (E8) medium (DMEM/F12 supplemented with 15 mM Hepes, 16 mg/mL L-ascorbic-acid, 0.7 mg/mL sodium selenite, 20 μ g/mL insulin, 10 μ g/mL holo-transferrin, 100 ng/mL bFGF, 1.74 ng/mL TGF β) containing

10 μM Rock inhibitor. Until 11 days in vitro (DIV), cells receive KSR medium (knock out DMEM, 15% knock out serum replacement, 1% GlutaMax, 1% MEM NEAA solution, 50 μM 2-mercaptoethanol) which is gradually replaced by 25% increments of N2-S medium (DMEM/F12, 1.55 mg/mL glucose, 1% GlutaMax, 0.1 mg/mL apotransferrin, 25 $\mu\text{g}/\text{mL}$ insulin, 20 nM progesterone, 100 μM putrescine, 30 nM selenium). From -1 DIV to 11 DIV, cells are cultured at 37 °C with 5% CO_2 and a daily medium change was performed. From 0 DIV to 2 DIV, medium is supplemented with 20 ng/mL Noggin. From 0 DIV to 3 DIV, it is supplemented with 10 μM SB431542 and from 2 DIV to 11 DIV with 3 μM CHIR 99021. After 11 DIV, cells are detached and resuspended in N2-S medium supplemented with 20 ng/mL EGF and 20 ng/mL FGF2 and seeded as droplets (10 μL) on poly-L-ornithine (PLO)/laminin/fibronectin-coated 10-cm dishes. Until 39 DIV, cells are expanded by weekly splitting in N2-S medium supplied with EGF and FGF2 and a medium change is performed every other day. On 39 DIV, cells are detached, resuspended in freeze medium (FBS with 10% DMSO), and frozen at a concentration of 4×10^6 cells per mL at -80 °C overnight. After 24 h, cells are stored in liquid nitrogen until further use.

For the NeuroTox assay (UKN4), LUHMES cells are cultured and handled as described before (Lotharius et al. 2005; Scholz et al. 2011; Krug et al. 2013a). They are maintained in proliferation medium (PMed; AdvDMEM/F12 supplemented with 2 mM glutamine, 1 \times N2 supplement and 40 ng/mL FGF) at 37 °C with 5% CO_2 . Cells are passaged every second or third day when reaching approximately 80% confluency. For pre-differentiation, 8×10^6 (45000 cells/cm²) cells are seeded one day before in PMed. Differentiation is started by switching to differentiation medium (DMed; AdvDMEM/F12 supplemented with 2 mM glutamine, 1 \times N2 supplement, 2.25 μM tetracycline, 1 mM dibutyryl cAMP and 2 ng/mL GDNF).

For the PeriTox assay (UKN5), sensory neurons are differentiated from the hiPSC line SBAD2, which was derived and characterized at the University of Newcastle from Lonza fibroblasts CC-2511, Lot 293971 with the tissue acquisition number 24245 (Baud et al. 2017). Culturing, handling, and differentiation are performed according to standard protocols (Thomson et al. 1998; Chambers et al. 2013; Hoelting et al. 2016). Generation of sensory neurons is started on -2 DIV by resuspending hiPSCs in E8 medium containing 10 μM

Rock inhibitor Y-27632. After replating cells at a density of 55000 cells/cm² on Matrigel coated 6-well plates (Falcon), a daily medium change is performed from -1 DIV until 10 DIV. E8 medium supplemented with rock inhibitor (10 μM) is refreshed on -1 DIV. On 0 DIV, neural differentiation is initiated and until 10 DIV cells receive KSR medium which is, from 4 DIV onward, gradually replaced by 25% increments of N2-S medium. Until 4 DIV medium is supplied with 35 ng/mL Noggin, 600 nM dorsomorphin and 10 μM SB431542 to initiate neutralization via dual-SMAD inhibition. From 2 DIV to 10 DIV, three further pathway inhibitors are added (1.5 μM CHIR99021, 5 μM SU5402, and 5 μM DAPT). On 10 DIV, cells are detached, resuspended in freeze medium (FBS with 10% DMSO) and frozen at a concentration of 8×10^6 cells per mL at -80 °C overnight. After 24 h, cells are stored in liquid nitrogen until further use.

The “neurosphere assay”—NPC1-5

hNPCs were chopped to 0.2 mm 2–3 days before plating to reach a defined size of 0.3 mm. Each compound was tested in serial dilution (1:3) with 7 concentrations and a solvent control (SC) plated in five replicate wells per condition in 96-well plates (proliferation U-bottom, Falcon; differentiation flat bottom, Greiner). Each well contained one sphere in 100 μL of the respective medium and FR/solvent(s) (proliferation medium (description in “Cell culture”); differentiation medium consisting of DMEM (Life Technologies), Hams F12 (Life Technologies) 3:1 supplemented with 1% of N2 (Life Technologies) and 1% penicillin and streptomycin (Pan-Biotech)). The 1:3 solution series and plate filling, LDH, CTB, and feeding step were performed automatically by STARlet 8 ML pipette robot system (MICROLAB STAR® M; Hamilton).

Proliferation

The proliferation by area (NPC1a) was assessed as slope of the increase in sphere size up to 3 DIV (0 h, 24 h, 48 h, and 72 h) measured by brightfield microscopy and using high content imaging (Cellomics Scan software, Version 6.6.0; Thermo Fisher Scientific). Proliferation by bromodeoxyuridine (BrdU; NPC1b) was analyzed after 3 DIV via a luminescence-based BrdU Assay (Roche) as previously published in Nimtz et al. (2019).

Immunocytochemical stainings

By plating neurospheres into 100 μ L differentiation medium on a poly-D-lysine (0.1 mg/mL, Sigma-Aldrich) and laminin (12.5 μ g/mL, Sigma-Aldrich)-coated 96-well plate (flat bottom, Greiner), spheres settle down and NPCs migrate radially out of the sphere core concurrently differentiating, into radial glia, neurons, and oligodendrocytes. After 5 days of migration and differentiation, human neurospheres were fixed with 4% paraformaldehyde (PFA, Merck) for 30 min at 37 °C and directly afterwards washed three times for 3 min with 250 μ L PBS (Biochrom) before stored at 4 °C until staining. Cells were always covered with 40 μ L PBS, and for staining, 10 μ L blocking solution (PBS, 50% Goat Serum (GS, Sigma-Aldrich) and 5% Bovines Serum Albumin (BSA, Serva Electrophoresis)) per well was added and incubated for 15 min at 37 °C. After removal of 10 μ L, cells were stained overnight at 4 °C with 10 μ L mouse IgM oligodendrocyte O4 antibody solution 1:400 (in PBS with 10% GS and 1% BSA; R&D System) followed by three 3-min washing steps by addition and removal of 250 μ L PBS. After the last washing step, 260 μ L was removed and 10 μ L secondary antibody solution in PBS (1:400 Alexa Fluor 488 anti-mouse IgM (Life Technologies), 10% GS, 5% BSA) was added for 30 min at 37 °C. After washing steps as previously described, cells were fixed a second time for 30 min at 37 °C in 4% PFA, followed by three 3-min washing steps and permeabilization in 0.5% PBS-T for 5 min at room temperature. Afterwards, cells were blocked for 15 min at 37 °C with 10 μ L PBS, 50% Rabbit Serum (RS, Sigma-Aldrich), and 5% BSA. For neuronal staining, neurospheres were incubated for 1 h at 37 °C with 10 μ L conjugated rabbit TUBB3 674 antibody (Abcam) 1:400 (in PBS with 10% RS, 1% BSA, and 5% Hoechst 33258 (Sigma-Aldrich)). After three additional 3-min washing steps, 250 μ L PBS was added to each well and the plates were stored in the dark at 4 °C. Images of immunocytochemical stainings of three channels (386 nm for Hoechst stained nuclei, 647 nm for β (III)tubulin stained neurons, 488 nm for O4 stained oligodendrocytes) were acquired with a 200-fold magnification and a resolution of 552 \times 552 pixel using the HCS Studio Cellomics software (version 6.6.0; Thermo Fisher Scientific).

Migration and differentiation

Radial glia migration distance (72 h, NPC2a) was analyzed by manual measurement of the radial migration

from the sphere core on brightfield images as number of pixels which is converted to micrometers. After 120 h, it is assessed by automatically identifying (Schmuck et al. 2016) the migration area of each sphere of Hoechst stained nuclei on fluorescence images. The migration distance of neurons (NPC2b) and oligodendrocytes (NPC2c) is defined as mean distance of all neurons/oligodendrocytes within the migration area divided by radial glia migration distance after 120 h. The differentiation into neurons (NPC3) and oligodendrocytes (NPC5) is determined as number of all β (III)tubulin and O4-positive cells in percent of the total amount of Hoechst-positive nuclei in the migration area and is performed automatically using two convolutional neural networks (CNN) based on the Keras architecture implemented in Python 3, which were trained to identify both cell types. All neurons that were identified in NPC3 are analyzed for their morphology (NPC4) by characterizing the neurite length (in μ m) and area (amount of pixel). Detection of migration (120 h, NPC2) and morphological analysis (NPC4) is calculated automatically by high-content image analysis (HCA) tool Omnisphero (Schmuck et al. 2016). Migrating/differentiating neurospheres were exposed to FRs/solvent(s) for 5 days. On day 3, half of the exposure/solvent medium was exchanged and the supernatant was used to detect cytotoxicity by measuring lactate dehydrogenase (LDH) leakage.

“cMINC assay” UKN2

NCCs were thawed and seeded into 96-well plates in N2-S medium containing FGF2 and EGF according to the previously published protocol (Nyffeler et al. 2017). Cells were seeded around stoppers to create a circular cell-free area and after 24 h stoppers were removed to allow cell migration. One day later, cells were exposed to FRs/solvent(s) for 24 h. The number of migrated cells into the cell free zone was quantified 48 h after stopper removal and 24 h after treatment. Cells were stained with Calcein-AM and Hoechst-33342 (H-33342), and high content imaging was performed. Four images for migration were taken to cover the region of interest (ROI) using a high content imaging microscope (Cellomics ArrayScanVTI), and Calcein and H-33342 double-positive cell numbers were determined by an automated algorithm (RingAssay software; <http://invitro-tox.uni-konstanz.de>). For viability, four fields close to the well borders, i.e., outside the ROI,

were imaged. Viable cells were defined by double-positivity for H-33342 and calcein and determined by an automated algorithm as described before (Nyffeler et al. 2017). TBBPA, BDE-47, BDE-99, IDDPHP, TCP, t-BPDPHP, and EHDPHP were tested in serial dilution (1:2) with 6 concentrations and SC, while TPHP and IPPHP were tested with 5 concentrations (Nyffeler et al. 2017). TCEP, TDCIPP, and TCIPP were negative within a 20- μ M pre-screening and therefore not tested further (data not shown). TBOEP, BBOEP, and TOCP were tested 1:3 with 6 concentrations and SC based on the method described in this study. Each compound concentration was plated in 4 replicate wells per condition.

“NeuriTox assay” UKN4

After 2 days of differentiation, 30000 LUHMES cells were reseeded into each well of a 96-well plate in DMed containing only tetracycline. After cells' attachment for 1 h, they were exposed to FRs/solvent(s) for 24 h. One hour before read-out, cells were stained with Calcein-AM and H-33342 and imaged via a high-content imaging microscope (Cellomics ArrayScanVTI, Thermo Fisher Scientific) to assess neurite area. For neurite area determination, an automated algorithm was used, which calculates the area of the cell soma and subtracts this area from all calcein-positive pixels imaged (Stiegler et al. 2011; Krug et al. 2013a). To assess viability, all stained nuclei (H-33342 positive) are used to determine total cell number and H-33342 and calcein double-positive cells are defined as viable cells (Stiegler et al. 2011; Krug et al. 2013a). Each compound was tested in serial dilutions (1:3) with 10 concentrations starting at 20 μ M and SC plated in three replica wells per condition. Effects of TBBPA, BDE-47, BDE-99, IDDPHP, TCP, t-BPDPHP, EHDPHP, TPHP, and IPPHP were assessed in a previous screening (Delp et al. 2018). TDCIPP, TOCP, and TCIPP were negative in a pre-screening at 20 μ M and therefore not tested any further (data not shown).

“PeriTox assay” UKN5

Differentiated sensory neurons were thawed and seeded in 25% KSR/75% N2-S medium supplemented with 1.5 μ M CHIR99021, 5 μ M SU5402, and 5 μ M DAPT into 96-well plates at a density of 100000 cells per cm^2 . After cells' attachment for 1 h, they were exposed to

FRs/solvent(s) for 24 h. Assessments of neurite area and viability of the cells were performed as described above for the UKN4 assay. Each compound concentration was tested in three wells per plate (technical replicates) in a serial dilution (1:3) with 6 concentrations starting at 20 μ M and SC. Effects of TBBPA, BDE-47, BDE-99, IDDPHP, TCP, t-BPDPHP, EHDPHP, TPHP, and IPPHP were assessed in a previous screening (Delp et al. 2018). TDCIPP, TOCP, and TCIPP were negative in a pre-screening at 20 μ M and therefore not tested any further (data not shown).

Viability and cytotoxicity

To distinguish compound effects from secondary effects due to loss of viability and cytotoxicity, respective assays were performed in parallel. Thereby, all viability and cytotoxicity assays are multiplexed within the respective assay. hNPC viability was assessed as mitochondrial activity by using an Alamar blue assay (CellTiter-Blue Assay (CTB); Promega) in the last 2 h of the respective compound treatment period (NPC1 at 3 DIV; NPC2-5 at 5 DIV). Cytotoxicity of treated hNPCs was detected by measuring LDH (CytoTox-ONE membrane integrity Assay; Promega) after 3 (NPC1; NPC2-5) and 5 (NPC2-5) DIV. It is of note that a reduced radial glia migration area causes a reduction in the CTB readout due to a diminished cell number without necessarily affecting cell viability (Fritsche et al. 2018a). Thus, when radial glia migration is inhibited by a compound, the LDH assay is solely the reference for DNT specificity of NPC2-5. Assessment of viability within the UKN assays was performed as described above.

RNA sequencing and RT-qPCR

For RNA sequencing (RNASeq) experiments, 1000 neurospheres per well with a defined size of 0.1 mm were plated onto PDL/laminin-coated 6-well plates and cultivated for 60 h in the presence and absence of selected FRs. The RNA isolation was performed using the RNeasy Mini Kit (Qiagen) according to the manufacturer's protocol. Total RNA was analyzed for high quality using the Agilent High Sensitivity RNA ScreenTape System for Agilent 4150 TapeStation Bioanalyzer (Agilent Technologies) for human samples with an RNA integrity number (RIN) \geq 8. All samples in this study showed high-quality RINs \geq 8.5. For RNASeq,

1.0 µg total RNA was used for library preparation using the TruSeq RNA Sample Prep Kit v2 according to the manufacturer's protocol (Illumina). All steps of the protocol were performed as described in the Illumina kit. DNA library templates were quantified using the Qubit™ 4 Fluorometer and the Qubit 1× dsDNA HS Assay Kit (Thermo Fisher Scientific). Quality control and fragment size analysis were performed on Agilent 4150 TapeStation System and the Agilent D1000 Screen Tape System (Agilent Technologies). Sequencing was performed on a MiSeq instrument (Illumina) using v3 chemistry, resulting in an average of 50 million reads per library with 1×76 bp paired end setup.

Raw data were uploaded on BaseSpace Sequence Hub (Illumina) for FastQ generation. RNAseq analysis was performed using the Illumina pipeline (Illumina Annotation Engine 2.0.10.0). The resulting raw reads were assessed for quality, adapter content and duplication rates with the Illumina FASTQ file generation pipeline. Trimmed and filtered reads were aligned versus the *Homo sapiens* reference genome (UCSC hg19) using STAR Aligner (STAR_2.6.1a). Total number of reads was quantified using both TopHat2 and Salmon Quantification (0.11.2). Strelka Variant Caller (2.9.9) was used to detect somatic single nucleotide variants (SNVs).

Quantitative real-time polymerase chain reaction (RT-qPCR) was performed with the QuantiFast SYBR Green PCR Kit (Qiagen) within the Rotor Gene Q Cycler (Qiagen). Therefore, 250 ng RNA was transcribed into cDNA using the QuantiTect Reverse Transcription Kit (Qiagen) according to manufacturer's instructions. Analysis was performed using the software Rotor-Gene Q Series version 2.3.4 (Qiagen). Copy numbers (CN) of the genes of interest were calculated by using gene-specific copy number standards as described previously in detail (Walter et al. 2019) and normalized to the housekeeping gene *beta-actin*. Gene CN of solvent control and FR treated differentiated spheres were normalized to proliferative spheres, which are thought to express very low numbers of oligodendrocyte-specific mRNA. Here, the solvent control visualizes oligodendrocyte-related gene expression as a function of normal NPC development that can directly be compared to sphere development in presence of FRs.

Toxicological Priority Index

For relative toxicological ranking and hierarchical clustering, the BMC values of the tested FRs were integrated

and visualized by using the Toxicological Priority Index Graphical User Interface (ToxPi GUI) version 2.3 (Gangwal et al. 2012). In ToxPi, the BMC values across the data set of each endpoint were scaled with the formula $-\log_{10}(x)+6$ from 0 to 1, while 1 represents the lowest BMC and therefore the most potent compound. If BMC was not reached, a concentration of 10^6 was applied before, which became 0 upon scaling. Data are visualized in a pie chart, where every slice represents one DNT endpoint (Fig. 7). The farther the slice extends from its origin, the more potent the compound in this endpoint. In comparison, ToxCast data was used to give an initial idea on the general toxicity of these FRs across a variety of assays. Regarding ToxCast AC_{50} (half-maximal activity concentration), values below a given cytotoxicity limit were used and scaled as described above. Each slide was assigned as one intended target family and contains several assays for respective endpoints.

Data analysis and statistics

All neurosphere experiments were performed with at least two different individuals. Experiments were defined as independent if they were generated with NPCs from different individuals or from a different passage of cells. For cMINC, NeuroTox, and PeriTox assays, biological replicates represent an independent experiment on another day with a different batch of NCCs, LUHMES cells, or 10 DIV sensory neurons thawed. If not otherwise indicated, results are presented as mean \pm SEM. For dose-response curves, a sigmoidal (variable slope) or bell-shaped curve fit was applied using GraphPad Prism 8.2.1. Statistical significance was calculated using the same software and one-way ANOVA with Bonferroni's post hoc tests ($p \leq 0.05$ was termed significant).

BMC as well as upper and lower confidence intervals (CI) were calculated with GraphPad Prism 8.2.1. Based on overlap of confidence intervals of the BMCs calculated for the DNT-specific endpoints and the endpoints related to cytotoxicity/viability, NPC endpoints were classified as DNT-specific (no CI overlap), unspecific (CI overlap $\geq 10\%$), or borderline ($0 > CI < 10\%$; Masjosthusmann et al. 2020). The classification model applied for UKN assays is based on a ratio cutoff for the ratio between the BMC for cell viability and the specific endpoints (ratio BMC_{10} viability/ BMC_{25} migration ≥ 1.3 in UKN2 assay; ratio BMC_{25} viability/ BMC_{25}

neurite area ≥ 4 in UKN4 assay or ≥ 3 in UKN5 assay). This is in line with the respective classification models suggested in previous publications (Krug et al. 2013b; Hoelting et al. 2016; Nyffeler et al. 2017).

Results

Experimental design of the human DNT testing battery

We assessed the neurodevelopmental hazard of 15 FRs (Table S1) and analyzed their adverse effects using a battery of human-based neurodevelopmental in vitro assays (Fig. 1). Within NPC assays, proliferation (NPC1), migration (NPC2), and differentiation into the main effector cells of the human brain, i.e., radial glia, neurons (NPC3), and oligodendrocytes (NPC5), were evaluated. NPC3 was multiplexed with NPC4, which quantifies neurite morphology by analyzing their length and area. The cMINC (UKN2) assay measures neural crest cell (NCC) migration and viability, while NeuroTox (UKN4) and PeriTox (UKN5) assays assess neurite morphology and viability of LUHMES cells and hiPSC-derived peripheral neurons, respectively. Finally, cytotoxicity was assessed after 3 (NPC1) and 5 (NPC2-5) DIV and cell viability was detected at the end of each assay. Additionally, RNA sequencing analyses provide further insight into the modes-of-action of FR toxicity.

Three out of the 15 analyzed FRs (BBOEP, TCIPP, and TCEP) did not produce significant effects in any of the tested endpoints up to a concentration of 20 μM . Therefore, the respective graphs are shown in supplementary Figs. S1–3.

hNPC proliferation is exclusively disturbed by alternative flame retardants

A fundamental neurodevelopmental KE is NPC proliferation. The analyzed PBDEs and aFRs did not affect sphere area increase over time (NPC1a; Fig. 2(a)). BrdU incorporation (NPC1b), however, as a direct measure of DNA synthesis has a higher sensitivity than NPC1a and EHDPHP and TCP reduced BrdU incorporation significantly (Fig. 2(b)) with EHDPHP being the more potent one with significant diminution of proliferation at 0.25 μM and 20 μM to $70.5 \pm 4.3\%$ and $37.4 \pm 2.7\%$ of the controls, respectively. TCP inhibited proliferation to $65.9 \pm 8.3\%$ and $58.5 \pm 6.8\%$ of controls at 6.6 μM and 20 μM ,

respectively. Neither viability nor cytotoxicity were altered by any of the analyzed FRs at the employed concentration levels, with the exception of IPPHP, which induced the mitochondrial activity at the highest concentration up to $121.1 \pm 4.9\%$ of control. The endpoint-specific control for NPC1 was hNPC cultivation in absence of growth factors causing significantly reduced proliferation (Suppl. Fig. 4(a, b)).

FRs affect migration in a cell type-specific manner

Next, we analyzed NCC (UKN2), radial glia (NPC2a), neuronal (NPC2b), and oligodendrocyte (NPC2c) migration in the presence and absence of FRs. NCC migration was affected by PBDEs, as well as organophosphorus aFRs and was significantly inhibited by 9 out of the 15 FRs tested (Fig. 3(a)). TBBPA reduced NCC migration to $52.6 \pm 9.2\%$ and $31.3 \pm 3.5\%$ of control at 2.5 μM and 5 μM , respectively (Fig. 3(a, c)). BDE-47, t-BDPHP, and TCP ($\geq 5 \mu\text{M}$) significantly reduced the number of migrating NCCs to $37.1 \pm 9.6\%$, $53.5 \pm 4.8\%$, and $56.6 \pm 4.4\%$ of controls, respectively. TOCP (6.67 μM) and BDE-99 (10 μM) significantly inhibited NCC migration to $43.2 \pm 7.6\%$ and $69.5 \pm 6.7\%$ of controls, respectively, while EHDPHP, IDDPHP, and TPHP disturbed NCC migration at the highest concentration to $31.8 \pm 23.1\%$, $52.7 \pm 10.6\%$, and $65.3 \pm 10.2\%$ of respective controls. NCC viability was significantly affected by 5 μM TBBPA ($81.1 \pm 1.7\%$); by $\geq 10 \mu\text{M}$ EHDPHP ($\leq 93.8 \pm 2.7\%$), TCP ($\leq 90.9 \pm 1.0\%$), and IPPHP ($\leq 93.1 \pm 1.2\%$); and by 20 μM BDE-47 ($86.6 \pm 5.5\%$) and TOCP ($63.3 \pm 10.2\%$; Fig. 3(b)). Cytochalasin D (200 nM) served as an endpoint specific control for UKN2 (data not shown). Similar to NCC migration, TBBPA is the most potent FR for hNPC migration inhibition, significantly disturbing radial glia (NPC2a), neuron (NPC2b), and oligodendrocyte (NPC2c) migration at concentrations $\geq 2.2 \mu\text{M}$ (Fig. 3(d, g)). Consequently, TBBPA decreased respective CTB values at concentrations $\geq 2.2 \mu\text{M}$ to $\leq 64.8 \pm 2.7\%$ of controls. However, also cytotoxicity was induced to $25.1 \pm 3.3\%$ (72 h) and $25.4 \pm 2.0\%$ (120 h) of the lysis control at concentrations $\geq 2.2 \mu\text{M}$ TBBPA (Fig. 3(e)).

The phased-out PBDEs did not affect migration behavior of differentiating hNPCs, while some OFFRs (TPHP, TDCIPP, IPPHP, and t-BDPHP) disturbed radial glia and oligodendrocyte migration selectively at the highest concentration of 20 μM . After 72 h, TPHP and TDCIPP inhibited radial glia migration to $86.3 \pm$

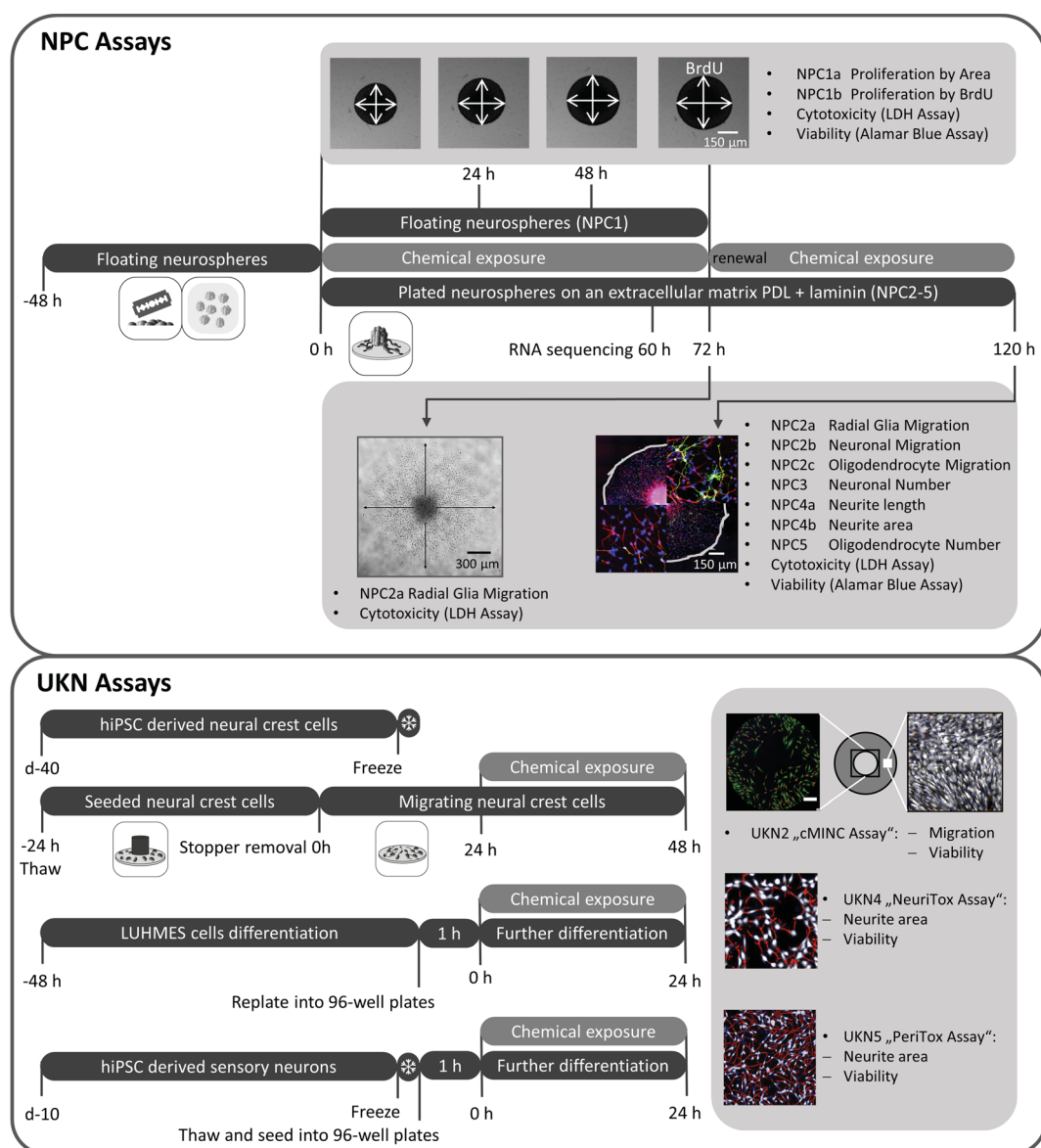


Fig. 1 Schematic overview of the battery of human-based neurodevelopmental in vitro assays. Experimental procedures for single assays are depicted schematically. Single endpoints

investigated by the battery assays are listed in gray boxes with their respective readout approach. PDL, poly-D-lysine; BrdU, bromodeoxyuridine; LDH, lactate dehydrogenase

2.9% and $90.5 \pm 2.5\%$ of controls, respectively (Fig. 3(f)). After 120 h, the influence of TPHP was reversed demonstrating the adaptive capabilities of the system. IPPHP, TDCIPP, and t-BPDPHP inhibited radial glia migration (120 h) decreasing the distance to $85.6 \pm 8.1\%$, $82.2 \pm 3.8\%$, and $71.5 \pm 14.0\%$ of respective controls (Fig. 3(h)). None of the tested FRs altered neuronal migration distance (Fig. 3(i)), while oligodendrocyte migration was significantly shortened at $20 \mu\text{M}$ of EHDPHP, IPPHP, and t-BPDPHP to $83.6 \pm 3.5\%$,

$83.0 \pm 7.2\%$, and $73.1 \pm 8.3\%$ of respective controls (Fig. 3(j)). Both phased-out PBDEs and OPFRs did not impact cell viability/cytotoxicity at the conditions tested, except for TDCIPP ($20 \mu\text{M}$) reducing mitochondrial activity (Fig. 3(k)). Strikingly, $6.6 \mu\text{M}$ and $20 \mu\text{M}$ IDDPHP increased cell viability to $133.2 \pm 4.9\%$ and $151.4 \pm 13.0\%$ of control, respectively, without affecting migration distance. The same effect was caused by $20 \mu\text{M}$ EHDPHP (Fig. 3(h, k)). The endpoint-specific control for NPC2 was the src-kinase inhibitor PP2

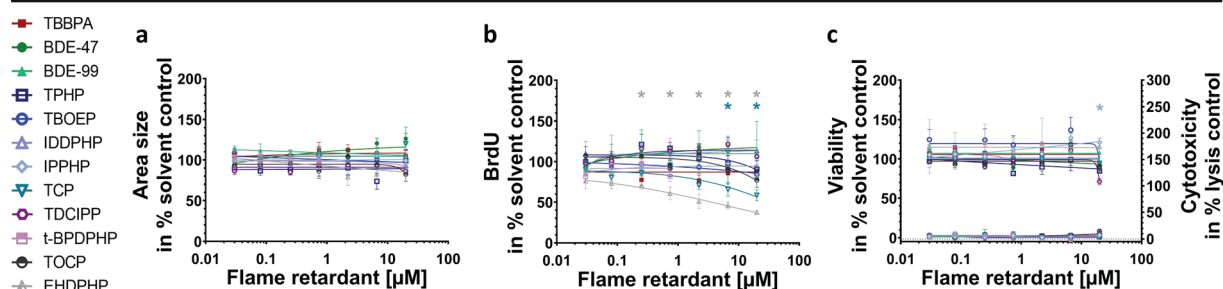


Fig. 2. Influence of FRs on proliferative hNPCs (NPC1). Spheres were plated in 96-well U-bottom plates and exposed to increasing FRs concentration over 72 h. Proliferation was studied by measuring the increase of sphere area (NPC1a) (a) and by quantifying BrdU incorporation (NPC1b) (b) into the DNA. In parallel, viability and cytotoxicity (c) were assessed by performing Alamar Blue Assay and LDH Assay. Data are represented as means \pm

SEM (except EHDPHP in NPC1a and CTB $n=2$ mean \pm SD). Highest concentrations (≥ 2.2 µM) of t-BPDPHP are not shown as spheres attached and differentiated. Statistical significance was calculated using one-way ANOVA followed by Bonferroni's post hoc tests ($p \leq 0.05$ was considered significant). BrdU, bromodeoxyuridine

significantly reducing migration to $36.9 \pm 29.9\%$ of control (Suppl. Fig. 4(c)).

Phased-out PBDEs and OPFRs do not interfere with neuronal differentiation and hardly affect neurite morphology

Within the migration area, hNPCs differentiate into different effector cells. In this study, 9.8% of the cells differentiated into neurons (Suppl. Fig. 4d). To analyze the influences of FRs on hNPC neuronal differentiation and neuronal morphology, NPC3 and NPC4 were performed. TBBPA (2.2 µM) reduced the total number of nuclei significantly to $60.8 \pm 7.0\%$ of control (Fig. 4(a, e)), which agrees with inhibition of radial glia migration (Fig. 3(d)). At higher TBBPA concentrations (6.6 µM and 20 µM), no nuclei and neurons were present (Fig. 4(a)) because migration was completely inhibited (Fig. 3(d)). The organophosphate-based IDDPHP (6.6 µM and 20 µM) increased the number of nuclei to $122.7 \pm 7.9\%$ and $133.4 \pm 6.2\%$ of controls, respectively (Fig. 4(c, e)) explaining the increased cell viability measures (Fig. 3(k)). All other FRs tested did not influence neuronal differentiation at concentrations up to 20 µM (Fig. 4(b, e)). For NPC3, the endpoint-specific control EGF significantly inhibited the total number of neurons to $1.0 \pm 0.2\%$ of total cell number (Suppl. Fig. 4(d)). The neurite length (NPC4) was significantly inhibited to $30.4 \pm 13.8\%$ of control by 20 µM TOCP only (Fig. 4(d)), while neurite area was not affected by any FR analyzed (Suppl. Fig. 3(f)). Additionally, LUHMES cells (UKN4) and hiPSC-derived peripheral neurons (UKN5) were used to analyze neurite morphology based

on two different cell types. Neurite outgrowth of both neuronal cell types (Fig. 4(f-h)) as well as their corresponding viability measures (Suppl. Fig. 3(i-j)) were not affected significantly by any of the FRs tested. As an endpoint-specific control for UKN4/5, cells were treated with 50 nM narciclasine which significantly reduced neurite outgrowth (data not shown).

Alteration of oligodendrocyte differentiation by all FR classes

Under differentiating conditions, 4.4% of the cells within the migration area differentiated into oligodendrocytes in this study (Suppl. Fig. 5c). Under the influence of TBBPA, differentiation into oligodendrocytes was specifically and significantly reduced starting from a concentration of 0.25 µM (to $66.2 \pm 8.9\%$ of control; Fig. 5(a, e)), as it was below the induction of cytotoxicity (Fig. 3(e)). BDE-47 significantly increased oligodendrocyte differentiation at low concentrations (0.03 µM to $147.4 \pm 4.1\%$; 0.08 µM to $172.5 \pm 6.4\%$ of control), whereas the highest concentration (20 µM) reduced their number to $10.9 \pm 5.9\%$ of control (Fig. 5(b, e)). Also, BDE-99 disturbed oligodendrocyte differentiation significantly at 2.5 µM to $35.2 \pm 11.7\%$, at 5 µM to $10.4 \pm 7.1\%$, and at 10 µM to $0.4 \pm 0.2\%$ (data taken from (Dach et al. 2017); Fig. 5(c, e)). The OPFR TDCIPP reduced the number of oligodendrocytes at 2.2 µM to $52.5 \pm 5.6\%$ of control (Fig. 5(d, e)). IDDPHP, TPHP, IPPHP, TOCP, and t-BPDPHP produced similar results as they significantly affected oligodendrocyte differentiation at the two highest concentrations of 6.6 µM and 20 µM (Fig. 5(f, g, h, i, j, k, o)).

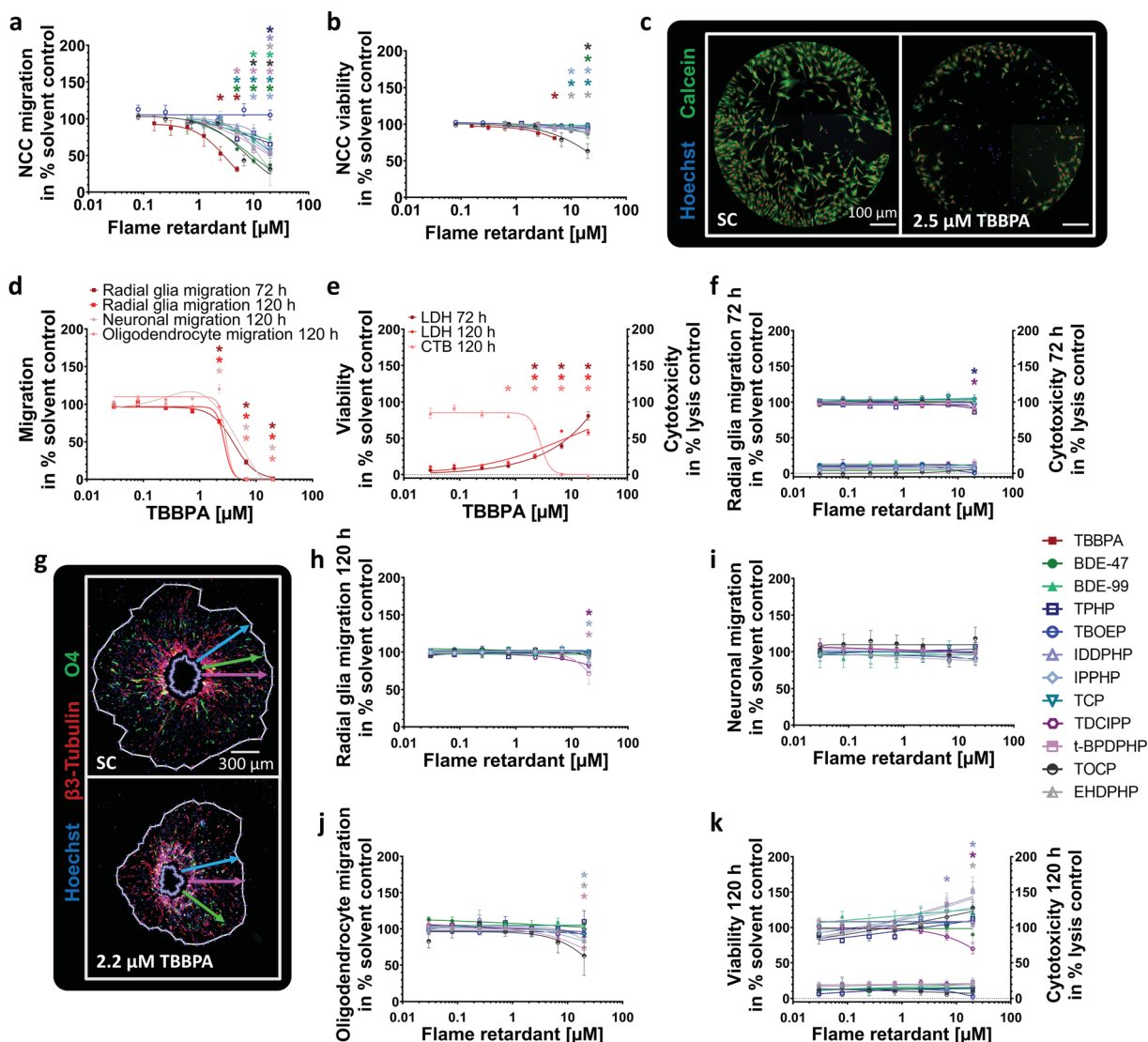


Fig. 3 Effects of FRs on different migration endpoints (NPC2, UKN2). NCCs were seeded around a stopper into 96-well plates. After stopper removal cells begin to migrate and were exposed to FRs/solvent(s) for 24 h. Cells were stained with Calcein-AM and H-33342, and the number of migrated cells (a) into the cell free zone was quantified using Cellomics ArrayScanVTI. Double-positive cell numbers were determined by an automated algorithm (marked with red dots, c). Viability was defined as the number of double-positive cells outside the ROI (b). Spheres were plated for hNPC migration analyses onto poly-D-lysine/laminin-coated 96-well plates in presence and absence of FRs for 120 h. Radial glia

migration (72 h) was determined by manually measuring the radial migration from the sphere core (d; f). After 120 h, the radial glia (d; h), neuronal (d; i), and oligodendrocyte migration (d; j) were assessed by automatically identifying (Omnisphero) the migration area of Hoechst stained nuclei, β (III)tubulin-stained neurons, and $O4^+$ oligodendrocytes (g). In parallel, viability and cytotoxicity (e; f; k) were assessed by the Alamar Blue and the LDH Assay. Data are represented as means \pm SEM (except BDE-99 NPC2b; TOCP LDH 120 h, $n=2$, means \pm SD). Statistical significance was calculated using one-way ANOVA followed by Bonferroni's post hoc tests ($p \leq 0.05$ was considered significant). ROI, region of interest

Despite the fact that IDDPHP caused an increase in the number of nuclei (Fig. 4(c)), there were still less oligodendrocytes differentiated (Fig. 5(f, j)). EHDPPH, TCP, and TBOEP significantly reduced oligodendrocyte differentiation only at 20 μ M to

36.5 \pm 8.3%, 31.1 \pm 7.4%, and 24.8 \pm 9.0% of controls, respectively (Fig. 5(l, m, n, o)). The endpoint-specific control BMP7 significantly reduced total number of oligodendrocytes to 0.4 \pm 0.1% (Suppl. Fig. 4(e)).

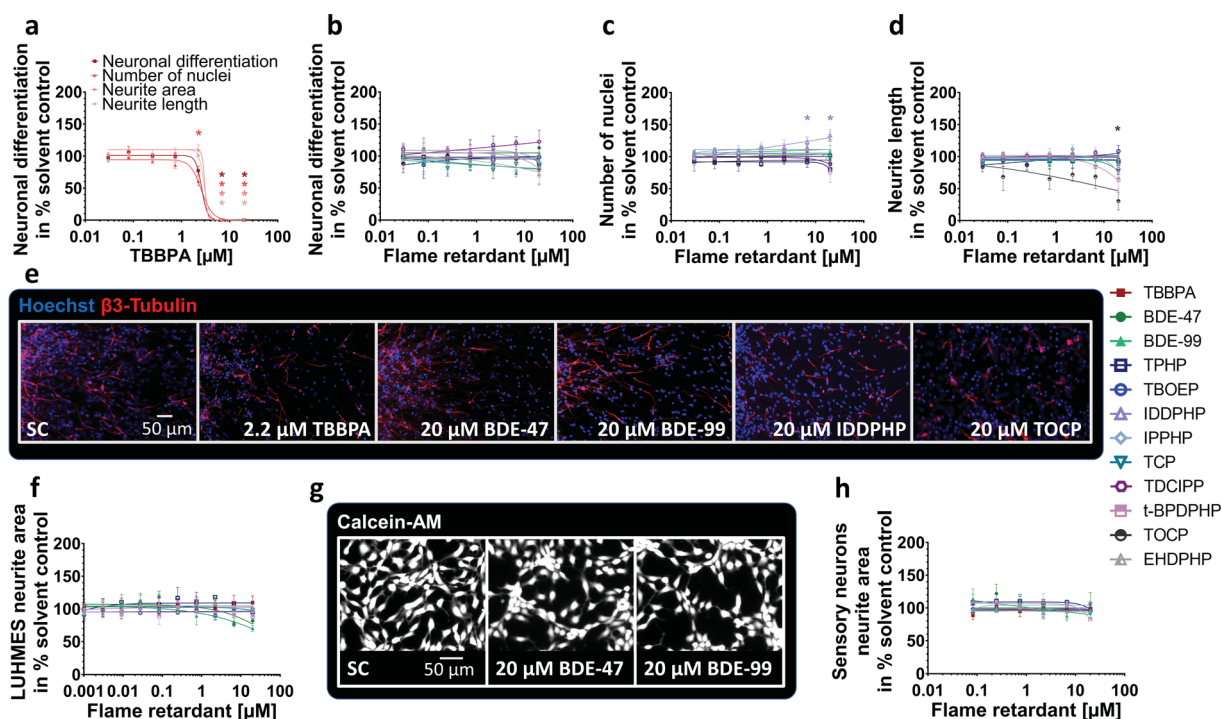


Fig. 4 Neuronal differentiation and morphology (NPC3, NPC4, UKN4, UKN5) in the presence and absence of FRs. Spheres were plated onto poly-D-lysine/laminin-coated 96-well plates in the presence and absence of FRs. Differentiation into neurons (**a**, **b**) was determined automatically by using a convolutional neural network (CNN) running on Keras implemented in Python 3. The number of all β (III)tubulin-positive cells (red) in percent of Hoechst positive nuclei (blue) in the migration area after 120 h of differentiation was calculated (**c**, **e**). Morphology (**d**) was determined automatically by using the software Omnisphero.

LUHMES cells and hiPSC derived sensory neurons were treated for 24 h in presence or absence of FRs and stained with Calcein-AM and H-333342 (**g**, LUHMES cells). An automated algorithm calculates the neurite area via subtraction of a calculated soma area from all calcein positive pixels (**f**, **h**). Data are represented as means \pm SEM (except BDE-99 NPC3, $n=2$, means \pm SD). Statistical significance was calculated using one-way ANOVA followed by Bonferroni's post hoc tests ($p < 0.05$ was considered significant)

Transcriptome changes in hNPCs

Since we identified 12 out of 15 FRs as disruptors of oligodendrocyte differentiation and for most of these compounds this endpoint was the only neurodevelopmental process disturbed in differentiating NPCs at these concentrations, we performed RNASeq analyses of neurospheres exposed to BMC₅₀ concentrations of selected FRs for 60 h. FR selection was based on DNTPi clustering choosing at least one FR from each DNTPi cluster (Fig. 7). For BDE-47, which produced a bell-shaped concentration-response curve, the highest significant concentration for the oligodendrocyte inducing effect was studied in addition. These experiments aimed at gaining understanding about similar or different modes-of-actions (MoA) underlying the observed endophenotype. The PCA analysis was based on 18941 genes and indicates the differences of individual FRs to the controls (Fig. 6(a)). The plot shows the highest

transcriptional variation in cells treated with EHDPHP compared to the controls. Both phased-out PBDEs (higher concentration for BDE-47), TOCP and IDDPHP, and t-BDPDHP, TDCIPP, and TBBPA clearly separated from the controls, while the low BDE-47 concentration did not lead to a separation from the controls. A hierarchical clustering of FRs based on their different gene expression levels was generated with Minkowski distance analyses (Fig. 6(b)). Similar to the PCA plot, EHDPHP was the most distanced FR to control and IDDPHP, TOCP, as well as BDE-99 and the higher concentration of BDE-47 form two clusters in an independent manner to the control. BDE-47 (0.08 μM), TDCIPP, TBBPA, and t-BDPDHP also form a cluster away from the controls, yet with less distance than the other compounds. This clustering is also reflected in the heatmap shown in Fig. 6(c). Here, the Z-score of up- and downregulated genes visually demonstrates that the pattern of BDE-47 (low), TDCIPP,

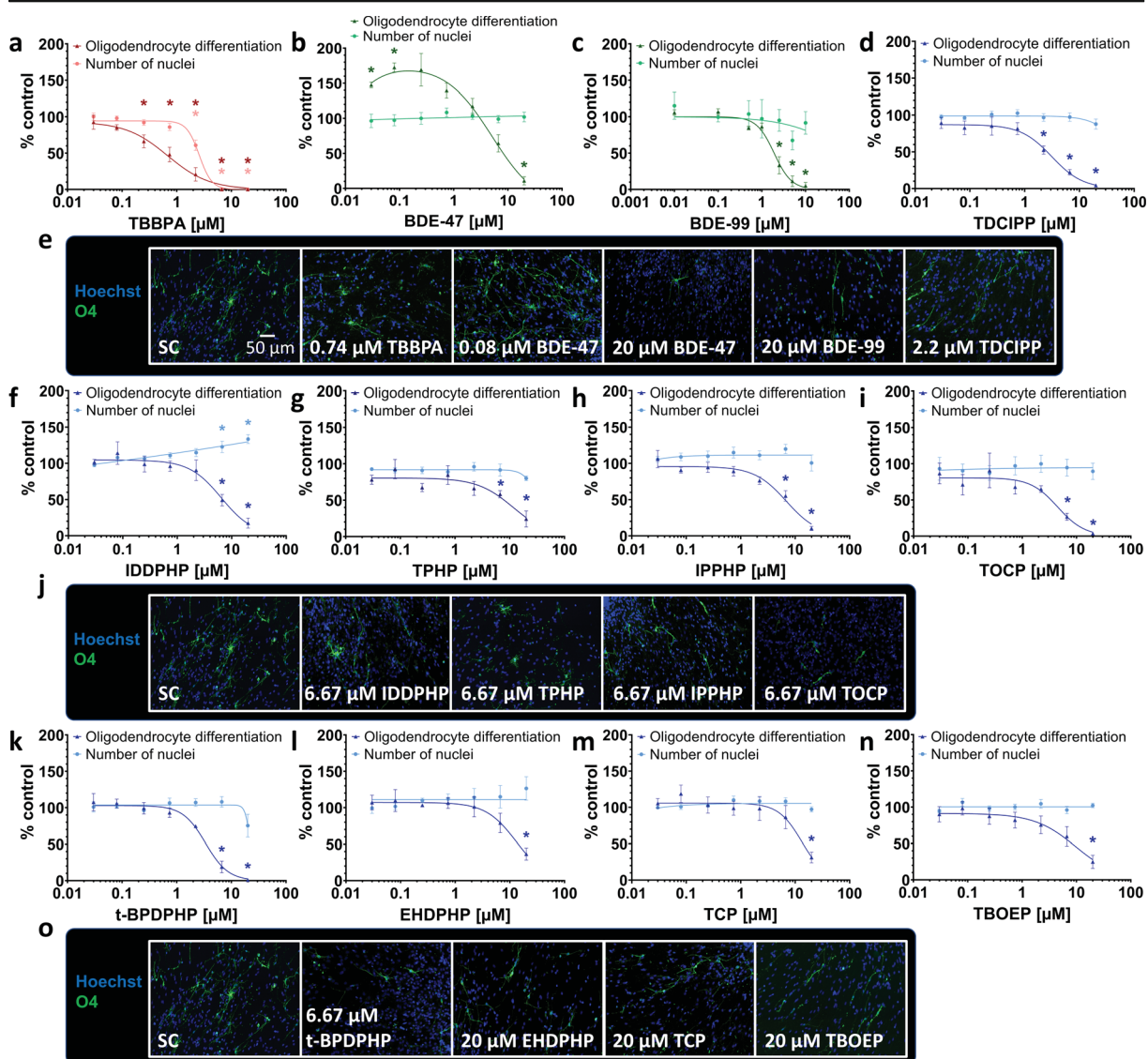


Fig. 5 Differentiation into oligodendrocytes (NPC5) in the presence and absence of FRs. Spheres were plated onto poly-D-lysine/laminin-coated 96-well plates in the presence and absence of FRs. Differentiation into oligodendrocytes was determined automatically based on immunocytochemical stainings (e, j, o) and by using a convolutional neural network (CNN) running on Keras

implemented in Python 3. The number of all O4-positive cells (green) in percent of Hoechst positive nuclei (blue) in the migration area after 120 h of differentiation was calculated (a, b, c, d, f, g, h, i, k, l, m, n). Data are represented as means \pm SEM. Statistical significance was calculated using one-way ANOVA followed by Bonferroni's post hoc tests ($p < 0.05$ was considered significant)

TBBPA, and t-BDPDHP is similar to the pattern of controls. Equally to the PCA variance and Minkowski cluster, the patterns of IDDPHP and TOCP, as well as of both phased-out PBDEs, are visually similar to each other. Again, EHDPHP was clearly different from the controls and the other FRs.

To understand qualitative changes in gene expression related to FR effects on oligodendrocytes, we analyzed genes involved in selected pathways that relate to

toxicity of the oligodendrocyte lineage (Simons and Trajkovic 2006; Káradóttir et al. 2008; Volpe et al. 2011; Marinelli et al. 2016) listed in Fig. 6(d) and visualized those in respective heatmaps (Suppl. Fig. 6). Heatmap hierarchical clusters were used for classification into several levels. Level 1 (dark blue) describes the most distanced cluster from control, while the separation between samples and controls decreases in hierarchy up to > level 4 (white). In all pathways analyzed except for

NOTCH1 signaling (level 3), EHDPHP reached level 1 suggesting that EHDPHP interfered with a wide variety of oligodendrocyte-relevant cell signaling. Similarly, the phased-out PBDEs affected a broad variety of genes belonging to these pathway gene clusters. Here it is of interest that BDE-99 did not affect genes involved in cholesterol biosynthesis or mitochondrial calcium transport. TOCP and IDDPHP, which clustered in the previous analyses (Fig. 6(a, b)), also displayed a similar pattern in the pathway analyses. Both most strongly influenced NOTCH1 signaling and at a lower level affected almost all other pathways except for ROS detoxification. TDCIPP and t-BDPHP both exerted the least effects on the pathways as they disturb multiple pathways at level 4 without pathway overlap.

A special case in MoA seems to be TBBPA as it strongly and selectively affected cholesterol biosynthesis at level 2 and endoplasmic reticulum stress at level 4, while all other pathways are unaffected. These RNASeq data confirm previous Affymetrix microarray data identifying altered cholesterol metabolism as the predominant non-endocrine pathway affected by TBBPA in differentiating neurospheres (Klose et al. 2020). These data indicate that the studied FRs disturb a variety of pathways that influence amongst others oligodendrocyte differentiation. As this is a mixed culture, we cannot exclude that the signals produced by FRs are also derived from the other cell types in differentiated neurospheres, i.e., radial glia and neurons. It is to note that these RNASeq results are based on an $n=1$ each that give an orientation on similar or distinct MoA of the individual FR but need to be substantiated by more in-depth work in the future.

Due to the low percentage of oligodendrocytes (4.4%) within the migration area, the depth of RNASeq was not sufficient to detect transcription of oligodendrocyte-related genes in detail. Therefore, we performed RT-qPCR analyses of five oligodendrocyte-specific transcripts representing their different maturation stages (Fig. 6(e)). Gene expression data of the solvent control of differentiated spheres normalized to proliferating spheres reveal “normal” neurosphere development over a time course of 60 h (gray bars). These can be directly compared to the FR-treated samples (blue bars). Gene products chosen are representative for increasing oligodendrocyte maturation stages ($PDGFR\alpha < PLP < CNP < GALC < MBP$; Baumann and Pham-Dinh 2001; Kuhn et al. 2019), although these are onsets of expression and the markers show considerable overlaps. All gene products were expressed at least twofold higher in differentiating versus

proliferating spheres supporting oligodendrocyte formation in the neurosphere system (Dach et al. 2017). FR exposure altered developmental gene expression changes from proliferating to 60 h differentiating neurospheres. Only t-BDPHP induced a twofold expression induction of $PDGFR\alpha$ mRNA, a gene expressed in oligodendrocyte progenitor cells (OPCs) and pre-oligodendrocytes (pre-OLs), but not in immature and mature oligodendrocytes (OLs), suggesting a delay in oligodendrocyte maturation. PLP is expressed in OPCs, pre-OLs, and OLs and was strongly reduced by TBBPA, BDE-99, TOCP, IDDPHP, BDE-47, and EHDPHP mirroring general reduction of OLs across maturation stages. In contrast, CNP and $GALC$ mRNA, which are expressed in all oligodendrocyte stages but the OPCs, were not affected by any of the compounds. MBP gene expression, one of the latest oligodendrocyte maturation markers, was reduced by BDE-47 (low concentration), TOCP, and EHDPHP (Fig. 6(e)). Interestingly, BDE-47 induced oligodendrocyte formation. These data demonstrate that despite the common phenotypical result of reduction in oligodendrocyte differentiation (besides BDE-47 low concentration), FRs’ molecular effects on oligodendrocyte marker expression patterns are compound-specific.

Compound classification based on BMC calculation

In order to provide a common metric of comparison across the different assays and substances, the benchmark dose (BMD) approach, which is recommended by the EFSA Scientific Committee (Hardy et al. 2017), was used. For in vitro toxicity testing, benchmark concentration (BMC) is comparable to the BMD (Krebs et al. 2020a) and derived from concentration-response information. The benchmark response (BMR) value was defined based on the variability of the respective endpoints (NPC1-5, Suppl. Fig. 4; UKN, Masjosthusmann et al. 2020). All BMCs calculated from all data points of the fitted concentration-response curves are listed in Table 1, with the respective upper and lower confidence intervals given in supplementary Table 2. From the FRs, which achieved BMCs, several questions can be drawn: (i) Are the observed effects DNT-specific or unspecific hits according to the classification models (Masjosthusmann et al. 2020)? (ii) What is the most sensitive endpoint (MSE) for each FR? And (iii) what is the potency ranking of the FRs? Most compound effects assessed by the battery are DNT-specific (Table 1), yet BBOEP, TCEP, and TCIPP did not reach DNT-specificity according to the

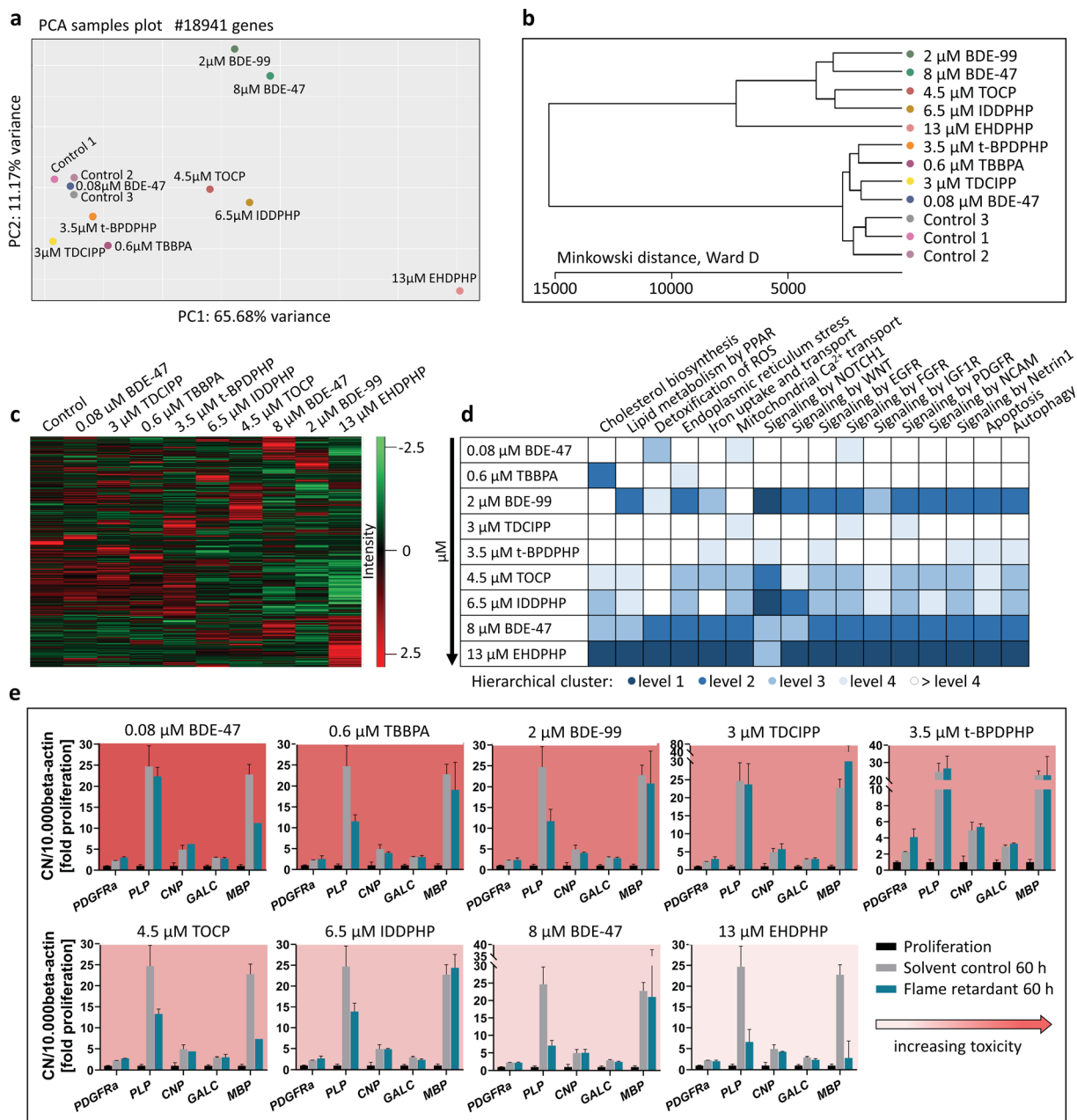


Fig. 6 RNA sequencing and RT-qPCR. Human NPCs differentiated for 60 h in the presence of 0.6 μM TBBPA, 2 μM BDE-99, 3 μM TDCIPP, 3.5 μM t-BPDPPH, 4.5 μM TOCP, 6.5 μM IDDPHP, 8 μM BDE-47, and 13 μM EHDPPH. These concentrations represent the BMC₅₀ values of oligodendrocyte differentiation inhibition. 0.08 μM BDE-47 induced oligodendrocyte differentiation. Controls 1–3 represent spheres plated in solvent control 0.1% DMSO. PCA (a) and Minkowski distance plot (b) analyses were performed using the PCAGO online software (<https://pcago.bioinf.uni-jena.de/>) as previously described (Gerst and Hölzer 2019). Both plots were generated by normalizing the total number of reads of different samples to the Transcript per Kilobase Million (TPM) count. The heatmap (c) was generated using Perseus Version 1.6.2.2 (<https://www.maxquant.org/perseus/>).

Therefore, the Z-scores of TPM values were used with a cut-off of one valid value per condition. Classification of impact on oligodendrocyte differentiation-relevant pathways (d) was performed by expert judgment based on hierarchical clustering of pathway-related genes (Suppl. Fig. 6) and was categorized into four levels (level 1 as most and level 4 as least distanced to one merged control). Gene expression (e) of *platelet-derived growth factor receptor A* (*PDGFRα*), *proteolipid protein* (*PLP*), *cyclic-nucleotide-phosphodiesterase* (*CNP*), *galactosylceramidase* (*GALC*) and *myelin basic protein* (*MBP*) was assessed via RT-qPCR and normalized to the housekeeping gene beta actin (*ACTB*). In addition to solvent control (gray bars), proliferative spheres (black bars) were used as an internal control. Data are represented as mean ± SD from 1 to 3 biological replicates

Table 1 Summary of BMCs across the DNT in vitro testing battery. Specific hits are highlighted bold and borderline hits are marked *curly*. Red colored specifies most sensitive endpoints(MSEs). *Induced effects. Numbers are given in μM . No value assumes BMCs > 20 μM

	Brominated (BFRs)			Organophosphates (OPFRs)											
	TBBPA	BDE-47	BDE-99	TPHP	TBOEP	IDDPHP	IPPHP	TCP	TDCIPP	t-BDPDHP	TOCP	EHDPHP	BBOEP	TCEP	TCIPP
Proliferation by area	-	-	-	-	-	-	-	-	-	-	-	-	-	-	-
Proliferation by BrdU	-	-	-	-	-	-	-	0.86	-	-	17.2	0.02	-	18.9	-
Proliferation CTB	-	-	-	-	-	-	9.62 [*]	-	19.2	-	-	-	19.9	-	-
Proliferation LDH	-	-	-	-	-	-	-	-	-	-	-	-	-	-	-
Radial glia migr. 72 h	1.93	-	-	-	-	-	-	-	-	-	-	-	-	-	-
Radial glia migr. 120 h	2.15	-	-	-	-	-	-	-	-	15.73	-	-	-	-	-
Neuronal migration	2.60	-	-	-	-	-	-	-	-	-	-	-	-	-	-
Oligo. migration	2.23	-	-	-	-	-	-	-	-	12.54	8.12	-	-	-	-
LDH 72 h	1.75 [*]	-	-	-	-	-	-	-	-	-	-	-	-	-	-
LDH 120 h	0.63 [*]	-	-	-	-	-	-	-	-	-	-	-	-	-	-
CTB 120 h	1.38	-	3.56 [*]	-	-	1.79 [†]	5.50 [†]	-	11.2	-	12.9 [*]	5.88 [*]	-	-	-
Neurite length	2.31	-	-	-	-	-	-	-	-	9.55	0.12	17.9	-	-	-
Neurite area	2.49	-	-	-	-	-	-	-	-	15.8	0.51	19.8	-	-	-
Number of nuclei	1.49	-	-	-	-	3.10[*]	-	-	-	19.8	-	8.72[*]	-	-	-
Number of neurons	2.18	-	-	-	-	-	-	-	12.8 [*]	-	18.8	10.3	-	-	-
Number of oligodendrocytes	-	0.03[*]	-	-	-	-	-	-	-	-	-	-	-	-	-
NCC migration	0.55	8.00	1.91	6.39	7.62	6.45	6.88	13.2	3.13	3.37	4.49	13.1	-	-	-
NCC viability	1.56	2.71	15.8	10.0	-	14.1	6.66	7.99	-	4.05	3.32	6.46	-	-	-
LUHMES neurite area	2.78	14.2	-	-	-	-	-	16.9	-	14.0	3.44	11.4	-	-	-
LUHMES viability	-	-	12.3	-	-	-	-	-	-	-	-	-	-	-	-
Sensory N. neurite area	-	13.5	15.0	-	-	-	-	-	-	-	-	-	-	-	-
Sensory N. viability	-	-	-	-	-	-	-	-	-	-	-	-	-	-	-

classification models. For TBBPA, most endpoints were affected at concentrations also inducing cytotoxicity. Based on specific DNT hits, the MSE for each compound across the DNT battery was assessed. In most cases (7/12), it was oligodendrocyte differentiation (NPC5), followed by NCC migration (UKN2; 2/12), NPC proliferation (NPC1; 2/12), and neurite morphology (NPC4; 1/12). The other assays did not provide MSE. Potency ranking was as follows: EHDPHP > BDE-47 > TOCP > TBBPA > TCP > BDE-99 > IDDPHP > TDCCP > t-BDPDHP > TPHP > IPPHP > TBOEP (Fig. 7).

Compound prioritization: ToxPi vs. DNTPi

Another currently propagated compound prioritization instrument is the Toxicological Prioritization Index (ToxPi) tool introduced by the US EPA (Reif et al. 2010; Marvel et al. 2018). Using this tool, FR testing results were visualized and prioritized according to their DNT profiles generated in this study by producing DNTPis (Fig. 7(b)), which are then compared to their toxicological profiles of the existing ToxCast data (ToxPis; Fig. 7(a); <https://www.epa.gov/chemical-research/toxicity-forecasting>). Here, the whole toxicological profiles are taken into account, i.e., also FR

effects on cell viability, and specific and non-specific hits are not distinguished. In general, the size of the Pi pieces does not reflect the actual BMC values but relates the BMCs for the studied compound to the BMCs of this endpoint across the highest and lowest values of the whole endpoint data set across all compounds irrespective of the values by distributing them between 0 and 1. Hence, it is a relative, not an absolute value. The ToxPi tool then hierarchically clusters the FRs within the ToxPis and the DNTPis according to their potency and assay hit patterns. Producing ToxPi information on compound clustering and ranking of a compound class for “general” (ToxPis) and “specific” toxicity, here DNT (DNTPis) gives information on the specificity of the compound effects.

Our ToxPi evaluation of the compound class of FRs clearly indicates that the Pi clustering is very different between the ToxPis and the DNTPis. For example, the two phased-out PBDEs are almost negative in the ToxCast assays and cluster collectively, while they evoke multiple responses in the DNT assays resulting in separate clusters. Similarly, e.g., TCIPP gives alerts in the ToxPi, while there is no effect in the DNTPis. Additionally, the program creates toxicity rankings and, in both rankings, TBBPA was classified as the most potent one. However, the overall ranking differs from each other, for example, t-

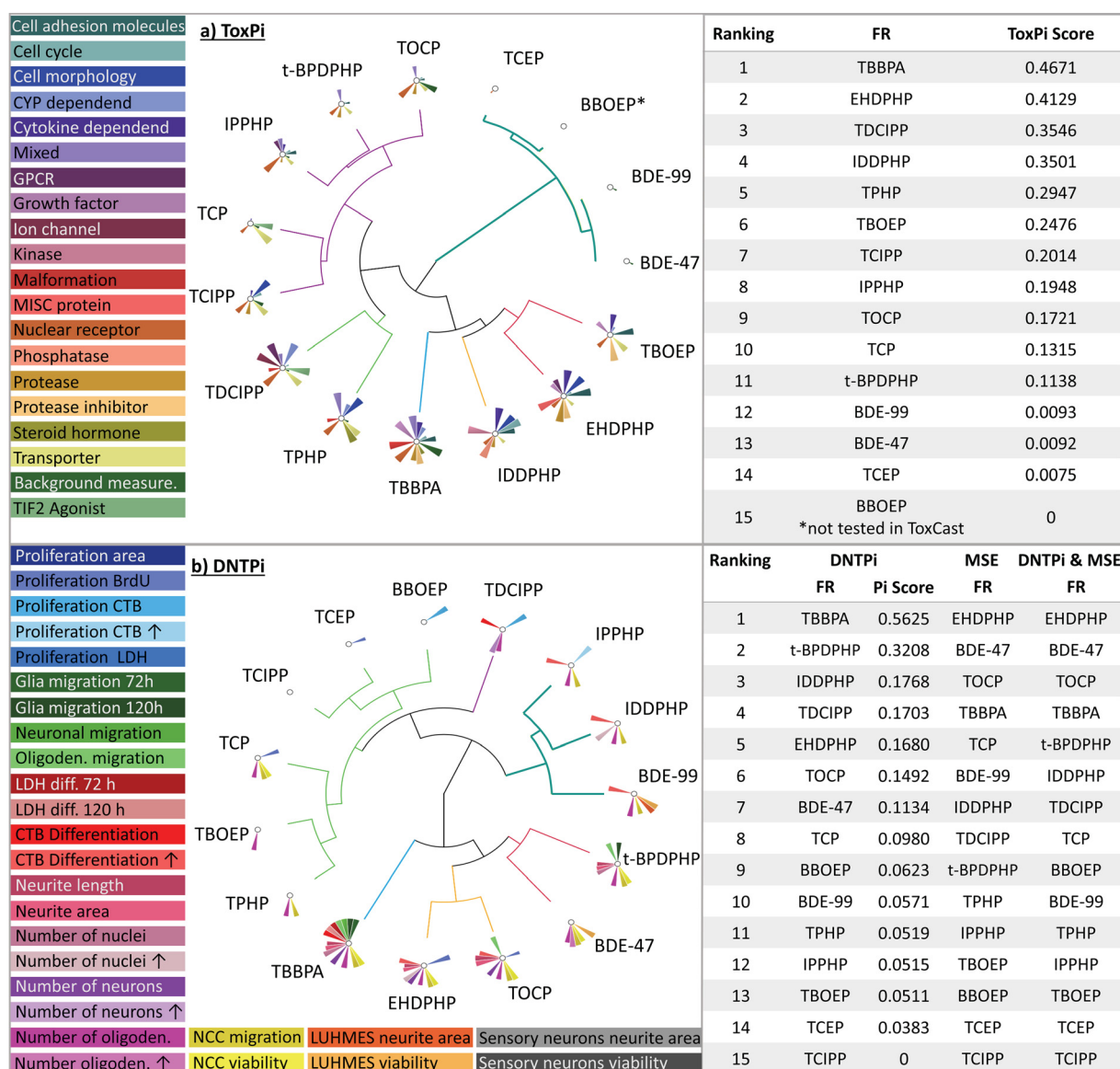


Fig. 7 Visualization and prioritization of FRs generated with ToxPi. ToxPis for general (a) and DNT-specific (b) toxicities using the ToxCast data and the results of the DNT in vitro battery, respectively. Graphs were produced with the Toxicological Prioritization Index (ToxPi) and Graphical User Interface (GUI) tool version 2.3. Size of pie slices represents relative strength of effect

on respective endpoint. For DNTPi and MSE ranking, first priority was given to MSE (Table 1); in the second line, ToxPi ranking was considered, e.g., for compounds with similar MSEs (starting from number 4 in the MSE analysis (Table 1; Suppl. Fig. 5a), due to overlapping 3-fold ranges for the MSE). *BBOEP was not tested in ToxCast

BPDPHP ranks on number 2 in the DNTPis and on number 11 in the ToxPis. Similarly, TCIPP ranks on number 15 in the DNTPis and on number 7 in the ToxPis suggesting that general toxicity is not a good predictor for DNT. As the ToxPi tool does not distinguish between DNT-specific and non-DNT-specific effects and the ranking takes rather the number of modified endpoints than the effective concentrations, which relate to potency, into

account, we next combined the MSE-based (Table 1; Fig. 7; Suppl. Fig. 5(a)) with the ToxPi (Fig. 7) ranking. Therefore, the MSE with DNT-specific hits (Table 1; Suppl. Fig. 5(a)) was set to the first priority and, in the second line, DNTPi ranking was considered, e.g., for compounds with similar MSEs (starting from number 4 in the MSE analysis (Table 1; Suppl. Fig. 5(a)) due to overlapping 3-fold ranges for the MSE (Masjosthusmann

et al. 2020). Merging the two ranking strategies changes some of the FR ranking, yet not the four most potent compounds EHDPHP, BDE-47, TOCP, and TBBPA and results in the final ranking of FRs due to the data of this study (DNTPi and MSE; Fig. 7).

Discussion

In this study, we applied a human-based DNT in vitro battery of tests as a first case study for screening and prioritization of 15 data-poor compounds belonging to the class of FRs including phased out and alternative FRs. By using the BMC concept, specific DNT hits and most sensitive endpoints were identified across the endpoints of the battery. These scatter across the broad variety of neurodevelopmental processes investigated in this study.

TCP and EHDPHP

Two FRs, TCP, and EHDPHP inhibited NPC proliferation (NPC1) as the MSE at fairly low concentrations (BMC_{20} 0.86 and 0.02 μ M, respectively). Proliferation is a fundamental neurodevelopmental KE that, when altered, might cause microcephaly (Tang et al. 2016). This is the first time that the specific impact of TCP and EHDPHP on cell proliferation was shown in human cells. Previous work demonstrated neurodevelopmental behavioral adversities in a zebrafish model of these compounds at concentrations of 4 and 5 μ M lowest nominal effect levels, respectively (Alzualde et al. 2018). This model is well suited for informing on adverse outcomes but does not provide mechanistic information. A strong DNT potential for TCP was also identified in a recent study using a rat primary cell-based spheroid model. Concentrations as low as 0.1 μ M decreased the neurotransmitter content and affected genes related to neurotransmitter production after an exposure period of 14 days (Hogberg et al. 2020).

TOCP

TOCP was the only FR altering neurite length of young, primary fetal neurons as the MSE (BMC_{20} 0.12 μ M). Neurotoxicity of TOCP was previously observed in ferret (Stumpf et al. 1989) and in the hen sciatic nerve accompanied by a reduction in nerve calcium (Luttrell et al. 1993). Interference with neuronal calcium levels

could hint to a potential TOCP developmental MoA as calcium signaling is crucial for neurite outgrowth via regulating growth cone motility (Gasperini et al. 2017). TOCP was also identified as a neurotoxicant, as it disturbed the neural network activity in rat cortical neurons (Behl et al. 2015). Yet, these studies did not investigate neurodevelopment, but adult neurotoxicity.

IDDPHP

Interestingly, the OPFR IDDPHP induced the number of nuclei in the migration area as the MSE, probably due to excessive migration or proliferation of radial glia cells, the major and still proliferative cell type in the migration area. As IDDPHP did not alter radial glia migration distance, the action of IDDPHP on their proliferation seems to be the more probable explanation. However, this has to be substantiated by further experiments in the future. When it comes to radial glia, species specificities become crucial, as this cell type regulates evolutionary specificities of cortex formation (Zilles et al. 2013). Their proliferation and migration are tightly regulated processes orchestrating species-specific development of the cortex, with a special role in its folding in gyrencephalic species, like humans (Borrell and Götz 2014). Hence, interference with radial glia neural progenitors underlie a number of cortical malformations and cause mental retardation in genetic and infectious diseases (Guerrini and Dobyns 2014; Hu et al. 2014; Juric-Sekhar and Hevner 2019). In a recent study, IDDPHP triggered an increase of *nestin* expression, and this was interpreted as evidence of reactive astrogliosis (Hogberg et al. 2020). However, there may be alternative explanations, as changes in *nestin* may also point to effects on the radial glia and neural stem cell compartments. Zebrafish behavior was also affected by IDDPHP, yet at fairly high nominal lowest effect levels (40 μ M) with no knowledge on the underlying mechanisms (Alzualde et al. 2018).

IPPHP and t-BPDPHP

NCC migration was the most sensitive endpoint (together with oligodendrocyte differentiation) upon IPPHP (BMC_{20} 6.66 μ M) and t-BPDPHP (BMC_{20} 4.05) exposure. Disturbance of NCC migration causes, e.g., cleft palate or loss of functional hearing (Mayor and Theveneau 2013). Our data from human cells are in good agreement with model systems from other species:

micromolar concentrations of IPPHP and t-BPDPHP were also toxic for zebrafish (Behl et al. 2015; Alzualde et al. 2018), *Caenorhabditis elegans* (Behl et al. 2015; Boyd et al. 2016), rat cortical neurons (Behl et al. 2015), and 3D rat brain spheres (Hogberg et al. 2020). t-BPDPHP specifically inhibits neurite outgrowth of rat cortical neurons at 14.9 μM (Behl et al. 2015), an effect that we observe at similar concentrations in the NPC4, but not in the UKN4/5 assays. Similarly, IPPHP solely inhibits NCC, but not radial glia, neuronal or oligodendrocyte migration, while t-BPDPHP does alter other cell type migration at higher concentrations. Why different migration or neurite outgrowth assays yield different hits and are thus complementary to each other is probably due to different cell types, species, and neurodevelopmental timing represented in the assays. Hence, toxicity patterns across the battery reflect compounds different MoA by specifically altering certain targets.

Oligodendrocyte differentiation

Oligodendrocyte differentiation was the endpoint most frequently altered as the MSE upon cellular FR exposure with the following compound potency ranking: BDE-47 (low) > TBBPA > BDE-99 > TDCCP > t-BPDPHP > TPHP > IPPHP > TBOEP. Oligodendrocytes are necessary for proper brain functioning as they form and keep myelin sheaths around axons, thereby allowing rapid saltatory conduction of neuronal action potentials (Baumann and Pham-Dinh 2001; Kuhn et al. 2019). Hence, impaired oligodendrogenesis and resulting hypomyelination due to genetic disorders or severe brain injury contribute to functional adverse outcomes manifesting in neurological disorders such as the Alan-Herndon-Dudley Syndrome (López-Espíndola et al. 2014; Tonduti et al. 2014) or periventricular leukomalacia (Back et al. 2001). Developing oligodendrocytes also exert a high susceptibility to stressors like reactive oxygen species and are sensitive to excitotoxicity and endoplasmic reticulum stress. They have a high energy and iron demand, are dependent on functional lipid metabolism, and their development and function are highly regulated by different hormones and growth factors (Bradl and Lassmann 2010; Volpe et al. 2011; Marinelli et al. 2016). Hence, developing oligodendrocytes can be concerned by a large variety of substances through a broad spectrum of MoA.

BDE-47 and oligodendrocyte differentiation

Since deviation from normal development into both directions, i.e., increase or decrease of a neurodevelopmental process, is considered adverse (Foti et al. 2013), the increase in oligodendrocyte differentiation by BDE-47 in the low nanomolar range needs attention. Consequences of increased oligodendrocyte differentiation are hypermyelination, an outcome observed for example in individuals with autism spectrum disorder (Ben Bashat et al. 2007; Wolff et al. 2013; Razek et al. 2014). So far, BDE-47 was found to reduce mouse and human oligodendrocyte differentiation similar to the effects observed in this study at higher concentrations (Schreiber et al. 2010; Li et al. 2013). Li et al. (2013) did not test with BDE-47 concentrations that induced oligodendrocytes here (< 0.3 μM), whereas Schreiber et al. (2010) used concentrations as low as 0.1 μM . Here, inter-individual differences could explain the missing inducing oligodendrocyte effect as neurospheres used were generated from a different donor. Thus, it is increasing confidence that the data produced in this paper represents data from three different individuals. In addition, Schreiber et al. (2010) quantified oligodendrocytes by manual counting, while cells in this work here were identified using a convolutional neuronal network (CNN), which is more reliable, reproducible, and free of human counting bias. The induction mechanism of oligodendrocyte differentiation by BDE-47 is so far unknown. The performed RNASeq analyses did not reach a sufficient depth for such a cell type-specific molecular clarification. Interestingly, oligodendrocyte toxicity pathways are already triggered at 80 nM BDE-47 (Fig. 6(d)), probably resulting in loss of MBP-expressing more mature oligodendrocytes that is overridden by an unknown, oligodendrocyte-inducing trigger. In rat brain spheres, BDE-47 (0.1–5 μM) did not appear to affect *mbp* gene expression, but it caused a transient increase in myelin-associated glycoprotein (*mag*) transcript at 5 μM (Hogberg et al. 2020). Our previous species comparison of in vitro oligodendrogenesis found significant differences in timing, regulation of gene expression and response to toxicants between human and mouse oligodendrocytes (Dach et al. 2017; Klose et al. 2020). On the basis of these observations, it is likely that human neurospheres (as used here) will show differences to rat spheres. The difference in exposure schemes and readouts further complicates direct comparisons. A striking difference is for instance that none of the 15 FRs had any effect on human neuronal differentiation, while all 5 FRs tested in rat spheres reduced

neurofilament and other specifically neuronal markers (Hogberg et al. 2020).

TBBPA and oligodendrocyte differentiation

Similarly, TBBPA reduces oligodendrocyte differentiation. From the toxicity pathways analyzed by RNASeq, mainly genes relating to cholesterol biosynthesis were deregulated by TBBPA. This MoA was previously described as a putative adverse outcome pathway (Klose et al. 2020). TBBPA did not affect the number of corpus callosum CNP⁺ oligodendrocytes (Saegusa et al. 2009) or Ret⁺ oligodendrocytes (Fujimoto et al. 2013) in developmental rat studies. This might be due to the markers used in the in vivo study, as e.g., *CNP* expression did not, but only *PLP* expression changed upon TBBPA treatment in this study. Also, species (Dach et al. 2017) or brain regions with heterogeneous oligodendrocyte populations (Hayashi and Suzuki 2019) might have affected the results.

RNASeq analyses

In the Minkowski distance cluster and gene heatmap (Fig. 6(b, c)), the low concentration BDE-47, TBBPA, TDCIPP, and t-BPDPHP clustered together close to the controls. Different from TBBPA, the latter two change gene expression in variable oligodendrocyte toxicity pathways. These data suggest that either one specific pathway, like cholesterol metabolism for TBBPA, or multiple hits across distinct converging pathways like in the case of TDCIPP or t-BPDPHP, can summit in the same endophenotype. Minkowski cluster further demonstrates that TOCP, IDDPHP, PBDEs, and EHDPHP differ most from the controls and they strongly affect a large variety of oligodendrocyte toxicity pathways. Because oligodendrocytes provide just around 4% of the cells in the migration area, it is highly unlikely that these strong alterations in mRNA expression profiles can be attributed to oligodendrocytes only, but probably also derive from radial glia and/or neurons in the migration area. Because all other phenotypic endpoints of the neurosphere assay were not affected, these data clearly show the high susceptibility of oligodendrocytes towards alterations of these pathways and thus supports the notion of “just being an oligodendrocyte seems enough to put these cells at greater risk of damage” (Bradl and Lassmann 2010).

Compound prioritization

Such DNT in vitro battery data can be used for compound prioritization. Here, different methods are at hand. For one, BMC values with CI allow distinguishing between DNT-specific and DNT-unspecific hits (Masjosthusmann et al. 2020) giving objective potency ranking measures. However, this method takes only the MSE and not, e.g., the number of affected endpoints into consideration. To account for both, we merged the MSE method with the ToxPi approach by prioritizing for BMCs first and secondly adding the ToxPi ranking when BMCs of MSE of different compounds were located within their 3-fold ranges. In our opinion, prioritization for DNT only by ToxPi might include high uncertainty, because altering only one DNT endpoint can have detrimental effects on neurodevelopment, especially when it happens at low concentrations. Using this merged approach, our study revealed that BDE-47 and BDE-99, which are already banned due to their neurodevelopmental toxicity, rank as 2nd and 10th out of the 15 FRs investigated. Of the currently used aFRs, only TCIPP did not produce a hit in the battery according to the BMCs. However, also TCEP and BBOEP did not yield statistically significant hits, but just reached their BMC₂₀ values. Therefore, these three aFRs are rated as the least toxic with the DNT in vitro battery, while EHDPHP together with BDE-47 summit at the top as the most hazardous FR. These data indicate that the DNT in vitro battery is a useful tool for prioritizing compounds for their DNT hazard potential. It has to be noted that the battery applied here still has known gaps that need to be closed in the future. These include test methods for neuronal network formation (Frank et al. 2017; Shafer et al. 2019; Nimitz et al. 2020) including synaptogenesis (Pistollato et al. 2020), astrocyte, and microglia performance.

One question that arises is if such a DNT in vitro battery is at all necessary or if DNT might as well be predicted by the general ToxCast assays. To answer this question, FR DNT in vitro battery is compared to ToxCast data by ToxPi versus DNTPi assessment. The results demonstrate the uniqueness of the DNT in vitro battery for DNT hazard assessment. Such an approach has never been executed before and was shown here to be very helpful for assays' specificity analyses.

Moving from hazard to risk

When moving from hazard characterization to risk assessment, exposure data is crucial. Biomonitoring data for parent compounds currently available (Table 2; Cariou et al. 2008; Sundkvist et al. 2010; Kim et al. 2014; Tang and Zhai 2017; Beser et al. 2019; Ma et al. 2019; Chupeau et al. 2020) reveal a gap on human FR exposure data, especially for OPFRs. While phased-out PBDEs and TBPPA can be measured in human samples, most OPFRs metabolize fast and parent compounds cannot be detected, e.g., in cord blood or breast milk. Therefore, the occurrence of OPFR metabolites is measured in urinary samples of adults (Bastiaensen et al. 2019b; Gibson et al. 2019; Chupeau et al. 2020; Li et al. 2020) and children (He et al. 2018a, b; Bastiaensen et al. 2019a; Gibson et al. 2019; Chupeau et al. 2020) or in

hair (Kucharska et al. 2015; Chupeau et al. 2020). These studies clearly demonstrate the existence of OPFR metabolites in human samples, especially in children.

For relating such biomonitoring data to the studied in vitro hazards, we converted the internal FR concentrations from cord blood or breast milk given in nanograms per gram of fat to molarity by using a fat content of 5.8 g/L for serum (Akins et al. 1989; Phillips et al. 1989; Covaci et al. 2006; Rylander et al. 2006) and 33 g/L for breast milk (Kent et al. 2006; Prentice et al. 2016). Such in vitro–in vivo comparisons are very crude and do not account for in vitro kinetics or for actual fetal brain concentrations in vivo.

Hence, advanced kinetic modelling would be eventually needed to perform proper in vitro to in vivo extrapolation (IVIVE). Nevertheless, our crude evaluations revealed cord blood values for BDE-99, BDE-47, and TBBPA of

Table 2 Exposure data collected from published FR measurements in human breast milk and cord blood samples (Cariou et al. 2008; Sundkvist et al. 2010; Kim et al. 2014; Tang and Zhai 2017; Beser et al. 2019; Ma et al. 2019; Chupeau et al. 2020)

	Breast milk						Cord blood					
	BDE-99		BDE-47		TBBPA		BDE-99		BDE-47		TBBPA	
	ng/g lw	μM	ng/g lw	μM	ng/g lw	μM	ng/g lw	μM	ng/g lw	μM	ng/g lw	μM
<i>Korea</i>	54.0	0.0316	31.0	0.0211	-	-	19.0	0.0020	36.0	0.0044	-	-
<i>China</i>	10.8	0.0063	27.5	0.0187	-	-	3.45	0.0004	8.49	0.0010	-	-
<i>Japan</i>	3.20	0.0019	4.90	0.0033	-	-	-	-	0.12	0.00001	-	-
<i>Philippines</i>	0.82	0.0005	3.60	0.0024	-	-	-	-	-	-	-	-
<i>Vietnam</i>	0.38	0.0002	0.40	0.0003	-	-	-	-	-	-	-	-
<i>USA</i>	6.40	0.0037	29.7	0.0202	-	-	23.3	0.0024	4.60	0.0006	-	-
<i>France</i>	0.53	0.0003	1.15	0.0008	4.1	0.0025	7.43	0.0008	-	-	103	0.0111
<i>Germany</i>	0.18	0.0001	0.45	0.0003	-	-	-	-	-	-	-	-
<i>UK</i>	0.80	0.0005	2.70	0.0018	-	-	-	-	-	-	-	-
<i>Sweden</i>	0.48	0.0003	2.28	0.0015	-	-	0.22	0.00002	3.4	0.0004	-	-
<i>Spain</i>	0.51	0.0003	0.54	0.0004	-	-	4.3	0.0004	3.3	0.0004	-	-
	Breast milk											
	TPHP		TBOEP		TCEP		TCIPP		EHDPHP		TCP	
	ng/g lw	μM	ng/g lw	μM	ng/g lw	μM	ng/g lw	μM	ng/g lw	μM	ng/g lw	μM
<i>Japan</i>	1.40	0.0014	0.24	0.0002	0.14	0.0002	-	-	-	-	-	-
<i>Philippines</i>	19.0	0.0192	22.0	0.0182	42.0	0.0554	-	-	-	-	2.30	0.0021
<i>Vietnam</i>	4.90	0.0050	-	-	-	-	-	-	-	-	0.28	0.0003
<i>Sweden</i>	8.50	0.0086	4.70	0.0039	4.90	0.0065	45.0	0.0453	6.50	0.0059	0.80	0.0007
<i>Spain</i>	9.90	0.0100	14.8	0.0123	-	-	12.5	0.0126	-	-	19.0	0.0170
	TPHP		TBOEP		TCEP		TCIPP		EHDPHP		IDDPHP	
	ng/mL	μM	ng/mL	μM	ng/mL	μM	ng/mL	μM	ng/mL	μM	ng/mL	μM
<i>USA</i>	0.15	0.0005	1.44	0.0036	0.04	0.0001	0.22	0.0005	0.02	0.00006	0.01	0.00003

0.002, 0.004, and 0.011 μM in a Korean (PBDEs) and French (TBBPA) cohort, respectively (Table 2). Breast milk concentrations calculated to 0.032 and 0.021 μM for BDE-99 and BDE-47 in Korea and 0.003 for TBBPA in France. OPFRs in breast milk occur with the highest measured values across all FRs with TCEP 0.055 μM , TPHP 0.019 μM , and TBOEP 0.018 μM (Philippines) and TCIPP 0.045 μM (Sweden). Assuming a breast milk intake of 1 L/day, exposure to these FRs approximates to 32 nmol/day BDE-99, 21 nmol/day BDE-47, 3 nmol/day TBBPA, 55 nmol/day TCEP, 19 nmol/day TPHP, 18 nmol/day TBOEP, and 45 nmol/day TCIPP. While the BMCs calculated for DNT in vitro hazard for BDE-99 and OPFRs are more than one order of magnitude lower than the estimated daily intake and cord blood concentrations, the BDE-47 BMC for the MSE is just one order of magnitude higher than the estimated exposure (suggesting a bioavailability of 100%, slow/no liver metabolism, perfect blood-brain-barrier (BBB) passage (1:1), and protein binding according to logP prediction model).

However, humans are generally exposed to compound mixtures including FRs, pesticides, pharmaceuticals, toxic metals, and other environmental contaminants. Therefore, individual compound exposure easily adds up to mixtures at relevant concentrations that might exert additive, synergistic, or antagonistic effects, especially when the same converging endpoint is affected. This is likely the case for oligodendrocytes because they seem to be the most susceptible cell type of the brain. Mixture experiments as well as sophisticated IVIVE are needed to substantiate these concerns.

Summary and conclusion

In summary, we tested 15 FRs including phased-out PBDEs, TBBPA and OPFRs for their neurodevelopmental toxicity in a human cell-based DNT in vitro battery. FR hazards across different neurodevelopmental endpoints were used for calculating BMC and CI leading to a potency ranking. Evaluation of the data with the ToxPi tool revealed a distinct ranking that we combined with the BMC ordering for final prioritization. In addition, comparison of DNT hazard ranking according to the ToxPi tool with the ToxCast data revealed DNT-specific hazard for this group of FRs that is not well predicted by ToxCast assays. Extrapolating DNT battery BMC to human FR exposure via breast milk suggests low risk for individual compounds but raises concern for mixture exposure, which

is the real-life situation. This is especially of apprehension when different compounds converge through diverse MoA on common endpoints like oligodendrocyte differentiation in this study.

This case study using FRs contextualized with the performance characteristics of the battery using diverse compound classes (Masjosthusmann et al. 2020) suggests that using a human cell-based DNT in vitro battery for hazard assessment for compound prioritization is a promising approach for future risk assessment procedures.

Supplementary Information The online version contains supplementary material available at <https://doi.org/10.1007/s10565-021-09603-2>.

Author contribution All authors read, commented, and approved the manuscript. Jördis Klose: study conception, investigation, data collection and analysis, figure design, writing. Melanie Pahl: investigation, data collection and analysis. Kristina Bartmann: investigation. Farina Bendt: investigation. Jonathan Blum: study conception, investigation, data collection and analysis. Xenia Dolde: study conception, investigation, data collection and analysis. Nils Förster: software. Anna-Katharina Holzer: study conception, investigation, data collection and analysis. Ulrike Hübenthal: investigation. Hagen Eike Keßel: software. Katharina Koch: study conception. Stefan Masjosthusmann: study conception and data analysis. Sabine Schneider: data analysis. Selina Woeste: investigation. Andrea Rossi: data analysis. Adrian Covaci: resources. Mamta Behl: resources. Marcel Leist: study conception, funding acquisition for all experiments performed with NCCs, LUHMES cells, and hiPSC-derived neurons; writing. Julia Tigges: study conception, supervision, project administration and writing. Ellen Fritsche: study conception, supervision, funding acquisition for all experiments performed with hNPCs, project administration, and writing.

Funding Open Access funding enabled and organized by Projekt DEAL. This work was supported by the FOKO (Forschungskommision of the medical faculty of the Heinrich-Heine-University) (2016-53), the EFSA (European Food Safety Authority) (OC/EFSA/PRAS/2017/01), CERST (Center for Alternatives to Animal Testing) of the Ministry for Culture and Science of the State of North-Rhine Westphalia, Germany) (file number 233-1.08.03.03-121972/131—1.08.03.03—121972), and the DFG Ursula M. Händel Tierschutzpreis to EF (DFG FR 1392/6-1). It has received funding from the European Union's Horizon 2020 research and innovation program under grant agreement No. 681002 (EU-ToxRisk) and No. 825759 (ENDpoiNTs).

Declarations

Ethics approval hNPCs were purchased from Lonza Verviers SPRL, Belgium, and work was approved by the ethics committee of the Heinrich-Heine University Duesseldorf.

Conflict of interest The authors declare that they have no conflicts of interest.

References

- Akins JR, Waldrep K, Bernert JT. The estimation of total serum lipids by a complete enzymatic 'summation' method. *Clin Chim Acta*. 1989;184:219–26.
- Alzualde A, Behl M, Sipes NS, Hsieh JH, Alday A, Tice RR, et al. Toxicity profiling of flame retardants in zebrafish embryos using a battery of assays for developmental toxicity, neurotoxicity, cardiotoxicity and hepatotoxicity toward human relevance. *Neurotoxicol Teratol*. 2018;70:40–50. <https://doi.org/10.1016/j.ntt.2018.10.002>.
- Andersen SL. Trajectories of brain development: point of vulnerability or window of opportunity? *Neurosci Biobehav Rev*. 2003;27:3–18. [https://doi.org/10.1016/S0149-7634\(03\)00005-8](https://doi.org/10.1016/S0149-7634(03)00005-8).
- Back SA, Luo NL, Borenstein NS, Levine JM, Volpe JJ, Kinney HC. Late oligodendrocyte progenitors coincide with the developmental window of vulnerability for human perinatal white matter injury. *J Neurosci*. 2001;21:1302–12. <https://doi.org/10.1523/jneurosci.21-04-01302.2001>.
- Bal-Price A, Crofton KM, Leist M, Allen S, Arand M, Buetler T, et al. International STakeholder NETwork (ISTNET): creating a developmental neurotoxicity (DNT) testing road map for regulatory purposes. *Arch Toxicol*. 2015;89:269–87. <https://doi.org/10.1007/s00204-015-1464-2>.
- Bal-Price A, Hogberg HT, Crofton KM, et al. Recommendation on test readiness criteria for new approach methods in toxicology: exemplified for developmental neurotoxicity. *ALTEX*. 2018;35:306–52. <https://doi.org/10.14573/altex.1712081>.
- Barenys M, Gassmann K, Baksmeier C, Heinz S, Reverte I, Schmuck M, et al. Epigallocatechin gallate (EGCG) inhibits adhesion and migration of neural progenitor cells in vitro. *Arch Toxicol*. 2017;91:827–37. <https://doi.org/10.1007/s00204-016-1709-8>.
- Bastiaansen M, Ait Bamai Y, Araki A, van den Eede N, Kawai T, Tsuboi T, et al. Biomonitoring of organophosphate flame retardants and plasticizers in children: associations with house dust and housing characteristics in Japan. *Environ Res*. 2019a;172:543–51. <https://doi.org/10.1016/j.envres.2019.02.045>.
- Bastiaansen M, Malarvannan G, Been F, Yin S, Yao Y, Huygh J, et al. Metabolites of phosphate flame retardants and alternative plasticizers in urine from intensive care patients. *Chemosphere*. 2019b;233:590–6. <https://doi.org/10.1016/j.chemosphere.2019.05.280>.
- Baud A, Wessely F, Mazzacuva F, McCormick J, Camuzeaux S, Heywood WE, et al. A multiplex high-throughput targeted proteomic assay to identify induced pluripotent stem cells. *Anal Chem*. 2017;89:2440–8. <https://doi.org/10.1021/acs.analchem.6b04368>.
- Baumann N, Pham-Dinh D. Biology of oligodendrocyte and myelin in the mammalian central nervous system. *Physiol Rev*. 2001;81:871–927. <https://doi.org/10.1152/physrev.2001.81.2.871>.
- Baumann J, Dach K, Barenys M, et al. Application of the neurosphere assay for DNT hazard assessment: challenges and limitations. *Methods Pharmacol Toxicol*. 2016;49:1–29. https://doi.org/10.1007/7653_2015_49.
- Behl M, Hsieh JH, Shafer TJ, Mundy WR, Rice JR, Boyd WA, et al. Use of alternative assays to identify and prioritize organophosphorus flame retardants for potential developmental and neurotoxicity. *Neurotoxicol Teratol*. 2015;52:181–93. <https://doi.org/10.1016/j.ntt.2015.09.003>.
- Ben Bashat D, Kronfeld-Duenias V, Zachor DA, Ekstein PM, Hendler T, Tarrasch R, et al. Accelerated maturation of white matter in young children with autism: a high b value DWI study. *Neuroimage*. 2007;37:40–7. <https://doi.org/10.1016/j.neuroimage.2007.04.060>.
- Bergman Å, Rydén A, Law RJ, de Boer J, Covaci A, Alae M, et al. A novel abbreviation standard for organobromine, organochlorine and organophosphorus flame retardants and some characteristics of the chemicals. *Environ Int*. 2012;49:57–82.
- Beser MI, Pardo O, Beltrán J, Yusà V. Determination of 21 perfluoroalkyl substances and organophosphorus compounds in breast milk by liquid chromatography coupled to orbitrap high-resolution mass spectrometry. *Anal Chim Acta*. 2019;1049:123–32. <https://doi.org/10.1016/j.aca.2018.10.033>.
- Blum A, Behl M, Birnbaum LS, Diamond ML, Phillips A, Singla V, et al. Organophosphate ester flame retardants: are they a regrettable substitution for polybrominated diphenyl ethers? *Environ Sci Technol Lett*. 2019;6:638–49. <https://doi.org/10.1021/acs.estlett.9b00582>.
- Borrell V, Götz M. Role of radial glial cells in cerebral cortex folding. *Curr Opin Neurobiol*. 2014;27:39–46. <https://doi.org/10.1016/j.conb.2014.02.007>.
- Boyd WA, Smith MV, Co CA, Pirone JR, Rice JR, Shockley KR, et al. Developmental effects of the ToxCast™ phase I and phase II chemicals in *Caenorhabditis elegans* and corresponding responses in zebrafish, rats, and rabbits. *Environ Health Perspect*. 2016;124:586–93. <https://doi.org/10.1289/ehp.1409645>.
- Bradl M, Lassmann H. Oligodendrocytes: biology and pathology. *Acta Neuropathol*. 2010;119:37–53. <https://doi.org/10.1007/s00401-009-0601-5>.
- Cariou R, Antignac J-P, Zalko D, Berrebi A, Cravedi JP, Maume D, et al. Exposure assessment of French women and their newborns to tetrabromobisphenol-A: occurrence measurements in maternal adipose tissue, serum, breast milk and cord serum. *Chemosphere*. 2008;73:1036–41. <https://doi.org/10.1016/j.chemosphere.2008.07.084>.
- Chambers SM, Qi Y, Mica Y, Lee G, Zhang XJ, Niu L, et al. Combined small molecule inhibition accelerates developmental timing and converts human pluripotent stem cells into nociceptors. *Nat Biotechnol*. 2013;30:715–20. <https://doi.org/10.1038/nbt.2249>.
- Chao HR, Wang SL, Lee WJ, Wang YF, Pöpke O. Levels of polybrominated diphenyl ethers (PBDEs) in breast milk from central Taiwan and their relation to infant birth outcome and maternal menstruation effects. *Environ Int*. 2007;33:239–45. <https://doi.org/10.1016/j.envint.2006.09.013>.

- Chupeau Z, Bonvallot N, Mercier F, le Bot B, Chevrier C, Glorennec P. Organophosphorus flame retardants: a global review of indoor contamination and human exposure in Europe and epidemiological evidence. *Int J Environ Res Public Health*. 2020;17:1–24. <https://doi.org/10.3390/ijerph17186713>.
- Covaci A, Voorspoels S, Thomsen C, van Bavel B, Neels H. Evaluation of total lipids using enzymatic methods for the normalization of persistent organic pollutant levels in serum. *Sci Total Environ*. 2006;366:361–6. <https://doi.org/10.1016/j.scitotenv.2006.03.006>.
- Crofton KM, Mundy WR, Shafer TJ. Developmental neurotoxicity testing: a path forward. *Congenit Anom (Kyoto)*. 2012;52:140–6. <https://doi.org/10.1111/j.1741-4520.2012.00377.x>.
- Crofton K, Fritsche E, Ylikomi T, Bal-Price A. International STakeholder NETwork (ISTNET) for creating a Developmental Neurotoxicity Testing (DNT) roadmap for regulatory purposes. *ALTEX*. 2014;31:223–4. <https://doi.org/10.14573/altex.1402121>.
- Dach K, Bendt F, Huebenthal U, Giersiefer S, Lein PJ, Heuer H, et al. BDE-99 impairs differentiation of human and mouse NPCs into the oligodendroglial lineage by species-specific modes of action. *Sci Rep*. 2017;7:1–11. <https://doi.org/10.1038/srep44861>.
- Darnerud PO, Eriksen GS, Jóhannesson T, Larsen PB, Viluksela M. Polybrominated diphenyl ethers: occurrence, dietary exposure, and toxicology. *Environ Health Perspect*. 2001;109:49–68. <https://doi.org/10.1289/ehp.01109s149>.
- De Wit CA. An overview of brominated flame retardants in the environment. *Chemosphere*. 2002;46:583–624. [https://doi.org/10.1016/S0045-6535\(01\)00225-9](https://doi.org/10.1016/S0045-6535(01)00225-9).
- Delp J, Gutbier S, Klima S, et al. A high-throughput approach to identify specific neurotoxicants/developmental toxicants in human neuronal cell function assays. *ALTEX*. 2018;35:235–53. <https://doi.org/10.14573/altex.1712182>.
- EFSA. Scientific Opinion on the developmental neurotoxicity potential of acetamiprid and imidacloprid. *EFSA J*. 2013;11:1–47. <https://doi.org/10.2903/j.efsa.2013.3471>.
- EPA 1998. EPA test guidelines for pesticides and toxic substances. Health effects test guidelines: OPPTS 870.6300 developmental neurotoxicity study. <https://www.epa.gov>
- Eskenazi B, Chevrier J, Rauch SA, Kogut K, Harley KG, Johnson C, et al. In utero and childhood polybrominated diphenyl ether (PBDE) exposures and neurodevelopment in the CHAMACOS study. *Environ Health Perspect*. 2013;121:257–62.
- Fischer D, Hooper K, Athanasiadou M, Athanassiadis I, Bergman Å. Children show highest levels of polybrominated diphenyl ethers in a California family of four: a case study. *Environ Health Perspect*. 2006;114:1581–4. <https://doi.org/10.1289/ehp.8554>.
- Foti F, Menghini D, Mandolesi L, Federico F, Vicari S, Petrosini L. Learning by observation: insights from Williams syndrome. *PLoS One*. 2013;8:1–10. <https://doi.org/10.1371/journal.pone.0053782>.
- Frank CL, Brown JP, Wallace K, Mundy WR, Shafer TJ. Developmental neurotoxicants disrupt activity in cortical networks on microelectrode arrays: results of screening 86 compounds during neural network formation. *Toxicol Sci*. 2017;160:121–35. <https://doi.org/10.1093/toxsci/kfx169>.
- Fritsche E, Alm H, Baumann J, Geerts L, Håkansson H, Masjosthusmann S, et al. Literature review on in vitro and alternative developmental neurotoxicity (DNT) testing methods. *EFSA Support Publ*. 2015;12:1–186. <https://doi.org/10.2903/sp.efsa.2015.en-778>.
- Fritsche E, Crofton KM, Hernandez AF, et al. OECD/EFSA workshop on developmental neurotoxicity (DNT): the use of non-animal test methods for regulatory purposes. *ALTEX*. 2017;34:311–5. <https://doi.org/10.14573/altex.1701171s>.
- Fritsche E, Barenys M, Klose J, Masjosthusmann S, Nimtz L, Schmuck M, et al. Current availability of stem cell-based in vitro methods for developmental neurotoxicity (DNT) testing. *Toxicol Sci*. 2018a;165:21–30. <https://doi.org/10.1093/toxsci/kfy178>.
- Fritsche E, Grandjean P, Crofton KM, Aschner M, Goldberg A, Heinonen T, et al. Consensus statement on the need for innovation, transition and implementation of developmental neurotoxicity (DNT) testing for regulatory purposes. *Toxicol Appl Pharmacol*. 2018b;354:3–6. <https://doi.org/10.1016/j.taap.2018.02.004>.
- Fujimoto H, Woo G-H, Morita R, et al. Increased cellular distribution of vimentin and ret in the cingulum of rat offspring after developmental exposure to decabromodiphenyl ether or 1,2,5,6,9,10-hexabromocyclododecane. *J Toxicol Pathol*. 2013;26:119–29. <https://doi.org/10.1293/tox.26.119>.
- Gangwal S, Reif DM, Mosher S, Egeghy PP, Wambaugh JF, Judson RS, et al. Incorporating exposure information into the toxicological prioritization index decision support framework. *Sci Total Environ*. 2012;435–436:316–25. <https://doi.org/10.1016/j.scitotenv.2012.06.086>.
- Gasparini RJ, Pavez M, Thompson AC, Mitchell CB, Hardy H, Young KM, et al. How does calcium interact with the cytoskeleton to regulate growth cone motility during axon pathfinding? *Mol Cell Neurosci*. 2017;84:29–35. <https://doi.org/10.1016/j.mcn.2017.07.006>.
- Gerst R, Hölzer M (2019) PCA-GO: an interactive web service to analyze RNA-Seq data with principal component analysis. *bioRxiv*. <https://doi.org/10.1101/433078>
- Gibson EA, Stapleton HM, Calero L, Holmes D, Burke K, Martinez R, et al. Differential exposure to organophosphate flame retardants in mother-child pairs. *Chemosphere*. 2019;219:567–73. <https://doi.org/10.1016/j.chemosphere.2018.12.008>.
- Guerrini R, Dobyns WB. Malformations of cortical development: clinical features and genetic causes. *Lancet Neurol*. 2014;13:710–26. [https://doi.org/10.1016/S1474-4422\(14\)70040-7](https://doi.org/10.1016/S1474-4422(14)70040-7).
- Hardy A, Benford D, Halldorsson T, et al. Update: use of the benchmark dose approach in risk assessment. *EFSA J*. 2017;15:1–41. <https://doi.org/10.2903/j.efsa.2017.4658>.
- Hayashi C, Suzuki N. Heterogeneity of Oligodendrocytes and Their Precursor Cells. *Adv Exp Med Biol*. 2019;1190:53–62. https://doi.org/10.1007/978-981-32-9636-7_5
- He C, English K, Baduel C, Thai P, Jagals P, Ware RS, et al. Concentrations of organophosphate flame retardants and plasticizers in urine from young children in Queensland, Australia and associations with environmental and behavioural factors. *Environ Res*. 2018a;164:262–70. <https://doi.org/10.1016/j.envres.2018.02.040>.
- He C, Toms L-ML, Thai P, van den Eede N, Wang X, Li Y, et al. Urinary metabolites of organophosphate esters: concentrations and age trends in Australian children. *Environ Int*.

- 2018b;111:124–30. <https://doi.org/10.1016/j.envint.2017.11.019>.
- Hirsch C, Striegl B, Mathes S, Adlhart C, Edelmann M, Bono E, et al. Multiparameter toxicity assessment of novel DOPO-derived organophosphorus flame retardants. *Arch Toxicol*. 2017;91:407–25. <https://doi.org/10.1007/s00204-016-1680-4>.
- Hoelting L, Klima S, Karreman C, Grinberg M, Meisig J, Henry M, et al. Stem cell-derived immature human dorsal root ganglia neurons to identify peripheral neurotoxicants. *Stem Cells Transl Med*. 2016;5:476–87. <https://doi.org/10.5966/sctm.2015-0108>.
- Hogberg HT, de Cássia da Silveira E, Sá R, Kleinsang A, et al. Organophosphorus flame retardants are developmental neurotoxicants in a rat primary brainsphere in vitro model. *Arch Toxicol*. 2020;95:207–28. <https://doi.org/10.1007/s00204-020-02903-2>.
- Hu WF, Chahrour MH, Walsh CA. The diverse genetic landscape of neurodevelopmental disorders. *Annu Rev Genomics Hum Genet*. 2014;15:195–213. <https://doi.org/10.1146/annurev-genom-090413-025600>.
- Juric-Sekhar G, Hevner RF. Malformations of cerebral cortex development: molecules and mechanisms. *Annu Rev Pathol Mech Dis*. 2019;14:293–318. <https://doi.org/10.1146/annurev-pathmechdis-012418-012927>.
- Káradóttir R, Hamilton NB, Bakiri Y, Attwell D. Spiking and nonspiking classes of oligodendrocyte precursor glia in CNS white matter. *Nat Neurosci*. 2008;11:450–6. <https://doi.org/10.1038/nn2060>.
- Kent JC, Mitoulas LR, Cregan MD, Ramsay DT, Doherty DA, Hartmann PE. Volume and frequency of breastfeedings and fat content of breast milk throughout the day. *Pediatrics*. 2006;117:387–95. <https://doi.org/10.1542/peds.2005-1417>.
- Kim JW, Isobe T, Muto M, Tue NM, Katsura K, Malarvannan G, et al. Organophosphorus flame retardants (PFRs) in human breast milk from several Asian countries. *Chemosphere*. 2014;116:91–7. <https://doi.org/10.1016/j.chemosphere.2014.02.033>.
- Klose J, Tigges J, Masjosthusmann S, et al. TBBPA targets converging key events of human oligodendrocyte development resulting in two novel AOPs. *ALTEX Prepr*. 2020;38:1–18. <https://doi.org/10.14573/altex.2007201>.
- Krebs A, Nyffeler J, Karreman C, et al. Determination of benchmark concentrations and their statistical uncertainty for cytotoxicity test data and functional in vitro assays. *ALTEX*. 2020a;37:155–63. <https://doi.org/10.14573/altex.1912021>.
- Krebs A, van Vugt-Lussenburg BMA, Waldmann T, Albrecht W, Boei J, ter Braak B, et al. The EU-ToxRisk method documentation, data processing and chemical testing pipeline for the regulatory use of new approach methods. *Arch Toxicol*. 2020b;94:2435–61. <https://doi.org/10.1007/s00204-020-02802-6>.
- Krug AK, Balmer NV, Matt F, Schönenberger F, Merhof D, Leist M. Evaluation of a human neurite growth assay as specific screen for developmental neurotoxicants. *Arch Toxicol*. 2013a;87:2215–31. <https://doi.org/10.1007/s00204-013-1072-y>.
- Krug AK, Kolde R, Gaspar JA, Rempel E, Balmer NV, Meganathan K, et al. Human embryonic stem cell-derived test systems for developmental neurotoxicity: a transcriptomics approach. *Arch Toxicol*. 2013b;87:123–43. <https://doi.org/10.1007/s00204-012-0967-3>.
- Kucharska A, Cequier E, Thomsen C, Becher G, Covaci A, Voorspoels S. Assessment of human hair as an indicator of exposure to organophosphate flame retardants. Case study on a Norwegian mother-child cohort. *Environ Int*. 2015;83:50–7. <https://doi.org/10.1016/j.envint.2015.05.015>.
- Kuhn S, Gritti L, Crooks D, Dombrowski Y. Oligodendrocytes in development, myelin generation and beyond. *cells* 2019;1424:1–23. <https://doi.org/10.3390/cells8111424>
- Law RJ, Covaci A, Harrad S, Herzke D, Abdallah MAE, Fernie K, et al. Levels and trends of PBDEs and HBCDs in the global environment: status at the end of 2012. *Environ Int*. 2014;65:147–58. <https://doi.org/10.1016/j.envint.2014.01.006>.
- Lein P, Silbergeld E, Locke P, Goldberg AM. In vitro and other alternative approaches to developmental neurotoxicity testing (DNT). *Environ Toxicol Pharmacol*. 2005;19:735–44. <https://doi.org/10.1016/j.etap.2004.12.035>.
- Li T, Wang W, Pan YW, Xu L, Xia Z. A hydroxylated metabolite of flame-retardant PBDE-47 decreases the survival, proliferation, and neuronal differentiation of primary cultured adult neural stem cells and interferes with signaling of ERK5 map kinase and neurotrophin 3. *Toxicol Sci*. 2013;134:111–24. <https://doi.org/10.1093/toxsci/kft083>.
- Li M, Yao Y, Wang Y, Bastiaensen M, Covaci A, Sun H. Organophosphate ester flame retardants and plasticizers in a Chinese population: significance of hydroxylated metabolites and implication for human exposure. *Environ Pollut*. 2020;257:257. <https://doi.org/10.1016/j.envpol.2019.113633>.
- López-Espíndola D, Morales-Bastos C, Grijota-Martínez C, Liao XH, Lev D, Sugo E, et al. Mutations of the thyroid hormone transporter MCT8 cause prenatal brain damage and persistent hypomyelination. *J Clin Endocrinol Metab*. 2014;99:E2799–804. <https://doi.org/10.1210/jc.2014-2162>.
- Lotharius J, Falsig J, Van Beek J, et al. Progressive degeneration of human mesencephalic neuron-derived cells triggered by dopamine-dependent oxidative stress is dependent on the mixed-lineage kinase pathway. *J Neurosci*. 2005;25:6329–42. <https://doi.org/10.1523/JNEUROSCI.1746-05.2005>.
- Luttrell WE, Olajos EJ, Pleban PA. Change in hen sciatic nerve clacium after a single oral dose of tri-O-tolyl phosphate. *Environ Res*. 1993;60:290–4.
- Ma Y, Salamova A, Venier M, Hites RA. Has the phase-out of PBDEs affected their atmospheric levels? Trends of PBDEs and their replacements in the great lakes atmosphere. *Environ Sci Technol*. 2013;47:11457–64. [dx.doi.org. https://doi.org/10.1021/es403029m](https://doi.org/10.1021/es403029m).
- Ma J, Zhu H, Kannan K. Organophosphorus flame retardants and plasticizers in breast milk from the United States. *Environ Sci Technol Lett*. 2019;6:525–31. <https://doi.org/10.1021/acs.estlett.9b00394>.
- Marinelli C, Bertalot T, Zusso M, Skaper SD, Giusti P. Systematic review of pharmacological properties of the oligodendrocyte lineage. *Front Cell Neurosci*. 2016;10:1–27. <https://doi.org/10.3389/fncel.2016.00027>.
- Marvel SW, To K, Grimm FA, et al. ToxPi Graphical User Interface 2.0: dynamic exploration, visualization, and sharing of integrated data models. *BMC Bioinformatics*. 2018;19:1–7. <https://doi.org/10.1186/s12859-018-2089-2>.

- Masjosthusmann S, Becker D, Petzuch B, Klose J, Siebert C, Deenen R, et al. A transcriptome comparison of time-matched developing human, mouse and rat neural progenitor cells reveals human uniqueness. *Toxicol Appl Pharmacol.* 2018;354:40–55. <https://doi.org/10.1016/j.taap.2018.05.009>.
- Masjosthusmann S, Blum J, Bartmann K, et al. Establishment of an a priori protocol for the implementation and interpretation of an in-vitro testing battery for the assessment of developmental neurotoxicity. *EFSA J.* 2020;17:1938e. <https://doi.org/10.2903/sp.efsa.2020.EN-1938>.
- Mayor R, Theveneau E. The neural crest. *Dev Glance.* 2013;140:2247–51. <https://doi.org/10.1242/dev.091751>.
- Mizouchi S, Ichiba M, Takigami H, Kajiwara N, Takamuku T, Miyajima T, et al. Exposure assessment of organophosphorus and organobromine flame retardants via indoor dust from elementary schools and domestic houses. *Chemosphere.* 2015;123:17–25. <https://doi.org/10.1016/j.chemosphere.2014.11.028>.
- Muñoz-Quezada MT, Lucero BA, Barr DB, Steenland K, Levy K, Ryan PB, et al. Neurodevelopmental effects in children associated with exposure to organophosphate pesticides: a systematic review. *Neurotoxicology.* 2013;39:158–68. <https://doi.org/10.1016/j.neuro.2013.09.003>.
- Nimtz L, Klose J, Masjosthusmann S, et al. The neurosphere assay as an in vitro method for developmental neurotoxicity (DNT) evaluation. *Cell Cult Tech Neuromethods.* 2019;145:141–68. <https://doi.org/10.1007/978-1-4939-9228-7>.
- Nimtz L, Hartmann J, Tigges J, Masjosthusmann S, Schmuck M, Keßel E, et al. Characterization and application of electrically active neuronal networks established from human induced pluripotent stem cell-derived neural progenitor cells for neurotoxicity evaluation. *Stem Cell Res.* 2020;45:101761. <https://doi.org/10.1016/j.scr.2020.101761>.
- Nyffeler J, Dolde X, Krebs A, Pinto-Gil K, Pastor M, Behl M, et al. Combination of multiple neural crest migration assays to identify environmental toxicants from a proof-of-concept chemical library. *Arch Toxicol.* 2017;91:3613–32. <https://doi.org/10.1007/s00204-017-1977-y>.
- OECD 2007. OECD guideline for the testing of chemicals: health effects. Test No. 426: developmental neurotoxicity study. <http://www.oecd.org/dataoecd/20/52/37622194.pdf>
- Phillips DL, Pirkle JL, Burse VW, Bemert JT Jr, Henderson LO, Needham LL. Chlorinated hydrocarbon levels in human serum: effects of fasting and feeding. *Arch Environ Contam Toxicol.* 1989;18:495–500. <https://doi.org/10.1007/BF01055015>.
- Pistollato F, De Gyves EM, Carpi D, et al. Assessment of developmental neurotoxicity induced by chemical mixtures using an adverse outcome pathway concept. *Environ Heal A Glob Access Sci Source.* 2020;19:1–26. <https://doi.org/10.1186/s12940-020-00578-x>.
- Prentice P, Ong KK, Schoemaker MH, Tol EAF, Vervoort J, Hughes IA, et al. Breast milk nutrient content and infancy growth. *Acta Paediatr Int J Paediatr.* 2016;105:641–7. <https://doi.org/10.1111/apa.13362>.
- Razek AA, Mazroa J, Baz H. Assessment of white matter integrity of autistic preschool children with diffusion weighted MR imaging. *Brain and Development.* 2014;36:28–34. <https://doi.org/10.1016/j.braindev.2013.01.003>.
- Reif DM, Martin MT, Tan SW, Houck KA, Judson RS, Richard AM, et al. Endocrine profiling and prioritization of environmental chemicals using toxcast data. *Environ Health Perspect.* 2010;118:1714–20. <https://doi.org/10.1289/ehp.1002180>.
- Roze E, Meijer L, Bakker A, van Braeckel KNJA, Sauer PJJ, Bos AF. Prenatal exposure to organohalogen, including brominated flame retardants, influences motor, cognitive, and behavioral performance at school age. *Environ Health Perspect.* 2009;117:1953–8. <https://doi.org/10.1289/ehp.0901015>.
- Rylander L, Nilsson-Ehle P, Hagmar L. A simplified precise method for adjusting serum levels of persistent organohalogen pollutants to total serum lipids. *Chemosphere.* 2006;62:333–6. <https://doi.org/10.1016/j.chemosphere.2005.04.107>.
- Sachana M, Bal-Price A, Crofton KM, Bennekou SH, Shafer TJ, Behl M, et al. International regulatory and scientific effort for improved developmental neurotoxicity testing. *Toxicol Sci.* 2019;167:45–57. <https://doi.org/10.1093/toxsci/kfy211>.
- Saegusa Y, Fujimoto H, Woo G-H, Inoue K, Takahashi M, Mitsumori K, et al. Developmental toxicity of brominated flame retardants, tetrabromobisphenol A and 1,2,5,6,9,10-hexabromocyclododecane, in rat offspring after maternal exposure from mid-gestation through lactation. *Reprod Toxicol.* 2009;28:456–67. <https://doi.org/10.1016/j.reprotox.2009.06.011>.
- Schmidt BZ, Lehmann M, Gutbier S, Nembo E, Noel S, Smirnova L, et al. In vitro acute and developmental neurotoxicity screening: an overview of cellular platforms and high-throughput technical possibilities. *Arch Toxicol.* 2017;91:1–33. <https://doi.org/10.1007/s00204-016-1805-9>.
- Schmuck MR, Temme T, Dach K, et al. Omnisphero: a high-content image analysis (HCA) approach for phenotypic developmental neurotoxicity (DNT) screenings of organoid neurosphere cultures in vitro. *Arch Toxicol.* 2016:1–12. <https://doi.org/10.1007/s00204-016-1852-2>.
- Scholz D, Pörtl D, Genewsky A, Weng M, Waldmann T, Schildknecht S, et al. Rapid, complete and large-scale generation of post-mitotic neurons from the human LUHMES cell line. *J Neurochem.* 2011;119:957–71. <https://doi.org/10.1111/j.1471-4159.2011.07255.x>.
- Schreiber T, Gassmann K, Götz C, Hübenal U, Moors M, Krause G, et al. Polybrominated diphenyl ethers induce developmental neurotoxicity in a human in vitro model: evidence for endocrine disruption. *Environ Health Perspect.* 2010;118:572–8. <https://doi.org/10.1289/ehp.0901435>.
- Shafer TJ, Brown JP, Lynch B, Davila-Montero S, Wallace K, Friedman KP. Evaluation of chemical effects on network formation in cortical neurons grown on microelectrode arrays. *Toxicol Sci.* 2019;169:436–55. <https://doi.org/10.1093/toxsci/kfz052>.
- Shy C-G, Huang H-L, Chang-Chien G-P, Chao HR, Tsou TC. Neurodevelopment of infants with prenatal exposure to polybrominated diphenyl ethers. *Bull Environ Contam Toxicol.* 2011;87:643–8. <https://doi.org/10.1007/s00128-011-0422-9>.
- Simons M, Trajkovic K. Neuron-glia communication in the control of oligodendrocyte function and myelin biogenesis. *J Cell Sci.* 2006;119:4381–9. <https://doi.org/10.1242/jcs.03242>.
- Stapleton HM, Klosterhaus S, Eagle S, Fuh J, Meeker JD, Blum A, et al. Detection of organophosphate flame retardants in furniture foam and U.S. house dust. *Environ Sci Technol.* 2009;43:7490–5. <https://doi.org/10.1021/es9014019>.

- Stapleton HM, Misenheimer J, Hoffman K, Webster TF. Flame retardant associations between children's handwipes and house dust. *Chemosphere*. 2014;116:54–60. <https://doi.org/10.1016/j.chemosphere.2013.12.100>.
- Stiegler NV, Krug AK, Matt F, Leist M. Assessment of chemical-induced impairment of human neurite outgrowth by multiparametric live cell imaging in high-density cultures. *Toxicol Sci*. 2011;121:73–87. <https://doi.org/10.1093/toxsci/kfi034>.
- Stumpf AM, Tanaka D, Aulerich RJ, Bursian SJ. Delayed neurotoxic effects of tri-*o*-tolyl phosphate in the european ferret. *J Toxicol Environ Health*. 1989;26:61–73. <https://doi.org/10.1080/15287398909531233>.
- Sugeng EJ, Leonards PEG, van de Bor M. Brominated and organophosphorus flame retardants in body wipes and house dust, and an estimation of house dust hand-loadings in Dutch toddlers. *Environ Res*. 2017;158:789–97. <https://doi.org/10.1016/j.envres.2017.07.035>.
- Sundkvist AM, Olofsson U, Haglund P. Organophosphorus flame retardants and plasticizers in marine and fresh water biota and in human milk. *J Environ Monit*. 2010;12:943–51. <https://doi.org/10.1039/b921910b>.
- Tang J, Zhai JX. Distribution of polybrominated diphenyl ethers in breast milk, cordblood and placentas: a systematic review. *Environ Sci Pollut Res*. 2017;24:21548–73. <https://doi.org/10.1007/s11356-017-9821-8>.
- Tang H, Hammack C, Ogden SC, Wen Z, Qian X, Li Y, et al. Zika virus infects human cortical neural progenitors and attenuates their growth. *Cell Stem Cell*. 2016;18:587–90. <https://doi.org/10.1016/j.stem.2016.02.016>.
- Terron A, Bennekou Hougaard S. Towards a regulatory use of alternative developmental neurotoxicity testing (DNT). *Toxicol Appl Pharmacol*. 2018;354:19–23. <https://doi.org/10.1016/j.taap.2018.02.002>.
- Thomson JA, Itskovitz-Eldor J, Shapiro SS, et al. Embryonic stem cell lines derived from human blastocysts. *Science*. 1998;282(80):1145–7. <https://doi.org/10.1126/science.282.5391.1145>.
- Toms L-ML, Sjödin A, Harden F, Hobson P, Jones R, Edenfield E, et al. Serum polybrominated diphenyl ether (PBDE) levels are higher in children (2-5 years of age) than in infants and adults. *Environ Health Perspect*. 2009;117:1461–5. <https://doi.org/10.1289/ehp.0900596>.
- Tonduti D, Vanderver A, Berardinelli A, et al. MCT8 deficiency: extrapyramidal symptoms and delayed myelination as prominent features. *Child Neurol Psychiatry*. 2014;28:795–800. <https://doi.org/10.1177/0883073812450944.MCT8>.
- Tsuji R, Crofton KM. Developmental neurotoxicity guideline study: issues with methodology, evaluation and regulation. *Congenit Anom (Kyoto)*. 2012;52:122–8. <https://doi.org/10.1111/j.1741-4520.2012.00374.x>.
- van der Veen I, de Boer J. Phosphorus flame retardants: properties, production, environmental occurrence, toxicity and analysis. *Chemosphere*. 2012;88:1119–53. <https://doi.org/10.1016/j.chemosphere.2012.03.067>.
- Volpe JJ, Kinney HC, Jensen FE, Rosenberg PA. The developing oligodendrocyte: key cellular target in brain injury in the premature infant. *Int J Dev Neurosci*. 2011;29:423–40. <https://doi.org/10.1016/j.ijdevneu.2011.02.012>.
- Waaijers SL, Kong D, Hendriks HS, et al. Persistence, Bioaccumulation, and Toxicity of Halogen-Free Flame Retardants. *Rev Environ Contam Toxicol*. 2013;222:1–71. <https://doi.org/10.1007/978-1-4614-6470-9>.
- Walter KM, Dach K, Hayakawa K, et al. Ontogenetic expression of thyroid hormone signaling genes: An in vitro and in vivo species comparison. *PLoS One*. 2019;14:1–26. <https://doi.org/10.1371/journal.pone.0221230>.
- Wolff JJ, Ph D, Gu H, et al. Differences in white matter fiber tract development present from 6 to 24 months in infants with autism. *Am J Psychiatry*. 2013;169:589–600. <https://doi.org/10.1176/appi.ajp.2011.11091447.Differences>.
- Yogui GT, Sericano JL. Polybrominated diphenyl ether flame retardants in the U.S. marine environment: a review. *Environ Int*. 2009;35:655–66. <https://doi.org/10.1016/j.envint.2008.11.001>.
- Zilles K, Palomero-Gallagher N, Amunts K. Development of cortical folding during evolution and ontogeny. *Trends Neurosci*. 2013;36:275–84. <https://doi.org/10.1016/j.tins.2013.01.006>.

Publisher's note Springer Nature remains neutral with regard to jurisdictional claims in published maps and institutional affiliations.

Neurodevelopmental toxicity assessment of flame retardants using a human DNT *in vitro* testing battery

Jördis Klose, Melanie Pahl, **Kristina Bartmann**, Farina Bendt, Jonathan Blum, Xenia Dolde, Anna-Katharina Holzer, Ulrike Hübenthal, Hagen Eike Keßel, Katharina Koch, Stefan Masjosthusmann, Sabine Schneider, Lynn-Christin Stürzl, Selina Woeste, Andrea Rossi, Adrian Covaci, Mamta Behl, Marcel Leist, Julia Tigges, Ellen Fritsche

Journal:	Cell Biology and Toxicology
Impact factor:	6.691 (2021-2022)
Contribution to the publication:	5%
	Performance and evaluation of TOCP experiments
Type of authorship:	co-authorship
Status of publication:	Published 10 May 2021

2.3 Establishment of a human cell-based *in vitro* battery to assess developmental neurotoxicity hazard of chemicals

Jonathan Blum, Stefan Masjosthusmann, **Kristina Bartmann**, Farina Bendt, Xenia Dolde, Arif Dönmez, Nils Förster, Anna-Katharina Holzer, Ulrike Hübenthal, Hagen Eike Keßel, Sadiye Kilic, Jördis Klose, Melanie Pahl, Lynn-Christin Stürzl, Iris Mangas, Andrea Terron, Kevin Crofton, Martin Scholze, Axel Mosig, Marcel Leist, Ellen Fritsche

Chemosphere

Die Entwicklungsneurotoxizität (DNT) ist ein wesentliches Sicherheitsproblem für alle Chemikalien des menschlichen Exposoms, doch DNT-Daten aus Tierstudien sind nur für wenige dieser Substanzen verfügbar. Daher werden dringend Testmethoden mit einem höheren Durchsatz als im Tierversuch und einer besseren Relevanz für den Menschen benötigt. Wir untersuchten daher die Durchführbarkeit einer DNT-Gefährdungsbeurteilung auf der Grundlage von sogenannten *new approach methods* (NAM). Eine *in vitro*-Batterie (IVB) wurde aus einzelnen NAMs zusammengestellt, die in den letzten Jahren entwickelt wurden, um die Auswirkung von Chemikalien auf verschiedene grundlegende Prozesse der Gehirnentwicklung zu untersuchen. Für alle Tests wurden menschliche neurale Zellen in verschiedenen Entwicklungsstadien entweder in 2D, 3D oder sekundärem 3D verwendet. Auf diese Weise konnten Störungen (i) der Proliferation neurale Vorläuferzellen (NPC), (ii) der Migration von Neuralleistenzellen, radialen Gliazellen, Neuronen und Oligodendrozyten, (iii) der Differenzierung von NPCs in Neuronen und Oligodendrozyten und (iv) des Neuritenwachstums peripherer und zentraler Neuronen in Verbindung mit Messungen der Zytotoxizität/Viabilität beurteilt werden. Die Durchführbarkeit eines konzentrationsabhängigen Screenings und einer zuverlässigen biostatistischen Verarbeitung der komplexen multidimensionalen Daten wurde mit einer Reihe von 120 Testsubstanzen untersucht, die eine Auswahl von vordefiniert positiven und negativen DNT-Substanzen enthielten. Die Batterie lieferte Hinweise (*Hit* oder *Borderline*) für 24 von 28 bekannten DNT-Toxika (82% Sensitivität), und die Spezifität lag bei >94%. Auf der Grundlage dieser Daten wurden Strategien entwickelt, wie die Daten im Rahmen von Risikobewertungsszenarien unter Verwendung integrierter Ansätze für die Prüfung und Bewertung verwendet werden können.

Chemosphere

Establishment of a human cell-based in vitro battery to assess developmental neurotoxicity hazard of chemicals

--Manuscript Draft--

Manuscript Number:	
Article Type:	Research paper
Section/Category:	Toxicology and Risk Assessment
Keywords:	testing battery, stem cell, brain development, in vitro testing, DNT
Corresponding Author:	Jonathan Blum University of Konstanz Konstanz, GERMANY
First Author:	Jonathan Blum
Order of Authors:	Jonathan Blum Stefan Masjosthusmann Kristina Bartmann Farina Bendt Xenia Dolde Arif Dönmez Nils Förster Anna-Katharina Holzer Ulrike Hübenthal Hagen Keßel Sadiye Kilic Jördis Klose Melanie Pahl Lynn-Christin Stürzl Iris Mangas Andrea Terron Kevin Crofton Martin Scholze Axel Mosig Marcel Leist Ellen Fritsche
Abstract:	Developmental neurotoxicity (DNT) is a major safety concern for all chemicals of the human exposome. However, DNT data from animal studies are available for only a small percentage of manufactured compounds. Test methods with a higher throughput than current regulatory guideline methods, and with improved human relevance are urgently needed. We therefore explored the feasibility of DNT hazard assessment based on new approach methods (NAMs). An in vitro battery (IVB) was assembled from ten individual NAMs that had been developed during the past years to probe effects of chemicals on various fundamental neurodevelopmental processes. All assays used human neural cells at different developmental stages. This allowed us to assess disturbances of: (i) proliferation of neural progenitor cells (NPC); (ii) migration of neural crest cells, radial glia cells, neurons and oligodendrocytes; (iii) differentiation of NPC into neurons and oligodendrocytes; and (iv) neurite outgrowth of peripheral and

	<p>central neurons. In parallel, cytotoxicity measures were obtained. The feasibility of concentration-dependent screening and of a reliable biostatistical processing of the complex multi-dimensional data was explored with a set of 120 test compounds, containing subsets of pre-defined positive and negative DNT compounds. The battery provided alerts (hit or borderline) for 24 of 28 known toxicants (82% sensitivity), and for none of the 17 negative controls. Based on the results from this screen project, strategies were developed on how IVB data may be used in the context of risk assessment scenarios employing integrated approaches for testing and assessment (IATA).</p>
<p>Suggested Reviewers:</p>	<p>Lena Smirnova Johns Hopkins University lsmirno1@jhu.edu</p> <p>Barbara Viviani University of Milan barbara.viviani@unimi.it</p> <p>Antonio Francisco Hernandez-Jerez University of Granada ajerez@ugr.es</p> <p>Pamela Lein University of California Davis College of Biological Sciences pjlein@ucdavis.edu</p> <p>Ellen Hessel National Institute for Public Health and the Environment ellen.hessel@rivm.nl</p> <p>David Pamies University of Lausanne David.Pamies@unil.ch</p>
<p>Opposed Reviewers:</p>	

Highlights

- An in vitro testing battery consisting of ten assays, all related to at least one key neurodevelopmental process, has been assembled and documented.
- Testing of 120 compounds has been performed across all assays of the developmental neurotoxicity in vitro test battery.
- Performance estimates (> 80% accuracy) have been obtained for the testing battery, based on 45 negative/positive controls.
- Gaps and uncertainties of the test battery have been analyzed, and recommendations for the use of the battery for regulatory testing have been put forward.

Blum & Masjosthusmann et al. (2022): In vitro battery for DNT testing

1 **Establishment of a human cell-based in vitro battery to assess** 2 **developmental neurotoxicity hazard of chemicals**

3 *Jonathan Blum^{1,#}, Stefan Masjosthusmann^{2,#}, Kristina Bartmann², Farina Bendt², Xenia Dolde¹,*
4 *Arif Dönmez², Nils Förster⁴, Anna-Katharina Holzer¹, Ulrike Hübenthal², Hagen Eike Keßel²,*
5 *Sadiye Kilic, Jördis Klose², Melanie Pahl², Lynn-Christin Stürzl², Iris Mangas⁵, Andrea Terron⁵,*
6 *Kevin M. Crofton⁶, Martin Scholze⁷, Axel Mosig⁴, Marcel Leist^{1,°}, Ellen Fritsche^{2,3,°}*

7 ¹In vitro Toxicology and Biomedicine, Dept inaugurated by the Doerenkamp-Zbinden
8 foundation, University of Konstanz, 78457 Konstanz, Germany

9 ²IUF - Leibniz Research Institute for Environmental Medicine, 40225 Düsseldorf, Germany

10 ³Medical Faculty, Heinrich-Heine-University, 40225 Düsseldorf, Germany

11 ⁴Bioinformatics Group, Ruhr University Bochum, 44801 Bochum, Germany

12 ⁵European Food Safety Authority, PREV Unit, 43126 Parma, Italy

13 ⁶R3Fellows LLC, Durham (NC), USA

14 ⁷Institute of Environment Health and Societies, Brunel University London, UK

15 [#]these authors contributed equally; [°]these authors contributed equally

16 **Running title:** In vitro battery for DNT testing

17 **Key words:** testing battery, stem cell, brain development, in vitro testing, DNT

18 Correspondence to be sent to:

19 Marcel Leist, In vitro Toxicology and Biomedicine, Dept inaugurated by the Doerenkamp-
20 Zbinden foundation at the University of Konstanz, Universitätsstraße 10, 78457 Konstanz,
21 Germany; Email: marcel.leist@uni-konstanz.de

22 Or: Ellen Fritsche, IUF – Leibniz Research Institute for Environmental Medicine, Auf'm
23 Hennekamp 50, 40225 Düsseldorf, Germany; Email: ellen.fritsche@iuf-duesseldorf.de

24 **Abstract**

25 Developmental neurotoxicity (DNT) is a major safety concern for all chemicals of the human
26 exposome. However, DNT data from animal studies are available for only a small percentage of
27 manufactured compounds. Test methods with a higher throughput than current regulatory
28 guideline methods, and with improved human relevance are urgently needed. We therefore
29 explored the feasibility of DNT hazard assessment based on new approach methods (NAMs). An
30 in vitro battery (IVB) was assembled from ten individual NAMs that had been developed during
31 the past years to probe effects of chemicals on various fundamental neurodevelopmental
32 processes. All assays used human neural cells at different developmental stages. This allowed us
33 to assess disturbances of: (i) proliferation of neural progenitor cells (NPC); (ii) migration of
34 neural crest cells, radial glia cells, neurons and oligodendrocytes; (iii) differentiation of NPC into
35 neurons and oligodendrocytes; and (iv) neurite outgrowth of peripheral and central neurons. In
36 parallel, cytotoxicity measures were obtained. The feasibility of concentration-dependent
37 screening and of a reliable biostatistical processing of the complex multi-dimensional data was
38 explored with a set of 120 test compounds, containing subsets of pre-defined positive and
39 negative DNT compounds. The battery provided alerts (hit or borderline) for 24 of 28 known
40 toxicants (82% sensitivity), and for none of the 17 negative controls. Based on the results from
41 this screen project, strategies were developed on how IVB data may be used in the context of risk
42 assessment scenarios employing integrated approaches for testing and assessment (IATA).

43

44 **1. Introduction**

45 Screening of chemicals for a potential neurodevelopmental toxicity (DNT) hazard has been
46 recognized as a pressing need by several large governmental and international organizations
47 concerned with consumer safety. For instance, the US EPA and the European JRC took important
48 roles in the organisation of a conference series (TestSmart) that was devoted to the development
49 of a DNT test strategy useful in a regulatory context (Coecke et al., 2007; Lein et al., 2007;
50 Crofton et al., 2011; Bal-Price et al., 2012). Also EFSA and the OECD embarked on similar
51 efforts (Fritsche et al., 2017). In this context, several experimental programs were launched to
52 probe novel approaches and to accelerate their implementation (Crofton et al., 2012; van Thriel et
53 al., 2012; Krug et al., 2013b; Bal-Price et al., 2015; Baumann et al., 2016; Fritsche et al., 2018;
54 Harrill et al., 2018; Behl et al., 2019; Lupu et al., 2020; Pistollato et al., 2021; Sachana et al.,
55 2021; Vinken et al., 2021; Koch et al., 2022).

56 DNT is a field of toxicology concerned with effects of chemicals on the developing nervous
57 system. Several experimental and epidemiological studies (on metals, pesticides and drugs) link
58 compound exposure during early live phases (of the embryo, fetus or child) to functional
59 alterations of the nervous system in adolescents or adults (Grandjean and Landrigan, 2014;
60 Smirnova et al., 2014; Bennett et al., 2016). A particular concern is the possible role of DNT in
61 the increased frequency of neurodevelopmental disorders, such as autism-spectrum disorders
62 (Grandjean and Landrigan, 2006; Bellinger, 2012; Grandjean and Landrigan, 2014; Modafferi et
63 al., 2021). The assessment is particularly challenging due to the multitude of potential toxicity
64 manifestations (structural and functional). Moreover, there may be a time offset between toxicant
65 exposure (before or after birth) and manifestation of effects.

Blum & Masjosthusmann et al. (2022): In vitro battery for DNT testing

66 The traditional methods to evaluate DNT hazard potential are based on animal studies following
67 the OECD (OECD, 2007) or EPA (USEPA, 1998) test guidelines. To date only about 180
68 compounds world-wide have been tested using these guidelines (Crofton and Mundy, 2021).
69 Several factors contribute to the limited availability of such studies: extensive time (e.g. 1-2
70 years) and resource requirement; limited triggered testing by chemical alerts; the need to reduce
71 animal use; and the limited regulatory requirement for DNT testing as compared to some other
72 test guidelines (e.g., carcinogenicity). The data available suffer from many uncertainties, and they
73 require species extrapolation from rodents to humans. Moreover, they provide limited
74 information on toxicity mechanisms. This can make them difficult to use in human risk
75 assessments (Makris et al., 2009; Tsuji and Crofton, 2012; Tohyama, 2016; Paparella et al.,
76 2020).

77 The strategic concepts of next generation risk assessment and of “toxicology for the 21st century”
78 (Leist et al., 2008; Thomas et al., 2018; Pallocca et al., 2022a) suggest reductions in use of
79 animal studies and development of new approach methods (NAMs) for toxicity assessments. The
80 non-animal test methods should ideally be based on human-relevant test systems, reduce costs,
81 allow a high throughput of test chemicals, and provide information on the toxicity mechanisms of
82 toxicants. Many recent activities on scientific and regulatory levels have been undertaken to
83 apply this strategy to the field of DNT (Sachana et al., 2019).

84 The establishment of DNT NAMs followed two major principles (Bal-Price et al., 2015; Aschner
85 et al., 2017). First, a concept was developed on how complex in vivo events and their
86 disturbances could be modeled by simplified in vitro systems. It was found that the biological
87 process of nervous system development can be broken down to less complex key
88 neurodevelopmental processes (KNDP). Moreover, it was assumed that the disturbance of any

Blum & Masjosthusmann et al. (2022): In vitro battery for DNT testing

89 KNDP may lead to DNT in man. On this basis, NAMs were developed for most of the crucial
90 KNDP. The second principle was that the performance and robustness of the NAMs should be at
91 a high level, so that data could be used with high confidence. The concept of test readiness was
92 developed to provide a measure of the NAM validation status (Bal-Price et al., 2018; Krebs et al.,
93 2019; Krebs et al., 2020b), and several assays were deemed ready and suitable for use in
94 chemical screening. They include: proliferation, migration and differentiation assays based on
95 neurospheres (NPC1-5 test methods); the neurite growth assays NeuroTox and PeriTox; the
96 neural crest migration assay (cMINC); and a assays for neural network formation and
97 synaptogenesis (Masjosthusmann et al., 2020; Crofton and Mundy, 2021; Carstens et al., 2022).
98 Instead of a formal OECD-type validation (e.g. skin sensitization NAMs (OECD, 2021;
99 Strickland et al., 2022)), the concept of a fit-for-purpose biological validation based on regulatory
100 needs has been suggested (Leist et al., 2012; Judson et al., 2013; Hartung et al., 2013; Bal-Price
101 et al., 2018; Cote et al., 2016; Griesinger et al., 2016; Andersen et al., 2019; Masjosthusmann et
102 al., 2020). Its application to DNT NAM involved: understanding of all technologies related to test
103 systems and endpoint assessment; a comparison of pivotal in vitro signaling pathways to those
104 relevant in vivo; and an assessment of the cellular presence of toxicity targets known to play a
105 role for human DNT (Aschner et al., 2017; Bal-Price et al., 2018; Koch et al., 2022).

106 No individual NAM covers all key aspects of neurodevelopmental biology. Thus no single test
107 will detect effects on all KNDP. Therefore, a battery of assays is needed, to sufficiently cover all
108 DNT toxicants. In 2016, participants of a meeting jointly organized by the European Food Safety
109 Authority (EFSA) and the organization for Economic Co-operation and Development (OECD)
110 agreed that “an in vitro testing battery (based on available DNT NAM) could be used
111 immediately to screen and prioritize chemicals” (Fritsche et al., 2017). A test run for such a

Blum & Masjosthusmann et al. (2022): In vitro battery for DNT testing

112 battery was planned, in order to evaluate the technical feasibility, to identify potential gaps and to
113 provide data and experience for setting up a draft guidance on how to run battery testing, and
114 how to interpret data therefrom (Crofton and Mundy, 2021).

115 The purpose of this manuscript is to describe the first test run of a DNT in vitro test battery based
116 on methods available in European laboratories (IVB-EU). Extensive raw data and method
117 documentations can be found in a report by EFSA (Masjosthusmann et al., 2020), and the
118 experience and learnings from the IVB-EU have led to the preparation of the draft of an OECD
119 guidance document, which is currently (July 2022) under revision in member countries (Crofton
120 and Mundy, 2021). However, the data from 10 assays on 120 compounds (including 28 positive
121 and 17 negative controls) have not been made available to academia and the interested public in a
122 peer-reviewed publication. The same applies to the preliminary performance evaluation of the
123 IVB-EU as a whole and the considerations concerning further use. The purpose of this
124 manuscript is to make this important information available, and to provide a basis for further
125 developments in academia, industry and by regulatory institutions concerned with NAM-based
126 DNT testing.

127

128

129 **2. Materials and Methods**

130 **2.1. Chemicals**

131 A list of screen compounds (n = 120) was assembled by an expert group with long experience,
132 based on their work at the US EPA, EFSA and/or their contribution to OECD test guidelines.
133 Compounds were selected to be chemically and biologically diverse and to reflect groups of
134 compounds with concern for a potential DNT hazard. For instance, flame retardants and
135 pesticides were included, as some compounds in these groups are known for biological properties
136 of relevance to DNT. One aspect of the selection process was also to allow for diversity of effects
137 on different fundamental neurodevelopmental processes (and respective assays), and it was
138 important to cover the full spectrum from compounds with no or low evidence for DNT liability
139 to compounds with rich background data to allow for a wide spread of screen results. A subset of
140 compounds (n=28) were included as positive controls for DNT hazard, based on human data or
141 robust animal data (Grandjean and Landrigan, 2006, 2014; Mundy et al., 2015; Ryan et al., 2016;
142 Aschner et al., 2017) (Fig. S1). Another subset (n=17) were compounds considered as negative
143 controls. They were selected for their safe use during human pregnancy or because the available
144 extensive data on their toxicity gave no evidence (by observation or mechanism) of any effects
145 related to DNT (at the test concentrations used) (Fig. S2). A description of chemicals, including
146 exact chemical identity is found in the [suppl. file 2 - sheet 1](#).

147 **2.2. Test methods**

148 All test methods used for screening were selected based on their high readiness level, which
149 included a very comprehensive test description, compatible with the OECD guidance document
150 GD211 on in vitro test method descriptions. These so-called ToxTemp files (Krebs et al., 2019)
151 are included in [suppl. file 1](#). Below, only brief descriptions are given for a quick overview.

Blum & Masjosthusmann et al. (2022): In vitro battery for DNT testing

152 UKN2 Assay (cMINC): The assay, is based on neural crest cells differentiated from hiPSC
153 (Nyffeler et al., 2017). Cells were seeded into 96-well plates around a stopper. The stopper was
154 removed after 24 h to allow migration into the cell free area. Cells were exposed to the test
155 compound for 24 h, and then stained with calcein-AM and Hoechst H-33342. The number of
156 migrated double positive cells was quantified independent of an observer by high content
157 imaging and image analysis (RingAssay software; <http://invitro-tox.uni-konstanz.de>). The cell
158 viability was also determined by an automated imaging algorithm. Concentration-response curves
159 from this test were based on six test compound concentrations (plus solvent control)

160 UKN4 assay (NeuriTox): The assay is based on LUHMES cells that were cultured and handled
161 as previously described (Lotharius et al., 2005; Scholz et al., 2011; Krug et al., 2013a). Cells
162 were pre-differentiated for two days to commit them towards the neuronal fate. They were then
163 re-seeded in 96-well plates and exposed to the chemical for 24 h. Viability and neurite area were
164 determined by high-content imaging after staining with calcein-AM and H-33342. The neurite
165 area was defined by a fully automated algorithm as the area of calcein-positive pixels minus the
166 area of all cell soma (Stiegler et al., 2011). Concentration-response curves from this test were
167 based on ten test compound concentrations (plus solvent control).

168 UKN5 Assay (PeriTox): The assay is based on immature sensory neurons differentiated from
169 hiPSC as previously described (Hoelting et al., 2016; Holzer et al., 2022). Frozen lots of
170 peripheral neuron precursors were thawed and seeded into 96-well plates. After 1 h, the cells
171 were exposed to test chemicals for 24 h. Testing and endpoint measurements were exactly as for
172 the UKN4 assay.

173 NPC1-5 Assays: The assays are based on human neural progenitor cells (hNPCs; gestational
174 week 16-19) cultivated as proliferating free-floating spheres.

Blum & Masjosthusmann et al. (2022): In vitro battery for DNT testing

175 For the NPC1 assay, spheres (0.3 mm) were plated in 96-well plates (U-bottom; 1 sphere/well)
176 and directly exposed to the test compound (in proliferation medium). DNA synthesis was
177 assessed as functional endpoint after 3 days in vitro (DIV), using a luminescence-based
178 bromodeoxyuridine (BrdU) ELISA (Nimtz et al., 2019). Cytotoxicity was assessed as a
179 membrane integrity assay (CytoTox-ONE Assay) measuring the LDH release into the
180 supernatant.

181 For the NPC2-5 assays, spheres (0.3 mm) were plated in poly-D-lysine / laminin-coated 96-well
182 plates (F-bottom; 1 sphere/well) and directly exposed to the test compounds (in differentiation
183 medium). Under control conditions, NPCs migrate radially out of the attached sphere and
184 differentiate into radial glia, neurons and oligodendrocytes. Data were obtained after 72 h and
185 120 h. After 72 h (3 DIV), bright field images were taken of live cell cultures, and radial glia
186 migration (NPC2a [72h]) was assessed using ImageJ software. The medium was partially
187 removed (50%) and used to assess cytotoxicity (CytoTox-ONE Assay). To continue the assay,
188 the medium was replenished and cells were allowed to further differentiate and migrate for 48 h.
189 At 5 DIV, cells were fixated and stained for TUBB3 (neuronal marker), O4 (oligodendrocyte
190 marker) and Hoechst H-33258 (nuclear marker). The endpoint assessment was done by high
191 content imaging followed by different image analysis algorithms. Neuronal and oligodendrocyte
192 differentiation (NPC3 and NPC5) was assessed as the number of all TUBB3-positive and O4-
193 positive cells in percent of the total number of nuclei in the migration area. Neurons and
194 oligodendrocytes were automatically recognized by a machine learning software based on
195 convolutional neural networks (Forster et al., 2022). The high-content image analysis software
196 Omnishpero was used to determine radial glia migration (NPC2a [120h]), neuronal migration
197 (NPC2b) and oligodendrocyte migration (NPC2c) as well as neuronal morphology (NPC4a:

Blum & Masjosthusmann et al. (2022): In vitro battery for DNT testing

198 neurite length; NPC4b: neurite area) (Schmuck et al., 2017). Cytotoxicity was assessed from
199 samples of medium removed before the fixation by the CytoTox-ONE LDH Assay. Some
200 additional cell viability data were obtained by using a resazurin reduction assay (CellTiter-Blue
201 Assay). Concentration-response curves from all these tests were based on seven test compound
202 concentrations.

203 **2.3. Screen strategy**

204 Compounds were assembled as DMSO stock solutions (usually 20 mM). Most of the compounds
205 (n = 75) were provided from the ToxCast repository at the US EPA, and the others were added
206 manually. A robotics platform was used to either produce replicates of the master plate for
207 different screening runs and different assays (UKN assays) or to directly prepare the compound
208 dilutions (1:3 steps) in the media in 96-well plates (NPC assays). Operators were blinded to the
209 compound identity. For the UKN assays serial dilutions (1:3 steps) were prepared from the
210 cloned master plates for each compound in DMSO on 96-well plates, and each of these stocks
211 was transferred to a pre-dilution plate so that compounds were dissolved in medium plus 1%
212 DMSO. Finally, pre-dilutions were transferred to assay plates with cells (e.g. 20 µl transfer to
213 180 µl cells in medium. Exact volumes and pre-dilutions were assay-dependent and are detailed
214 in ToxTemp files. For few compounds, data had already been obtained during other testing
215 campaigns or during the assay setup. Some of these were tested in an adapted concentration range
216 (e.g. it is known that valproic acid is a human teratogen and DNT toxicant at clinically used
217 concentrations of 0.5-1 mM. Therefore, such high concentrations were also tested, and master
218 stock were prepared accordingly).

219 For some assays (e.g. UKN2), a pre-screening step was included, in which only 1-2 (highest) test
220 compound concentrations were run. When they showed no effect, screening was ended. When

Blum & Masjosthusmann et al. (2022): In vitro battery for DNT testing

221 there was an effect (at least 20% change of endpoint), a full concentration-response was obtained.
222 Pre-screen and full concentration-response screen were performed three times independently. For
223 the UKN assays this meant the use of different cell lots, for the NPC assays it meant the use of
224 cells from different donors and/or passages. Each screen contained 2-6 replicates (details in
225 [ToxTemps; suppl. file 1](#)). In some cases, follow-up tests were run, when e.g. only the highest
226 concentration showed a response, or when already additional information was present on a
227 compound. Then new stocks were produced, and the concentration range was extended to 60 or
228 100 μM , depending on the solubility of the compound.

229 **2.4. Data analysis**

230 A fully automated data analysis workflow was implemented on the programming platform R. It
231 included the following steps and outputs: (1) Pre-processing of data, where required by the
232 definitions of the assay endpoints ([see ToxTemps; suppl. file 1](#)). For instance, the background
233 signal was subtracted from all data points for the BrdU fluorescence readings. (2) Normalization
234 of test compound data to the median of solvent controls. (3) Calculation of the median of the
235 replicates for each experimental condition. (4) Concentration response fitting of the data for each
236 compound. The best-fitting model (general logistic, 3-parameter log-logistic, 4-parameter log-
237 logistic, 2-parameter exponential, 3-parameter exponential, 3-parameter Weibull, 4-parameter
238 Weibull) was selected by the AKAIKE information criteria. (5) Re-normalization of the data, so
239 that the starting point of the selected curve fit was at 100% ([Krebs et al., 2018](#); [Kappenberg et al.,](#)
240 [2020](#)). (6) Calculation of the mean values for each condition across independent test runs. (7)
241 Concentration response fitting of the data for each compound. The best-fitting model (general
242 logistic, 3-parameter log-logistic, 4-parameter log-logistic, 2-parameter exponential, 3-parameter
243 exponential, 3-parameter Weibull, 4-parameter Weibull) was selected by the AKAIKE

Blum & Masjosthusmann et al. (2022): In vitro battery for DNT testing

244 information criteria. (8) Determination of the benchmark concentration (BMC) as the point of the
245 concentration-response curve that intersected with the benchmark response level (BMR). The
246 BMR was determined and described for each assay (see [ToxTemp](#); [suppl. file 1](#)), based on a
247 biological and statistical rationale. It marked the extent of response considered to be statistically
248 significant and toxicologically meaningful. It thus depended on the endpoint and on the base line
249 noise. For most functional endpoints it was set at 75% (= 25% reduced normal function). For
250 some assays it was set at 70% (higher baseline noise). For some viability measures it was set at
251 90% (a deviation of > 10% was considered to potentially influence the functional endpoint). (9)
252 After determination of the BMC, the upper (BMCU) and lower limit (BMCL) of its 95%
253 confidence interval were calculated ([Krebs et al., 2020a](#)).

254 **2.5. Hit definitions and prediction models**

255 All NAM of the IVB-EU had at least two endpoints, and all of them used different prediction
256 models. These were defined during the original test setup, as documented in the literature and the
257 [ToxTemp files](#). A key feature of all assays was that they had a specific functional endpoint
258 (related to ta KNDP) and an endpoint characterizing compound effects on cell viability. Within
259 each NAM, a compound was considered a specific hit (toxicant), when it affected the functional
260 endpoint at least at one concentration that did not affect viability ([Fig. S3](#)). Notably, this does not
261 mean that specific cytotoxicity of a given cell population (e.g. neural crest cells) would not lead
262 to DNT. However, specific toxicity to a subpopulation can only be determined across assays, not
263 within one assay. Within a given assay, cytotoxicity just has the technical consequence that the
264 functional endpoint cannot be measured. Specific cytotoxicity to subpopulations was not
265 considered in this first application of the IVB-EU, as no prediction model for this endpoint had
266 been established. For the UKN assays, specific effects were determined by the ratio of

Blum & Masjosthusmann et al. (2022): In vitro battery for DNT testing

267 benchmark concentrations for the functional endpoint (e.g. neurite growth in UKN4) and
268 cytotoxicity (e.g. a 4-fold offset for UKN4). For the NPC assays. Specific toxicity was assumed
269 when the 95% confidence intervals of the functional endpoint and the viability endpoint did not
270 overlap. As the separation between “hit” and “non-hit” leads to binary data with high
271 uncertainties at the hit/non-hit boundary (Leontaridou et al., 2017; Delp et al., 2018), we
272 introduced a borderline category for transition compounds (e.g. when confidence intervals in
273 NPC assays overlapped by > 10%). Thus, a given compound was classified in each assay as “no
274 hit”, “unspecific hit”, “specific hit” or “borderline hit” (Fig. S3).

275 **2.6. Performance parameters**

276 A set of reference compounds (28 DNT positives; 17 DNT negatives) was used for a preliminary
277 evaluation of the IVB-EU predictivity. Various hit definitions were used (e.g. only specific hits,
278 or specific+borderline hits). If a positive control was a hit, it was considered true positive (TP), if
279 it was not a hit, it was considered a false negative (FN). If a negative control was a hit, it was
280 considered a false positive (FP) and if it was not a hit, it was considered a true negative (TN).
281 Using these four numbers (FP, FN, TP, TN), the following performance parameters were defined:

$$282 \text{ sensitivity } [\%] = \frac{TP}{(TP + FN)} * 100$$

$$283 \text{ specificity } [\%] = \frac{TN}{(TN + FP)} * 100$$

$$284 \text{ accuracy} = \frac{(TP + TN)}{(TP + TN + FP + FN)} * 100$$

$$285 \text{ balanced accuracy} = \frac{\text{sensitivity} + \text{specificity}}{2}$$

$$286 \text{ positive predictive value (PPV)} = \frac{TP}{(TP + FP)} * 100$$

Blum & Masjosthusmann et al. (2022): In vitro battery for DNT testing

$$287 \quad F1 \text{ score} = \frac{2}{\frac{1}{\text{sensitivity}} + \frac{1}{PPV}} = \frac{1}{2} * (\text{sensitivity} + PPV)$$

$$288 \quad \text{Matthews correlation coefficient (MCC)} = \frac{(TP * TN) - (FP * FN)}{\sqrt{(TP + FP)(TP + FN)(TN + FP)(TN + FN)}}$$

289 **2.7. Data accessibility**

290 The full data set as raw data will be available in the ToxCast data base after the new 2022

291 ToxCast release (fall 2022).

292

293

294 **3. Results and discussion**

295 **3.1. The DNT in vitro battery (IVB)**

296 A large panel of assays with direct or indirect relevance to DNT can be found in the literature.
297 Criteria needed to be developed to select a prototype battery that was large enough for the main
298 objective of this study, i.e. providing a basis for preparation of a general technical guidance
299 document on battery testing for regulatory applications. At the same time, reasons of feasibility
300 and limited resources called for keeping the number of NAMs included in the test run low.
301 Experts with a regulatory background (from the US and Europe) were involved in the selection.
302 The overall plan was to start testing in some European laboratories on a core battery (IVB-EU) of
303 fully ready NAMs, and then to combine data on the same set of compounds with tests established
304 at the US EPA. The three main selection criteria for the DNT NAMs were: (i) complementarity,
305 (ii) documentation, and (iii) the readiness level (Fig. 1A). The first point meant that the assays
306 were selected in a way to fill gaps of knowledge and to cover many KNDP. It was also
307 considered here to use assays for overlapping biological functions to learn about their
308 orthogonality and to provide a basis for later designs of tiered testing and sub-batteries. The
309 second point referred to the availability of method documentations useful at a regulatory level
310 (i.e. defined by OECD guidance document GD211) for the use of NAMs. Linked to this was the
311 third criterion which referred to the technical performance of the NAMs, and the level of
312 confidence into their predictivity and relevance. These issues are in some legislations referred to
313 as validation state. In the selection of assays for the IVB-EU, we used a more flexible definition,
314 termed “readiness” (Krebs et al., 2020b; Patterson et al., 2021). The assays used here all had
315 undergone such an evaluation (Bal-Price et al., 2018; Klose et al., 2021a; Koch et al., 2022). A
316 final criterion for inclusion of further assays after this pilot run was defined, as having run a

Blum & Masjosthusmann et al. (2022): In vitro battery for DNT testing

317 common pool of test compounds. This has many important reasons: demonstrating a sufficient
318 throughput of the method, providing a basis for robustness and performance evaluation, allowing
319 a rough assessment of added value/gap filling (Fig. 1A).

320 Ten assays fulfilled all criteria, and they were considered to be suitable for forming the IVB-EU.
321 They all use human cells, cover four major KNDP, reflect seven different brain cell types and
322 represent different neurodevelopmental stages (Fig. 2).

323 The neurosphere assays (NPC1-5) are based on primary human neural progenitor cells (hNPC),
324 that are grown as floating 3D neurospheres. Their growth and viability is assessed in the 3D
325 neurospheres (NPC1). Alternatively, spheres can be plated onto a laminin-coated matrix, where
326 the cells start migration and differentiation to form a secondary 3D co-culture. The latter
327 approach allows the simultaneous assessment of radial glia migration (NPC2a), neuronal
328 differentiation (NPC3), neuronal migration (NPC2b) and neurite outgrowth (NPC4) as well as
329 oligodendrocyte differentiation (NPC5) and their migration (NPC2c) by fully automated high
330 content imaging analyses and subsequent cell identification using artificial intelligence (Fig. 1B)
331 (Forster et al., 2022; Koch et al., 2022). The UKN assays use several cell types in conventional
332 2D cultures that are evaluated by fully automated high content imaging. The UKN2 test
333 (alternative name: cMINC) uses iPSC-derived neural crest cells and assesses their migration
334 (Nyffeler et al., 2017). The UKN4 test (alternative name: NeuriTox) utilizes immature LUHMES
335 neurons to assess neurite outgrowth in central nervous system neurons (Delp et al., 2018). The
336 UKN5 test (alternative name: PeriTox) is based on hiPSC derived sensory neurons and measures
337 neurite outgrowth in peripheral neurons (Fig. 1C). All IVB-EU assays assess at least one
338 indicator of cell health (viability/ cytotoxicity) in addition to their specific endpoint.

Blum & Masjosthusmann et al. (2022): In vitro battery for DNT testing

339 Despite the broad coverage of endpoints, IVB-EU gap analyses revealed KNDP currently not
340 covered by this battery. These concern very early processes such as stem cell differentiation into
341 neural progenitor cells and subsequent neural tube construction, as well as processes necessary
342 for neuronal circuit building, like formation, maturation and function of neuronal networks. As
343 such gaps may reduce the sensitivity of DNT predictions, we explored the availability of assays
344 that fulfill the IVB-EU inclusion criteria and could become part of an expanded full battery (Fig.
345 2). Many assays for network formation have indeed already shown to be at high readiness, yet
346 these are based on rat cortical cells (Carstens et al., 2022) calling for human cell-based neuronal
347 network formation assays. The early embryonal stages of neural development may be covered by
348 the UKN1 assay (Dresler et al., 2020; Meisig et al., 2020). Some functional endpoints related to
349 non-neuronal cells are also desirable for the IVB, as these cells (astrocytes, microglia,
350 myelinating oligodendrocytes, microvascular endothelial cells) do not only have support and
351 immune function, but rather participate in multiple neurodevelopmental processes (Allen and
352 Lyons, 2018). Several 3D systems have been described to include the necessary cell types (Brull
353 et al., 2020; Chesnut et al., 2021; Nunes et al., 2022), but they still need some additional
354 development to meet basic inclusion criteria (set up of test methods, throughput, documentation)
355 for the IVB. The same applies to dedicated assays to investigate neurotransmitter systems (e.g.
356 glutamate and acetylcholine signalling) (Klima et al., 2021; Loser et al., 2021b). However, a
357 large part of signalling systems is covered already by the emerging neural network assays (Frank
358 et al., 2017; Nimtz et al., 2020).

359 **3.2 Readiness overview**

360 The readiness of the assays of the DNT IVB was assessed on two tiers: first, the readiness of
361 individual assays, as assessed earlier in individual publications, was an inclusion criterion (Fig. 1)

Blum & Masjosthusmann et al. (2022): In vitro battery for DNT testing

362 of the IVB-EU. Second, the readiness of the overall battery and the performance of the assays
363 under screening conditions was evaluated.

364 Concerning the first point, the underlying considerations are briefly re-iterated here, as they
365 impinge on the interpretation and on the overall confidence into data from the NAMs of the IVB-
366 EU. As for all toxicological assays, relevance, predictivity and reliability/robustness were
367 considered. A major focus was put on the latter point, as suggested earlier (Leist et al., 2014;
368 Krebs et al., 2019; Pallocca et al., 2022b). Earlier publications (summarized in Masjosthusmann
369 et al. (2020)), and the ToxTemp (suppl. file 1) give more background information. One aspect
370 helping to keep typical sources of variability low is that the selected IVB-EU assays all used a
371 fully automated data capturing and evaluation procedure. However, the ultimate proof of the
372 pudding for robustness, a blinded inter-lab comparison study, still has to be done for the assays.

373 When simple methods for 1:1 replacement of acute toxicity endpoints were evaluated, relevance
374 and predictivity have been defined as separate aspects of NAMs. However, this concept has been
375 modified for complex endpoints and batteries. In such more complex cases, the predictivity of a
376 single NAM (for a given regulatory endpoint derived from animal studies) cannot be calculated,
377 and the aspects of predictivity and relevance are strongly intertwined (Escher et al., 2022). In
378 such cases, a scientific validation process is suggested that builds on two pillars: (i) comparison
379 of the biological basis of the test system to that of the modelled human biology, and (ii)
380 comparison of pathway modulations that lead to endpoint changes in the NAM to pathway
381 changes known to be relevant to the respective human pathophysiology (Hartung, 2007; Leist et
382 al., 2012; Hartung et al., 2013; Bal-Price et al., 2018; Piersma et al., 2018; Patterson et al., 2021).
383 For the NAMs included in the IVB-EU, the test systems have been extensively documented and
384 compared to the respective human developing nervous system counterparts. This involved the

Blum & Masjosthusmann et al. (2022): In vitro battery for DNT testing

385 levels of cell morphology, cell function, and cell markers (see [ToxTemps](#); [suppl. file 1](#)).
386 Moreover, the relevant systems were profiled for their respective transcriptomes ([Krug et al.,](#)
387 [2014](#); [Hoelting et al., 2016](#); [Pallocca et al., 2017](#); [Gutbier et al., 2018](#); [Masjosthusmann et al.,](#)
388 [2018](#); [Klose et al., 2021a](#); [Klose et al., 2021b](#); [Klose et al., 2022](#)). Also, the responses of the
389 NAMs to modulation of signaling pathways relevant for brain development have been
390 investigated by the use of compounds known to specifically affect signaling pathways (for
391 overview: [Klose et al. \(2021b\)](#); [Koch et al. \(2022\)](#); [Krebs et al. \(2020b\)](#); [Masjosthusmann et al.](#)
392 [\(2020\)](#)). A high-level summary of the responses to such “mechanistic tool compounds” is
393 summarized in [Fig. S4](#). One example is the Notch pathway, which determines a crucial switch
394 between neurogenesis and oligodendrogenesis in vivo. By using the Notch pathway inhibitor
395 DAPT, we can mimic this differentiation switch also in vivo with the NPC3/5 tests ([Koch et al.,](#)
396 [2022](#)). Another illustrative example is the Rho pathway, which is involved in neurite growth in
397 vivo. Activation of the RhoA kinase by narciclasine decreases neurite outgrowth in the NPC4,
398 UKN4 and UKN5 assays. This successful characterization of neurodevelopmentally-relevant
399 signaling in the IVB-EU assays is considered as the physiological basis and qualitative evidence
400 for relevance and predictivity.

401 While the above-mentioned steps were mainly important for the selection of NAMs and for
402 giving confidence into their individual function within the IVB-EU, we also took some effort to
403 validate the IVB-EU as a battery. Concerning relevance, it was mainly considered how many cell
404 types and how many signaling pathways important for brain development were covered. A gap
405 analysis showed that there was a need for few additional cells (e.g. microglia) and for some
406 additional functions (e.g. neuronal network formation, astrocyte function). Moreover, some more
407 coverage of signaling (e.g. BDNF pathway and nicotinic signaling pathway) would be desirable.

408 However, most relevant cell types were already represented, and many pathways known to be
409 affected by toxicants were shown to be identifiable by at least one assay (Fig. 2; Fig. S4).

410 For getting an impression on the robustness of screen results from the test battery, we determined
411 the baseline noise. As the results of all assays are normalized to solvent control data (which are
412 set to 100%, and therefore do not vary by default), we used a surrogate baseline data set: from
413 each concentration-response curve of the screen compounds, we selected the lowest
414 concentration and assumed that this was in most cases a no-effect concentration. This assumption
415 was consistent with the average of all these data points being about 100% for all assays. With this
416 approach it was possible to visualize the baseline noise (as standard deviation around the average
417 signal, Fig. 3a). From such data, we also calculated the assay-specific coefficients of variation
418 (CoVs, see ToxTemp; suppl. file 1). As a second measure of robustness, we evaluated the
419 responses of each test to the positive controls, which were run along on each plate/for every
420 experiment during the screen (Fig. 3b). The positive controls were also used to determine
421 acceptability of the respective plates/experiments for further evaluation. The plates/experiments,
422 for which the acceptance criteria (see ToxTemp; suppl. file 1) were not met, were discarded.

423 **3.3. Performance analysis**

424 The predictivity of the overall battery is a key feature of regulatory applicability, and therefore
425 got special attention here. The first tier of this evaluation concerns all of the above discussed
426 aspects of mechanistic validation. The biology and pathophysiology covered by the entirety of
427 assays of the IVB-EU suggested a high, but not perfect applicability domain and thus expected
428 predictivity.

Blum & Masjosthusmann et al. (2022): In vitro battery for DNT testing

429 As a second tier approach, we evaluated the capacity of the IVB-EU to correctly identify negative
430 and positive controls. A list of 45 such calibration compounds was assembled from various
431 literature references (Kadereit et al., 2012; Grandjean and Landrigan, 2014; Mundy et al., 2015;
432 Aschner et al., 2017; Paparella et al., 2020; Crofton and Mundy, 2021). The challenges and
433 shortcomings of this approach have been widely discussed (see above references), but our
434 compound selection appeared to be a good compromise at the present state of knowledge (Fig.
435 4A,B).

436 Prediction models for test batteries are an active field of research, and many possibilities exist
437 (tiered approaches, Bayesian models, Boolean rules and decision trees). The difficulty to agree on
438 the defined approaches for the small (3 NAM) battery used to predict dermal sensitization
439 exemplifies these difficulties (Strickland et al., 2022). Here, we used a simple Boolean rule to
440 define a battery hit as any compound that was a hit in one of the included DNT IVB-EU NAMs.
441 A negative was defined as a compound not being a hit in any of the assays. This rule allows for a
442 high transparency and simplicity, but it may be associated with a high false discovery rate. The
443 use of full concentration-response curves (instead of single data points) for hit definition and the
444 use of data from three independent experiments were our approaches to dampen the false positive
445 rate, and to ensure sufficient specificity.

446 The 28 positive controls were used to obtain a preliminary measure of assay sensitivity (to be
447 refined with time and the addition of more control compounds). We used different stringencies of
448 hit definitions to obtain an estimate of the IVB-EU performance with respect to detection of DNT
449 toxicants. When only the specific hits (compounds causing functional impairment at non-
450 cytotoxic concentrations) were counted, the sensitivity of the IVB-EU was 68%. When borderline
451 hits were included, this went up to 82%. A further increase to 86% was found, when also

Blum & Masjosthusmann et al. (2022): In vitro battery for DNT testing

452 cytotoxic compounds were included in the “hits” (Fig. 4A,C). The 17 negative controls were used
453 to obtain data on specificity. When specific and borderline hits were counted a value of 100%
454 was obtained. Specificity dropped to 94%, when also cytotoxic effects were counted as “hit” (Fig.
455 4B,C).

456 Altogether, these preliminary performance estimates indicate that a balanced accuracy of about
457 80% or higher can be reached. Based on the set of control compounds, several additional
458 performance measures were calculated (Fig. 4C) and it is particularly noteworthy that the IVB-
459 EU had a high positive predictive value (PPV). That means that a compound identified as a
460 battery hit was very likely associated with a DNT hazard. This feature is important for the use of
461 the IVB-EU for prioritization of compounds for further testing, or for excluding compounds at
462 early stages from further development.

463 Nicotine serves as a good example for gaps in the IVB-EU, identified by the performance
464 evaluation. It was identified as FN, and thus is indicative of the shortcomings with respect to
465 sensitivity. Nicotine stimulates ionotropic acetylcholine receptors, and the battery does not
466 include NAMs that would cover this biological function. This information is important when it
467 comes to the interpretation of data from compounds that target nicotinic receptors, like
468 neonicotinoid insecticides (Sheets et al., 2016; Loser et al., 2021a). Assays that fill these gaps are
469 already under development (Fig. 2), and inclusion of assays based on zebra fish embryos and
470 other model organisms (e.g. *C. elegans*) are considered an additional approach to close battery
471 gaps (Atzei et al., 2021; Dasgupta et al., 2022).

472 Another limitation of the DNT IVB-EU is hard to overcome: the number of control compounds
473 with clearly documented human effects is very limited, and also the compounds having been

Blum & Masjosthusmann et al. (2022): In vitro battery for DNT testing

474 tested in DNT guideline studies in animals is small (Aschner et al., 2017). For this reason,
475 performance metrics on the basis of control-compound predictivity will remain coarse and
476 superficial. The realistic way forward will be to further refine mechanistic validation approaches.
477 This seems at present the most realistic way forward to gain further confidence into the
478 predictivity of the battery for human adversities.

479 A final, but very important, consideration on predictivity is that this is highly context-dependent.
480 While defining predictivity “in general” may be an illusion for such a complex endpoint as DNT,
481 it is realistic to consider test predictivity in sharply defined application domains. In each of these
482 contexts, it seems important to ask how far the battery is fit-for-purpose. Four issues need to be
483 specified: (i) which problem is to be addressed (e.g. risk assessment of a new chemical, or
484 prioritization of compounds for further testing); (ii) is there a focus on high positive predictivity
485 or high negative predictivity; (iii) which type of chemicals is examined (predictivity may be very
486 high within certain groups, while it may be low for other compound classes); (iv) which type of
487 biology (targets, pathways) plays a role. It is likely that some adverse outcome pathways (AOP)
488 are covered well, while others not at all. E.g. acetylcholine esterase inhibitors may not be
489 detected easily by the current IVB-EU, but this gap would be easily filled by an additional
490 enzymatic assay (Li et al., 2017).

491 **3.3 Compound testing and hit identification**

492 In addition to the 45 compounds tested for the IVB-EU performance analyses, all 10 assays were
493 challenged with additional 75 test compounds, so that the total screen comprised 120 chemicals
494 (suppl. file 2). The result of the screen were benchmark concentrations (BMC) of effect (or no
495 effect data within the used concentration range) for 120 compounds on ten functional and six
496 viability endpoints, i.e. 1920 concentration response curves. A matrix including 405 BMCs for

Blum & Masjosthusmann et al. (2022): In vitro battery for DNT testing

497 the IVB hits (with measures of uncertainty) was generated. To allow a better overview and focus,
498 all compounds were compiled that affected at least one functional endpoint at a non-cytotoxic
499 concentration (n = 59). To better visualize the activity profile of compounds, the endpoints for
500 which toxicants had the highest potency (most sensitive endpoint(s)) were highlighted (Fig. 5).
501 Compounds were considered to be about equally potent across test endpoints, when their activity
502 did not differ by more than a factor of three. This is due to technical issues (the test
503 concentrations were separated by a factor of three in the concentration-response curves), but also
504 due to statistical considerations (the confidence intervals of BMCs separated by factor 3
505 overlapped in 85 % of all cases).

506 Besides the 59 compounds that produced at least one specific hit (comprising 23 positive controls
507 and 33 other compounds), there were also 61 compounds that had no specific hit in any of the 10
508 functional endpoints. Ten of these compounds were cytotoxic to one or more cell populations
509 (Fig. S4A), while 51 compounds (including the 17 negative controls) had no effect at all (Fig.
510 S4B). This finding of 34 fully negatives (excluding the known negative controls) extends
511 observations from the preliminary predictivity evaluation (using known negative control
512 compounds) that showed that the IVB-EU, despite its large number of tests and endpoints, is not
513 highly unspecific.

514 **3.4 Hit patterns in the DNT IVB screen**

515 Concerning the further analysis of battery hits, several strategies were followed. One approach
516 was to select some individual hit compounds or groups of compounds for further toxicological
517 evaluation. For instance, an expert group of EFSA and the OECD used IVB-EU data on
518 deltamethrine and flufenacet for a case study within the OECD IATA program (EFSA PPR
519 Panel, 2021). Another example is the group of flame retardants, for which the battery data were

Blum & Masjosthusmann et al. (2022): In vitro battery for DNT testing

520 used to support a comprehensive hazard assessment (Klose et al., 2021a). Such specific
521 toxicological follow-ups were beyond the scope of the present study. Instead, we analyzed
522 general hit patterns of the screen to learn more about the relationship (complementarity/necessity)
523 of the various assays and endpoints.

524 The first question was, how functional endpoints and specific hits related to the viability
525 endpoints and cytotoxicity hits. To understand the overall data structure, we generated an
526 overview, comparing for each specific hit compound the potency for the most sensitive functional
527 endpoint in the battery (MSE) with the potencies for all cytotoxic effects across the battery test
528 systems (cytotoxicity hits). There were 57 specific hits, plus two compounds (maneb and
529 clorpyrifos), which were classified as borderline hits, and are being included here in the group of
530 functional hits. Altogether 17 of the 59 compounds (29%) did not affect any of the battery's
531 viability endpoints. For this subgroup, the functional endpoint provided a definite gain in
532 sensitivity, compared to cytotoxicity assays. It is also very likely that the functional endpoint was
533 directly affected by the test compounds, i.e. it was not an indirect effect of unspecific
534 cytotoxicity.

535 As an alternative approach to understand the role of cytotoxicity, we asked, how the MSE
536 concentration related to the cytotoxic potency in the same or in any other assay. There were only
537 five compounds (8%) for which a cytotoxic endpoint was observed at higher (\geq factor 2) potency
538 than the functional MSE (Fig. 6A). One example is carbaryl (CBR), which specifically inhibited
539 neurite growth in the UKN4 assay (functional endpoint). It was particularly potent as
540 cytotoxicant for peripheral neurons and mixed NPC cultures. This may indicate that CBR exerts a
541 cell type-specific cytotoxicity for such neural cell populations. Such viability effects may be

Blum & Masjosthusmann et al. (2022): In vitro battery for DNT testing

542 relevant for neurodevelopment, but further investigations would be required to allow clear
543 conclusions.

544 We used a comparison to published data as one preliminary approach to test whether cytotoxicity
545 hits of the IVB-EU are specific for neurodevelopmental cell types. We hypothesized that we may
546 see a difference between cytotoxic potencies on conventional cell lines (HepG2, HE293, etc.) and
547 on the test systems used here, if a compound shows a developmental-stage specific cytotoxicity.
548 Information on unspecific toxicity (called: cytotoxicity lower bound) was obtained from the
549 ToxCast data base (Judson et al., 2016). For the 41 compounds, for which sufficient data was
550 available, we found that cytotoxicity hit potency in the IVB-EU was at least 10-fold below the
551 cytotoxicity lower bound for 7 compounds; 34 compounds showed no particular sensitivity in
552 IVB-EU test systems compared to cell lines used for ToxCast screening (Fig. S5A). This may
553 indicate that some, but not all cytotoxicity hits may be specific for neurodevelopmental cell
554 types. To complete this comparison, we also checked how the functional hits of the IVB-EU
555 compared to the cytotoxicity lower bound. In general, the cytotoxicity threshold in ToxCast was
556 often in the range of 5-20 μM . Thus, the 17 IVB screen hits with MSEs $< 1 \mu\text{M}$ (for which the
557 cytotoxicity lower bound was available), seemed to separate clearly from general cytotoxicity
558 except for TETB. The situation is complex for compounds with higher MSE potency in the IVB-
559 EU. The data set is too small and compound behaviour is very heterogeneous. However, it is
560 plausible, that specificity may be reduced (or lost) at higher screen concentrations ($> 20 \mu\text{M}$). It
561 has been shown that unspecific baseline toxicity increases from this threshold on, due to
562 membrane incorporation and alterations of protein conformations (Escher et al., 2019; Lee et al.,
563 2021; Lee et al., 2022). Therefore, hits in a higher concentration range (e.g. MAM, VPA, AAM)
564 need good justifications (e.g. clinically-observed plasma levels at hit concentration levels) and/or

Blum & Masjosthusmann et al. (2022): In vitro battery for DNT testing

565 a detailed mechanistic follow-up providing a rationale for specific functional effects in the
566 observed concentration range (Fig. S5B)

567 All these potency comparisons have an important caveat: the data we obtained are based on
568 nominal concentrations, and these might differ from the free effective concentrations in the
569 medium, and especially at the target sites (Kisitu et al., 2020). Especially, for comparisons to
570 assays with tumor cell lines, it needs to be considered, that such systems usually use serum
571 supplements containing protein and lipids, while most stem cell culture media used here had a
572 low protein and lipid content. Under the conditions used for the IVB-EU, the free concentrations
573 are very close to the total concentrations in medium (Krebs et al., 2020b), while this is not
574 necessarily the case for serum-containing media.

575 The second question we asked was, how the hits distributed over the different assays of the
576 battery. Altogether 67 compounds affected at least one test endpoint: 57 specific, 2 borderline 10
577 cytotoxic and 51 compounds affected no endpoint at concentrations up to 20 μ M (Fig. 6B, Fig.
578 S5&S7). All cytotoxic compounds had potencies of ≥ 8 μ M (Fig. S5A). The number of hits
579 obtained in each assay was also compiled. For instance, the NPC5 assay (examining the KNDP
580 oligodendrocyte differentiation) identified the highest number ($n = 34$) of specific hits (Fig. 6B).
581 Moreover, 10 compounds were hits only in this assay and would have been missed as potential
582 toxicants without the NPC5 test as part of the IVB-EU (Fig. 6C). The second highest hit rate ($n =$
583 30) was found for the UKN2 assay (represents the KNDP of neural crest cell migration). Three
584 compounds were unique hits in this test, i.e. not identified by another endpoint. Most other assays
585 (UKN4, UKN5, NPC1, NPC2a NPC3 and NPC4) identified 8-15 specific hits, and each of the
586 assay identified at least one test compound that would have been missed by the other tests of the
587 battery (Fig. 6C). This illustrates that the cell types and endpoints assembled in the IVB-EU all

Blum & Masjosthusmann et al. (2022): In vitro battery for DNT testing

588 differ in the pattern of toxicity pathways and targets they represent. This analysis also showed
589 that the test methods are not redundant, even with this small number (n = 120) of screened
590 chemicals. We anticipate that the broad coverage of cell types, developmental stages and
591 endpoints of the IVB-EU will be even more required to ensure maximal sensitivity, when the
592 chemical space is enlarged by broader test campaigns and a more-wide spread use of the battery.

593 A third question we asked dealt with resource optimization. Some assays, such as NPC2b/c
594 (migration of neurons and oligodendrocytes) or UKN4 (neurite outgrowth) contributed relatively
595 little to the overall hit rate, and one may consider them to be deleted from the battery or replaced.
596 This would be a step towards a faster, more economical “mini-battery”, which would be expected
597 to have a slightly reduced sensitivity, but not greatly reduced overall performance (accuracy;
598 Matthews coefficient). However, in case of the neurosphere assay, individual readouts are
599 multiplexed, meaning that omission of one endpoint will not lead to saving resources, e.g.
600 NPC2b/c are automatically assessed when NPC3/5 are evaluated. As NPC3 is multiplexed with
601 NPC2 and 5, also this assay adds negligible extra time and costs to the overall assays NPC2-5.
602 Hence, a mini-battery should only omit assays that practically save resources, i.e. individual
603 assays. If one continues this line of thought, a minimal DNT IVB may consist of NPC1 (NPC
604 proliferation), NPC2-5 and UKN2 (NCC migration) test methods (Fig. 6C). In our screen, this
605 mini-battery would have identified 52 compounds (88% of all specific and borderline hits) of the
606 59 hits covered by the whole IVB-EU. Such a reduced approach may be used e.g. for
607 quick/inexpensive pre-screens, e.g. in situations where sensitivity is of low importance, but
608 compounds are to be ranked according to their priority for further testing. However, one may also
609 consider adding an assay to a mini-battery that is not yet included in the IVB-EU. The gap
610 analysis (Fig. 2) suggested that some biological domains are still poorly covered, and that an

Blum & Masjosthusmann et al. (2022): In vitro battery for DNT testing

611 important gap would be filled by a neural network formation assay ([Carstens et al. 2022](#)). Thus,
612 future batteries would need to consider the assays presented here, in addition to other established
613 and emerging DNT NAM.

614 **4. Conclusions and outlook**

615 We have demonstrated here how NAMs with endpoints related to KNDP can be selected and
616 assembled to an in vitro battery to screen for DNT hazard of chemicals. The technical feasibility
617 and the implementation of solid reporting standards have been demonstrated by the use of 120
618 test compounds in a battery test-run that produced close to 2000 BMCs. These were used to
619 provide battery performance estimates and to classify test compounds as specific hits,
620 cytotoxicants or non-hits. The pattern of results was used to discuss the contribution of the assays
621 and their endpoints to the overall IVB-EU and to define gaps still to be filled.

622 Pivotal questions for the future are (i) how battery hits would be further used and (ii) how the
623 IVB-EU (or its future expanded version = IVB) could be implemented in a regulatory context
624 (Fig. 7A,B). We anticipate that the first application of the IVB will be for screening of data-poor
625 compounds to explore their DNT liabilities. As the overwhelming majority of chemicals lacks
626 data on DNT hazard, compounds of particular concern (because of high exposure or structural
627 alerts) may be screened first. The IVB would produce alerts for further testing. The underlying
628 toxicological rationale is that disturbance of any KNDP covered by the IVB has the potential to
629 lead to DNT. In a regulatory environment, the IVB data would provide a hazard characterization,
630 and could be used as point-of-departure for further steps. In this context, physiology-based
631 kinetic modelling (PBK) followed by in vitro-to-in vivo extrapolations (IVIVE) could be applied
632 to convert the BMCs to estimated adverse doses (AEDs). These would be used to perform a risk
633 assessment.

634 With growing experience and confidence into the IVB, its output could become a pivotal element
635 of DNT risk assessment. Such a development is supported by the guidance document on the
636 generation and use of the NAM-based DNT data (Crofton and Mundy, 2021). In a risk

Blum & Masjosthusmann et al. (2022): In vitro battery for DNT testing

637 assessment situation with a defined problem formulation (e.g. for pesticide marketing re-approval
638 in the EU, or during registration of a chemical in Japan) the compound to be evaluated would be
639 run through the battery to provide hazard data. These might be clear and unambiguous. Or they
640 may need to be complemented by additional rounds of testing in battery extensions. Together
641 with the use of ADME data or other information (such as QSAR) and an IVIVE procedure,
642 sufficient information for risk assessment would be generated (Fig. 7A).

643 One important aspect of using the battery data as hazard characterization is the interpretation and
644 follow-up of hits. It is at present unclear, whether the number of positive battery endpoints
645 correlates with the strength of DNT hazard. Hence, in the hazard characterization scenario one
646 would be equally concerned if a compound produced one or several hits. However, the BMCs
647 producing the hits have to be considered as multiple hits in the same order of magnitude suggest
648 a higher concern than hits that only produce one low BMC. In the screening and prioritization
649 scenario concern could be based on a combination of BMC magnitude and number of hits similar
650 to the approach practiced in Klose et al. (2021) in the flame retardant case study. However,
651 singleton-hit chemicals can be of high concern as exemplified by the illustrative example lead,
652 which is one of the best-proven human DNT toxicants and only affected one functional endpoint
653 of the IVB-EU.

654 For each battery hit, there is always the uncertainty, that it is either a true positive, i.e. that the
655 battery results reflect real DNT hazard for humans, or that it is a false positive (FP). A reasons for
656 the latter scenario may be toxicokinetic (ADME) properties. E.g. a compound may never reach
657 the foetal or child brain because of barrier functions, but there is no such barrier in vitro. Some
658 FP will also arise from test classification uncertainties (alpha error) and the IVB false discovery
659 rate (FDR) due to the combination of a large number of assays. Fortunately, there are also ways

Blum & Masjosthusmann et al. (2022): In vitro battery for DNT testing

660 to build confidence into the hit pattern and to reduce the uncertainty of a hit being a FP. The
661 assays and their prediction models can be trimmed for high specificity (multiple test runs, full
662 concentration-response curves, conservative thresholds for hit definition). Another powerful
663 approach is to functionally group hit compounds and to use information on one compound to read
664 across to others. This way, consistency and plausibility can be established and/or strengthened.

665 For some applications, also non-hits play an important role, e.g. for providing confidence to
666 consumers on the safety of food constituents or contaminants. Non-hits may either be true (no
667 hazard) or be false negatives (FN), i.e. have non-discovered toxic properties. The main sources of
668 uncertainty on negatives are the gaps in the battery (KNDP or specific signalling pathway not
669 covered) and toxicokinetic aspects. For instance, a tested parent compound may not be toxic, but
670 a metabolite generated only in vivo may be a DNT toxicant. Fortunately, there are also strategies
671 available to increase confidence in negative hits. If this is of particular importance, the sensitivity
672 of assays can be increased by running a higher number of replicates. Also, a less conservative
673 prediction model may be applied. This strategy is demonstrated here by the introduction of a
674 borderline category, to capture toxic compounds that would otherwise have dropped out of the hit
675 definition. Another major approach is the extension of the battery, e.g. by combination with the
676 US EPA assays (Carstens et al., 2022). Last, but not least, grouping, and other information from
677 data bases and the literature could be used for further evaluation of negative hits and decisions on
678 potential extended testing (Fig. 7A).

679

680

681 ***Acknowledgements***

682 The authors are very grateful to Tim Shafer, Katie Paul Friedman and Kelly Carstens (all
683 employees of the US EPA, involved in compound selection, study design, data interpretation and
684 transfer of data to the ToxCast data base). We would like to thank Rebecca Göttler for the
685 experimental and Julia Kapr for layout support. Furthermore, we thank Thomas Mayer, Silke
686 Müller, and the screening centre of the University of Konstanz for the experimental and technical
687 support.

Blum & Masjosthusmann et al. (2022): In vitro battery for DNT testing

688 **Funding**

689 This work was supported by the European Food Safety Authority (EFSA- Q- 2018- 00308), the
690 Danish Environmental Protection Agency (EPA) under the grant number MST-667-00205, the
691 State Ministry of Baden-Wuerttemberg, Germany, for Economic Affairs, Labour and Tourism
692 (NAM-Accept), the project CERST (Center for Alternatives to Animal Testing) of the Ministry
693 for culture and science of the State of North-Rhine Westphalia, Germany (file number 233-
694 1.08.03.03- 121972/131 – 1.08.03.03 – 121972), the European Chemical Industry Council Long-
695 Range Research Initiative (Cefic LRI) under the project name AIMT11 and the BMBF
696 (NeuroTool). It has also received funding from the European Union's Horizon 2020 research and
697 innovation program under grant agreements No. 964537 (RISK-HUNT3R), No. 964518
698 (ToxFree) and No. 825759 (ENDpoiNTs).

699 **Abbreviations**

700	AOP	– adverse outcome pathway
701	BMC	– benchmark concentration
702	BMCL	– lower limit of 95% confidence interval of BMC
703	BMCU	– upper limit of 95% confidence interval of BMC
704	DIV	– days <i>in vitro</i>
705	DNT	– developmental neurotoxicity
706	EFSA	– European Food Safety Authority
707	FDR	– false discovery rate
708	hNPC	– human neural progenitor cell
709	hiPSC	– human induced pluripotent stem cell
710	IVB	– <i>in vitro</i> battery
711	IVB-EU	– DNT IVB based on methods available in European laboratories
712	IVIVE	– <i>in vitro</i> to <i>in vivo</i> extrapolation
713	KNDP	– key neurodevelopmental process
714	MSE	– most sensitive endpoint
715	NAM	– new approach methods
716	PPV	– positive predictive value
717	IATA	– integrated approaches for testing and assessment

Blum & Masjosthusmann et al. (2022): In vitro battery for DNT testing

718 OECD – Organisation for Economic Co-operation and Development

719 TN – true negative

720 TP – true positive

721 UKN – University of Konstanz

722 US EPA – United States Environmental Protection Agency

723

724

725

726 **References**

- 727 Allen, N.J., Lyons, D.A., 2018. Glia as architects of central nervous system formation and
728 function. *Science* 362, 181-185.
729
- 730 Andersen ME, McMullen PD, Phillips MB, Yoon M, Pendse SN, Clewell HJ, Hartman JK,
731 Moreau M, Becker RA, Clewell RA. 2019. Developing context appropriate toxicity testing
732 approaches using new alternative methods (nams). *Altex*. 36(4):523-534.
733
- 734 Aschner, M., Ceccatelli, S., Daneshian, M., Fritsche, E., Hasiwa, N., Hartung, T., Hogberg, H.T.,
735 Leist, M., Li, A., Mundi, W.R., Padilla, S., Piersma, A.H., Bal-Price, A., Seiler, A.,
736 Westerink, R.H., Zimmer, B., Lein, P.J., 2017. Reference compounds for alternative test
737 methods to indicate developmental neurotoxicity (DNT) potential of chemicals: example lists
738 and criteria for their selection and use. *ALTEX* 34, 49-74.
739
- 740 Atzei, A., Jense, I., Zwart, E.P., Legradi, J., Venhuis, B.J., van der Ven, L.T.M., Heusinkveld,
741 H.J., Hessel, E.V.S., 2021. Developmental Neurotoxicity of Environmentally Relevant
742 Pharmaceuticals and Mixtures Thereof in a Zebrafish Embryo Behavioural Test. *Int J*
743 *Environ Res Public Health* 18.
744
- 745 Bal-Price, A., Crofton, K.M., Leist, M., Allen, S., Arand, M., Buetler, T., Delrue, N., FitzGerald,
746 R.E., Hartung, T., Heinonen, T., Hogberg, H., Bennekou, S.H., Lichtensteiger, W., Oggier,
747 D., Paparella, M., Axelstad, M., Piersma, A., Rached, E., Schilter, B., Schmuck, G.,
748 Stoppini, L., Tongiorgi, E., Tiramani, M., Monnet-Tschudi, F., Wilks, M.F., Ylikomi, T.,
749 Fritsche, E., 2015. International STakeholder NETwork (ISTNET): creating a developmental
750 neurotoxicity (DNT) testing road map for regulatory purposes. *Arch Toxicol* 89, 269-287.
751
- 752 Bal-Price, A., Hogberg, H.T., Crofton, K.M., Daneshian, M., FitzGerald, R.E., Fritsche, E.,
753 Heinonen, T., Hougaard Bennekou, S., Klima, S., Piersma, A.H., Sachana, M., Shafer, T.J.,
754 Terron, A., Monnet-Tschudi, F., Viviani, B., Waldmann, T., Westerink, R.H.S., Wilks, M.F.,
755 Witters, H., Zurich, M.G., Leist, M., 2018. Recommendation on test readiness criteria for
756 new approach methods in toxicology: Exemplified for developmental neurotoxicity. *ALTEX*
757 35, 306-352.
758
- 759 Bal-Price, A.K., Coecke, S., Costa, L., Crofton, K.M., Fritsche, E., Goldberg, A., Grandjean, P.,
760 Lein, P.J., Li, A., Lucchini, R., Mundy, W.R., Padilla, S., Persico, A.M., Seiler, A.E.,
761 Kreysa, J., 2012. Advancing the science of developmental neurotoxicity (DNT): testing for
762 better safety evaluation. *ALTEX* 29, 202-215.
763
- 764 Baumann, J., Gassmann, K., Masjosthusmann, S., DeBoer, D., Bendt, F., Giersiefer, S., Fritsche,
765 E., 2016. Comparative human and rat neurospheres reveal species differences in chemical
766 effects on neurodevelopmental key events. *Arch Toxicol* 90, 1415-1427.
767
- 768 Behl, M., Ryan, K., Hsieh, J.H., Parham, F., Shapiro, A.J., Collins, B.J., Sipes, N.S., Birnbaum,
769 L.S., Bucher, J.R., Foster, P.M.D., Walker, N.J., Paules, R.S., Tice, R.R., 2019. Screening

Blum & Masjosthusmann et al. (2022): In vitro battery for DNT testing

- 770 for Developmental Neurotoxicity at the National Toxicology Program: The Future Is Here.
771 *Toxicol Sci* 167, 6-14.
772
- 773 Bellinger, D.C., 2012. A strategy for comparing the contributions of environmental chemicals
774 and other risk factors to neurodevelopment of children. *Environ Health Perspect* 120, 501-
775 507.
- 776 Bennett, D., Bellinger, D.C., Birnbaum, L.S., Bradman, A., Chen, A., Cory-Slechta, D.A., Engel,
777 S.M., Fallin, M.D., Halladay, A., Hauser, R., Hertz-Picciotto, I., Kwiatkowski, C.F.,
778 Lanphear, B.P., Marquez, E., Marty, M., McPartland, J., Newschaffer, C.J., Payne-Sturges,
779 D., Patisaul, H.B., Perera, F.P., Ritz, B., Sass, J., Schantz, S.L., Webster, T.F., Whyatt, R.M.,
780 Woodruff, T.J., Zoeller, R.T., Anderko, L., Campbell, C., Conry, J.A., DeNicola, N., Gould,
781 R.M., Hirtz, D., Huffling, K., Landrigan, P.J., Lavin, A., Miller, M., Mitchell, M.A., Rubin,
782 L., Schettler, T., Tran, H.L., Acosta, A., Brody, C., Miller, E., Miller, P., Swanson, M.,
783 Witherspoon, N.O., American College of, O., Gynecologists, Child Neurology, S.,
784 Endocrine, S., International Neurotoxicology, A., International Society for Children's, H.,
785 the, E., International Society for Environmental, E., National Council of Asian Pacific
786 Islander, P., National Hispanic Medical, A., National Medical, A., 2016. Project TENDR:
787 Targeting Environmental Neuro-Developmental Risks The TENDR Consensus Statement.
788 *Environ Health Perspect* 124, A118-122.
789
- 790 Brull, M., Spreng, A.S., Gutbier, S., Loser, D., Krebs, A., Reich, M., Kraushaar, U., Britschgi,
791 M., Patsch, C., Leist, M., 2020. Incorporation of stem cell-derived astrocytes into neuronal
792 organoids to allow neuro-glial interactions in toxicological studies. *ALTEX* 37, 409-428.
793
- 794 Carstens, K.E., Carpenter, A.F., Martin, M.M., Harrill, J.A., Shafer, T.J., Paul Friedman, K.,
795 2022. Integrating Data From In Vitro New Approach Methodologies for Developmental
796 Neurotoxicity. *Toxicol Sci* 187, 62-79.
797
- 798 Chesnut, M., Paschoud, H., Repond, C., Smirnova, L., Hartung, T., Zurich, M.G., Hogberg, H.T.,
799 Pamies, D., 2021. Human iPSC-Derived Model to Study Myelin Disruption. *Int J Mol Sci*
800 22.
801
- 802 Coecke, S., Goldberg, A.M., Allen, S., Buzanska, L., Calamandrei, G., Crofton, K., Hareng, L.,
803 Hartung, T., Knaut, H., Honegger, P., Jacobs, M., Lein, P., Li, A., Mundy, W., Owen, D.,
804 Schneider, S., Silbergeld, E., Reum, T., Trnovec, T., Monnet-Tschudi, F., Bal-Price, A.,
805 2007. Workgroup report: incorporating in vitro alternative methods for developmental
806 neurotoxicity into international hazard and risk assessment strategies. *Environ Health*
807 *Perspect* 115, 924-931.
808
- 809 Cote I, Andersen ME, Ankley GT, Barone S, Birnbaum LS, Boekelheide K, Bois FY, Burgoon
810 LD, Chiu WA, Crawford-Brown D et al. 2016. The next generation of risk assessment multi-
811 year study-highlights of findings, applications to risk assessment, and future directions.
812 *Environmental health perspectives*. 124(11):1671-1682.
813

Blum & Masjosthusmann et al. (2022): In vitro battery for DNT testing

- 814 Crofton, K.M., Mundy, W.R., 2021. External Scientific Report on the Interpretation of Data from
815 the Developmental Neurotoxicity In Vitro Testing Assays for Use in Integrated Approaches
816 for Testing and Assessment. EFSA Supporting Publications 18, 6924E.
817
- 818 Crofton, K.M., Mundy, W.R., Lein, P.J., Bal-Price, A., Coecke, S., Seiler, A.E., Knaut, H.,
819 Buzanska, L., Goldberg, A., 2011. Developmental neurotoxicity testing: recommendations
820 for developing alternative methods for the screening and prioritization of chemicals. ALTEX
821 28, 9-15.
822
- 823 Crofton, K.M., Mundy, W.R., Shafer, T.J., 2012. Developmental neurotoxicity testing: a path
824 forward. *Congenit Anom (Kyoto)* 52, 140-146.
825
- 826 Dasgupta, S., Simonich, M.T., Tanguay, R.L., 2022. Zebrafish Behavioral Assays in Toxicology.
827 *Methods Mol Biol* 2474, 109-122.
828
- 829 Delp, J., Gutbier, S., Klima, S., Hoelting, L., Pinto-Gil, K., Hsieh, J.H., Aichem, M., Klein, K.,
830 Schreiber, F., Tice, R.R., Pastor, M., Behl, M., Leist, M., 2018. A high-throughput approach
831 to identify specific neurotoxicants/ developmental toxicants in human neuronal cell function
832 assays. ALTEX 35, 235-253.
833
- 834 Dreser, N., Madjar, K., Holzer, A.K., Kapitza, M., Scholz, C., Kranaster, P., Gutbier, S., Klima,
835 S., Kolb, D., Dietz, C., Trefzer, T., Meisig, J., van Thriel, C., Henry, M., Berthold, M.R.,
836 Bluthgen, N., Sachinidis, A., Rahnenfuhrer, J., Hengstler, J.G., Waldmann, T., Leist, M.,
837 2020. Development of a neural rosette formation assay (RoFA) to identify
838 neurodevelopmental toxicants and to characterize their transcriptome disturbances. *Arch*
839 *Toxicol* 94, 151-171.
840
- 841 Escher, B.I., Glauch, L., Konig, M., Mayer, P., Schlichting, R., 2019. Baseline Toxicity and
842 Volatility Cutoff in Reporter Gene Assays Used for High-Throughput Screening. *Chem Res*
843 *Toxicol* 32, 1646-1655.
844
- 845 Escher, S.E., Partosch, F., Konzok, S., Jennings, P., Luijten, M., Kienhuis, A., de Leeuw, V.,
846 Reuss, R., Lindemann, K.-M., Bennekou, S.H., 2022. Development of a Roadmap for Action
847 on New Approach Methodologies in Risk Assessment. EFSA Supporting Publications 19,
848 7341E.
849
- 850 Forster, N., Butke, J., Kessel, H.E., Bendt, F., Pahl, M., Li, L., Fan, X., Leung, P.C., Klose, J.,
851 Masjosthusmann, S., Fritsche, E., Mosig, A., 2022. Reliable identification and quantification
852 of neural cells in microscopic images of neurospheres. *Cytometry A* 101, 411-422.
853
- 854 Frank, C.L., Brown, J.P., Wallace, K., Mundy, W.R., Shafer, T.J., 2017. From the Cover:
855 Developmental Neurotoxicants Disrupt Activity in Cortical Networks on Microelectrode
856 Arrays: Results of Screening 86 Compounds During Neural Network Formation. *Toxicol Sci*
857 160, 121-135.
858

Blum & Masjosthusmann et al. (2022): In vitro battery for DNT testing

- 859 Fritsche, E., Crofton, K.M., Hernandez, A.F., Hougaard Bennekou, S., Leist, M., Bal-Price, A.,
860 Reaves, E., Wilks, M.F., Terron, A., Solecki, R., Sachana, M., Gourmelon, A., 2017.
861 OECD/EFSA workshop on developmental neurotoxicity (DNT): The use of non-animal test
862 methods for regulatory purposes. *ALTEX* 34, 311-315.
863
- 864 Fritsche, E., Grandjean, P., Crofton, K.M., Aschner, M., Goldberg, A., Heinonen, T., Hessel,
865 E.V.S., Hogberg, H.T., Bennekou, S.H., Lein, P.J., Leist, M., Mundy, W.R., Paparella, M.,
866 Piersma, A.H., Sachana, M., Schmuck, G., Solecki, R., Terron, A., Monnet-Tschudi, F.,
867 Wilks, M.F., Witters, H., Zurich, M.G., Bal-Price, A., 2018. Consensus statement on the
868 need for innovation, transition and implementation of developmental neurotoxicity (DNT)
869 testing for regulatory purposes. *Toxicol Appl Pharmacol* 354, 3-6.
870
- 871 Grandjean, P., Landrigan, P.J., 2006. Developmental neurotoxicity of industrial chemicals.
872 *Lancet* 368, 2167-2178.
873
- 874 Grandjean, P., Landrigan, P.J., 2014. Neurobehavioural effects of developmental toxicity. *Lancet*
875 *Neurol* 13, 330-338.
876
- 877 Griesinger C, Desprez B, Coecke S, Casey W, Zuang V. 2016. Validation of alternative in vitro
878 methods to animal testing: Concepts, challenges, processes and tools. *Adv Exp Med Biol*.
879 856:65-132.
880
- 881 Gutbier, S., May, P., Berthelot, S., Krishna, A., Trefzer, T., Behbehani, M., Efremova, L., Delp,
882 J., Gstraunthaler, G., Waldmann, T., Leist, M., 2018. Major changes of cell function and
883 toxicant sensitivity in cultured cells undergoing mild, quasi-natural genetic drift. *Arch*
884 *Toxicol* 92, 3487-3503.
885
- 886 Harrill, J.A., Freudenrich, T., Wallace, K., Ball, K., Shafer, T.J., Mundy, W.R., 2018. Testing for
887 developmental neurotoxicity using a battery of in vitro assays for key cellular events in
888 neurodevelopment. *Toxicol Appl Pharmacol* 354, 24-39.
889
- 890 Hartung, T., 2007. Food for thought ... on validation. *ALTEX* 24, 67-80.
891
- 892 Hartung, T., Hoffmann, S., Stephens, M., 2013. Mechanistic validation. *ALTEX* 30, 119-130.
893
- 894 Hoelting, L., Klima, S., Karreman, C., Grinberg, M., Meisig, J., Henry, M., Rotshteyn, T.,
895 Rahnenfuhrer, J., Bluthgen, N., Sachinidis, A., Waldmann, T., Leist, M., 2016. Stem Cell-
896 Derived Immature Human Dorsal Root Ganglia Neurons to Identify Peripheral
897 Neurotoxicants. *Stem Cells Transl Med* 5, 476-487.
898
- 899 Holzer, A.K., Suciu, I., Karreman, C., Goj, T., Leist, M., 2022. Specific Attenuation of
900 Purinergic Signaling during Bortezomib-Induced Peripheral Neuropathy In Vitro. *Int J Mol*
901 *Sci* 23.
902

Blum & Masjosthusmann et al. (2022): In vitro battery for DNT testing

- 903 Judson R, Kavlock R, Martin M, Reif D, Houck K, Knudsen T, Richard A, Tice RR, Whelan M,
904 Xia M. 2013. Perspectives on validation of high-throughput assays supporting 21st century
905 toxicity testing. *Altex*. 30(1):51.
906
- 907 Judson, hR., Houck, K., Martin, M., Richard, A.M., Knudsen, T.B., Shah, I., Little, S.,
908 Wambaugh, J., Woodrow Setzer, R., Kothiyia, P., Phuong, J., Filer, D., Smith, D., Reif, D.,
909 Rotroff, D., Kleinstreuer, N., Sipes, N., Xia, M., Huang, R., Crofton, K., Thomas, R.S.,
910 2016. Editor's Highlight: Analysis of the Effects of Cell Stress and Cytotoxicity on In Vitro
911 Assay Activity Across a Diverse Chemical and Assay Space. *Toxicol Sci* 152, 323-339.
912
- 913 Kadereit, S., Zimmer, B., van Thriel, C., Hengstler, J.G., Leist, M., 2012. Compound selection
914 for in vitro modeling of developmental neurotoxicity. *Front Biosci (Landmark Ed)* 17, 2442-
915 2460.
916
- 917 Kappenberg, F., Brecklinghaus, T., Albrecht, W., Blum, J., van der Wurp, C., Leist, M.,
918 Hengstler, J.G., Rahnenfuhrer, J., 2020. Handling deviating control values in concentration-
919 response curves. *Arch Toxicol* 94, 3787-3798.
920
- 921 Kisitu, J., Hollert, H., Fisher, C., Leist, M., 2020. Chemical concentrations in cell culture
922 compartments (C5) - free concentrations. *ALTEX* 37, 693-708.
923
- 924 Klima, S., Brull, M., Spreng, A.S., Suci, I., Falt, T., Schwamborn, J.C., Waldmann, T.,
925 Karreman, C., Leist, M., 2021. A human stem cell-derived test system for agents modifying
926 neuronal N-methyl-D-aspartate-type glutamate receptor Ca(2+)-signalling. *Arch Toxicol* 95,
927 1703-1722.
928
- 929 Klose, J., Li, L., Pahl, M., Bendt, F., Hubenthal, U., Jungst, C., Petzsch, P., Schauss, A., Kohrer,
930 K., Leung, P.C., Wang, C.C., Koch, K., Tigges, J., Fan, X., Fritsche, E., 2022. Application of
931 the adverse outcome pathway concept for investigating developmental neurotoxicity
932 potential of Chinese herbal medicines by using human neural progenitor cells in vitro. *Cell*
933 *Biol Toxicol*.
- 934 Klose, J., Pahl, M., Bartmann, K., Bendt, F., Blum, J., Dolde, X., Forster, N., Holzer, A.K.,
935 Hubenthal, U., Kessel, H.E., Koch, K., Masjosthusmann, S., Schneider, S., Sturzl, L.C.,
936 Woeste, S., Rossi, A., Covaci, A., Behl, M., Leist, M., Tigges, J., Fritsche, E., 2021a.
937 Neurodevelopmental toxicity assessment of flame retardants using a human DNT in vitro
938 testing battery. *Cell Biol Toxicol*.
939
- 940 Klose, J., Tigges, J., Masjosthusmann, S., Schmuck, K., Bendt, F., Hubenthal, U., Petzsch, P.,
941 Kohrer, K., Koch, K., Fritsche, E., 2021b. TBBPA targets converging key events of human
942 oligodendrocyte development resulting in two novel AOPs. *ALTEX* 38, 215-234.
943
- 944 Koch, K., Bartmann, K., Hartmann, J., Kapr, J., Klose, J., Kuchovska, E., Pahl, M.,
945 Schluppmann, K., Zuhr, E., Fritsche, E., 2022. Scientific Validation of Human Neurosphere
946 Assays for Developmental Neurotoxicity Evaluation. *Front Toxicol* 4, 816370.
947

Blum & Masjosthusmann et al. (2022): In vitro battery for DNT testing

- 948 Krebs, A., Nyffeler, J., Karreman, C., Schmidt, B.Z., Kappenberg, F., Mellert, J., Pallocca, G.,
949 Pastor, M., Rahnenfuhrer, J., Leist, M., 2020a. Determination of benchmark concentrations
950 and their statistical uncertainty for cytotoxicity test data and functional in vitro assays.
951 ALTEX 37, 155-163.
952
- 953 Krebs, A., Nyffeler, J., Rahnenfuhrer, J., Leist, M., 2018. Normalization of data for viability and
954 relative cell function curves. ALTEX 35, 268-271.
955
- 956 Krebs, A., van Vugt-Lussenburg, B.M.A., Waldmann, T., Albrecht, W., Boei, J., Ter Braak, B.,
957 Brajnik, M., Braunbeck, T., Brecklinghaus, T., Busquet, F., Dinnyes, A., Dokler, J., Dolde,
958 X., Exner, T.E., Fisher, C., Fluri, D., Forsby, A., Hengstler, J.G., Holzer, A.K., Janstova, Z.,
959 Jennings, P., Kisitu, J., Kobolak, J., Kumar, M., Limonciel, A., Lundqvist, J., Mihalik, B.,
960 Moritz, W., Pallocca, G., Ulloa, A.P.C., Pastor, M., Rovida, C., Sarkans, U., Schimming,
961 J.P., Schmidt, B.Z., Stober, R., Strassfeld, T., van de Water, B., Wilmes, A., van der Burg,
962 B., Verfaillie, C.M., von Hellfeld, R., Vrieling, H., Vrijenhoek, N.G., Leist, M., 2020b. The
963 EU-ToxRisk method documentation, data processing and chemical testing pipeline for the
964 regulatory use of new approach methods. Arch Toxicol 94, 2435-2461.
965
- 966 Krebs, A., Waldmann, T., Wilks, M.F., Van Vugt-Lussenburg, B.M.A., Van der Burg, B.,
967 Terron, A., Steger-Hartmann, T., Ruegg, J., Rovida, C., Pedersen, E., Pallocca, G., Luijten,
968 M., Leite, S.B., Kustermann, S., Kamp, H., Hoeng, J., Hewitt, P., Herzler, M., Hengstler,
969 J.G., Heinonen, T., Hartung, T., Hardy, B., Gantner, F., Fritsche, E., Fant, K., Ezendam, J.,
970 Exner, T., Dunkern, T., Dietrich, D.R., Coecke, S., Busquet, F., Braeuning, A., Bondarenko,
971 O., Bennekou, S.H., Beilmann, M., Leist, M., 2019. Template for the description of cell-
972 based toxicological test methods to allow evaluation and regulatory use of the data. ALTEX
973 36, 682-699.
974
- 975 Krug, A.K., Balmer, N.V., Matt, F., Schonenberger, F., Merhof, D., Leist, M., 2013a. Evaluation
976 of a human neurite growth assay as specific screen for developmental neurotoxicants. Arch
977 Toxicol 87, 2215-2231.
978
- 979 Krug, A.K., Gutbier, S., Zhao, L., Poltl, D., Kullmann, C., Ivanova, V., Forster, S., Jagtap, S.,
980 Meiser, J., Leparac, G., Schildknecht, S., Adam, M., Hiller, K., Farhan, H., Brunner, T.,
981 Hartung, T., Sachinidis, A., Leist, M., 2014. Transcriptional and metabolic adaptation of
982 human neurons to the mitochondrial toxicant MPP(+). Cell Death Dis 5, e1222.
983
- 984 Krug, A.K., Kolde, R., Gaspar, J.A., Rempel, E., Balmer, N.V., Meganathan, K., Vojnits, K.,
985 Baquie, M., Waldmann, T., Ensenat-Waser, R., Jagtap, S., Evans, R.M., Julien, S., Peterson,
986 H., Zagoura, D., Kadereit, S., Gerhard, D., Sotiriadou, I., Heke, M., Natarajan, K., Henry,
987 M., Winkler, J., Marchan, R., Stoppini, L., Bosgra, S., Westerhout, J., Verwei, M., Vilo, J.,
988 Kortenkamp, A., Hescheler, J., Hothorn, L., Bremer, S., van Thriel, C., Krause, K.H.,
989 Hengstler, J.G., Rahnenfuhrer, J., Leist, M., Sachinidis, A., 2013b. Human embryonic stem
990 cell-derived test systems for developmental neurotoxicity: a transcriptomics approach. Arch
991 Toxicol 87, 123-143.
992

Blum & Masjosthusmann et al. (2022): In vitro battery for DNT testing

- 993 Lee, J., Braun, G., Henneberger, L., Konig, M., Schlichting, R., Scholz, S., Escher, B.I., 2021.
994 Critical Membrane Concentration and Mass-Balance Model to Identify Baseline Cytotoxicity
995 of Hydrophobic and Ionizable Organic Chemicals in Mammalian Cell Lines. *Chem Res*
996 *Toxicol* 34, 2100-2109.
997
- 998 Lee, J., Escher, B.I., Scholz, S., Schlichting, R., 2022. Inhibition of neurite outgrowth and
999 enhanced effects compared to baseline toxicity in SH-SY5Y cells. *Arch Toxicol* 96, 1039-
1000 1053.
1001
- 1002 Lein, P., Locke, P., Goldberg, A., 2007. Meeting report: alternatives for developmental
1003 neurotoxicity testing. *Environ Health Perspect* 115, 764-768.
1004
- 1005 Leist, M., Hartung, T., Nicotera, P., 2008. The dawning of a new age of toxicology. *ALTEX* 25,
1006 103-114.
1007
- 1008 Leist, M., Hasiwa, N., Daneshian, M., Hartung, T., 2012. Validation and quality control of
1009 replacement alternatives – current status and future challenges. *Toxicology Research* 1, 8-22.
1010
- 1011 Leist, M., Hasiwa, N., Rovida, C., Daneshian, M., Basketter, D., Kimber, I., Clewell, H., Gocht,
1012 T., Goldberg, A., Busquet, F., Rossi, A.M., Schwarz, M., Stephens, M., Taalman, R.,
1013 Knudsen, T.B., McKim, J., Harris, G., Pamies, D., Hartung, T., 2014. Consensus report on
1014 the future of animal-free systemic toxicity testing. *ALTEX* 31, 341-356.
1015
- 1016 Leontaridou, M., Urbisch, D., Kolle, S.N., Ott, K., Mulliner, D.S., Gabbert, S., Landsiedel, R.,
1017 2017. The borderline range of toxicological methods: Quantification and implications for
1018 evaluating precision. *ALTEX* 34, 525-538.
1019
- 1020 Li, S., Huang, R., Solomon, S., Liu, Y., Zhao, B., Santillo, M.F., Xia, M., 2017. Identification of
1021 acetylcholinesterase inhibitors using homogenous cell-based assays in quantitative high-
1022 throughput screening platforms. *Biotechnol J* 12.
1023
- 1024 Loser, D., Hinojosa, M.G., Blum, J., Schaefer, J., Brull, M., Johansson, Y., Suci, I., Grillberger,
1025 K., Danker, T., Moller, C., Gardner, I., Ecker, G.F., Bennekou, S.H., Forsby, A., Kraushaar,
1026 U., Leist, M., 2021a. Functional alterations by a subgroup of neonicotinoid pesticides in
1027 human dopaminergic neurons. *Arch Toxicol* 95, 2081-2107.
1028
- 1029 Loser, D., Schaefer, J., Danker, T., Moller, C., Brull, M., Suci, I., Uckert, A.K., Klima, S., Leist,
1030 M., Kraushaar, U., 2021b. Human neuronal signaling and communication assays to assess
1031 functional neurotoxicity. *Arch Toxicol* 95, 229-252.
1032
- 1033 Lotharius, J., Falsig, J., van Beek, J., Payne, S., Dringen, R., Brundin, P., Leist, M., 2005.
1034 Progressive degeneration of human mesencephalic neuron-derived cells triggered by
1035 dopamine-dependent oxidative stress is dependent on the mixed-lineage kinase pathway. *J*
1036 *Neurosci* 25, 6329-6342.
1037

Blum & Masjosthusmann et al. (2022): In vitro battery for DNT testing

- 1038 Lupu, D., Andersson, P., Bornehag, C.G., Demeneix, B., Fritsche, E., Gennings, C.,
1039 Lichtensteiger, W., Leist, M., Leonards, P.E.G., Ponsonby, A.L., Scholze, M., Testa, G.,
1040 Tresguerres, J.A.F., Westerink, R.H.S., Zalc, B., Ruegg, J., 2020. The ENDpoiNTs Project:
1041 Novel Testing Strategies for Endocrine Disruptors Linked to Developmental Neurotoxicity.
1042 Int J Mol Sci 21.
1043
- 1044 Makris, S.L., Raffaele, K., Allen, S., Bowers, W.J., Hass, U., Alleva, E., Calamandrei, G., Sheets,
1045 L., Amcoff, P., Delrue, N., Crofton, K.M., 2009. A retrospective performance assessment of
1046 the developmental neurotoxicity study in support of OECD test guideline 426. Environ
1047 Health Perspect 117, 17-25.
1048
- 1049 Masjosthusmann, S., Becker, D., Petzuch, B., Klose, J., Siebert, C., Deenen, R., Barenys, M.,
1050 Baumann, J., Dach, K., Tigges, J., Hubenthal, U., Kohrer, K., Fritsche, E., 2018. A
1051 transcriptome comparison of time-matched developing human, mouse and rat neural
1052 progenitor cells reveals human uniqueness. Toxicol Appl Pharmacol 354, 40-55.
1053
- 1054 Masjosthusmann, S., Blum, J., Bartmann, K., Dolde, X., Holzer, A.-K., Stürzl, L.-C., Keßel,
1055 E.H., Förster, N., Dönmez, A., Klose, J., Pahl, M., Waldmann, T., Bendt, F., Kisitu, J.,
1056 Suciú, I., Hübenthal, U., Mosig, A., Leist, M., Fritsche, E., 2020. Establishment of an a priori
1057 protocol for the implementation and interpretation of an in-vitro testing battery for the
1058 assessment of developmental neurotoxicity. EFSA Supporting Publications 17, 1938E.
1059
- 1060 Meisig, J., Dreser, N., Kapitza, M., Henry, M., Rotshteyn, T., Rahnenfuhrer, J., Hengstler, J.G.,
1061 Sachinidis, A., Waldmann, T., Leist, M., Bluthgen, N., 2020. Kinetic modeling of stem cell
1062 transcriptome dynamics to identify regulatory modules of normal and disturbed
1063 neuroectodermal differentiation. Nucleic Acids Res 48, 12577-12592.
1064
- 1065 Modafferi, S., Zhong, X., Kleensang, A., Murata, Y., Fagiani, F., Pamies, D., Hogberg, H.T.,
1066 Calabrese, V., Lachman, H., Hartung, T., Smirnova, L., 2021. Gene-Environment
1067 Interactions in Developmental Neurotoxicity: a Case Study of Synergy between Chlorpyrifos
1068 and CHD8 Knockout in Human BrainSpheres. Environ Health Perspect 129, 77001.
1069
- 1070 Mundy, W.R., Padilla, S., Breier, J.M., Crofton, K.M., Gilbert, M.E., Herr, D.W., Jensen, K.F.,
1071 Radio, N.M., Raffaele, K.C., Schumacher, K., Shafer, T.J., Cowden, J., 2015. Expanding the
1072 test set: Chemicals with potential to disrupt mammalian brain development. Neurotoxicol
1073 Teratol 52, 25-35.
1074
- 1075 Nimtz, L., Hartmann, J., Tigges, J., Masjosthusmann, S., Schmuck, M., Kessel, E., Theiss, S.,
1076 Kohrer, K., Petzsch, P., Adjaye, J., Wigmann, C., Wiczorek, D., Hildebrandt, B., Bendt, F.,
1077 Hubenthal, U., Brockerhoff, G., Fritsche, E., 2020. Characterization and application of
1078 electrically active neuronal networks established from human induced pluripotent stem cell-
1079 derived neural progenitor cells for neurotoxicity evaluation. Stem Cell Res 45, 101761.
1080
- 1081 Nimtz, L., Klose, J., Masjosthusmann, S., Barenys, M., Fritsche, E., 2019. The Neurosphere
1082 Assay as an In Vitro Method for Developmental Neurotoxicity (DNT) Evaluation. in:

Blum & Masjosthusmann et al. (2022): In vitro battery for DNT testing

- 1083 Aschner, M., Costa, L. (Eds.). Cell Culture Techniques. Springer New York, New York, NY,
1084 pp. 141-168.
1085
- 1086 Nunes, C., Singh, P., Mazidi, Z., Murphy, C., Bourguignon, A., Wellens, S., Chandrasekaran, V.,
1087 Ghosh, S., Zana, M., Pamies, D., Thomas, A., Verfaillie, C., Culot, M., Dinnyes, A., Hardy,
1088 B., Wilmes, A., Jennings, P., Grillari, R., Grillari, J., Zurich, M.G., Exner, T., 2022. An in
1089 vitro strategy using multiple human induced pluripotent stem cell-derived models to assess
1090 the toxicity of chemicals: A case study on paraquat. *Toxicol In Vitro* 81, 105333.
1091
- 1092 Nyffeler, J., Karreman, C., Leisner, H., Kim, Y.J., Lee, G., Waldmann, T., Leist, M., 2017.
1093 Design of a high-throughput human neural crest cell migration assay to indicate potential
1094 developmental toxicants. *ALTEX* 34, 75-94.
1095
- 1096 OECD, 2021. Guideline No. 497: Defined Approaches on Skin Sensitisation.
1097
- 1098 OECD. 2007. Test no. 426: Developmental neurotoxicity study. OECD Publishing.
1099
- 1100 Pallocca, G., Mone, M.J., Kamp, H., Luijten, M., Van de Water, B., Leist, M., 2022a. Next-
1101 generation risk assessment of chemicals - Rolling out a human-centric testing strategy to
1102 drive 3R implementation: The RISK-HUNT3R project perspective. *ALTEX*.
1103
- 1104 Pallocca, G., Nyffeler, J., Dolde, X., Grinberg, M., Gstraunthaler, G., Waldmann, T.,
1105 Rahnenfuhrer, J., Sachinidis, A., Leist, M., 2017. Impairment of human neural crest cell
1106 migration by prolonged exposure to interferon-beta. *Arch Toxicol* 91, 3385-3402.
1107
- 1108 Pallocca, G., Rovida, C., Leist, M., 2022b. On the usefulness of animals as a model system (part
1109 I): Overview of criteria and focus on robustness. *ALTEX* 39, 347-353.
1110
- 1111 Paparella, M., Bennekou, S.H., Bal-Price, A., 2020. An analysis of the limitations and
1112 uncertainties of in vivo developmental neurotoxicity testing and assessment to identify the
1113 potential for alternative approaches. *Reprod Toxicol* 96, 327-336.
1114
- 1115 Patterson, E.A., Whelan, M.P., Worth, A.P., 2021. The role of validation in establishing the
1116 scientific credibility of predictive toxicology approaches intended for regulatory application.
1117 *Comput Toxicol* 17, 100144.
1118
- 1118 Piersma, A.H., van Benthem, J., Ezendam, J., Kienhuis, A.S., 2018. Validation redefined.
1119 *Toxicol In Vitro* 46, 163-165.
1120
- 1121 Pistollato, F., Carpi, D., Mendoza-de Gyves, E., Paini, A., Bopp, S.K., Worth, A., Bal-Price, A.,
1122 2021. Combining in vitro assays and mathematical modelling to study developmental
1123 neurotoxicity induced by chemical mixtures. *Reprod Toxicol* 105, 101-119.
1124
- 1125 Products, E.Panel o.P.P., Residues, t., Hernández-Jerez, A., Adriaanse, P., Aldrich, A., Berny, P.,
1126 Coja, T., Duquesne, S., Focks, A., Marinovich, M., Millet, M., Pelkonen, O., Pieper, S.,
1127 Tiktak, A., Topping, C., Widenfalk, A., Wilks, M., Wolterink, G., Crofton, K., Hougaard
1128 Bennekou, S., Paparella, M., Tzoulaki, I., 2021. Development of Integrated Approaches to

Blum & Masjosthusmann et al. (2022): In vitro battery for DNT testing

- 1129 Testing and Assessment (IATA) case studies on developmental neurotoxicity (DNT) risk
1130 assessment. *EFSA Journal* 19, e06599.
1131
- 1132 Ryan, K.R., Sirenko, O., Parham, F., Hsieh, J.H., Cromwell, E.F., Tice, R.R., Behl, M., 2016.
1133 Neurite outgrowth in human induced pluripotent stem cell-derived neurons as a high-
1134 throughput screen for developmental neurotoxicity or neurotoxicity. *Neurotoxicology* 53,
1135 271-281.
1136
- 1137 Sachana, M., Bal-Price, A., Crofton, K.M., Bennekou, S.H., Shafer, T.J., Behl, M., Terron, A.,
1138 2019. International Regulatory and Scientific Effort for Improved Developmental
1139 Neurotoxicity Testing. *Toxicol Sci* 167, 45-57.
1140
- 1141 Sachana, M., Willett, C., Pistollato, F., Bal-Price, A., 2021. The potential of mechanistic
1142 information organised within the AOP framework to increase regulatory uptake of the
1143 developmental neurotoxicity (DNT) in vitro battery of assays. *Reprod Toxicol* 103, 159-170.
1144
- 1145 Schmuck, M.R., Temme, T., Dach, K., de Boer, D., Barenys, M., Bendt, F., Mosig, A., Fritsche,
1146 E., 2017. Omnisphero: a high-content image analysis (HCA) approach for phenotypic
1147 developmental neurotoxicity (DNT) screenings of organoid neurosphere cultures in vitro.
1148 *Arch Toxicol* 91, 2017-2028.
1149
- 1150 Scholz, D., Poltl, D., Genewsky, A., Weng, M., Waldmann, T., Schildknecht, S., Leist, M., 2011.
1151 Rapid, complete and large-scale generation of post-mitotic neurons from the human
1152 LUHMES cell line. *J Neurochem* 119, 957-971.
1153
- 1154 Sheets, L.P., Li, A.A., Minnema, D.J., Collier, R.H., Creek, M.R., Peffer, R.C., 2016. A critical
1155 review of neonicotinoid insecticides for developmental neurotoxicity. *Crit Rev Toxicol* 46,
1156 153-190.
1157
- 1158 Smirnova, L., Hogberg, H.T., Leist, M., Hartung, T., 2014. Developmental neurotoxicity -
1159 challenges in the 21st century and in vitro opportunities. *ALTEX* 31, 129-156.
1160
- 1161 Stiegler, N.V., Krug, A.K., Matt, F., Leist, M., 2011. Assessment of chemical-induced
1162 impairment of human neurite outgrowth by multiparametric live cell imaging in high-density
1163 cultures. *Toxicol Sci* 121, 73-87.
- 1164 Strickland, J., Truax, J., Corvaro, M., Settivari, R., Henriquez, J., McFadden, J., Gullledge, T.,
1165 Johnson, V., Gehen, S., Germolec, D., Allen, D.G., Kleinstreuer, N., 2022. Application of
1166 Defined Approaches for Skin Sensitization to Agrochemical Products. *Front Toxicol* 4,
1167 852856.
1168
- 1169 Thomas, R.S., Paules, R.S., Simeonov, A., Fitzpatrick, S.C., Crofton, K.M., Casey, W.M.,
1170 Mendrick, D.L., 2018. The US Federal Tox21 Program: A strategic and operational plan for
1171 continued leadership. *ALTEX* 35, 163-168.
1172
- 1173 Tohyama, C., 2016. Developmental neurotoxicity test guidelines: problems and perspectives. *J*
1174 *Toxicol Sci* 41, SP69-SP79.

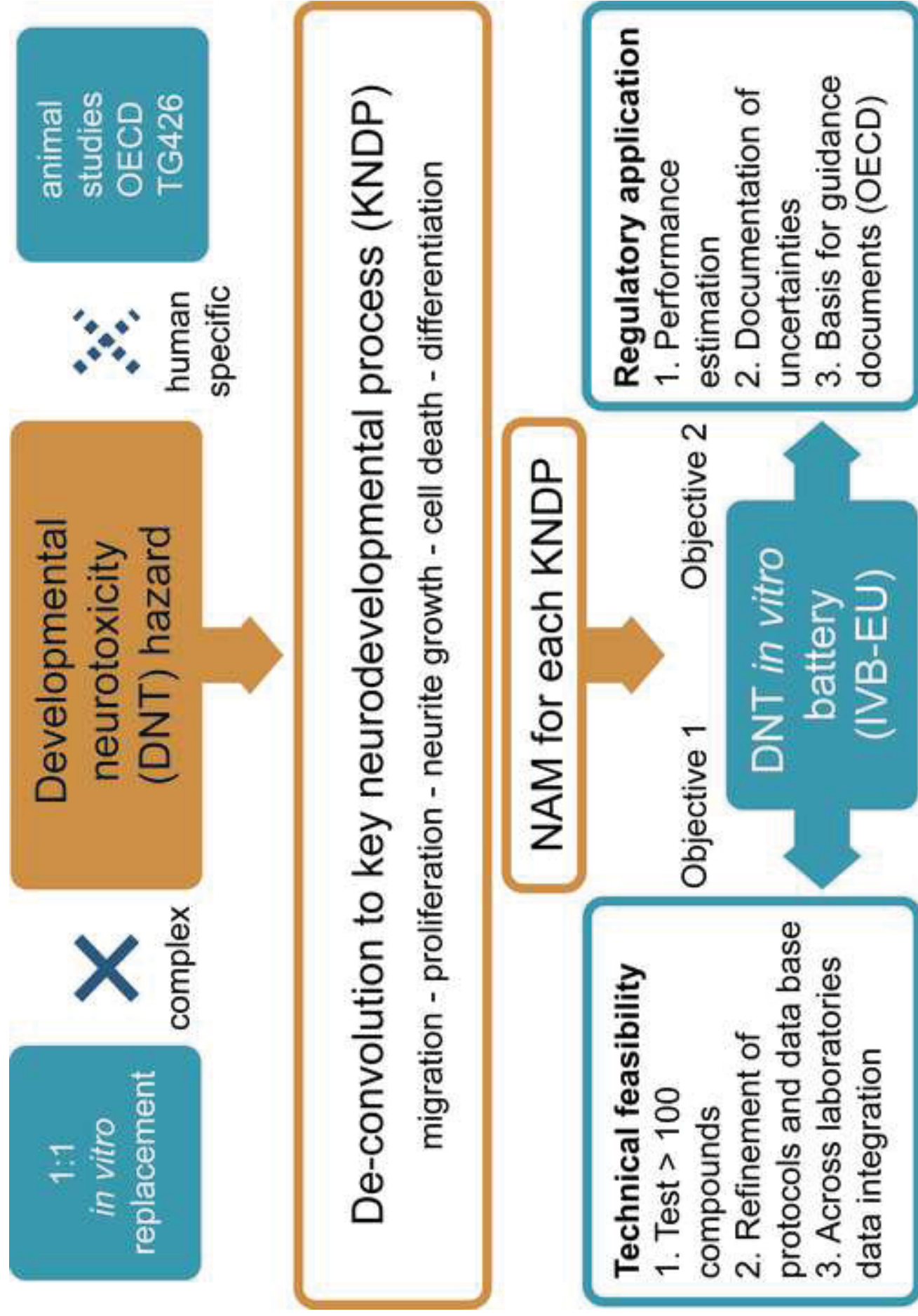
Blum & Masjosthusmann et al. (2022): In vitro battery for DNT testing

- 1175
1176 Tsuji, R., Crofton, K.M., 2012. Developmental neurotoxicity guideline study: issues with
1177 methodology, evaluation and regulation. *Congenit Anom (Kyoto)* 52, 122-128.
1178
1179 USEPA. 1998. Health effects guidelines oppts 970.6300: Developmental neurotoxicity study.
1180
1181 van Thriel, C., Westerink, R.H., Beste, C., Bale, A.S., Lein, P.J., Leist, M., 2012. Translating
1182 neurobehavioural endpoints of developmental neurotoxicity tests into in vitro assays and
1183 readouts. *Neurotoxicology* 33, 911-924.
1184
1185 Vinken, M., Benfenati, E., Busquet, F., Castell, J., Clevert, D.A., de Kok, T.M., Dirven, H.,
1186 Fritsche, E., Geris, L., Gozalbes, R., Hartung, T., Jennen, D., Jover, R., Kandarova, H.,
1187 Kramer, N., Krul, C., Luechtefeld, T., Masereeuw, R., Roggen, E., Schaller, S., Vanhaecke,
1188 T., Yang, C., Piersma, A.H., 2021. Safer chemicals using less animals: kick-off of the
1189 European ONTOX project. *Toxicology* 458, 152846.
1190

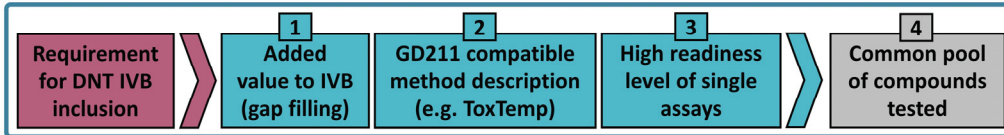
Blum & Masjosthusmann et al. (2022): In vitro battery for DNT testing

1 **Author Contributions**

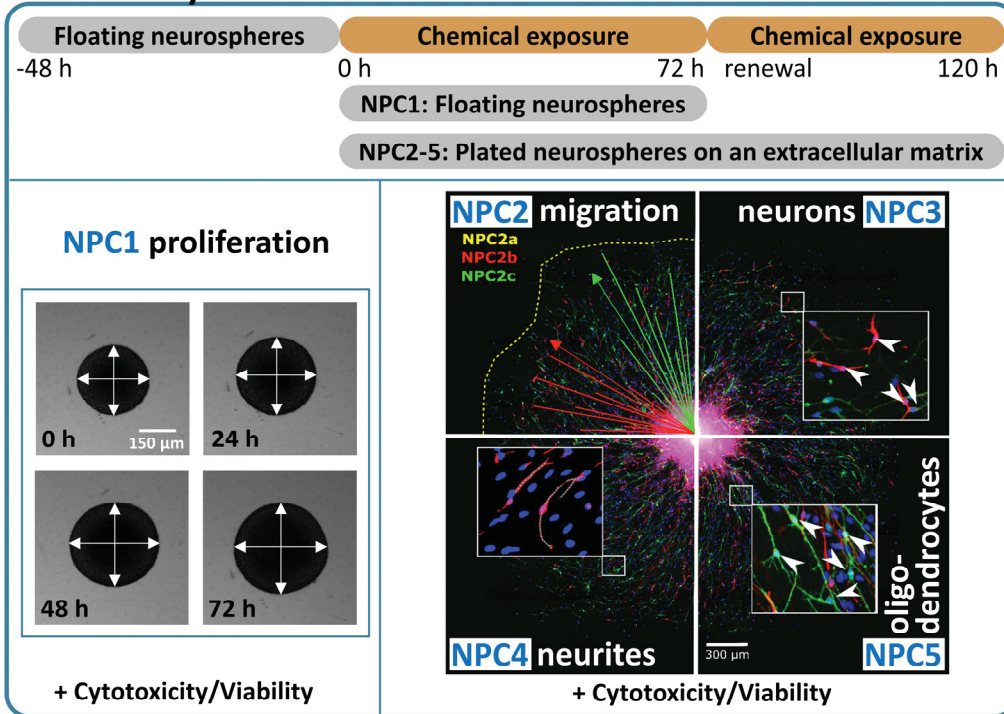
2 All authors read, commented, and approved the manuscript. **Jonathan Blum:** study conception,
3 investigation, data analysis, supervision, figure design, writing of article. **Stefan**
4 **Masjosthusmann:** study conception, data analysis, supervision, figure design, writing of article.
5 **Kristina Bartmann:** investigation. **Farina Bendt:** investigation. **Xenia Dolde:** investigation,
6 data analysis. **Anna-Katharina Holzer:** investigation, data analysis. **Ulrike Hübenthal:**
7 investigation. **Sadiye Kilic:** investigation. **Jördis Klose:** investigation. **Melanie Pahl:**
8 investigation. **Lynn-Christin Stürzl:** investigation. **Arif Dönmez:** software development, data
9 analysis. **Nils Förster:** software development, data analysis. **Hagen Eike Keßel:** software
10 development, data analysis. **Martin Scholze:** software development, data analysis. **Axel Mosig:**
11 software development, supervision. **Iris Mangas:** editing of article. **Andrea Terron:** editing of
12 article. **Kevin Crofton:** editing of article. **Marcel Leist:** study conception, supervision, funding
13 acquisition, project administration, figure design, writing of article. **Ellen Fritsche:** study
14 conception, supervision, funding acquisition, project administration, figure design, writing of
15 article.



A IVB-EU



B NPC Assays



C UKN Assays

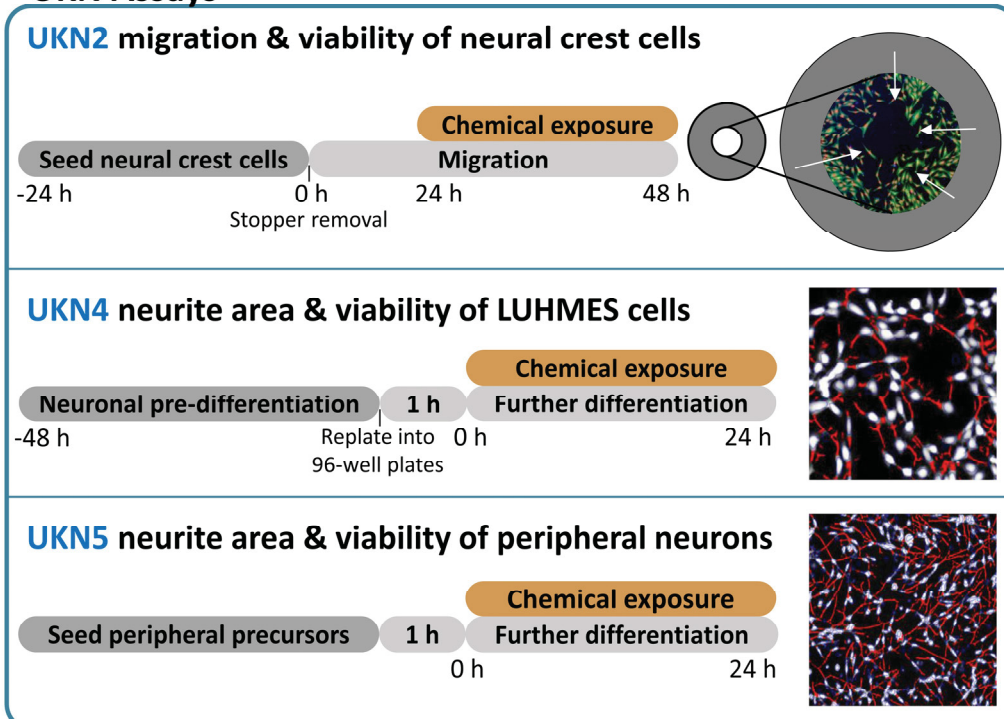


Fig. 1: Requirements and composition of the IVB-EU

(A) Criteria for assays to be included in the DNT test battery designated here IVB-EU. Criteria 1-3 were applied to this study. Criterion 4 was fulfilled in the course of this study and is suggested to be considered for future battery expansion.

GD211 = OECD guidance document 211 on documentation of in vitro methods.

(B) Schematic representation of the assays based on human neural progenitor cells (NPC) and their progeny. The general test system generation and exposure scheme is indicated on top. For the NPC1 test, floating neurospheres were exposed to toxicants for 72 h, and bromodeoxyuridine (BrdU) incorporation was used as endpoint for proliferation of NPC. For the NPC2-5 assays, neurospheres were plated and allowed to form secondary co-cultures of various cell types. Endpoints related to migration (NPC2) neuronal differentiation (NPC3), neurite growth (NPC4) and oligodendrocyte formation (NPC5) were assessed after 120 h by immunostaining and high content imaging. **(C)** Schematic representation of UKN assays. Cell types used and exposure schemes are indicated. Viability and migration of the cells in all assays were determined simultaneously by automated high content imaging after staining of the cell cultures with calcein-AM and Hoechst H-33342. The UKN2 assay evaluated the migration of neural crest cells into an empty circular area. The UKN4/UKN5 assays evaluated neural outgrowth of central nervous system and peripheral nervous system immature neurons. Detailed descriptions of NPC and UKN assays are given in the [ToxTemps \(suppl. file 1\)](#).

KNDPs	Precursor proliferation	Migration	Differentiation	Neurite outgrowth	Neural network formation and function	Cell activation & stimulation
	Death of specific cell populations					
In vitro methods	NPC1 NPCs	NPC2a radial glia	NPC3 neuron	NPC4 CNS neuron	MEA based assays*	transport activity
	hiPSC based NPCs*	NPC2b neuronal	NPC5 oligo-dendrocytes	UKN4 CNS neuron	maturation & synaptogenesis	neuro-transmitter signals*
	radial glia	NPC2c oligo-dendrocytes	(NPC6) oligo-dendrocyte maturation*	UKN5 PNS neuron	myelination	inflammation (glia activation)
		UKN2 neural crest	NEPs (UKN1 & RoFA)*			signal transduction gaps
			astrocytes & radial glia*			
*established with good readiness level for toxicity testing, but not part of initial IVB-EU					Covered in IVB-EU	Potential gap

Fig. 2: Key neurodevelopmental processes (KNDP) covered by IVB-EU

Categories of KNDPs, according to Bal-Price et al (Bal-Price et al., 2018) are listed on top. Specific cell death in a neurodevelopmental sub-population may either be considered a KNDP or an adverse effect. As it is measured as endpoint in all assays of others KNDP, it was considered to be broadly covered by the IVB-EU without a dedicated own assay. The lower part of the figure indicates NAM (designated here: *in vitro* methods) that are related to the respective KNDP on top of each column. The coverage of KNDPs by assays that are part of the current IVB-EU is shown (bold). For some KNDPs, more than one test was available. The reason was that several distinct subpopulations e.g. migrate (radial glia, neurons, oligodendrocytes and neural crest cells) or grow neurites (different types of CNS and PNS neurons). Potential gaps of the current IVB-EU are shown as assays in the non-bold *in vitro* method boxes. Assays that have already been established in the co-authors' labs are indicated by asterisks. They may be included in an extended version of the IVB, once they fulfill all inclusion criteria (Fig. 1). CNS: central nervous system; hiPSC: human induced pluripotent stem cells; NEP: neuroepithelial precursor; NPC: neural progenitor cell; MEA: microelectrode array; PNS: peripheral nervous system; RoFA: rosette formation assay.

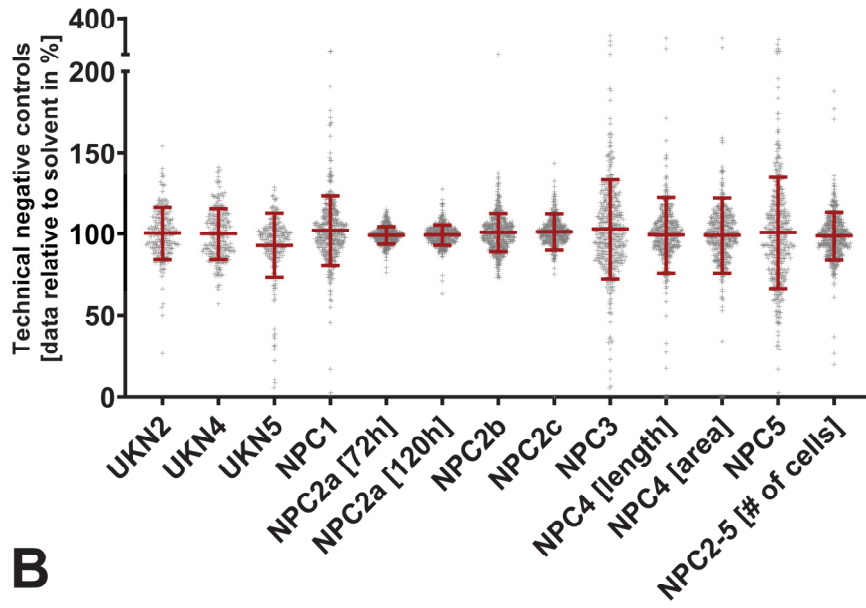
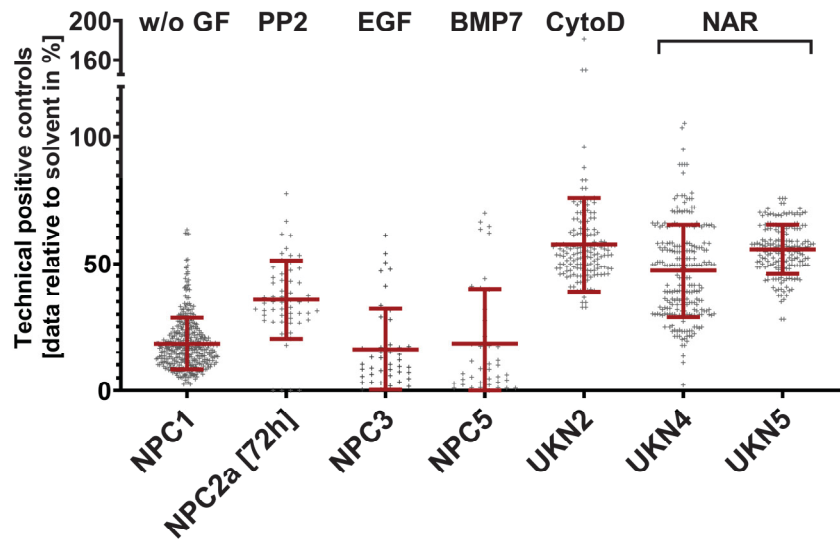
A**B**

Fig. 3: Baseline noise and signal variation of acceptance controls in the IVB-EU assays

All tests were performed in a way so that each assay plate or experimental run contained wells with (i) negative controls, and at least one (ii) positive control. The reading of (ii) vs. (i) was used as acceptance criterion of the respective plate for UKN2,4 and 5. If the positive control was not in a pre-specified range, the plate data were not included in screen results and measurements were repeated. Depending on the assay, plates contained different numbers of compounds. For some tests, the different concentrations of a given compound were on different plates. Thus, some plates contained the (iii) lowest concentration of a compound, and some did not. **(A)** To obtain a measure of inter-plate and intra-experimental variability of the baseline signal, the lowest concentration of each test compound (iii) was compared to the solvent control (i) on each plate. Altogether > 200 data points were obtained for each IVB-EU endpoint from the testing campaign. For easier overview, the means \pm SD are indicated on top of the data points. **(B)** For each plate, the reading of the positive controls (ii) was compared to that of the negative controls (i) and normalized to negative control readings. The means \pm SD of data for positive controls are given for the IVB-EU endpoints. The compounds used to set acceptance criteria were as follows: w/o GF: without growth factor (omission of normally present growth factors in the positive control well); PP-2: SRC-kinase inhibitor; EGF: epidermal growth factor; BMP7: bone morphogenetic protein 7; CytoD: cytochalasin D; NAR: narciclasine. Details on concentrations are found in the [ToxTemps \(suppl. file 1\)](#).

A

Positive controls	specific + brdl. + cytotox	specific + brdl.	specific
Cadmium chloride	TP	TP	TP
Chlorpyrifos	TP	TP	FN
Dexamethasone	TP	TP	TP
Hexachlorophene	TP	TP	TP
Lead (II) acetate trihydrate	TP	TP	TP
Manganese (II) chloride	TP	TP	TP
Methylmercury chloride	TP	TP	TP
PBDE 47	TP	TP	TP
PBDE 99	TP	TP	FN
(±) Ketamine hydrochloride	FN	FN	FN
5,5-Diphenylhydantoin	FN	FN	FN
Acrylamide	TP	TP	TP
all-trans-Retinoic acid	TP	TP	TP
Chlorpromazine hydrochloride	TP	TP	TP
Deltamethrin	TP	TP	TP
Domoic acid	FN	FN	FN
Haloperidol	TP	TP	TP
Maneb	TP	TP	FN
Methylazoxymethanol acetate	TP	TP	TP
Nicotine	FN	FN	FN
Paraquat dichloride hydrate	TP	TP	TP
PFOA	TP	FN	FN
PFOSK	TP	TP	TP
Sodium valproate	TP	TP	TP
Tebuconazole	TP	TP	TP
Tributyltin chloride	TP	TP	TP
Trichlorfon	TP	TP	TP
Triethyl-tin bromide	TP	TP	FN

B

Negative controls	Acetaminophen	TN	TN	TN
	Amoxicillin	TN	TN	TN
	Aspirin	TN	TN	TN
	Bupirone	FP	TN	TN
	Chlorpheniramine maleate	TN	TN	TN
	D-Glucitol	TN	TN	TN
	Diethylene glycol	TN	TN	TN
	D-Mannitol	TN	TN	TN
	Doxylamine succinate	TN	TN	TN
	Famotidine	TN	TN	TN
	Ibuprofen	TN	TN	TN
	Metformin	TN	TN	TN
	Metoprolol	TN	TN	TN
	Penicillin	TN	TN	TN
	Saccharin	TN	TN	TN
	Sodium benzoate	TN	TN	TN
	Warfarin	TN	TN	TN

C

Performance [%]	Sensitivity	86	82	68
	Specificity	94	100	100
	Accuracy	89	89	80
	Balanced accuracy	90	91	84
	PPV	96	100	100
	F1 score	91	91	84
	MCC	78	80	67

Fig. 4: Performance overview of the test battery (IVB-EU)

A set of predefined negative (n=17) and positive (n=28) control compounds was included in the set of screening compounds (n=120). The rationale for their selection is given in Fig. S2. Note that the controls were randomly included in the overall screening workflow without being given any preferences or special treatment. This means that the standard prediction models of the assays were applied to them, so that they were classified as “no hit”, “cytotoxic”, “borderline (brdl) ” or “specific hit” in individual NAM (see Fig. S3). A reference compound was considered to be a “positive” on the level of the overall IVB-EU, when it was an “alert” in at least one of the individual assays. The tabular display of the figure uses three definitions for an alert: anything that is not a “no hit” (first column), anything that was a specific hit or brdl (second column) or only specific hits (third column). **(A)** Alerts were considered true positives (TP), non-alerts were considered false negatives (FN). **(B)** Non-alerts were considered true negatives (TN), alerts were considered false positives (FP). **(C)** Performance parameters of the current DNT IVB-EU in percent. All parameters were calculated based on the TP, FN, TN, FP as indicated in (A) and (B). PPV: positive predictive value; MCC: Matthews correlation coefficient.

	M S E	within 3-fold MSE range	outside 3-fold range	Compound / Test method ¹												
				UKN2	UKN4	UKN5	NPC1	NPC2a [72h]	NPC2a [120h]	NPC2b	NPC2c	NPC3	NPC4 [length]	NPC4 [area]	NPC5	NPC2-5 [# of cells]
positive control compounds	Dexamethasone (DEX)				7.3						5.7					
	Tributyltin chloride (TTC)	6.9			7.2									6.8		
	Hexachlorophene (HCP)	6.4			4.9	6.9					7.1					
	Methylmercury(II) chloride (MMC)		7.0	6.4		6.2	6.3			6.3	6.7	6.3			6.1	
	Chlorpromazine hydrochloride (CPH)	5.2		5.5	6.0						5.4	5.3	6.4			
	Deltamethrin (DM)	4.8				6.0		5.4			4.9		6.4			
	Cadmium chloride (CCL)	6.3			5.3	5.8	5.6								5.5	
	Triethyltin bromide (TETB)			6.2												
	all-trans-RetInoic acid (RA)	5.3			5.7											
	Tebuconazole (TBN)													5.6		
	Haloperidol (HPD)		4.9	4.9		4.9								5.6		
	PBDE-47 ²	4.3											5.4			
	Trichlorfon (TCF)										5.3				4.9	
	PFOSK ³	4.5								5.0						
	Maneb (MAB)	5.0														
	PBDE 99 (BDE)		4.9													
	Paraquat dichloride hydrate (PQ)	4.0	4.0	3.8			4.9									
	Manganese(II) chloride (MC)												4.7			
	Lead(II) acetate trihydrate (LAT)	4.6														
	Chlorpyrifos (CPF)	4.4	4.0													
Methylazoxymethanol acetate (MAM)				3.8												
Sodium valproate (VPA)				3.3					3.3			3.3				
Acrylamide (AAM)			2.9													
all other hits	Narciclasine (NAR)	7.3	7.9	7.7	7.8				7.2	8.3	7.9	8.0	7.8	7.6		
	Rotenone (RTN)	7.5	7.0	7.2		6.8	7.0			6.3	6.3	6.2		6.7		
	Glufosinate-ammonium (GFA)									7.1						
	Alpha-Endosulfan (AES)	5.1					4.8						6.4			
	Metaflumizone (MFM)												6.3			
	Endosulfan sulfate (ESS)	5.4											6.3			
	Indoxacarb (IXC)	5.0			6.3								5.8			
	3,3',5,5'-Tetrabromobisphenol A (TBBPA)	5.9											6.3			
	gamma-Cyhalothrin (CHT)												6.1			
	Emamectin benzoate (EMB)	6.0			6.0											
	2-Ethylhexyl diphenyl phosphate (EDP)	5.3			6.0								5.2			
	Beta-Cypermethrin (BCPM)												6.0			
	Malathion (MLT)												5.9			
	Endosulfan (EDS)						4.9						5.7			
	tau-Fluvalinate (TFV)												5.7			
	tert-Butylphenyl diphenyl phosphate (BDP)	5.3					5.1						5.7			
	MPP ⁴		5.7		5.6											
	Tris(1,3-dichloro-2-propyl) phosphate (TDCPP)						4.9						5.6			
	Flubendiamide (FBD)												5.5			
	Fipronil (FPN)	4.8	5.0			4.9				4.9	4.9	4.9	5.5	4.8		
	Triphenyl phosphates isopropylated (TPI)	5.2											5.4			
	Tri-o-tolyl phosphate (TOTP)	5.4					5.3						5.2	4.7		
	Isodecyl diphenyl phosphate (IDDP)	5.0											5.4			
	Penthiopyrad (PP)					4.8							5.3			
	Chlorpyrifos-oxon (CPFO)				5.2		5.0				4.9					
	Tris(2-butoxyethyl)phosphate (TBOEP)												5.2			
	beta-Cyfluthrin (BCFT)												5.2			
	Carbaryl (CBR)	5.0	4.8			5.1	5.2				5.1	5.0				
	Acibenzolar-S-methyl (ABM)				5.1											
	Tris(methylphenyl) phosphate (TTP)	5.1														
	Clothianidin (CTN)										5.0					
	Triphenylphosphate (TPHP)	5.0											4.9			
Bisphenol A (BPA)	4.9											4.9				
Thiacloprid (TC)														4.9		
1-Naphthol (NT)	4.7				4.9											
Azinphos-methyl (APM)					4.8	4.8										

¹all concentrations are given in -logM; ²2,2',4,4'-Tetrabromodiphenyl ether;

³Heptadecafluorooctanesulfonic acid potassium salt; ⁴1-Methyl-4-phenylpyridinium iodide,

Fig. 5: Hit summary of the IVB-EU screen

Overall, 120 compounds were screened in the current DNT IVB-EU. Screened substances were considered as “hits” when they were classified as a “specific hit” or a “borderline compound” in at least one assay of the battery (assays indicated on top of the columns). The upper section of the table shows all 23 hits amongst the 28 positive controls used in the screen (the remaining five positive controls were no hits). The lower section shows all additional 36 hits amongst the screened compounds. Within the groups, the compounds are ranked based on potency (indicated in units of $-\log [M]$). The table includes all hits of the screen. For each compound, the most sensitive endpoint (MSE) is highlighted. In addition, hits of the respective chemical in other assays, which were of similar potency as in the MSE assay (within a 3-fold range), are also highlighted. The compounds that affected only viability endpoints in the IVB-EU are listed in Fig. S5A. The compounds that affected no endpoint at all are listed in Fig. S5B. Exact and complete screen data (including the uncertainties assessed as 95% confidence interval) are included in a [suppl. file 2 – sheet 2 & 3](#).

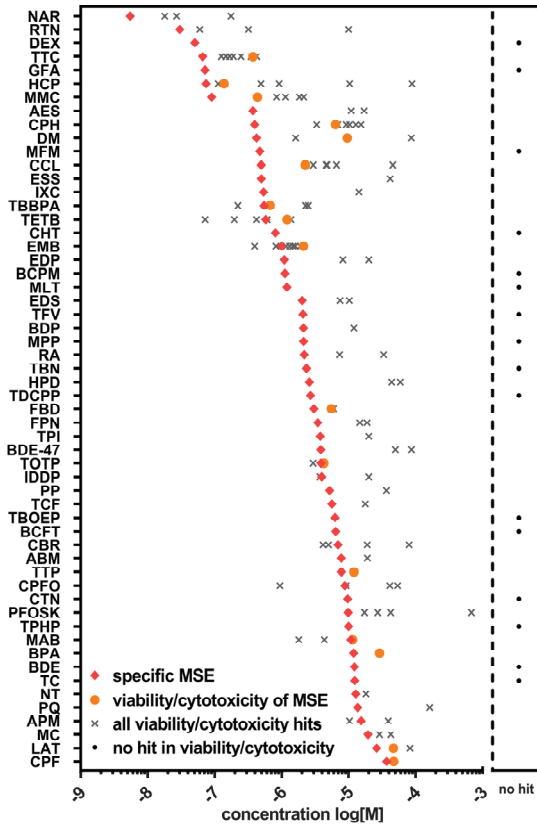
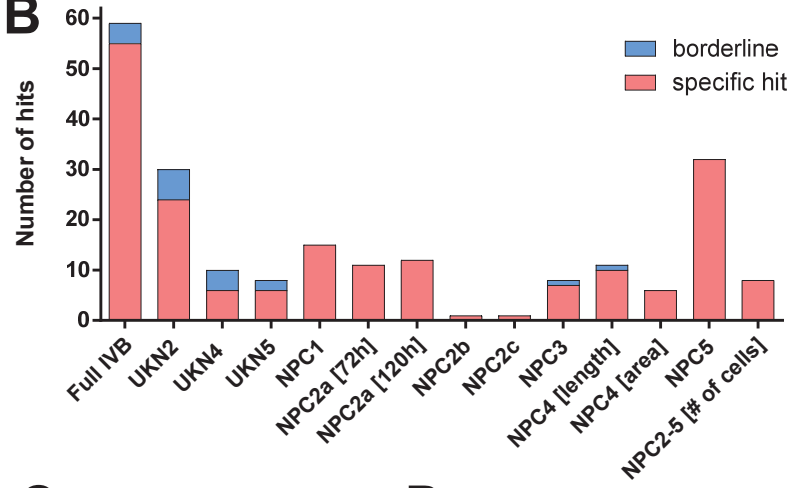
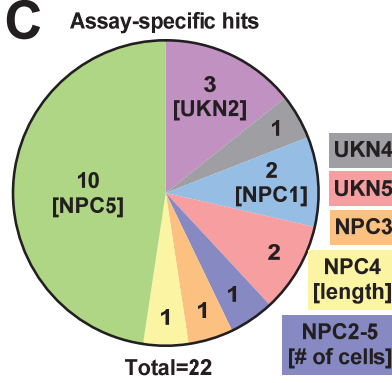
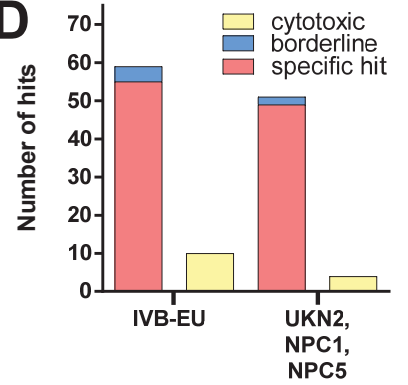
A**B****C****D**

Fig. 6: Contribution of individual NAM to the overall IVB-EU

The screen was performed, hits were identified and the most sensitive endpoint (MSE) was defined for each compound as detailed in Fig. 5. **(A)** A potency overview of all hit compounds (see Fig. 5 for abbreviation) is displayed: The compounds are sorted according to the potency of their MSE. Note that all MSE data refer to a specific test endpoint (i.e. migration, differentiation, proliferation, neurite growth). In addition, the concentrations at which compounds were detected to be cytotoxic are indicated. Compounds that were not cytotoxic in any assay are indicated by a dot right of the dashed line. The cytotoxic concentration measured in the same assay as the MSE is given a separate symbol (filled circle) to allow an easy overview. Note that for many compounds, no cytotoxicity was measured in the assay that produced the MSE. For design reasons, three low potency compounds were not included in the figure: MAM (MSE = -3.8) orange point at x, 3 additional cytotoxic hits; VPA (MSE = -3.3) orange point at -2.7, four other cytotoxicity hits; AAM (MSE = -2.9) no other cytotoxic hit. All data are given in log(M). **(B)** The number of hits (out of 120 screen compounds) is indicated for each assay of the battery, and for the total IVB-EU (most leftward bar). The number of specific hits and of borderline hits can both be seen within one bar. The respective set of data for cytotoxic compounds is visualized in Fig. S7 **(C)** The number of compounds that were a hit in only one assay is displayed for all assays, e.g. 10 compounds were detected only in NPC5, but no other assay; one compound was detected only in UKN4 and no other assay. **(D)** The number of hits (separated in specific hits, borderline hits and cytotoxic-only compounds) was compared for the full IVB-EU and a hypothetical mini-battery consisting of 3 assays (UKN2, NPC1, NPC5).

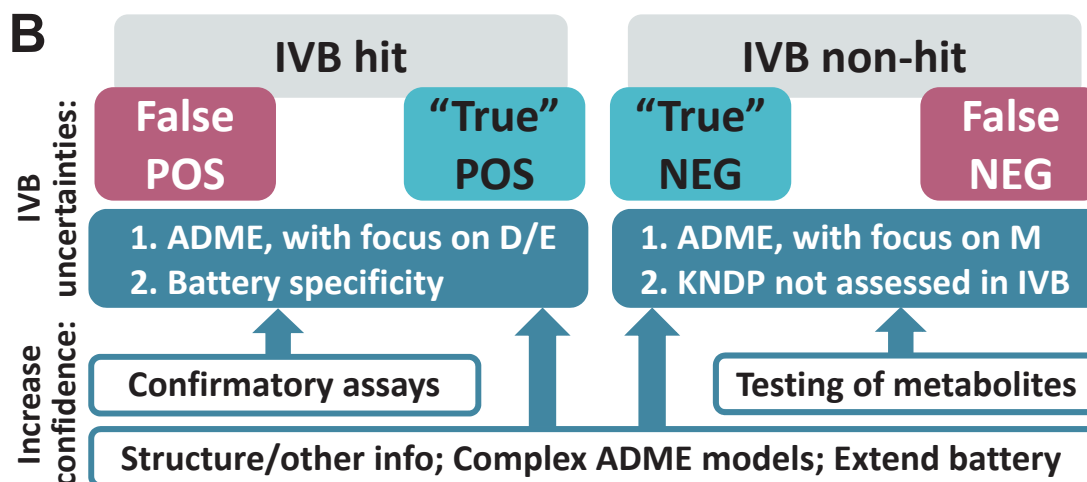
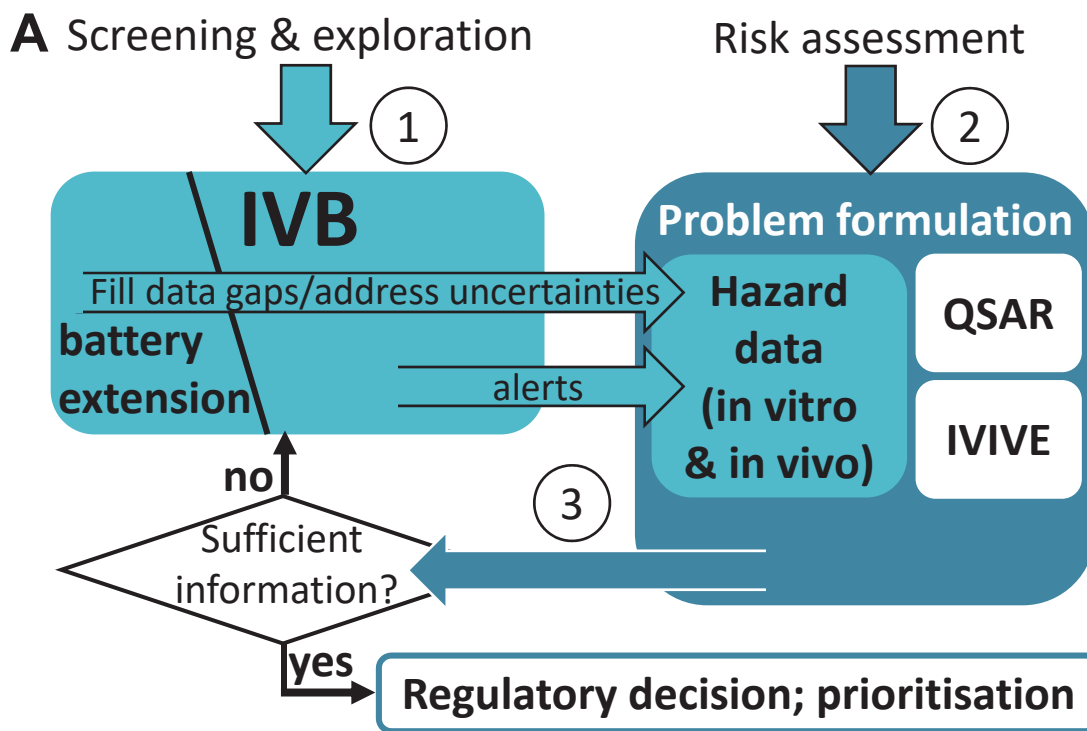


Fig. 7: Outlook on further uses and extensions of the IVB

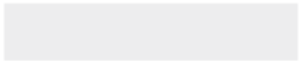
(A) Incorporation of the IVB into an integrated approach to testing and assessment (IATA): Two different scenarios are depicted. In the first (1) the IVB will be used for screening of compound groups to generate hazard alerts (IVB hits). One way to follow up on these would be in the context of an IATA. In the second scenario (2), risk assessment of single chemicals would be performed in an IATA. This approach starts with a problem formulation (considering or not considering particular exposure situations). In this context all available data on hazard identification and characterization are collected. These may be extended via data of scenario (1). Quantitative structure activity relationships (QSAR) and in vitro-to-in vivo extrapolation (IVIVE) are shown as exemplary elements of the IATA framework. Further elements could include absorption, distribution, metabolism and excretion data (ADME) or an exposure assessment. If the hazard data of the assessed compound are considered not sufficient to derive a robust point of departure (PoD), further information could be obtained from the IVB. (3) In some cases, IVB extensions would be needed to fill data gaps and to reduce uncertainties, until sufficient information is available for regulatory action.

(B) Each test method or battery has some uncertainties. The level of uncertainties that can be accepted depends on the problem formulation. For IVB hits and non-hits, one needs to consider that these may be either false positives/negatives, or compounds with a correctly identified hazard (“true” positives/negatives). One potential reason for misidentification is a lack of ADME features represented in the in vitro test systems. For example in vivo distribution and elimination (D/E) features may be misrepresented in the in vitro system. As a result, a compound never reaching the fetal brain because of the placental barrier may show effects on neurons in vitro. In contrast, some false negatives can be explained by a lack of metabolism (M) i.e. in vivo toxic metabolites which are not present in the IVB. Another reason is that a toxicant affects a key neurodevelopmental process (KNDP) that is not included in the IVB. In order to reduce the level of uncertainties and gain confidence in to the results, further information can be added (low, yellow boxes). This includes information transfer across tested compounds (grouping and readacross (RAX)), complex ADME models, confirmatory assays (battery extension), and direct testing of potential metabolites.





Click here to access/download
Supplementary Material
Supplementary File 2.xlsx



Establishment of a human cell-based *in vitro* battery to assess developmental neurotoxicity hazard of chemicals

Jonathan Blum, Stefan Masjosthusmann, **Kristina Bartmann**, Farina Bendt, Xenia Dolde, Arif Dönmez, Nils Förster, Anna-Katharina Holzer, Ulrike Hübenthal, Hagen Eike Keßel, Sadiye Kilic, Jördis Klose, Melanie Pahl, Lynn-Christin Stürzl, Iris Mangas, Andrea Terron, Kevin Crofton, Martin Scholze, Axel Mosig, Marcel Leist, Ellen Fritsche

Journal:	Chemosphere
Impact factor:	7.086 (2021)
Contribution to the publication:	15 %
	Performance of NPC experiments and evaluation
Type of authorship:	co-authorship
Status of publication:	Submitted to Chemosphere

2.4 Measurement of electrical activity of differentiated human iPSC-derived neurospheres recorded by microelectrode arrays (MEA)

Kristina Bartmann, Julia Hartmann, Julia Kapr, Ellen Fritsche

Springer Protocols

Neurotoxizität wird durch eine Vielzahl von Substanzklassen hervorgerufen und betrifft alle Lebensstadien, vom sich entwickelnden Kind bis zum älteren Menschen. Für Neurotoxizitätsstudien werden häufig Tiermodelle verwendet, die sehr ressourcenintensiv sind und das Problem der Speziesunterschiede mit sich bringen. Daher werden für humane Fragestellungen wie Medikamentenentwicklung und Toxizitätstests alternative humanbasierte Modelle benötigt, um diese Speziesunterschiede zu überwinden. In den letzten Jahren wurden weitreichende Fortschritte auf dem Gebiet der Neurotoxizitätstestung gemacht, primär durch die Reprogrammierung humaner somatischer Stammzellen (hiPSC). Diese hiPSC können in Neurone und Astrozyten differenziert werden, die *in vitro* spontan funktionelle neurale Netzwerke (NN) bilden. Mikroelektroden-Arrays (MEA) sind ein wertvolles Instrument zur Beurteilung der Elektrophysiologie solcher Netzwerke. In diesem Buchkapitel wird die neurale Induktion von hiPSCs zu humanen neuronalen Vorläuferzellen (hiNPC) in Form von freischwimmenden Sphäroiden und deren anschließende Differenzierung zu funktionellen Neuronen auf MEAs erläutert. Die Messung der elektrischen Netzwerkaktivität sowie die Auswertung der erhaltenen Daten wird beschrieben.



Measurement of Electrical Activity of Differentiated Human iPSC-Derived Neurospheres Recorded by Microelectrode Arrays (MEA)

Kristina Bartmann, Julia Hartmann, Julia Kapr, and Ellen Fritsche

Abstract

Neurotoxicity is caused by a large variety of compound classes and affects all life stages from the developing child to the elderly. Studying for neurotoxicity often involves animal models, which are very resource-intensive and bear the problem of species-differences. Thus, alternative human-based models are needed to overcome these issues. Over the last years, far-reaching advancements in the field of neurotoxicity were made possible by the ability to reprogram human somatic cells into induced pluripotent stem cells (hiPSC). These hiPSCs can be differentiated into neurons and astrocytes, which spontaneously form functional neuronal networks (NN) in vitro. Microelectrode arrays (MEA) are a valuable tool to assess the electrophysiology of such networks. This chapter explains the neural induction of hiPSCs to human neural progenitor cells (hiNPC) in the form of free-floating spheres and their subsequent differentiation into functional neurons on MEAs. The measurement of the electrical network activity, as well as the evaluation of the received data is described.

Key words Neurotoxicology, Neurotoxicity, Human induced pluripotent stem cells (hiPSC), Human induced neural progenitor cells (hiNPC), Microelectrode array (MEA), Neuronal network, Electrical activity

1 Introduction

Adverse effects on the peripheral or central nervous system caused by chemical, biological, or physical agents are referred to as neurotoxicity [1]. Substances such as metals (e.g., lead), industrial chemicals (e.g., acrylamide), pharmaceutical drugs (e.g., doxorubicin), pesticides (e.g., deltamethrin), and natural toxins (e.g., domoic acid) have been shown to cause neurotoxicity [1, 2]. They are often included in industrial, agricultural, and consumer products, which must then be registered and approved by the European Chemical Agency (ECHA) and the European Food Safety

Kristina Bartmann and Julia Hartmann are contributed equally to this chapter.

Authority (EFSA), prior to entering the European market. Depending on the production volume, different toxicity tests have to be conducted. Current neurotoxicity guideline studies [3, 4] that precede the approval of such products are performed *in vivo* and are thus highly resource-intensive with regard to time, money, and animals [5]. Additionally, animal and human interspecies variations greatly challenge the translation of the generated data, especially for the nervous system [6–8]. Therefore, we are in urgent need of animal-free alternatives that better mimic human nervous system physiology [9]. The ability to reprogram human somatic cells into induced pluripotent stem cells (hiPSC) [10] has extensively advanced the field of neurotoxicity evaluation [11–14].

The use of human cellular models gave rise to a very important component of hazard identification—the neurophysiological assessment. Cultured *in vitro*, hiPSCs are able to grow, migrate, and differentiate into functional neuronal networks (NN) [15–19]. Important tools to study the electrophysiology of such NN are microelectrode arrays (MEA). These integrated arrays of electrodes, photoetched into a glass slide or “chip”, allow the simultaneous extracellular recording of electrical activity from a large number of individual sites in one tissue [20]. So far, neurotoxicological testing with MEAs has mainly been performed with rodent NN [21–30]. However, the use of human *in vitro* cultures is preferred, because responses to test compounds might be affected by species differences in toxicodynamics [31–35]. For this reason, human cells are increasingly used to measure neurotoxicity on MEAs [36–40]. In this chapter, we describe the neural induction of hiPSCs to free-floating neural progenitor cells (hiNPC), their differentiation on poly-d-lysine (PDL)/laminin-coated MEAs and the subsequent formation and measurement of functional NN (Fig. 1) [15, 16].

2 Materials

All cell culture procedures need to be performed in a Class II Biological Safety Cabinet under sterile conditions. The cells are cultivated in an incubator at 37 °C and 5% CO₂.

2.1 Generation of Human Induced Neural Progenitor Cells (hiNPC)

2.1.1 Preparation of Neural Induction Medium (NIM)

Mix **DMEM** (high glucose, GlutaMAX™ Supplement, pyruvate, Thermofisher Scientific #31966-021) and **Ham’s F12 Nutrient Mix** (GlutaMAX™ Supplement, Thermofisher Scientific #31765-027) 3:1 and add **1% Penicillin-Streptomycin** (10.000 U/mL, Thermofisher Scientific #15140-122), **2% B27™ supplement** (serum-free (50×), Thermofisher Scientific #17504-044), **0.2% Human recombinant epidermal growth factor** (EGF, Thermofisher Scientific #PHG0313), **1% N2 Supplement** (100×, Thermofisher Scientific #17502-048), **20% KnockOut™ Serum**

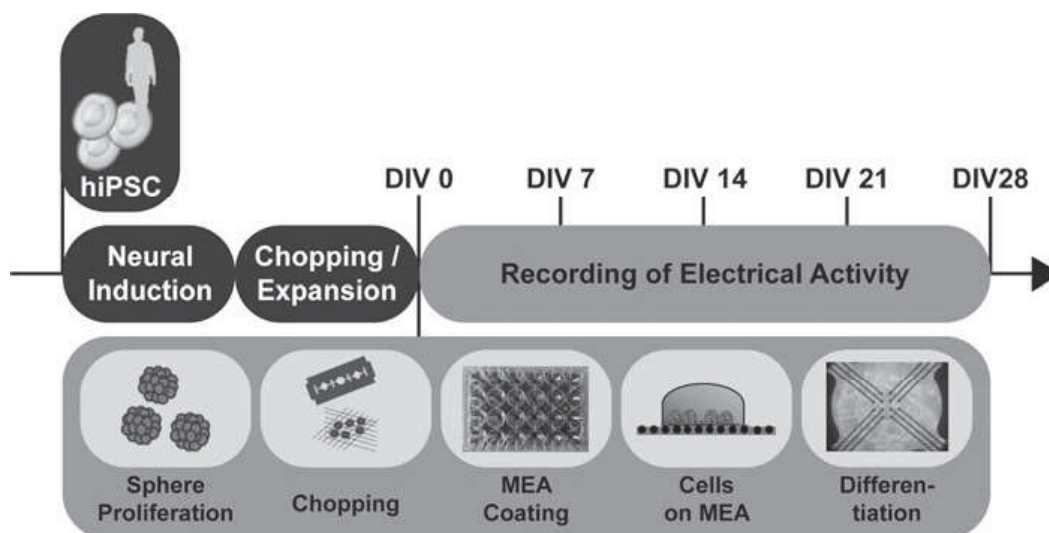


Fig. 1 Experimental setup (adapted from Nimitz et al. [15]). Human iPSCs were neurally induced to hiNPC and cultivated as free-floating 3D neurospheres. Neurospheres proliferate in neural proliferation medium (NPM) supplemented with basic fibroblast growth factor (FGF2) and epidermal growth factor (EGF). By mechanical passaging with a razorblade (chopping), neurospheres are cut into small pieces (100 μ m) and directly plated onto a PDL-Laminin-coated mwMEA plate. In CINDA the NN differentiate and can be cultured for multiple weeks. The electrical activity can be measured from day 7. *DIV*: days in vitro

Replacement (KSR, Thermofisher Scientific #10828-028), **10 μ M SB-431542 hydrate** (Sigma #S4317, dissolved at 10 mM in DMSO), and **0.5 μ M LDN-193189 hydrochloride** (Sigma #SML0559, dissolved at 500 μ M in ultrapure water).

The medium can be stored at 2–8 °C for at least 3 weeks. Warm it to 37 °C prior to use.

2.1.2 Preparation of Neural Proliferation Medium (NPM)

Mix **DMEM** (high glucose, GlutaMAX™ Supplement, pyruvate, Thermofisher Scientific #31966-021) and **Ham's F12 Nutrient Mix** (GlutaMAX™ Supplement, Thermofisher Scientific #31765-027) 3:1 and add **1% Penicillin-Streptomycin** (10,000 U/mL, Thermofisher Scientific #15140-122), **2% B27™ supplement** (serum-free (50 \times), Thermofisher Scientific #17504-044), and **0.2% human recombinant epidermal growth factor** (EGF, Thermofisher Scientific #PHG0313). Previously, EGF is dissolved at 10 μ g/mL in sterile PBS, containing 0.1% bovine serum albumin (BSA, Serva #11920) and 1 mM DL-Dithiothreitol solution (DTT, Sigma #646563-10 \times). EGF is stored at –20 °C.

The NPM, containing supplements, antibiotics, and growth factors, can be stored up to 2 weeks at 2–8 °C. Prior to use, warm it to 37 °C and add **basic human recombinant fibroblast growth factor** (FGF2, R&D Systems #233-FB) to a final concentration of **20 ng/mL**. FGF2 is dissolved at 10 μ g/mL in sterile PBS, containing 0.1% bovine serum albumin (BSA, Serva #11920) and 1 mM DL-Dithiothreitol solution (DTT, Sigma #646563-10 \times). The reconstituted FGF2 can be stored for a maximum of 3 months at –20 °C.

2.1.3 Preparation of Poly-HEMA Solution

Dissolve 1.2 g of Poly(2-hydroxyethyl methacrylate) (Poly-HEMA, Sigma-Aldrich #P3932) in 40 mL ethanol (94.8%) using a magnetic stirrer for 5–16 h (*see Note 1*).

2.1.4 Neural Induction

- iPSC (IMR90) clone (#4), WiCell (*see Note 2*).
- mTeSR1, Stemcell Technologies #05850.
- Corning® Matrigel® Growth Factor Reduced (GFR) Basement Membrane Matrix, Phenol Red-free, LDEV-free, Corning #356231.
- Y-27632 (Rock Inhibitor), Tocris #1254, diluted to 10 mM in ultrapure water.
- StemPro™ EZPassage™ Disposable Stem Cell Passaging Tool, ThermoFisher Scientific #23181010.
- Corning® cell lifter, Merck #CLS3008.
- McIlwain tissue chopper, Mickle Laboratory Engineering Co. Ltd.
- NIM (*see Subheading 2.1.1*).
- NPM (*see Subheading 2.1.2*).
- Dulbecco's phosphate-buffered saline with CaCl₂ and MgCl₂ (DPBS, 1×, Gibco).
- Culture dish (Ø10 cm and Ø6 cm).

2.2 Multiwell Microelectrode Arrays (mwMEAs)

2.2.1 Preparation of Differentiation Medium—CINDA

Mix **DMEM** (high glucose, GlutaMAX™ Supplement, pyruvate, ThermoFisher Scientific #31966-021) and **Ham's F12 Nutrient Mix** (GlutaMAX™ Supplement, ThermoFisher Scientific #31765-027) 3:1 and add **1% Penicillin-Streptomycin** (10,000 U/mL, ThermoFisher Scientific #15140-122), **2% B27™ supplement** (serum-free (50×), ThermoFisher Scientific #17504-044), **1% N2 Supplement** (100×, ThermoFisher Scientific #17502-048), **5 mM creatine monohydrate** (Sigma #C3630), **100 U/mL human recombinant interferon-γ** (IFN-γ, Peprtech #300-02), **20 ng/mL human recombinant neurotrophin-3** (Peprtech #450-03) and **20 μM L-Ascorbic acid** (Sigma #A5960).

Store the medium at 2–8 °C for up to 2 weeks. Warm the differentiation medium to 37 °C and add **300 μM N⁶,2'-O-Dibutyryl adenosine 3',5'-cyclic monophosphate sodium salt** (Dibutyryl cAMP, Sigma #D0260) prior to use (*see Note 3*).

2.2.2 Differentiation on Poly-D-Lysin/Laminin-Coated 24-Multiwell MEAs

- 24-Well plate with PEDOT electrodes on glass (mw-MEA), Multichannelsystems #24W300/30G-288.
- Poly-D-lysine hydrobromide (PDL), Sigma #P0899.
- Laminin from Engelbreth-Holm-Swarm sarcoma basement membrane (Laminin, working solution: $c = 1$ mg/mL), Sigma #L2020 (*see Note 4*).

- Autoclaved ultrapure water.
- McIlwain tissue chopper, Mickle Laboratory Engineering Co. LTD.
- Dulbecco's phosphate-buffered saline with CaCl_2 and MgCl_2 (DPBS, 1 \times , Gibco).
- Counting Chamber Nageotte, Marienfeld #KHY3.1.

2.2.3 Devices and Software for mwMEA Recordings and Analysis

- Multiwell-MEA headstage, Multi Channel Systems MCS GmbH.
- Multiwell-Screen, Version 1.11.6.0, Multi Channel Systems MCS GmbH.
- Multiwell-Analyzer, Version 1.8.6.0, Multi Channel Systems MCS GmbH.

2.3 Lactate- Dehydrogenase Assay

- CytoTox-ONE Homogenous Membrane Integrity Assay Kit (#G7891, Promega; $-20\text{ }^\circ\text{C}$).
 - Substrate mix.
 - Assay buffer.
- Triton X-100 (10% in H_2O), Sigma-Aldrich #T8787.
- CINDA (*see* Subheading 2.2.1).
- 96-Well plate compatible with fluorometer.
- Fluorescence plate reader with excitation 530–570 nm and emission 580–620 nm filter pair.

3 Methods

All experiments need to be performed under sterile conditions.

3.1 Neural Induction of hiPSCs into Human Induced Neural Progenitor Cells (hiNPC)

During embryogenesis the human central nervous system develops from the ectoderm, one of the three germ layers that compose the entire body. These complex procedures can now be taken into a dish due to the unique technique of stem cell differentiation. In vitro, pluripotent stem cells, such as hiPSCs, can be directed to the ectodermal lineage by using neural induction media (NIM). The NIM used in this protocol is based on dual SMAD inhibition, and contains the small molecules LDN-193189 and SB431542 [15]. These factors inhibit TGF- β and SMAD signaling pathways and thereby prevent differentiation into non-neural ectodermal directions [41]. The neural induction is performed in Poly-HEMA-coated culture dishes to prevent cell adhesion to the dishes' surface and to ensure neurosphere formation. From day 7, 10 ng/mL FGF2 are added to the NIM. On day 21, the NPCs are

transferred to the NPM for further maintenance. With time, the neurospheres grow and need to be reduced in size by cutting into smaller pieces in order to avoid a necrotic sphere core (chopping; [42]). By using this method, neurospheres can be expanded and cultivated over several months. The number of possible passages depends on the cell line.

1. Add 1.5 mL Poly-HEMA solution to a 6 cm, or 3 mL to a 10 cm, culture dish and distribute the solution evenly across the surface. Let the solution evaporate overnight under sterile conditions or at least for 2 h (*see Note 5*).
2. The iPSC colonies are cultivated on Matrigel in a 6-well plate, with mTeSR1 medium. Assess the cell morphology under a microscope. If there are differentiated cells, mark the culture dish at the respective point and scratch off the cells with a pipette (*see Note 6*).
3. Add 10 μ M Y-27632 into the culture medium and swivel the plate in order to distribute it evenly.
4. Incubate the cells for 1 h at 37 °C and 5% CO₂.
5. After the incubation, discard the medium and wash each well with 1 mL pre-warmed DPBS.
6. Add 1 mL NIM with 10 μ M Y-27632 to the culture and cut the iPSC colonies into pieces by rolling them with StemPro™ EZPassage™ Disposable Stem Cell Passaging Tool once from top to bottom and once from left to right (*see Note 7*).
7. Scrape the resulting cell-clusters off the plate using a cell lifter. Use a microscope to make sure that uncut colonies are not lifted from the edge of the well.
8. Transfer the scratched colonies of each two wells to one 6 cm Poly-HEMA-coated culture dish and add 5 mL NIM including 10 μ M Y-27632 to each dish to reach a final volume of 7 mL.
9. After 2 days, move the culture dish in small circles to collect the formed neurospheres in the middle of the dish and replace 3.5 mL culture medium with the same volume NIM, without Y-27632.
10. Place the dishes into the incubator and carefully move the dish six times horizontally left and right as well as back and forth to distribute the spheres evenly and to avoid clumping.
11. Replace half of the medium every other day by following instructions 9 and 10.
12. Starting from day 7, add 10 ng/mL FGF2 to the NIM.
13. On day 21, collect all neurospheres by gathering them in the middle of the dish and transfer them into a 10 cm Poly-HEMA-coated culture dish. Further cultivate them in 20 mL NPM with 20 ng/mL FGF2.

14. Replace half of the media with fresh NPM every other day, by following instructions 9 and 10.
15. Neurospheres with a diameter of 0.7 mm or above are mechanically passaged with a razor blade (chopped). This is necessary approximately every 7 days.
16. For chopping, use the McIlwan tissue chopper and attach a sterilized razor blade onto the chopping arm. Make sure the razor blade is positioned correctly and screwed on tightly (*see Note 8*).
17. Adjust the chop distance to 0.25 mm.
18. Transfer neurospheres from the culture dish to the lid of a sterile 6 cm culture dish, with less medium as possible. Remove the supernatant medium, to prevent moving of neurospheres during the process.
19. Place the lid in the holder of the tissue chopper, move it to the start position, and start the device, by pressing “reset”.
20. Stop the tissue chopper when the razor blade reached the end of the dish lid, rotate the lid 90°, and repeat **step 19**.
21. Resuspend the chopped neurospheres in 1 mL NPM by carefully pipetting up and down. Equally distribute the cell suspension into two to three new Poly-HEMA-coated culture dishes (Ø 10 cm), each with 20 mL NPM.
22. Cultivate the cells in an incubator at 37 °C and 5% CO₂.

3.2 Recording Electrical Activity of Neural Networks with mwMEAs

By plating the neurospheres as a monolayer onto an extracellular matrix, here PDL and laminin, and cultivating them in neural differentiation medium, they differentiate into an electrically active NN. Laminin is one of the major integrin interaction factors and, besides facilitating cell adherence, it supports growth, survival, and functional development in iPSC-based neural cultures in vitro [43]. The differentiation medium CINDA contains additional maturation supporting factors (Creatine, Interferon- γ , Neurotrophin-3, Dibutyl cAMP and Ascorbic acid) that support neuronal maturation, synapse formation, and spontaneous NN activity [15]. This NN activity can be measured on MEAs, which simultaneously derive the membrane potential of numerous neurons via an electrode recording field. The here used 24-multiwell MEAs have an electrode field of 12 PEDOT-coated gold-electrodes plus four reference electrodes per well. Each electrode has a diameter of 30 μ m and an interelectrode distance of 300 μ m. The measured neuronal activity is detected and displayed as spikes and bursts, whereas each spike is derived from one action potential and several consecutive spikes are defined as one burst. Another measurable parameter is network bursts, which occur when the network matures over time and develops a synchronous bursting pattern.

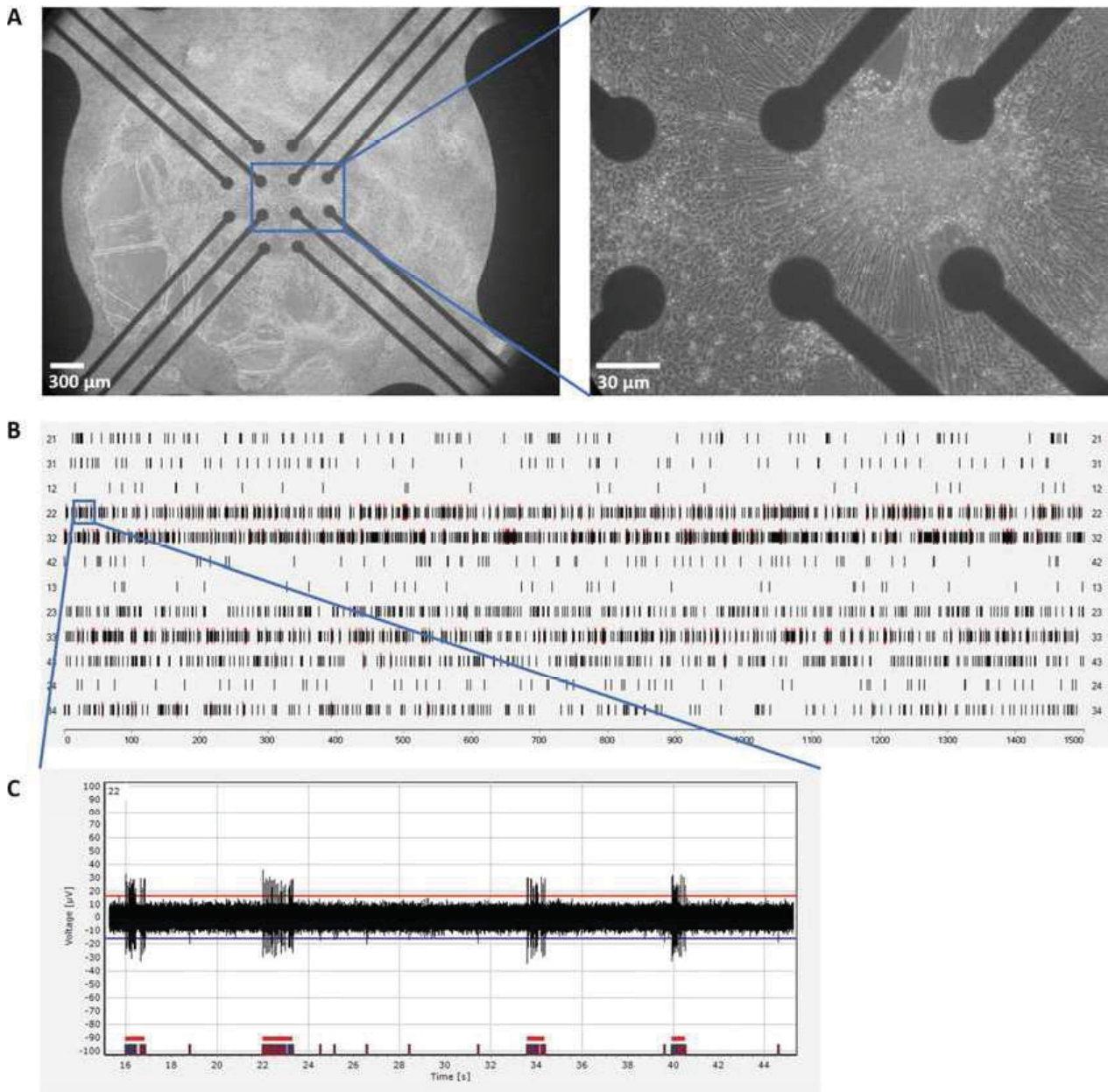


Fig. 2 Measurement of electrical NN activity on mwMEA. (a) Representative phase-contrast images of a human NN, differentiated on mwMEA electrodes for 12 days. (b) SRP of one well of a 24-mwMEA, after 10 days of differentiation. Each vertical black line represents a spike and each horizontal red bar represents a burst. (c) Spike train of the blue marked position in the SRP

During the measurement, the signals are shown as spike raster plots (SRP) and spike trains (Figs. 2 and 3). By setting certain values and thresholds, which have to be adapted for each network, the sensitivity of the measurement can be adjusted and the background noise can be filtered. The measurement data give information about spike count, spike rate [Hz], burst count, mean burst duration [μs], mean burst spike count, percentage of spikes in a burst, mean interburst interval [μs], and number of active electrodes, as well as the same information about network bursts. The combined data set allows a good characterization of the network activity and

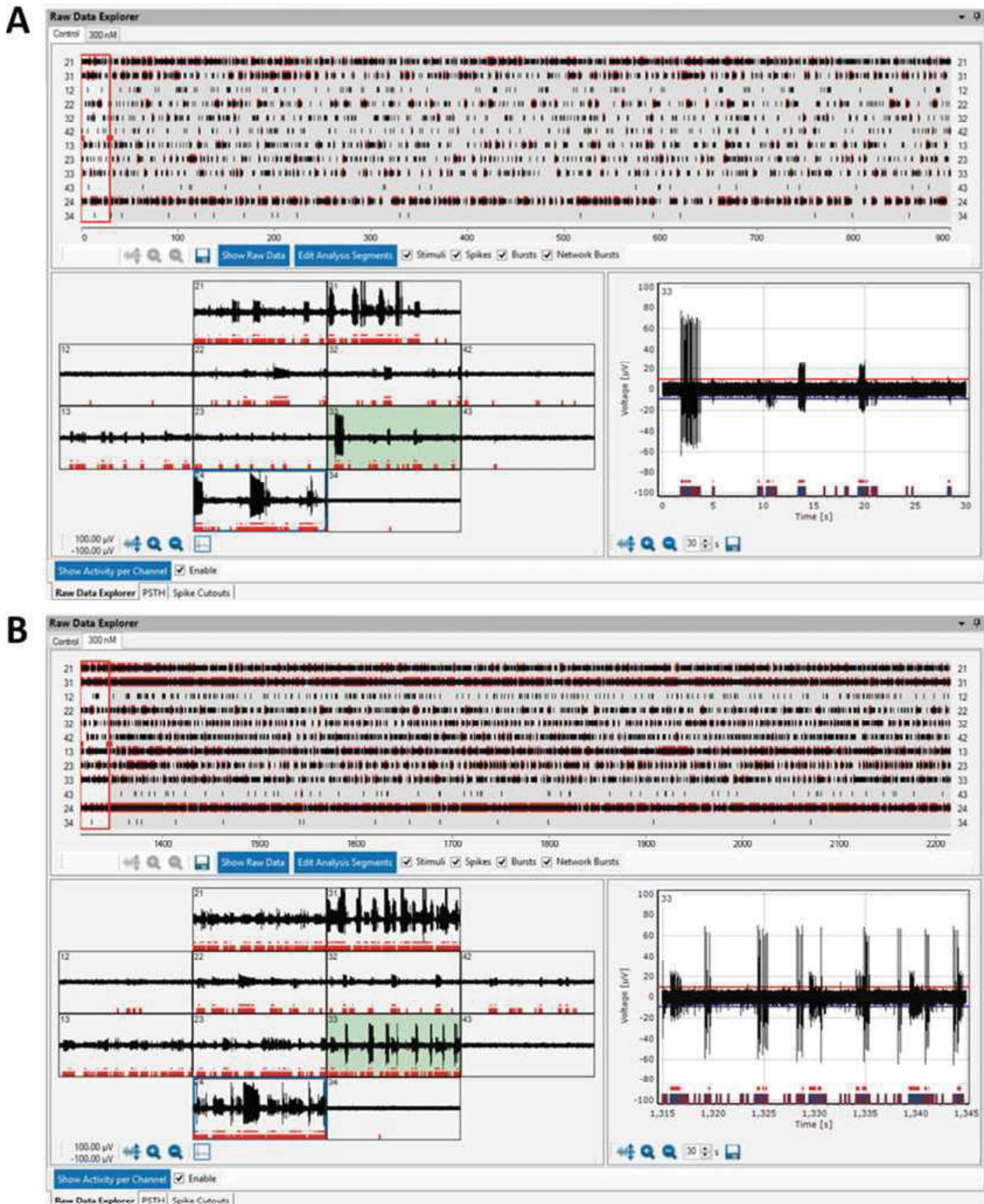


Fig. 3 Neuronal network activity before and during treatment with domoic acid. Domoic acid binds to glutamate receptors with a higher affinity than glutamate itself. This results in an overreaction that can lead to excitotoxicity and finally to cell death. The images show representative software screen shots after 10 DIV of the **a**) baseline activity and **b**) the activity during the treatment with 300 nM domoic acid (after wash-in-phase of 5 min). Each vertical black line represents a spike and each horizontal red line represents a burst. Software: Multiwell-Analyzer, Version 1.8.6.0, Multi Channel Systems MCS GmbH

its response to neurotoxic substance exposure. In order to define a valid experiment, the two parameters minimum spike rate/electrode and number of active electrodes/well need to be monitored. The limit values for these parameters can vary depending on the cell line used.

3.2.1 Differentiation on PDL/Laminin-Coated 24-Multiwell MEAs

1. Dilute PDL in sterile ultrapure water to reach a final concentration of 100µg/mL and store working stocks at -20°C until use. Prior to coating, thaw the PDL solution at 37°C .
2. Add 100µL PDL solution (100µg/mL) to each well of a 24-mwMEA plate and incubate at least for 1 h at 37°C or for 48 h at 4°C .
3. Thaw laminin in the fridge ($4-8^{\circ}\text{C}$) to avoid gel formation and dilute the laminin with sterile ultrapure water 1:80 to obtain a final concentration of 12.5 ng/mL.
4. Aspirate the PDL solution and wash wells once with sterile ultrapure water.
5. Add 100µL laminin (12.5µg/mL) solution to each well and incubate at least for 1 h at 37°C (*see Note 9*).
6. Aspirate the laminin solution, wash the wells once with sterile ultrapure water, and directly use the coated plate.
7. Chop the neurospheres to a size of 0.1 mm (for details *see* Subheading 3.1, step 16–21).
8. Resuspend the cut spheres in 1 mL prewarmed CINDA.
9. Transfer 80µL of the cut spheres suspension into a Nageotte counting chamber and count the sphere parts. Dilute the cut spheres solution if necessary to reach a maximum of 4000 sphere parts/mL.
10. Collect 200 sphere parts in up to 100µL CINDA and carefully pipet them directly onto the electrodes of a mwMEA well. The solution should form a droplet on top of the electrodes. Allow the spheres to settle and adhere to the well surface, by incubating the droplet for 2 h at 37°C and 5% CO_2 .
11. Add 1 mL CINDA to each well and incubate the plate at 37°C and 5% CO_2 .
12. Feed the cells once a week, by replacing half of the medium in each well.
13. From day 7, measure the electrical activity twice a week as long as the neurons are electrically active (*see Note 10*). Preheat the mwMEA headstage to 37°C and gas the device with carbogen, before adding the mwMEA. For parameter settings *see* Table 1.
14. Let the mwMEA acclimatize for 15 min, before starting the 15 min baseline recording.

Table 1
Parameter settings for mwMEA measurement

Parameter	Setting
Sampling rate	20,000 Hz
Low-pass filter type	Butterworth
Low-pass-filter order	4
Low-pass filter cutoff frequency	3,500 Hz
High-pass filter type	Butterworth
High-pass-filter order	2
High-pass filter cutoff frequency	300 Hz

15. For acute toxicity measurements, stick to the following time schedule:
 - Baseline measurement: 15 min recording.
 - Wash-in-phase: add the substance and equilibrate for 5 min.
 - Treatment: 15 min recording.
 - Cytotoxicity analysis: remove the medium and transfer it into a new 24-well plate for cytotoxicity analysis (*see* Sub-heading 3.3 for further details).
 - Wash-out-phase: wash each well twice with CINDA to wash out the substance.
16. Further cultivate the cells in fresh CINDA medium at 37 °C and 5% CO₂.

3.2.2 Analysis of mwMEA Recordings

1. Load the .mwr file, which is automatically generated during recording, into the Multiwell-Analyzer Software.
2. Set the “Spike Detector Configuration” to an automatic threshold estimation of 500 ms baseline duration and rising/falling edge of 5× standard deviation (*see* **Note 11**).
3. For the “Burst Detector Configuration” choose the following settings (*see* **Note 12**):
 - Max. Interval to start burst: 100 ms.
 - Max. Interval to end burst: 100 ms.
 - Min. Interval between bursts: 20 ms.
 - Min. Duration of burst: 10 ms.
 - Min. Spike count in burst: 3.
4. To select active wells only, set the “Channel Selection Configuration” to a minimum of 5 spikes/minute (=0.083 Hz) for

each channel and a minimum of 3 active channels for each well [21].

5. Run the analysis.
6. Check each channel for artifacts and defective electrodes (*see Note 13*).
7. Export the analysis of all intact electrodes without artifacts as a .csv file.
8. Open the .csv file and copy the data into a software for statistical analysis and data plotting.

3.3 Assessment of Cytotoxicity via the Lactate-Dehydrogenase Assay

To ensure that the adverse effects are due to neurotoxicity and not cytotoxicity, we perform the Lactate-Dehydrogenase (LDH) Assay. The substrate mix contains lactate, NAD⁺, and resazurin. If the cell membrane is damaged, the cytosolic lactate dehydrogenase enzyme is released into the cell culture medium and can be quantified by subsequent enzymatic reactions. LDH first catalyzes the conversion of lactate to pyruvate, with a simultaneous reduction of NAD⁺ to NADH. By oxidation of NADH to NAD⁺, the enzyme diaphorase reduces resazurin to resorufin, which can be measured with a fluorometer (excitation: 540 nm; emission: 590 nm). The amount of produced resorufin is thus proportional to the amount of released LDH. Cells with an intact membrane do not release LDH and therefore no fluorescence is measurable in the culture medium. Two controls are required to perform this assay: a 100% cell lysis control (LC) and a background control (BG; culture medium without cells). By lysing the cells of the LC with Triton X-100, the maximum amount of LDH present is determined.

1. Prepare the CytoTox-ONE Reagent as indicated in the supplier's manual and protect it from light (*see Note 14*).
2. For the LC, add 10% (v/v) Triton X-100 solution 1:5 to the desired number of wells (final concentration 2%).
3. Preincubate the LC for 30 min at 37 °C and 5% CO₂.
4. Transfer the complete medium of each well into a new 24-well plate.
5. Transfer 50µL medium of each well of interest of the 24-well plate into a 96-well plate, including the LC and the BG.
6. Add 50µL CytoTox-ONE Reagent to each of the wells.
7. Incubate at room temperature for 2 h, protected from light.
8. Measure the fluorescence of the samples at an excitation wavelength of 540 nm and an emission wavelength of 590 nm in a plate reader (*see Note 15*).
9. Calculate the mean of all technical replicate measurements and normalize data by subtracting the mean of the BG from the mean of the different conditions.

10. Calculate the values of each condition as percent of the mean of the LC.
11. The results of at least three independent experiments are pooled, and mean, standard deviation (SD), and standard error of the mean (SEM) are calculated. Data analyses, statistical analyses, and data plotting are performed in GraphPad Prism, using OneWay ANOVA and Bonferroni's post hoc test.

4 Notes

1. The Poly-HEMA solution is stable for up to 2 months at 4 °C.
2. When using a different hiPSC line, the protocol may have to be adapted.
3. Dibutyl cAMP is sensitive to light and moisture. The CINDA medium should therefore not be exposed to light for more than 1 h.
4. The product concentration depends on the batch number and has to be adjusted to 1 mg/mL with autoclaved ultrapure water.
5. Poly-HEMA-coated dishes can be used for up to 3 months if stored sealed at room temperature and in the dark.
6. iPSCs are small and round in shape and have a high nucleus-to-cytoplasm ratio, with prominent nucleoli. Differentiating cells have a lower nucleus-to-cytoplasm ratio and the morphology differs visibly from the original round shape.
7. We banked our hiPSCs so that we can start each neural induction with a similar passage number. We use the cells starting from passage 3 post-thawing at the earliest and up to passage 10 post-thawing at the latest. This must be adapted for other cell lines.
8. Each side of a razor blade can be used three times.
9. PDL/Laminin-coated plates can be stored in the refrigerator (4–8 °C) for a maximum of 2 weeks prior to use.
10. During cell differentiation, the burst behavior changes and begins to synchronize as the network matures. For this reason, exposure to the same substance in different experiments should always be carried out in the same time frame.
11. This eliminates the detected background signals.
12. These settings need to be adapted to the specific cell signals and vary depending on the cell line.
13. An artifact can be caused by external influences and is visible as an exactly simultaneous signals on all electrodes. Furthermore,

artifacts and defective electrodes can be excluded by observing the spike signal that should resemble a waveform.

14. Aliquot unused CytoTox-ONE reagent and protect the reagent from light. Aliquots should be labeled with preparation date and reagent number and can be stored tightly capped at $-20\text{ }^{\circ}\text{C}$ for 6–8 weeks.
15. If the plate reader measures from above, remove the lid of the plate before measurement.

References

1. Costa LG, Giordano G, Guizzetti M, Vitalone A (2008) Neurotoxicity of pesticides: a brief review. *Front Biosci* 13:1240–1249. <https://doi.org/10.2741/2758>
2. Massaro EJ (2002) *Handbook of neurotoxicology*. Humana Press, Totowa, NJ
3. OECD guideline for the testing of Chemicals (1997) Test no. 424: neurotoxicity study in rodents. In: *OECD guideline for the testing of chemicals*. OECD, Paris, pp 1–15
4. Forum RA (1998) *Guidelines for neurotoxicity risk assessment*
5. Bal-Price AK, Suñol C, Weiss DG et al (2008) Application of in vitro neurotoxicity testing for regulatory purposes: symposium III summary and research needs. *Neurotoxicology* 29:520–531. <https://doi.org/10.1016/j.neuro.2008.02.008>
6. Leist M, Hartung T (2013) Inflammatory findings on species extrapolations: humans are definitely no 70-kg mice. *Arch Toxicol* 87:563–567
7. Borrell V, Götz M (2014) Role of radial glial cells in cerebral cortex folding. *Curr Opin Neurobiol* 27:39–46
8. Toutain P-L, Ferran A, Bousquet-Melou A (2010) Species differences in pharmacokinetics and pharmacodynamics. In: *Comparative and Veterinary Pharmacology, Handbook of Experimental Pharmacology*, Springer, pp 19–48. https://doi.org/10.1007/978-3-642-10324-7_2
9. Masjosthusmann S, Barenys M, El-Gamal M et al (2018) Literature review and appraisal on alternative neurotoxicity testing methods. *EFSA Support Publ* 15:1–108. <https://doi.org/10.2903/sp.efsa.2018.en-1410>
10. Takahashi K, Tanabe K, Ohnuki M et al (2007) Induction of pluripotent stem cells from adult human fibroblasts by defined factors. *Cell* 131:861–872. <https://doi.org/10.1016/j.cell.2007.11.019>
11. Pei Y, Peng J, Behl M et al (2016) Comparative neurotoxicity screening in human iPSC-derived neural stem cells, neurons and astrocytes. *Brain Res* 1638:57–73. <https://doi.org/10.1016/j.brainres.2015.07.048>
12. Barenys M, Fritsche E (2018) A historical perspective on the use of stem/progenitor cell-based in vitro methods for neurodevelopmental toxicity testing. *Toxicol Sci* 165:10–13. <https://doi.org/10.1093/toxsci/kfy170>
13. de Groot MWGDM, Westerink RHS, Dingemans MML (2013) Don't judge a neuron only by its cover: neuronal function in in vitro developmental neurotoxicity testing. *Toxicol Sci* 132:1–7. <https://doi.org/10.1093/toxsci/kfs269>
14. Tukker AM, De Groot MWGDM, Wijnolts FMJ et al (2016) Research article is the time right for in vitro neurotoxicity testing using human iPSC-derived neurons? *ALTEX* 33:261–271. <https://doi.org/10.14573/altex.1510091>
15. Nimtz L, Hartmann J, Tigges J et al (2020) Characterization and application of electrically active neuronal networks established from human induced pluripotent stem cell-derived neural progenitor cells for neurotoxicity evaluation. *Stem Cell Res* 45:101761. <https://doi.org/10.1016/j.scr.2020.101761>
16. Hofrichter M, Nimtz L, Tigges J et al (2017) Comparative performance analysis of human iPSC-derived and primary neural progenitor cells (NPC) grown as neurospheres in vitro. *Stem Cell Res* 25:72–82. <https://doi.org/10.1016/j.scr.2017.10.013>
17. Izsak J, Seth H, Andersson M et al (2019) Robust generation of person-specific, synchronously active neuronal networks using purely isogenic human iPSC-3D neural aggregate cultures. *Front Neurosci* 13. <https://doi.org/10.3389/fnins.2019.00351>

18. Hyvärinen T, Hyysalo A, Kapucu FE et al (2019) Functional characterization of human pluripotent stem cell-derived cortical networks differentiated on laminin-521 substrate: comparison to rat cortical cultures. *Sci Rep* 9:17125. <https://doi.org/10.1038/s41598-019-53647-8>
19. Pamies D, Barreras P, Block K et al (2017) A human brain microphysiological system derived from induced pluripotent stem cells to study neurological diseases and toxicity. *ALTEX* 34:362–376. <https://doi.org/10.14573/altext.1609122>
20. Johnstone AFM, Gross GW, Weiss DG et al (2010) Microelectrode arrays: a physiologically based neurotoxicity testing platform for the 21st century. *Neurotoxicology* 31:331–350
21. McConnell ER, McClain MA, Ross J et al (2012) Evaluation of multi-well microelectrode arrays for neurotoxicity screening using a chemical training set. *Neurotoxicology* 33:1048–1057. <https://doi.org/10.1016/j.neuro.2012.05.001>
22. Hogberg HT, Sobanski T, Novellino A et al (2011) Application of micro-electrode arrays (MEAs) as an emerging technology for developmental neurotoxicity: evaluation of domoic acid-induced effects in primary cultures of rat cortical neurons. *Neurotoxicology* 32:158–168. <https://doi.org/10.1016/j.neuro.2010.10.007>
23. Mack CM, Lin BJ, Turner JD et al (2014) Burst and principal components analyses of MEA data for 16 chemicals describe at least three effects classes. *Neurotoxicology* 40:75–85
24. Shafer TJ, Brown JP, Lynch B et al (2019) Evaluation of chemical effects on network formation in cortical neurons grown on microelectrode arrays. *Toxicol Sci* 169:436–455. <https://doi.org/10.1093/toxsci/kfz052>
25. Alloisio S, Nobile M, Novellino A (2015) Multiparametric characterisation of neuronal network activity for in vitro agrochemical neurotoxicity assessment. *Neurotoxicology* 48:152–165. <https://doi.org/10.1016/j.neuro.2015.03.013>
26. Shafer TJ, Rijal SO, Gross GW (2008) Complete inhibition of spontaneous activity in neuronal networks in vitro by deltamethrin and permethrin. *Neurotoxicology* 29:203–212. <https://doi.org/10.1016/j.neuro.2008.01.002>
27. Defranchi E, Novellino A, Whelan M et al (2011) Feasibility assessment of microelectrode chip assay as a method of detecting neurotoxicity in vitro. *Front Neuroeng* 4:1–12. <https://doi.org/10.3389/fneng.2011.00006>
28. Valdivia P, Martin M, LeFew WR et al (2014) Multi-well microelectrode array recordings detect neuroactivity of ToxCast compounds. *Neurotoxicology* 44:204–217. <https://doi.org/10.1016/j.neuro.2014.06.012>
29. Wallace K, Strickland JD, Valdivia P et al (2015) A multiplexed assay for determination of neurotoxicant effects on spontaneous network activity and viability from microelectrode arrays. *Neurotoxicology* 49:79–85. <https://doi.org/10.1016/j.neuro.2015.05.007>
30. Novellino A, Scelfo B, Palosaari T et al (2011) Development of micro-electrode array based tests for neurotoxicity: assessment of Interlaboratory reproducibility with neuroactive chemicals. *Front Neuroeng* 4:1–14. <https://doi.org/10.3389/fneng.2011.00004>
31. Gassmann K, Abel J, Bothe H et al (2010) Species-specific differential ahr expression protects human neural progenitor cells against developmental neurotoxicity of PAHs. *Environ Health Perspect* 118:1571–1577. <https://doi.org/10.1289/ehp.0901545>
32. Dach K, Bendt F, Huebenthal U et al (2017) BDE-99 impairs differentiation of human and mouse NPCs into the oligodendroglial lineage by species-specific modes of action. *Sci Rep* 7:1–11. <https://doi.org/10.1038/srep44861>
33. Masjosthusmann S, Becker D, Petzuch B et al (2018) A transcriptome comparison of time-matched developing human, mouse and rat neural progenitor cells reveals human uniqueness. *Toxicol Appl Pharmacol* 354:40–55. <https://doi.org/10.1016/j.taap.2018.05.009>
34. Oberheim NA, Takano T, Han X et al (2009) Uniquely hominid features of adult human astrocytes. *J Neurosci* 29:3276–3287. <https://doi.org/10.1523/JNEUROSCI.4707-08.2009>
35. Perreault M, Feng G, Will S et al (2013) Activation of TrkB with TAM-163 results in opposite effects on body weight in rodents and non-human primates. *PLoS One* 8:e62616. <https://doi.org/10.1371/journal.pone.0062616>
36. Tukker AM, Wijnolts FMJ, de Groot A, Westerink RHS (2018) Human iPSC-derived neuronal models for in vitro neurotoxicity assessment. *Neurotoxicology* 67:215–225. <https://doi.org/10.1016/j.neuro.2018.06.007>
37. Tukker AM, Wijnolts FMJ, de Groot A, Westerink RHS (2020) Applicability of hiPSC-derived neuronal co-cultures and rodent primary cortical cultures for in vitro seizure liability assessment. *Toxicol Sci*. <https://doi.org/10.1093/toxsci/kfaa136>

38. Tukker AM, Bouwman LMS, van Kleef RGDM et al (2020) Perfluorooctane sulfonate (PFOS) and perfluorooctanoate (PFOA) acutely affect human $\alpha 1\beta 2\gamma 2L$ GABAA receptor and spontaneous neuronal network function in vitro. *Sci Rep* 10. <https://doi.org/10.1038/s41598-020-62152-2>
39. Ylä-Outinen L, Heikkilä J, Skottman H et al (2010) Human cell-based micro electrode array platform for studying neurotoxicity. *Front Neuroeng* 3. <https://doi.org/10.3389/fneng.2010.00111>
40. Odawara A, Matsuda N, Ishibashi Y et al (2018) Toxicological evaluation of convulsant and anticonvulsant drugs in human induced pluripotent stem cell-derived cortical neuronal networks using an MEA system. *Sci Rep* 8:10416. <https://doi.org/10.1038/s41598-018-28835-7>
41. Qi Y, Zhang XJ, Renier N et al (2017) Combined small-molecule inhibition accelerates the derivation of functional cortical neurons from human pluripotent stem cells. *Nat Biotechnol* 35:154–163. <https://doi.org/10.1038/nbt.3777>
42. Svendsen CN, Ter Borg MG, Armstrong RJE et al (1998) A new method for the rapid and long term growth of human neural precursor cells. *J Neurosci Methods* 85:141–152. [https://doi.org/10.1016/S0165-0270\(98\)00126-5](https://doi.org/10.1016/S0165-0270(98)00126-5)
43. Farrukh A, Zhao S, del Campo A (2018) Microenvironments designed to support growth and function of neuronal cells. *Front Mater* 5:1–22. <https://doi.org/10.3389/fmats.2018.00062>

Measurement of electrical activity of differentiated human iPSC-derived neurospheres recorded by microelectrode arrays (MEA)

Kristina Bartmann, Julia Hartmann, Julia Kapr, Ellen Fritsche

Journal:	Springer Protocols
Impact factor:	not calculated for book chapters
Contribution to the publication:	40 % Writing of the manuscript's introduction and part of material & methods
Type of authorship:	first authorship
Status of publication:	Published 30 July 2021

2.5 A human iPSC-based *in vitro* neural network formation assay to investigate neurodevelopmental toxicity of pesticides

Kristina Bartmann, Farina Bendt, Arif Dönmez, Daniel Haag, Eike Keßel, Stefan Masjosthusmann, Christopher Noel, Ji Wu, Peng Zhou, Ellen Fritsche

ALTEX

Eine einwandfreie Gehirnentwicklung basiert auf der Orchestrierung wichtiger neurologischer Schlüsselprozesse (*key neurodevelopmental processes*, KNDP) einschließlich der Bildung und Funktionalität neuraler Netzwerke. Wenn mindestens ein KNDP durch eine Chemikalie beeinträchtigt wird, ist ein nachteiliges Ergebnis zu erwarten. Um einen höheren Testdurchsatz als die in den Richtlinien vorgesehenen Tierversuche zu ermöglichen, wurde eine *in-vitro*-Testbatterie für Entwicklungsneurotoxizität (DNT, DNT-IVB) eingerichtet, die eine Vielzahl von Tests umfasst, welche mehrere KNDPs abbilden. Eine Analyse der in der Batterie vorhandenen Lücken ergab, dass ein human-basierter Test für die Modellierung der Formierung und Funktionalität neuraler Netzwerke (NNF) erforderlich ist und bisher in der DNT-IVB fehlt. Daher haben wir hier den humanen NNF (hNNF)-Assay entwickelt. Eine Co-Kultur basierend auf aus hiPSC-generierten exzitatorischen und inhibitorischen Neuronen sowie primären humanen Astrozyten wurde 35 Tage lang auf Mikroelektrode-Arrays (MEA) differenziert, und die spontane elektrische Aktivität zusammen mit der Zytotoxizität wöchentlich bewertet, nachdem die Substanzen 24 Stunden vor den Messungen ausgewaschen worden waren. Zusätzlich zur Charakterisierung des Testsystems wurden 28 Substanzen, hauptsächlich Pestizide, im hNNF Assay getestet, um deren DNT-Potenzial durch Auswertung spezifischer Spike-, Burst- und Netzwerkparametern zu ermitteln. Dieser Ansatz bestätigte die Eignung des Assays für das Screening von Umweltchemikalien. Ein direkter Vergleich von Benchmark-Konzentrationen zwischen dem hNNF Assay und einem auf primären kortikalen Rattenzellen basierenden NNF-Assay (rNNF) ergab Unterschiede in der Sensitivität. Zusammen mit der erfolgreichen Implementierung von hNNF-Daten in ein postuliertes AOP-Netzwerk (*adverse outcome pathway*) zur Deltamethrin-Exposition empfiehlt diese Studie den hNNF-Assay als nützliche Ergänzung zu der derzeitigen DNT-IVB.

1 **A human iPSC-based *in vitro* neural network formation assay to investigate neurodevelopmental**
2 **toxicity of pesticides**

3 Kristina Bartmann¹, Farina Bendt¹, Arif Dönmez¹, Daniel Haag², Eike Keßel¹, Stefan Masjosthusmann¹,
4 Christopher Noel², Ji Wu², Peng Zhou², Ellen Fritsche^{1,3}

5

6 ¹IUF - Leibniz Research Institute for Environmental Medicine, Duesseldorf, Germany

7 ²NeuCyte Inc., Mountain View, CA, USA

8 ³Medical Faculty, Heinrich-Heine-University, Duesseldorf, Germany

9

10 Corresponding Author:

11 Prof. Dr. Ellen Fritsche

12 IUF-Leibniz Research Institute for Environmental Medicine

13 Auf'm Hennekamp 50

14 40225 Duesseldorf, Germany

15 E-Mail address: ellen.fritsche@iuf-duesseldorf.de

16 Keywords: developmental neurotoxicity, microelectrode arrays, electrical activity, human induced
17 pluripotent stem cells, new approach methodologies

18

19 **Abstract**

20 Proper brain development is based on the orchestration of key neurodevelopmental processes (KNDP),
21 including the formation and function of neural networks. If at least one KNDP is affected by a chemical,
22 an adverse outcome is expected. To allow a higher testing throughput than the guideline animal
23 experiments, a developmental neurotoxicity (DNT) *in vitro* testing battery (DNT-IVB) has been set up
24 that includes a variety of assays, which model several KNDPs. Gap analyses of the DNT-IVB revealed
25 the need of a human-based assay to assess neural network formation and function (NNF). Therefore,
26 here we established the human NNF (hNNF) assay. A co-culture comprised of human-induced
27 pluripotent stem cell (hiPSC)-derived excitatory and inhibitory neurons, as well as primary human
28 astroglia, was differentiated for 35 days on micro-electrode arrays (MEA) and spontaneous electrical
29 activity, together with cytotoxicity, was assessed on a weekly basis after washout of the compounds

30 24 h prior to measurements. In addition to the characterization of the test system, the assay was
31 challenged with 28 compounds, mainly pesticides, identifying their DNT potential by evaluation of
32 specific spike-, burst- and network parameters. This approach confirmed the suitability of the assay for
33 screening environmental chemicals. Comparison of benchmark concentrations (BMC) with an NNF *in*
34 *vitro* assay (rNNF) based on primary rat cortical cells, revealed differences in sensitivity. Together with
35 the successful implementation of hNNF data into a postulated adverse outcome pathway (AOP)
36 network on deltamethrin exposure, this study suggests the hNNF assay as a useful complement to the
37 current DNT-IVB.

38 **1 Introduction**

39 The developing central nervous system (CNS) is known to be more sensitive to exposure to toxic agents
40 than the adult CNS (Rodier, 1995). There is evidence that environmental chemicals contribute to
41 neurodevelopmental disorders in children such as autism spectrum disorder (AD), mental retardation,
42 and cerebral palsy (National Research Council, 2000; Grandjean and Landrigan, 2006; Kuehn, 2010;
43 Sagiv et al., 2010; Bennett et al., 2016). One compound class demonstrably associated with causing
44 developmental neurotoxicity (DNT) is pesticides (Bjørning-Poulsen et al., 2008). Today, only 35 of the
45 485 pesticides currently approved in the EU have been tested in DNT studies (Ockleford et al., 2018).
46 The reason for this lack of testing, which generally expands to all chemicals (Goldman and Koduru,
47 2000; Crofton et al., 2012) lies in the current DNT *in vivo* testing guidelines: the OECD 426 (OECD, 2007)
48 or EPA 870.6300 guideline (U.S. EPA, 1998). Their high resource intensity regarding time, money, and
49 animals substantiate the limited throughput of these studies (Smirnova et al., 2014). Furthermore, high
50 variability and low reproducibility of *in vivo* experiments, as well as species differences, increase the
51 uncertainty of *in vivo* guideline studies for DNT testing (Tsuji and Crofton, 2012; Terron and Bennekou,
52 2018; Sachana et al., 2019; Paparella et al., 2020). In the last years, scientists from academia, industry,
53 and regulatory authorities across the world agreed on the need for a standardized *in vitro* testing
54 strategy, aiming for a cheaper and faster generation of additional data for DNT hazard assessment
55 (EFSA, 2013; Crofton et al., 2014; Bal-Price et al., 2015 a, 2018; Fritsche, Crofton, Hernandez, Hougaard
56 Bennekou, et al., 2017; Fritsche, Barenys, et al., 2018; Fritsche, Grandjean, et al., 2018). Following this
57 consensus, a DNT *in vitro* battery (IVB) was compiled, which includes not one, but various DNT test
58 methods, covering different neurodevelopmental processes, so-called key events (KEs), and
59 developmental stages to approximate the complexity of human brain development (Fritsche, 2017;
60 Fritsche, Crofton, Hernandez, Bennekou, et al., 2017; Bal-Price et al., 2018). Within this DNT-IVB,
61 neurodevelopment is described by *in vitro* assays covering the following KEs: human neural progenitor
62 cell (hNPC) proliferation (Baumann et al., 2014, 2015; Harrill et al., 2018; Nimitz et al., 2019;
63 Masjosthusmann et al., 2020; Koch et al., 2022) and apoptosis (Druwe et al., 2015; Harrill et al., 2018),

64 cell migration (Baumann et al., 2015, 2016; Nyffeler et al., 2017; Schmuck et al., 2017; Masjosthusmann
65 et al., 2020; Koch et al., 2022), hNPC-neuronal (Baumann et al., 2015; Schmuck et al., 2017;
66 Masjosthusmann et al., 2020; Koch et al., 2022) and oligodendrocyte differentiation (Fritsche et al.,
67 2015; Dach et al., 2017; Schmuck et al., 2017; Masjosthusmann et al., 2020; Klose et al., 2021; Koch et
68 al., 2022), neurite outgrowth (human: Harrill et al., 2010, 2018; Krug et al., 2013; Hoelting et al., 2016;
69 Masjosthusmann et al., 2020; Koch et al., 2022; rat: Harrill et al., 2013, 2018), as well as neuronal
70 maturation and synaptogenesis (rat: Harrill et al., 2011, 2018).

71 Another crucial key neurodevelopmental process, also represented within the DNT-IVB is the
72 formation and function of neural networks, since the nervous system development requires functional
73 networks consisting of different types of neurons and glial cells (Brown et al., 2016; Frank et al., 2017;
74 Shafer, 2019). Furthermore, certain brain disorders, like autism spectrum disorder (ASD), Alzheimer's
75 disease, and Parkinson's are associated with dysfunctional neural synchronization (Uhlhaas and Singer,
76 2006). Important tools to study electrophysiology of such neural networks are microelectrode arrays
77 (MEA), which record extracellular local field potentials on multiple electrodes thus at different
78 locations of the network and provide information on electrical activity, firing patterns, and
79 synchronicity of the neural networks (Johnstone et al., 2010). So far, DNT *in vitro* testing for
80 synaptogenesis and neuronal activity is mainly performed in assays based on rat primary cortical cells
81 (Brown et al., 2016; Frank et al., 2017). The use of a human cell model to assess this endpoint has been
82 identified as a gap in the current DNT-IVB, precisely because the potential for species-specific features
83 is still unknown (Crofton and Mundy, 2021).

84 The introduction of human-induced pluripotent stem cells (hiPSC) (Takahashi et al., 2007) has
85 extensively advanced the field of biomedical sciences including testing for DNT. It has been proven that
86 hiPSC-derived neural networks growing directly on MEAs exhibit spontaneous neuronal activity with
87 organized spiking and bursting patterns (Odawara et al., 2016; Ishii et al., 2017; Nimtz et al., 2020;
88 Tukker, Wijnolts, et al., 2020; Bartmann et al., 2021), which can be further modulated with known
89 neurotoxicants and drugs (Odawara et al., 2018; Nimtz et al., 2020; Tukker, Bouwman, et al., 2020).
90 The neural induction of hiPSCs towards functional neuronal cultures comes with many advantages,
91 especially with regard to disease modeling but bears the issue of high variability between batches and
92 cell lines. This variability is mostly due to the fact, that every single neural network differentiates into
93 a variable number of neuronal subtypes. In addition, the generation of sufficiently active networks
94 takes weeks to months (Hofrichter et al., 2017; Hyvärinen et al., 2019). The usage of commercially
95 available hiPSC-derived neurons circumvents these problems with quality- and cell ratio-controlled,
96 reproducible cells in large quantities (Little et al., 2019).

97 In this study, we present the establishment of a human neural network formation (hNMF) assay based
98 on a commercially available kit, which consists of hiPSC-derived excitatory and inhibitory neurons and
99 primary astroglia (SynFire, NeuCyte, USA). Pharmacological modulation confirmed the functionality of
100 both neuronal subtypes and chronic treatment over 35 days revealed the ability of the cell model to
101 detect alterations by Bis-I through a known mode of action. Moreover, the assay was challenged with
102 a test set of 28 substances and displayed compound-specific effects on network development.

103

104 **2 Material & Methods**

105 **2.1 Compounds**

106 In the present study, 28 substances were tested with various concerns regarding their DNT potential.
107 As an assay negative control, Acetaminophen was included in the test set (assay negative control). The
108 protein kinase C (PKC) inhibitor bisindolylmaleimide I (Bis-I) was used as an assay positive control,
109 together with bicuculline and cyanquixaline (6-cyano-7-nitroquinoxaline-2,3-dione; CNQX) for acute
110 pharmacological treatment of networks. Bis-I is known to decrease neurite outgrowth and
111 firing/bursting rates of rat neural networks (Harrill et al., 2011; Robinette et al., 2011), whereas
112 bicuculline and CNQX are GABAergic and glutamatergic receptor inhibitors, respectively. Compounds
113 were dissolved in dimethyl sulfoxide (DMSO) or water to a stock concentration of 20 mM with
114 exception of rotenone (100 mM), bicuculline (15 mM), and CNQX (30 mM). Applied concentrations
115 ranged from 0.027 to 20 μ M and 0.0004 to 0.3 μ M for rotenone. Bis-I was applied at 5 μ M, bicuculline
116 at 3 μ M, and CNQX at 30 μ M. CAS registry numbers (CASRN), suppliers, and further information are
117 collected in **Tab. S1**.

118

119 **2.2 Cell Culture**

120 SynFire glutamatergic neurons (LOT#000172 and 000131), SynFire GABAergic neurons (Lot#000172
121 and 000131) and SynFire astrocytes (Lot#13029-050 and 00190820; all from NeuCyte, USA) were
122 thawed and cultured according to the manufacturer's protocol. In short, all three cell types were
123 thawed and resuspended in a defined ratio in supplemented seeding medium (NeuCyte). Cells were
124 seeded at a density of 270×10^3 cells/well (140×10^3 glutamatergic neurons, 60×10^3 GABAergic
125 neurons, 70×10^3 astrocytes) on 48 well MEA plates (Axion M768-KAP-48) pre-coated with 0.05%
126 polyethyleneimine and 20 μ g/ml mouse laminin. The seeding was performed in a 50 μ l droplet ($270 \times$
127 10^3 cells/droplet) of supplemented seeding medium (NeuCyte) per well. After cells were allowed to

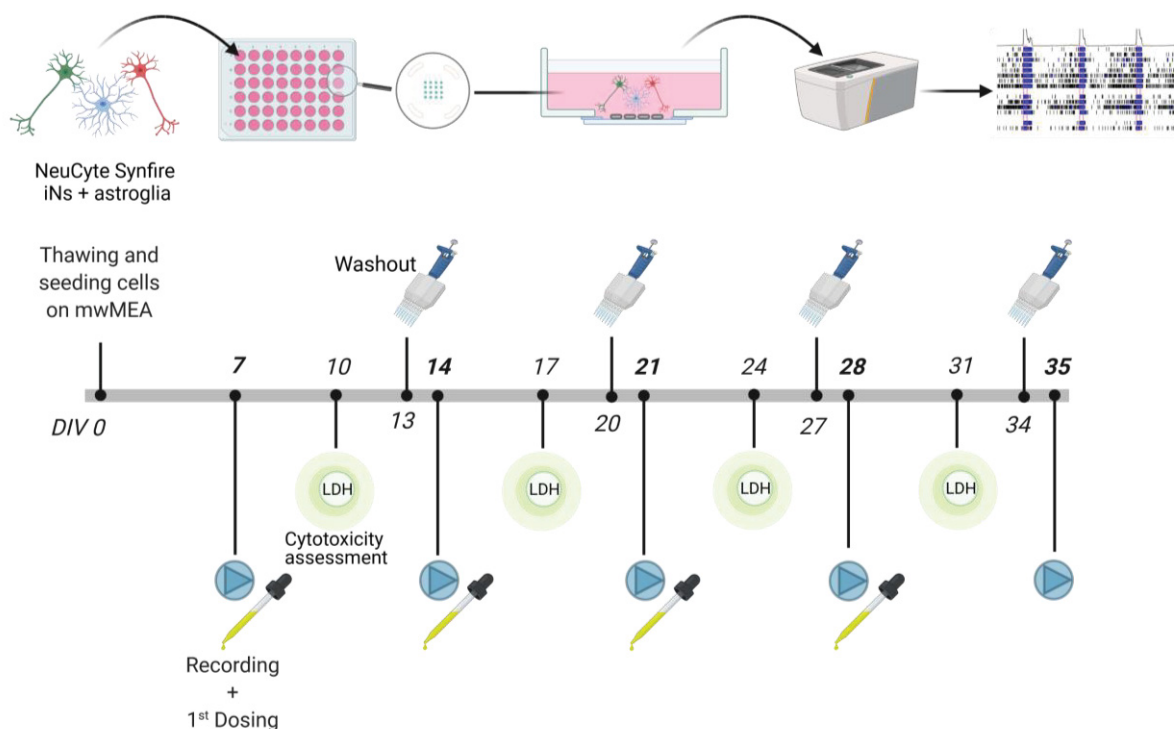
128 adhere for 24h each well was filled with 250 μ l supplemented short-term medium (NeuCyte). At days
129 *in vitro* (DIV) 3 and 5 cells were fed by changing half of the medium with supplemented short-term
130 medium. From DIV 7 onwards, medium was gradually changed to supplemented long-term medium
131 (NeuCyte). Following the same plating procedure and seeding density, 20 wells of a pre-coated 96-well
132 flat bottom plate (Greiner) were prepared for weekly cytotoxicity assessments (see section 2.5).

133

134 **2.3 Experimental Design**

135 Following the first recording of spontaneous electrical network activity at DIV 7, cells were exposed to
136 the respective test compound by changing half of the medium with supplemented long-term medium
137 containing double-concentrated compound. Half medium changes with the compounds were
138 conducted at DIV 10, 17, 24, and 31. The removed media was used for cytotoxicity assessment using
139 the CytoTox-ONE homogenous membrane integrity (LDH) assay (see 2.5). 24 hours before weekly
140 recordings at DIV 7, 14, 21, 28, and 35 a washout with PBS was performed prior to replacing the
141 medium with chemical-free supplemented long-term medium. After recording, the media was again
142 replaced with long-term medium containing the test compound. Two compounds were tested per 48-
143 well MEA plate including solvent and endpoint-specific controls. Each independent experiment
144 (biological replicate) results from a different thawing procedure done on a different day and composes
145 three technical replicates (replicate wells). In this study, we followed a two-step testing paradigm,
146 where primarily each compound was tested twice independently. If the two independent experiments
147 showed the same results, e.g no effect, no additional experiment was conducted. In case of conflicting
148 outcomes, a third experiment was performed. The experimental setup is summarized in **Figure 1**.

149



150

151 **Figure 1: Experimental Setup of the human NNF assay.** A co-culture of hiPSC-derived excitatory and inhibitory
 152 neurons and primary astroglia (NeuCyte, USA) was plated in a defined cell type ratio on 48-well MEA plates at
 153 DIV0. Cultures were allowed to mature for 7 days before exposure to the test compounds. 24 hours before the
 154 weekly recording of spontaneous electrical network activity on DIV7, 14, 21, 28, and 35 a washout of the
 155 respective compounds was performed. Additionally, cytotoxicity was assessed every week by the CytoTox-ONE
 156 (LDH) assay on DIV10, 17, 24, and 31 three days after dosing.

157

158 2.4 MEA recording

159 Spontaneous electrical network activity on DIV7, 14, 21, 28, and 35 was recorded with the Axion
 160 Maestro Pro system, a 768-channel amplifier, and the Axion Integrated Studio (AxIS) software version
 161 1.5.3 or later (Axion Biosystems, Atlanta, USA). After an equilibration time of 15 minutes, recordings
 162 were performed two times 15 minutes, whereas only the last 15 minutes were used for further
 163 analyses. For acute response measurements (CNQX, BIC) only the first 15 minutes recording was
 164 analysed. All recordings were conducted at 37°C and 5% CO₂. The activity was measured using a gain
 165 of 1000 x and a sampling frequency of 12.5 kHz. A Butterworth band-pass filter was used (200 - 3000
 166 Hz) prior to spike detection (threshold of 6x root mean square [RMS] noise on each electrode) via the
 167 AxIS adaptive spike detector. An active electrode was defined as ≥ 5 spikes/min.

168

169 2.5 Cytotoxicity assessment

170 Cytotoxicity was assessed every week and three days after re-dosing (at DIV10, DIV17, DIV24, and
171 DIV31) using the CytoTox-ONE Homogeneous Membrane Integrity assay according to the
172 manufacturer's instructions (CytoTox-ONE Homogeneous Membrane Integrity Assay; #G7891,
173 Promega, Madison, United States). Therefore, 50 μ l medium from each well was removed, transferred
174 to a 96-well plate (Sarstedt) and 50 μ l CytoTox-ONE reagent was added. 30 minutes prior to the
175 cytotoxicity assay, 3 wells of the lysis plate were treated with 10% Triton-X 100, and the supernatant
176 was used as lysis positive control. As a background control, 50 μ l of supplemented long-term medium
177 were incubated with the same volume of CytoTox-ONE reagent. Following 2 hours of incubation at
178 room temperature, the fluorescence was detected with a Tecan infinite M200 Pro reader (ex: 540 nm;
179 em: 590 nm).

180

181 2.6 Data analyses

182 After recording with the Axion Integrated Studio (AxIS) software, recordings were re-recorded using
183 the same software, resulting in spk. files. For single electrode burst detection, the Inter-Spike Interval
184 (ISI) Threshold Algorithm was used with a maximum ISI of 100 ms with at least 5 spikes. Additionally,
185 network bursts were detected using the Axion Neural Metric Tool and the Envelope algorithm with a
186 threshold factor of 1.5, a minimum Inter-Burst Interval (IBI) of 100 ms, and 60% of active electrodes.
187 The Synchrony Window was set to 20 ms. This resulted in 72 network parameters for five timepoints
188 and seven concentrations. As the manual evaluation of all 72 parameters was not possible, an
189 automated evaluation workflow that calculates the trapezoidal area under the curve (AUC) and
190 benchmark concentrations (BMC) was set up. AUC was calculated as previously described by Brown
191 and colleagues (Brown et al., 2016). Consecutively, spline interpolations with degree 1 polynomials for
192 the data points given for conditions are made for each endpoint in each plate. If the response for an
193 endpoint for the DIV7 measurement was missing, it was set using random sampling throughout overall
194 available first days-*in-vitro* responses for that endpoint on the same plate when at least 50% of these
195 responses were available. In the final preprocessing step a common time duration (DIV) with available
196 responses in the resulting data is determined for each endpoint and experiment. Finally, the area under
197 the resulting curves from these common durations was determined.

198 The pesticides data presented in this paper were derived from 2-3 individual experiments per
199 compound as stated in **Tab. S2**. The data was normalized to the median solvent control and re-
200 normalized to the starting point of a concentration-response curve generated with the R package drc

201 as described below. For cytotoxicity data a different normalization was used: The normalized
202 cytotoxicity response equalled the lysis control (LC) median minus the response of the respective
203 concentration divided by the lysis control median minus the solvent control (SC) median
204 ($normalized\ response = \frac{LC\ (median) - response}{LC\ (median) - SC\ (median)}$). Benchmark concentrations (BMC; as BMC₅₀ and
205 BMC₅₀) with their upper and lower confidence intervals were calculated based on the R package drc.
206 Linear, sigmoidal, monotonic, and non-monotonic models were run with the concentration-response
207 data of each endpoint, and Akaike's information criteria were used to determine the best fit. Endpoints
208 were classified as DNT-specific if CIs of the BMCs calculated for the DNT-specific endpoint did not
209 overlap with the cytotoxicity endpoint. If the overlap exceeded 10%, the endpoint was classified as
210 unspecific. Statistical significance was calculated using Graphpad Prism 8.2.1 and OneWay ANOVA with
211 Dunnett's post-hoc tests or two-tailed Student's t-tests ($p \leq 0.05$ was termed significant).

212

213 **2.7 RNAseq**

214 NeuCyte's iPSC-derived glutamatergic, GABAergic induced neurons and human astrocytes were
215 seeded to form iN:glia co-culture. Cells were harvested on DIV 7, 14, 21, 28, and 35, four biological
216 replicates per time point. RNA-Seq was performed by Novogene (CA, USA). Total RNA was extracted
217 by Qiagen's RNA Extraction Kit (Qiagen, Germany). For library preparation, NEBNext[®] Ultra[™] II RNA
218 Library Prep Kit for Illumina[®] was used (New England Biolabs, MA, USA). For sequencing, NovaSeq 6000
219 was used, utilizing paired-end 150 bp read length. Downstream data analysis was performed using a
220 combination of programs. Alignments were parsed using STAR program. Reads were aligned to the
221 reference genome GRCh37 using STAR (v2.S). STAR counted number of reads per gene while mapping.
222 The counts coincide with those produced by HTseq-count with default parameters. Then FPKM of each
223 gene was calculated based on the length of the gene and reads count mapped to this gene.

224 **2.8 Immunostainings**

225 SynFire iN:glia co-cultures were validated by immunostaining of markers including: Goat anti-MAP2
226 (1:1000, Synaptic Systems, 188 004), Chicken anti-NeuN (1:1000, Synaptic Systems, 266 006), Rabbit
227 anti-Synapsin1/2 (1:1000, Synaptic Systems, 106 002), Rabbit anti-VGLUT2 (1:1000, Synaptic Systems,
228 135 403), Rabbit anti-VGAT (1:1000, Synaptic Systems, 131 003), Chicken anti-GFAP (1:250, Abcam,
229 ab4674). Secondary antibodies were conjugated to AlexaFluor647 (1:2000, Invitrogen).

230 On DIV35, the co-cultures were fixed with 4% paraformaldehyde (PFA; Alfa Aesar, J61899-AK) at room
231 temperature for 15 min, washed 3 times with PBS (Gibco, 14190-144), and then incubated overnight

232 at 4°C with primary antibodies diluted in blocking solution [5% Cosmic Calf Serum (GE Life Sciences,
233 SH30087) + 0.2% Triton X-100 (VWR, 97063-996) in PBS]. On the second day, co-cultures were washed
234 3 times with PBS, and then incubated on a shaker at room temperature in the dark, with secondary
235 antibodies diluted in blocking solution with DAPI (1 µg/mL, Thermo Scientific, 62248). After 3 times
236 washing with PBS, co-cultures were imaged using an Operetta CLS High Content Analysis System
237 (PerkinElmer).

238

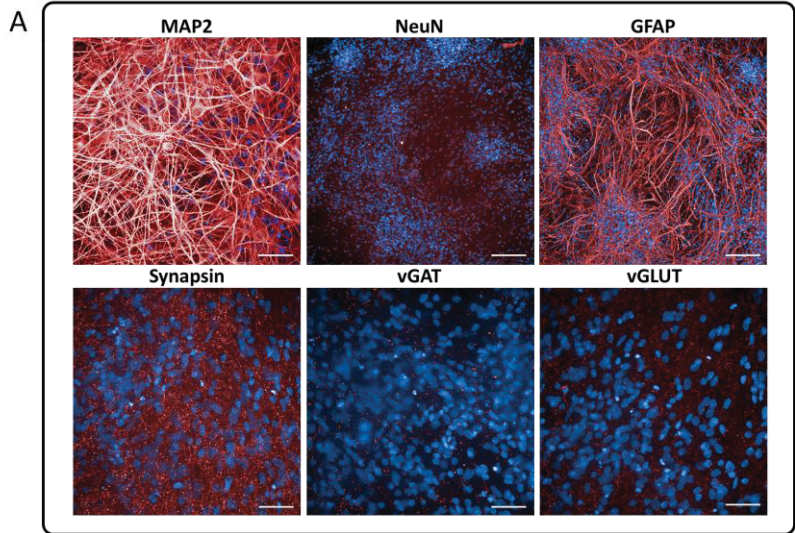
239 **3 Results**

240 **3.1 Characterization of an MEA-Based Assay for Network Formation**

241 The present study describes the establishment and characterization of a human iPSC-based neural
242 network formation assay. Furthermore, the assay was challenged with 27 pesticides and
243 acetaminophen as a negative control. 270,000 cells of a defined cell type ratio (52% glutamatergic
244 neurons, 22% GABAergic neurons, 26% astrocytes) were seeded as a monolayer culture on each MEA
245 well containing 16 electrodes. This cell system is commercially available (NeuCyte, USA) and has been
246 intensively characterized. **Figure 2** illustrates the characteristics of neural networks at different
247 maturation time points (DIV7-35) using transcriptome profiling (RNA-seq), as well as
248 immunocytochemical staining of DIV35 networks. Stainings of differentiated co-cultures at DIV35 (**Fig.**
249 **2A**) show a strong presence of MAP2-positive neurons and a lower amount of NeuN (RBFOX3),
250 indicating a high maturation of the networks. In addition, the glial marker GFAP is strongly expressed.
251 Furthermore, the co-cultures are positive for the pre-synaptic marker synapsin and exhibit the
252 vesicular GABA transporter vGAT, as well as vGLUT, a vesicular glutamate transporter.

253 These characteristics are also confirmed by RNA sequencing of co-cultures at different time points (**Fig.**
254 **2B**). The proceeded maturation of neurons within the system is verified by a high expression of
255 neuronal maturation markers, e.g. *MAP2*, *DLG4* and *SYP*, compared to genes, coding for immature
256 neurons (e.g. *TUBB3*, *NEUROD1*). Additionally, the high expression of *GFAP* and *AQP4*, compared to
257 *S100B*, describes the mature glial system. Also, genes coding for GABA and AMPA receptors and
258 glutamate transporters showed expression at DIV7 with gradations within their subtypes (e.g. *SLC1A2*
259 vs. *SLC1A3*). In addition, voltage- (VG) and ligand-gated (LG) ion channels are enriched in the culture.
260 In comparison to VG- and LG-calcium channels, VG-sodium channels are higher expressed. Moreover,
261 decent expression levels were detected for transcripts coding for dopaminergic, cholinergic (nicotinic
262 and muscarinic), and NMDA receptors. Especially *CHRNA3* and *DRD3* expressions were enhanced at
263 DIV7 and decreased with increasing maturation of the networks. The higher expression of *SLC12A5*

264 (*KCC2*) compared to *SLC12A2* (*NKCC1*) at DIV14 gives an indication that the cells are in a stage after the
265 GABA switch.



B

Neurons						
Family	Gene	DIV7	DIV14	DIV21	DIV28	DIV35
Neuronal	ASCL1	0.41	0.41	0.44	0.60	0.61
	DCX	74.12	73.08	90.43	81.84	82.18
	DLG4	29.10	28.63	26.28	28.48	34.00
	FOXP1	19.56	11.74	9.77	8.49	7.88
	MAP2	69.94	85.44	109.89	110.93	121.45
	NES	174.10	95.06	81.90	72.43	56.10
	NEUROD1	6.10	3.46	3.11	2.40	1.81
	RBFOX3	11.28	7.06	8.42	8.72	10.01
	SYN1	16.75	19.27	24.69	28.54	37.81
	SYP	55.80	97.72	109.23	145.22	166.37
	TUBB3	4.47	2.06	2.52	2.22	1.90

Astrocytes						
Family	Gene	DIV7	DIV14	DIV21	DIV28	DIV35
Glial	GFAP	779.49	1700.0	1995.0	2095.3	1862.1
	ALDH1L1	0.16	0.20	0.29	0.43	0.63
	AQP4	13.19	64.70	110.02	118.66	116.47
	GLUL	36.38	42.48	47.55	46.76	39.97
	S100B	19.27	41.30	58.97	54.95	43.87

GABA system						
Family	Gene	DIV7	DIV14	DIV21	DIV28	DIV35
GABAR	GABBR1	40.95	35.30	40.00	42.77	48.78
	GABBR2	8.91	10.70	15.47	17.56	21.29
	GABRA1	0.10	0.53	1.02	1.53	1.40
	GABRA2	2.34	5.48	7.33	8.51	10.56
	GABRA3	10.72	13.57	17.47	18.29	20.93
	GABRA4	0.23	0.31	0.29	0.30	0.39
	GABRA5	3.96	10.30	13.23	12.27	13.96
	GABRB1	0.47	1.09	1.94	2.23	3.21
	GABRB2	1.28	1.85	2.69	3.07	3.46
	GABRB3	20.61	24.21	29.97	28.78	29.47
	GABRD	0.09	0.26	0.25	0.26	0.46
	GABRE	8.33	4.45	5.16	4.13	3.95
	GABRG1	0.16	0.55	0.86	1.24	1.49
GABRG2	2.10	7.38	10.24	12.62	13.09	
GABRG3	2.07	1.97	2.47	3.00	3.59	
GAD	GAD1	4.64	6.29	8.47	9.69	11.91
	GAD2	1.78	1.80	1.82	1.83	1.67
GABA switch	SLC12A2	6.05	4.48	4.39	4.18	3.56
	SLC12A5	5.75	6.27	8.64	8.61	9.84

Glutamate system						
Family	Gene	DIV7	DIV14	DIV21	DIV28	DIV35
ionotropic glutamate receptors (AMPA/kainate)	GRIA1	3.70	5.17	7.37	8.27	8.35
	GRIA2	5.76	10.70	18.90	18.88	19.64
	GRIA3	5.14	4.81	5.76	5.39	4.40
	GRIA4	9.96	12.86	15.87	17.02	18.89
	GRIK1	7.75	7.02	7.75	6.84	6.01
GRIK2	6.19	7.17	7.91	7.49	6.81	
GRIK5	35.25	21.19	21.07	19.32	18.73	
ionotropic glutamate receptors (NMDA)	GRIN1	6.26	9.52	18.24	20.01	23.93
	GRIN2A	1.04	1.16	1.41	1.14	1.44
	GRIN2B	0.09	0.37	0.85	0.85	1.23
	GRIN2C	0.62	0.35	0.46	0.49	0.60
	GRIN2D	14.59	8.64	9.77	9.74	11.78
	GRIN3A	0.54	0.99	1.06	1.11	1.39
GRIN3B	0.12	0.20	0.24	0.27	0.36	
GLS	27.77	28.75	32.47	33.82	35.62	
glutamate transporter	SLC17A6	22.30	25.73	31.73	41.61	47.14
	SLC17A7	10.76	7.81	5.23	6.83	9.70
	SLC1A1	4.19	6.07	8.13	9.04	8.95
	SLC1A2	6.63	6.08	6.61	6.20	7.00
	SLC1A3	93.84	121.49	148.07	119.37	102.00
	SLC1A6	4.95	7.25	8.67	9.54	10.27
	SLC4A10	2.41	6.92	10.62	10.20	8.45
	SLC6A9	4.44	3.68	3.85	3.76	4.39
SLC8A2	4.86	4.72	5.67	6.00	7.65	

Ion channels						
Family	Gene	DIV7	DIV14	DIV21	DIV28	DIV35
VG-Na channels	SCN2A	6.07	15.26	23.20	23.42	22.31
	SCN3A	11.31	17.54	22.00	21.88	20.81
	CACNA1A	8.22	4.62	6.23	5.81	5.74
VG-Ca channels	CACNA1B	11.28	6.73	8.61	7.82	7.99
	CACNA1C	6.16	4.16	5.36	4.40	5.06
	CACNA1D	1.62	1.51	2.27	2.00	2.33
	CACNA1E	6.74	4.62	6.17	5.66	6.55
	CACNA1F	0.05	0.04	0.02	0.01	0.05
	CACNA1H	11.47	6.19	6.83	6.23	7.16
	CACNA1I	2.37	2.11	3.17	2.58	3.08
LG-Ca channels	ITPR1	0.89	0.69	0.78	0.72	0.85
	ITPR2	7.08	6.91	8.26	7.04	6.86
	ITPR3	4.75	2.62	2.27	2.03	2.18
	ORAI1	4.35	4.38	3.29	3.33	3.38
	ORAI2	11.63	11.69	10.64	11.10	11.13
	RYR1	1.97	0.71	0.90	0.84	1.39
	RYR2	0.74	1.09	1.99	1.99	2.48
	TPCN1	7.27	5.46	5.41	5.06	5.95
TPCN2	5.73	3.22	3.84	2.77	2.35	

Cholinergic						
Family	Gene	DIV7	DIV14	DIV21	DIV28	DIV35
Acetylcholine-R	CHRM1	0.00	0.00	0.00	0.00	0.00
	CHRM2	0.75	1.91	4.09	4.37	4.53
	CHRM3	1.15	1.73	2.06	2.23	2.32
	CHRM4	3.36	3.22	2.52	2.65	3.39
	CHRNA3	22.50	12.32	10.98	10.61	12.04
	CHRNA4	6.83	6.12	6.75	7.81	9.20
	CHRNA6	0.17	0.75	1.29	1.80	2.18
	CHRNA7	1.98	1.26	1.40	1.41	1.45
	CHRNA9	0.57	0.47	0.26	0.43	0.39
	CHRNB2	6.93	5.84	4.95	4.82	5.25
	CHRNB3	0.55	0.25	0.12	0.13	0.13
	CHRNB4	10.03	4.91	3.71	3.42	4.13

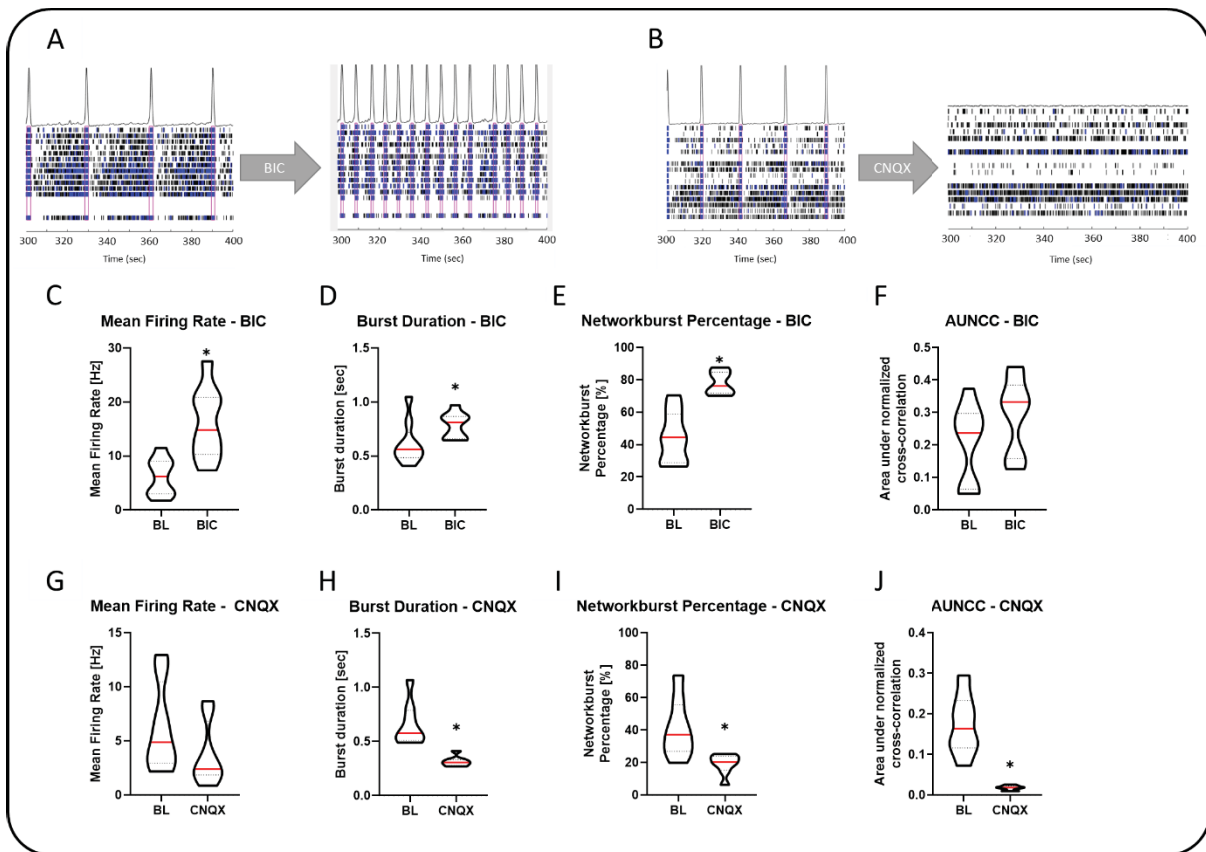
Dopaminergic						
Family	Gene	DIV7	DIV14	DIV21	DIV28	DIV35
Dopamine	DRD1	0.38	0.49	0.47	0.38	0.44
	DRD2	18.37	8.52	6.47	8.00	10.48
	DRD3	0.02	0.03	0.04	0.11	0.05
	DRD4	4.95	3.33	3.74	3.85	4.75
	DRD5	0.40	0.95	0.50	0.46	0.52
	TH	10.42	12.34	5.16	5.75	8.54

raw signal intensity (FPKM)

267 **Figure 2: Immunocytochemical stainings and gene expression profiles of SynFire neuronal/glia co-cultures at**
268 **different maturation time points. (A)** Immunocytochemical stainings of different neuronal and glial markers of
269 differentiated co-cultures at DIV35. Nuclei were stained with DAPI (blue) together with the respective marker
270 (red). MAP2, Synapsin, vGAT, vGLUT: scale bar = 50 μm ; NeuN, GFAP: scale bar = 200 μm . **(B)** RNA-seq data was
271 used to generate gene expression profiles on DIV7, 14, 21, 28, and 35. Values are presented as fragments per
272 kilobase per million mapped reads (FPKM). VG: voltage-gated; LG: ligand-gated; Ca: calcium; Na: sodium.

273 Taken together, these gene expression data show that the neural networks develop over time and
274 express a broad variety of genes related to neuronal and glial function as a prerequisite for neural
275 network function.

276 Important tools to study electrophysiology of such networks are MEAs. MEA recordings provide high
277 content data based on the recording of extracellular action potentials, so-called spikes, which are the
278 basic unit of activity of a neural network. During the development of a network, spikes can group into
279 bursts and also synchronize their activity resulting in network bursts. To confirm the contribution of
280 functional GABAergic and glutamatergic neurons in the development of the networks, we performed
281 an acute pharmacological modulation of neural networks on DIV21. Therefore, the neuronal subtypes
282 included in the cell model were challenged with the two receptor antagonists bicuculline (BIC) and
283 cyanquixaline (6-cyano-7-nitroquinoxaline-2,3-dione; CNQX). BIC is a well-studied GABA_A receptor
284 antagonist (Johnston, 2013), whereas CNQX antagonizes AMPA-type glutamate receptors. After
285 baseline recording at DIV21, cells were exposed to the respective modulator and the electrical activity
286 was measured subsequently. Exposure to 3 μM BIC increased general electrical activity, especially
287 synchronous bursting (**Fig. 3A**, pink boxes), whereas 30 μM CNQX led to a loss of organized activity, as
288 illustrated by representative 100-second spike raster plots (**Fig. 3A, B**). For additional quality control
289 of the test method, acute treatments with the two described modulators were included in every assay
290 run. Violin plots for each compound and four different network parameters (**Fig. 3C-F**) illustrate the
291 distribution of these data and the median of 8-9 independent experiments (median of 3 technical
292 replicates each) reveals the effect of both receptor antagonists. 3 μM BIC significantly enhanced the
293 mean firing rate and burst duration. Consistent with the spike raster plots, bicuculline doubled the
294 percentage of overall spikes contributing to network bursts from 40% to 80% ("Networkburst
295 percentage", **Fig. 3E**) and increased the synchronicity ("AUNCC", **Fig. 3F**). In contrast, CNQX inhibited
296 the overall activity and organization of the networks. Especially burst duration and synchronicity were
297 impaired with a low degree of variation (**Fig. 3H, J**).



298

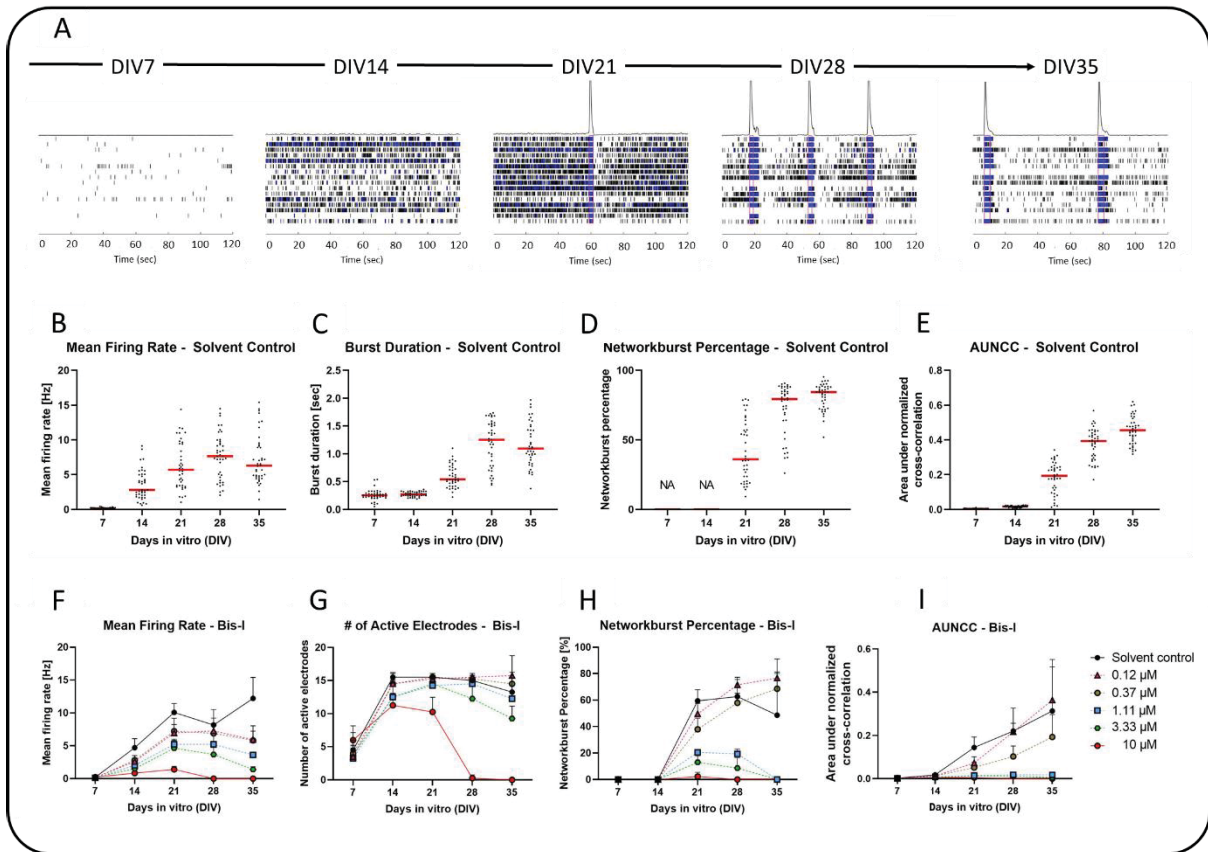
299 **Figure 3: Acute pharmacological modulation of DIV21 neural network activity.** Untreated DIV21 neural
 300 networks (baseline, BL) were exposed to 3 μ M bicuculline (BIC) and 30 μ M CNQX, respectively. **(A, B)** 100-second
 301 spike raster plots reveal the effects of 3 μ M BIC and 30 μ M CNQX on DIV21 neural networks. Spikes are
 302 represented as black bars, bursts as blue bars. Pink boxes indicate networkbursts. **(C-F)** 3 μ M BIC enhanced neural
 303 network activity as indicated by the increase of different network parameters compared to the baseline. **(G-J)** 30
 304 μ M CNQX decreased neural network activity through different network parameters. Data are represented as
 305 violin plot distribution of 9 **(C-F)** or 8 **(G-J)** independent experiments. Dotted lines represent quartiles of
 306 distribution and red bars the median. Statistical significance was calculated using two-tailed Student's t-tests. A
 307 p-value below 0.05 was termed significant. *significant compared to the respective BL.

308

309 As already indicated by gene expression data **(Fig. 2)**, electrophysiological measurements over time
 310 confirm maturation of the neural networks by displaying specific firing patterns, like organized spiking
 311 and synchronicity at later points of differentiation **(Fig. 3A)**. Representative spike raster plots illustrate
 312 these features over the 35-day development of the networks **(Fig. 4A)**. At DIV7 spikes (black bars) are
 313 the sole form of activity, whereas at DIV14 bursts (blue bars) start to form on single electrodes. Along
 314 with the increase in bursting activity and the emergence of a synchronous network starting on DIV21,
 315 the number of spikes between network bursts decreases at DIV28 and 35. This transition in network
 316 development is reflected by the evaluation of different network parameters of untreated solvent

317 control wells (0.1% DMSO) from all plates contributing to this study (n=41 plates and 123 wells). **Figure**
318 **4B-E** shows the distribution of different parameters between experiments (each data point reflects the
319 median of 3 wells of each independent experiment) and indicates the variation of the hNNF assay. On
320 DIV7 and 14, the mean firing rate is notably below 5 Hz, but raises to 10 Hz, with its peak at DIV28 (**Fig.**
321 **4B**). The same trend can be observed for the duration of bursts between DIV7 and 35 (**Fig. 4C**).
322 Nevertheless, some parameters, like the network burst percentage or the area under normalized cross-
323 correlation, which describes the synchronicity of the network, continuously increase and find their
324 peak at DIV35 (**Fig. 4D, E**). Because the highly organized activity of the network is rarely observed at
325 DIV7 and 14 (**Fig. 4E**), networkburst parameters were only considered from DIV21 to 35 for the
326 following evaluations.

327 To show that neural network development within the hNNF assay can be altered by a specific
328 mechanism, DIV7 networks were exposed to increasing concentrations of the protein kinase C inhibitor
329 Bisindolylmaleimide I (Bis-I), following the exposure scheme described in **Figure 1**. Bis-I inhibits neurite
330 outgrowth in PC-12 cells (Das et al., 2004), rat cortical neurons, and human iPSC-derived neurons
331 (Druwe et al., 2016). In particular, Bis-I decreased firing and bursting rates of rat neural networks *in*
332 *vitro* (Robinette et al., 2011). We observed that network activity was affected by Bis-I in a
333 concentration-dependent manner, as illustrated by representative network parameters in **Figure 4F-I**.
334 Untreated controls showed a mean firing rate of more than 10 Hz on DIV35, whereas Bis-I interfered
335 with the formation of a functional network starting at low concentrations of 0.12 μ M resulting in about
336 5 Hz (**Fig. 4F**). Exposure to 10 μ M Bis-I resulted in a fully muted network at DIV28 and DIV35 observable
337 in every of the four displayed network parameters. Not only the general activity was affected, but also
338 the network burst percentage was reduced to 20% at DIV21 and 28 by 1.11 μ M Bis-I and culminate in
339 0% at DIV35 (**Fig. 4H**). This impairment in network bursting is also reflected in the area under
340 normalized cross-correlation (AUNCC; **Fig. 4I**). After this initial proof-of-concept, Bis-I was introduced
341 as an endpoint-specific positive control for the hNNF test method. For this purpose, each experimental
342 run in the compound screening contained control wells, treated with 5 μ M Bis-I. The data of 13
343 independent experiments (39 wells) showed that Bis-I reliably and significantly inhibits different
344 network parameters, e.g. burst duration, networkburst percentage and network synchronicity
345 (AUNCC, **Fig. S1**). The overall effect of Bis-I on the mean firing rate was not significant, which may be
346 explained by the higher variability of this parameter, as explained in the next section (see **Fig. S1**).



347

348 **Figure 4: Neural network development on 48-well microelectrode arrays (MEA) and its inhibition by**
 349 **Bisindolylmaleimide I (Bis-I).** (A) Representative 120 second raster plots referring to DIV7 to DIV35. Spikes
 350 are represented as black bars, bursts as blue bars. Pink boxes indicate network bursts. (B-E) Dot plots showing
 351 the distribution of untreated (solvent control; 0.1% DMSO) network activities from DIV7 to DIV35 over four
 352 network parameters (mean firing rate, burst duration, networkburst percentage, and area under normalized
 353 cross-correlation (AUNCC)). Single dots represent the median of 3 replicates of each experiment. The red bar
 354 defines the median overall plates (n=41). (F-I) Starting at DIV7 networks were treated with increasing
 355 concentrations (0.12; 0.37; 1.11; 3.33 and 10 μ M) of the PKC inhibitor Bis-I. Different network parameters (mean
 356 firing rate, number of active electrodes, networkburst percentage, area under normalized cross-correlation
 357 (AUNCC)) reflect the impairment of Bis-I on neural network development over 35 days of differentiation. Data
 358 are shown as mean \pm SD of 4 wells.

359

360 3.2 Selection of Parameters to Evaluate

361 MEA recordings generated in this study result in 72 network parameters, which are predominantly
 362 correlated and can be grouped into spike-, burst- and network-related parameters. A plethora of these
 363 define the same characteristic of the network (e.g., “mean firing rate” and “weighted mean firing rate”)
 364 or use a different statistical method to describe the parameter (e.g. “inter-burst interval - Avg” vs
 365 “inter-burst interval (median) - Avg”). The evaluation of one 48-well MEA plate during a time course

366 of 35 days results in over 17,000 data points, which enormously exacerbates the processing of data
367 and interpretation of possible compound effects. To reduce the number of data points and only
368 concentrate on the most informative and at the same time robust parameters, we analyzed the
369 variability of all parameters across all 41 wells treated with the lowest compound concentration. We
370 therefore calculated the inter-experimental standard deviation (SD) for each parameter. The higher
371 the SD, the greater is the dispersion. Additionally, we included parameters that were previously
372 described in the literature (Brown et al., 2016; Frank et al., 2017; Kosnik et al., 2020) and which
373 represent a broad variety of network development. We then selected a final set of 14 network
374 parameters, that covers the three categories “General activity”, “Bursting activity” and “Connectivity”
375 of the neural networks and shows a SD between 6 and 29 (Table 1).

376

377 **Table 1: 14 Parameters from MEA recordings and their respective inter-experimental standard deviation (SD).**

Category	Parameter	Definition	Inter-experimental SD
General Activity	Mean Firing Rate	Total number of spikes divided by the duration of the analysis [Hz]	28.45
	Number of Active Electrodes	Number of electrodes with activity > 5 spikes / minute	9.97
	Number of Bursting Electrodes	Total number of electrodes within the well with bursts/minute greater than the burst electrode criterion (min# of spikes: 5; max ISI: 100 ms)	11.14
Bursting Activity	Burst Duration	Average time from the first spike to last spike in a single-electrode burst	11.24
	Number of Spikes per Burst	Average number of spikes in a single-electrode burst	25.17
	Mean ISI within Burst	Mean inter-spike interval, time between spikes, for spikes in a single-electrode burst	5.94
	Inter-Burst Interval	Average time between the start of single-electrode bursts	19.18
	Burst Frequency	Total number of single-electrode bursts divided by the duration of the analysis [Hz]	28.60
	Burst Percentage	The number of spikes in single-electrode bursts divided by the total number of spikes, multiplied by 100	14.67
Connectivity	Networkburst Frequency	Total number of networkbursts divided by the duration of the analysis [Hz]	20.83
	Networkburst Duration	Average time from the first spike to last spike in a network burst	11.42
	Networkburst Percentage	The number of spikes in network bursts divided by the total number of spikes, multiplied by 100	7.08

Number of Spikes per Networkburst	Average number of spikes in a network burst	29.01
Area Under Normalized Cross-Correlation (AUNCC)	Area under the well-wide pooled inter-electrode cross-correlation normalized to the auto-correlations	14.73

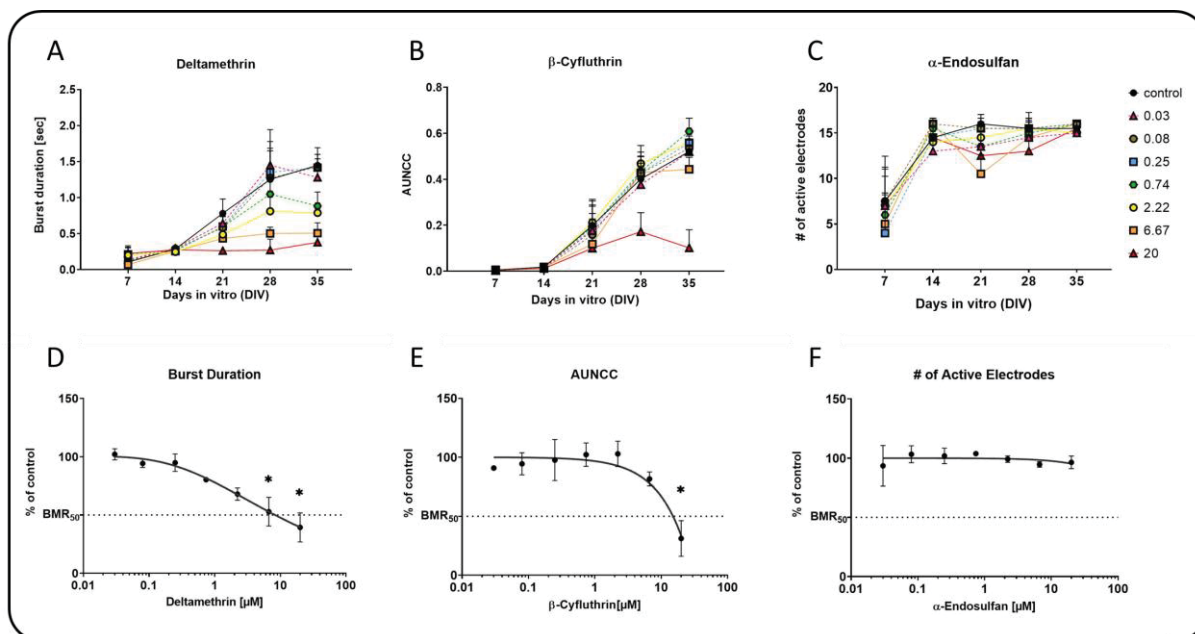
378

379

380 3.3 Concentration-Dependent Effects of Pesticides on Network Activity

381 After having set up the hNNF assay by setting up a defined treatment scheme and standard operation
382 procedure, establishing an endpoint-specific control and evaluating variability over wells and plates,
383 we next applied the hNNF assay for screening of 28 chemicals. The set consists of 27 pesticides and
384 acetaminophen as a negative control compound. To identify concentration-dependent effects of
385 substances that impaired neural network formation, cells were weekly exposed from DIV7 to DIV35,
386 including respective washout steps 24h before each recording. As an example, deltamethrin and β -
387 cyfluthrin reduced the mean firing rate (**Fig. 5A**) and area under normalized cross-correlation (**Fig. 5B**)
388 of neural networks, respectively, in a time- and concentration-dependent manner. Acibenzolar-S-
389 methyl, on the other hand, did not affect the number of active electrodes (**Fig. 5C**). These time-
390 concentration relationships can be translated into concentration-response curves as illustrated in
391 **Figure 5D-F**. For each concentration, the trapezoidal area under the curve was calculated to include all
392 five time points in one single value per concentration. This approach, as adapted from Brown et al.
393 (2016) and Shafer, et al. (2019) simplifies the comparison of effects over different days of neural
394 network development. In the next step, the AUC information and resulting concentration-response
395 curves were used to estimate BMCs with upper and lower confidence limits for each compound and
396 parameter. For estimation of the BMCs a bench mark response (BMR) of 50% (BMR₅₀) was selected as
397 this best reflects the variability of the most variable parameters (**see Tab. 1**).

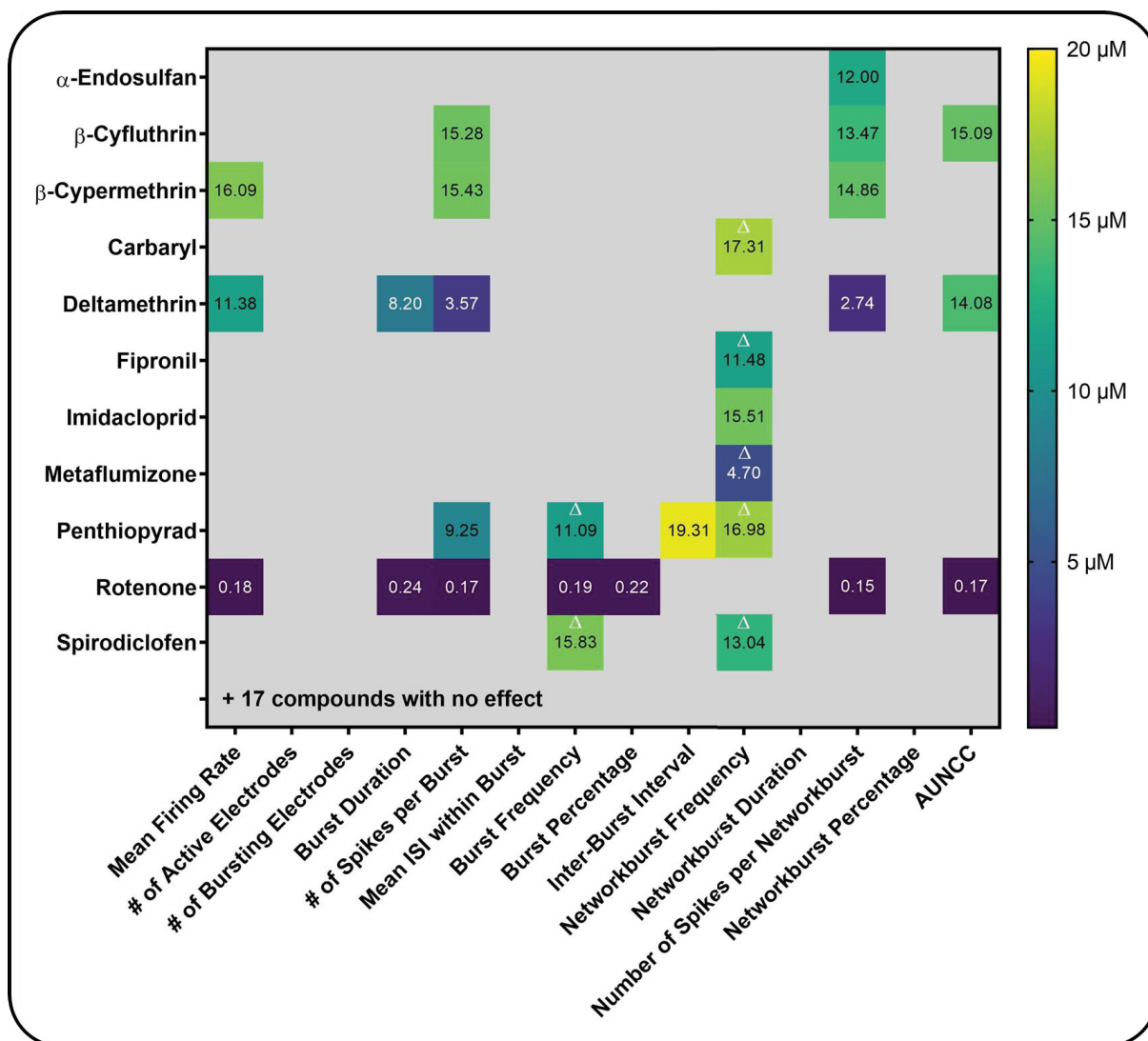
398



399
 400 **Figure 5: Example data for area under the curve (AUC) summary of time- and concentration-dependent MEA**
 401 **readouts. (A-C)** Starting at DIV7, neural networks were treated with increasing concentrations of deltamethrin
 402 **(A)**, β -cyfluthrin **(B)**, and α -endosulfan **(C)**, and exemplary network parameters were evaluated. Time- and
 403 concentration-dependent data are shown as the mean of three **(A, B)** or two **(C)** independent experiments \pm SEM
 404 **(A, B)** or SD **(C)**. Area under curve values were computed for these data and plotted in a concentration-dependent
 405 relationship **(D-F)**. Data are represented as the mean of three **(D, E)** or two **(F)** independent experiments \pm SEM
 406 **(D, E)** or \pm SD **(F)**. Replicates within one experiment are summarize by median. Curve fitting was conducted as
 407 described in section 2.6. Statistical significance was calculated using one-way ANOVA. A p-value below 0.05 was
 408 termed significant. *significant compared to the respective solvent control.

409
 410 **Figure 6** summarizes the concentration-dependent effects of the 28 tested compounds on neural
 411 network development that produced a 50% change (reduction or induction) from the curves starting
 412 point. 5 of the 14 network parameters were not affected by any compound, including number of active
 413 electrodes and mean ISI within bursts. Furthermore, 17 compounds were tested negative, e.g.
 414 acetaminophen, chlorpyrifos, and its derivate chlorpyrifos-methyl (data not shown). 11 of the 27
 415 pesticides are considered positive, for which at least one network parameter had to be affected,
 416 without cytotoxic effects at any administered concentration. β -cyfluthrin, β -cypermethrin,
 417 deltamethrin, penthiopyrad, and rotenone evoked effects in more than 2 parameters, whereas the
 418 other 6 pesticides affected 2 or less parameters. Networkburst frequency points out as the most
 419 sensitive parameter with 6 hits, of which 5 represent inductive effects. Furthermore, spirodiclofen and
 420 penthiopyrad additively increased the burst frequency. Predominantly, the observed effects are all in
 421 a similar range between 9 and 20 μ M. In contrast, deltamethrin and metaflumizone influenced

422 different network parameters below 9 μM . Rotenone points out as the most potent compound,
 423 specifically reducing 7 parameters in a concentration range between 0.15 and 0.24 μM without causing
 424 cytotoxicity.



425
 426 **Figure 6: Summary of BMCs across 14 network parameters of the hNNF assay.** No cytotoxicity was observed.
 427 17 compounds had no effect (acetaminophen, acetamiprid, acibenzolar-s-methyl, aldicarb, chlorpyrifos,
 428 chlorpyrifos-methyl, clothianidin, diazinon, dimethoate, dinotefuran, disulfoton, etofenprox, flufenacet,
 429 methamidophos, thiacloprid, thiamethoxam, triallate; data not shown). Δ Induced effects. Numbers are given in
 430 μM . No value assumes BMCs $> 20 \mu\text{M}$ ($> 0.3 \mu\text{M}$ for rotenone). Confidence intervals are listed in **Tab. S2**. AUNCC:
 431 area under normalized cross-correlation.

432
 433
 434

435 4 Discussion

436 In the last years, scientists from academia, industry, and regulatory authorities across the world agreed
437 on the need for a standardized *in vitro* testing strategy, aiming for a cheaper and faster generation of
438 additional data for DNT hazard assessment (EFSA, 2013; Crofton et al., 2014; Bal-Price et al., 2015 a,
439 2018; Fritsche, Crofton, Hernandez, Hougaard Bennekou, et al., 2017; Fritsche, Barenys, et al., 2018;
440 Fritsche, Grandjean, et al., 2018). Therefore, a DNT-IVB was compiled, including various test methods
441 covering different KEs of neurodevelopment, including the formation and function of neural networks
442 (Fritsche, 2017; Fritsche, Crofton, Hernandez, Bennekou, et al., 2017; Bal-Price et al., 2018). One of the
443 identified gaps of the DNT-IVB is the assessment of network formation and function in a human-based
444 cell model (Crofton and Mundy, 2021). This is why we established the human neural network formation
445 assay (hNNF), which consists of hiPSC-derived excitatory and inhibitory neurons and primary astroglia
446 (SynFire, NeuCyte, USA). By pharmacological modulation, the functionality of neuronal subtypes and
447 the ability of the cell model to detect alterations by a known mode of action were confirmed.
448 Furthermore, the assay was challenged with a test set of 28 substances and revealed compound-
449 specific effects of different pesticides on network development.

450 Assay establishment

451 Under most circumstances, newly developed methods for DNT testing are restricted by their ability to
452 test large numbers of chemicals (Coecke et al., 2007; Crofton et al., 2011). To tackle this issue, Crofton
453 et al. provided a set of 15 principles, which should enhance the amenability of higher throughput
454 screening (Crofton et al., 2011). The establishment of the hNNF assay in this study was realized by
455 considering these principles, which are described in more detail in the following (P1-15). During early
456 brain development, neurons start to mature and build connections via synapses (Okado et al., 1979;
457 Zhang and Poo, 2001). Neural network formation and function is therefore a key aspect of
458 neurodevelopment (P1 “Key Event of Neurodevelopment”). By measuring extracellular local field
459 potentials on MEAs, network formation and function can be assessed, thus providing information on
460 electrical activity, firing patterns, and synchronicity of the neural networks (P2 “Endpoint
461 Measurement”). Each MEA recording performed in the hNNF assay results in about 3500 data points
462 and by calculating the AUC for each concentration and normalizing the values to the respective solvent
463 control, the assay can reflect alterations of network activity in both directions (increase and decrease;
464 P3 “Dynamic Range”). Furthermore, Crofton et al. emphasize the importance of parametric controls,
465 meaning parameters of the assay that evoke predictable changes in the endpoint (P4 “Parametric
466 Controls”). One aspect that was confirmed within the presented study is the increase in electrical
467 activity and synchronicity of the networks with increasing culture time (**Fig. 3**). Furthermore, Saavedra
468 and colleagues showed that an excitatory:inhibitory (ex:inh) ratio of 70:30 using SynFire neurons

469 exhibits the steadiest spiking increase and coverage of electrodes over differentiation time, compared
470 to other ex:inh ratios (Saavedra et al., 2021). Principle 5 (“Response Characterization”) highlights the
471 relevance of a precise effect characterization, based on the degree of variability in the assay. Within
472 the hNNF assay, as recommended by the EFSA Scientific Committee, the BMC approach was applied,
473 to derive a reference point or point of departure (Hardy et al., 2017), whereby the benchmark response
474 (BMR) should be defined as an effect size that is higher than the general variability of the measured
475 endpoint. Based on the inter-experimental standard deviation ($1.5 \times SD$), which was calculated for every
476 parameter presented in this study (**Tab. 1**), we defined the BMR_{50} (reduction) and BMR_{-50} (induction)
477 as the degree of change that, if exceeded, results in a positive response (hit). Furthermore, Crofton
478 and colleagues state, that the concentration range and the resulting concentration-response holds a
479 very significant role in terms of comparison of sensitivity between different endpoints. For this study,
480 we selected a concentration range that has already been chosen in other *in vitro* DNT assays and has
481 elicited little to no cytotoxicity (Frank et al., 2017; Masjosthusmann et al., 2020). To discriminate
482 specific from unspecific effects, we assessed the cytotoxicity of each compound on a weekly level
483 during the 35-day culture period (P7 “Endpoint Selectivity”). Another crucial requirement for assay
484 development is the selection of endpoint-specific controls, altering the endpoint by known mode of
485 action, both negatively and positively. In the present study, Bis-I, a PKC inhibitor was selected as an
486 endpoint-specific control (P8 “Endpoint-selective controls). In primary rat cortical cells the inhibition
487 of PKC blocked the local astrocytic contact and thus the facilitation of excitatory synaptogenesis
488 throughout the neuron (Hama et al., 2004). Furthermore, Bis-I inhibits neurite outgrowth in PC-12 cells
489 (Das et al., 2004), rat cortical neurons, and human iPSC-derived neurons (Druwe et al., 2016). In
490 particular, in MEA experiments, Bis-I decreased the firing and bursting rates of rat neural networks *in*
491 *vitro* (Robinette et al., 2011). Within the hNNF assay, Bis-I reliably reduced network parameters e.g.
492 burst duration, networkburst percentage and network synchronicity (AUNCC). Due to the enhanced
493 variability of the mean firing rate, no significant effect of Bis-I could be observed over all conducted
494 experimental runs. Nevertheless, Bis-I is an appropriate endpoint-specific control for assessing neural
495 network activity *in vitro*. As a negative control compound, Acetaminophen showed no effect on
496 network activity. A plethora of studies confirmed the use of Acetaminophen as an apt negative control
497 for DNT *in vitro* testing (Radio et al., 2008; Stern et al., 2014; Brown et al., 2016; Masjosthusmann et
498 al., 2020). Following the recommendations of Crofton and colleagues, a training set of chemicals
499 should be designed and assayed (P9 “Training Set Chemicals”), after demonstrating that the test
500 method has the aforementioned characteristics. Chemicals should be included that produce a reliable
501 effect on the endpoint in focus and chemicals that do not, which allows both specificity and sensitivity
502 of the assay to be determined (P11 “Specificity and Sensitivity”). The hNNF assay was established and
503 used within a research project with a focus on pesticides. In consideration of the high cost involved in

504 performing substances screening in the assay, it was not possible to distinguish between training and
505 testing set of chemicals during the establishment process. Instead, we selected pesticides that have
506 different DNT potentials, according to several *in vivo* and *in vitro* studies (P10 “Testing Set Chemicals”).
507 Pyrethroids, for example, are linked to epidemiological studies that report neurodevelopmental
508 disorders during childhood after pyrethroid pesticides exposure (Oulhote and Bouchard, 2013; Xue et
509 al., 2013; Pitzer et al., 2021). Especially deltamethrin is a thoroughly studied type II pyrethroid, for
510 which animal studies reported long-term effects on the brain (summarized in Pitzer et al., 2021), which
511 was also observed *in vitro* (Shafer et al., 2008; Masjosthusmann et al., 2020). In contrast, the
512 neonicotinoid dinotefuran was described as DNT negative *in vivo* (Sheets et al., 2016) and also
513 recommended as a negative tool compound for alternative DNT test methods (Aschner et al., 2017).
514 In the future the hNNF assay will also be challenged with more chemicals that are well-described DNT
515 positive and negative compounds to assess specificity and sensitivity of the assay and to enhance the
516 readiness of the test method (Bal-Price et al. 2018). Currently, the academic setup of the hNNF assay
517 allows parallel testing of 12 compounds (n=1) within the 35-day experimental period. However, it is
518 possible to increase the throughput by increasing the plate size format from 48- to 96-well or by
519 introducing automation (P12 “HighThroughput”). Principles 13-15 deal with documentation and
520 transferability of the test method and sharing of assessed data. Progress is currently being made with
521 regard to these points as well. Currently, a standardized protocol is being transferred to a laboratory
522 of the U.S. EPA. After initial establishment of the assay in the collaborating laboratory, the hNNF assay
523 will be challenged with a set of test substances to inform about the robustness and inter-laboratory
524 transferability of the assay.

525 In summary, the hNNF assay fulfills the majority of the principles proposed by Crofton for the
526 establishment of *in vitro* DNT assays for substance screening. Currently, the low number of tested
527 chemicals defines the lack of readiness of the assay (Phase I Readiness Score B, Phase II Readiness
528 Score C; Bal-Price et al., 2018) and the improvements required for the assay to be ready will be tackled
529 in the future by testing of known DNT positive substances (Aschner et al., 2017).

530

531 The hNNF assay compared to its rat counterpart

532 The hNNF assay was established to model neural network formation and function in a human-based
533 cell model and to become a valuable addition to the current DNT-IVB, which comprises 17 different
534 test methods, able to measure changes in key neurodevelopmental processes (Masjosthusmann et al.,
535 2020; Crofton and Mundy, 2021). Neural network formation and function is currently modeled in an
536 assay based on rat primary cortical cells (rNNF), assessing the developmental effects of chemicals over

537 12 days of differentiation. In this rat cell-based NNF assay, exposure with the test substances starts
 538 two hours after cell plating on 48-well MEAs and is refreshed on a regular basis with cytotoxicity
 539 assessment solely on the last day *in vitro* (Brown et al., 2016). It is important to mention that we aligned
 540 the hNNF assay with the parameter set of the rNNF assay and thus both assays provide comparable
 541 parameters of network development (e.g. number of active electrodes or burst duration) to reduce
 542 uncertainty. **Table 2** juxtaposes the results obtained in this study with rNNF data (Frank et al., 2017).
 543 Comparing the BMC₅₀ values of the most sensitive endpoint (MSE) between the hNNF and rNNF assay,
 544 it becomes clear that the observed positive hits differ in sensitivity across all substances. The rNNF
 545 seems to be more sensitive as it detects effects on network activity even at lower concentrations of
 546 the tested substances, e.g. Deltamethrin (BMC₅₀ MSE hNNF: 2.74 μM; BMC₅₀ MSE rNNF: 0.5 μM).
 547 Aldicarb and chlorpyrifos were negative in the hNNF, but altered network formation in the rNNF assay.
 548 Acetaminophen was identified as a negative in both assays.

549 **Table 2:** Comparison of benchmark concentration (BMC₅₀) values of the most sensitive endpoint (MSE) for
 550 chemicals (same CAS No.) tested in the hNNF (this study) and rNNF assay (Frank et al., 2017). ↑ indicates an
 551 inductive effect (BMC₅₀).

	Acetaminophen	Aldicarb	Carbaryl	Chlorpyrifos	Deltamethrin	Fipronil	Imidacloprid
BMC₅₀ MSE hNNF	no hit	no hit	17.31↑	no hit	2.74	11.48 ↑	15.51
BMC₅₀ MSE rNNF	no hit	0.66	0.08	1.4	0.5	1.33	9.99

552

553 The hNNF and rNNF assay are referred to as complementary assays because they measure similar
 554 endpoints, i.e. several MEA parameters, but differ with regards to species (rat vs. human) and assay
 555 technology (beginning and wash-out of compounds before MEA recordings). Therefore, differences in
 556 data obtained within these assays are not necessarily evidential of a false detection (Crofton and
 557 Mundy, 2021). These differences may be justified by several distinctions in the assay setup, i.e. species
 558 differences and exposure schemes. The hNNF and rNNF assays are based on the same basic cell types,
 559 namely neurons and astrocytes, but derived from different species (hNNF: human iPSC-derived
 560 neurons and primary astroglia; rNNF: rat primary neocortical cells). It is widely accepted that the
 561 predictability of non-human-based assays for human health is limited by species differences (Leist and
 562 Hartung, 2013). Also primary neural progenitor cells (NPC) derived from rats (PND5), are more sensitive
 563 towards exposure with DNT compounds compared to time-matched primary human NPCs *in vitro*
 564 (Baumann et al., 2016). These two systems differ not only in their sensitivity but also with regard to
 565 their molecular equipment notwithstanding similar cellular functions (e.g. NPC migration and
 566 differentiation; Masjosthusmann et al., 2018). Recently, the co-culture system applied in this study

567 was used for comparing acute effects of neurotoxic compounds on network activity to rodent cultures
568 (rNNF) and revealed a considerable delay in human iPSC-derived neuronal and glial co-culture
569 compared to rat cortical cultures (Saavedra et al., 2021). In general, the developing rat brain exhibits
570 some crucial differences from human brain development *in vivo*, such as the absence of gyrification,
571 which adds complexity to the human brain (Dubois et al., 2008). Furthermore it has been
572 demonstrated, that embryonic day (E) 18 and E21 during rat brain development match with week 8-9
573 and week 15-16 after fertilization in human embryo, when looking at neurogenesis (Bayer et al., 1993).
574 The faster maturation of rodent cells compared to human cells *in vitro* was also suggested by
575 Masjosthusmann et al. (2018).

576 As the compound set presented in **Table 2** is rather small and focussed on pesticides, we cannot draw
577 general conclusions about species-specific sensitivity of the rNNF and hNNF assays. As suggested by
578 Bauman et al. (2016), testing of additional compounds with known MoA required to infer more general
579 species-specific sensitivity. Nevertheless, our data highlights the importance of considering species
580 specificities when comparing screening results.

581 Besides the species, experimental procedures differ between the human and rat NNF assays and may
582 also lead to differences in assay sensitivity. Two major exposure differences are crucial. First, the
583 timepoint when the compound is administered differs between hNNF and rNNF assay. Rat cortical
584 cultures are exposed to the compound 2 hours after seeding the cell on MEAs, whereas the first day
585 of dosing in hNNF experiments is DIV7, when first single spike activities are visible. The respective
586 networks are at different stages of development at this time, i.e. in contrast to human cells, rat cortical
587 cells are barely established in the culture dish. Not yet established cells shortly after the plating process
588 may be more susceptible to substance exposure than networks that have already been able to
589 differentiate for a week in chemical-free medium. In the rNNF assay, early processes like neurite
590 initiation and outgrowth, as well as glial proliferation are potentially disrupted within the first 24h
591 (Harrill et al., 2011; Frank et al., 2017), whereas these processes can proceed undisturbed during the
592 first seven days of differentiation and contribute to network development in the hNNF assay. Both
593 assays thus depict different stages of neural network development and hence include different
594 windows of neurodevelopmental processes. In addition, the hNNF culture medium is supplemented
595 with fetal bovine serum, whereas the rNNF medium is not.

596 Secondly, the washout of the respective compound 24h prior to the recording is a unique feature of
597 the hNNF assay and aims at minimizing acute substance effects during MEA recordings. There is
598 evidence that specific substances directly target synaptic receptors and acutely affect brain function.
599 For example, the NMDA receptor (NMDAR) is a prime target of the heavy metal lead, leading to the
600 inhibition of glutamatergic synapse activity (Toscano and Guilarte, 2005). To diminish the

601 measurement of these acute effects and to only assess the effects of substances on neural network
602 development, we introduced washout steps into the experimental procedure of the hNNF. In
603 comparison to the rNNF results (**Tab. 2**) it is possible that presence of compounds during MEA
604 measurements contributes to higher sensitivity of the rat versus the human NNF assay.

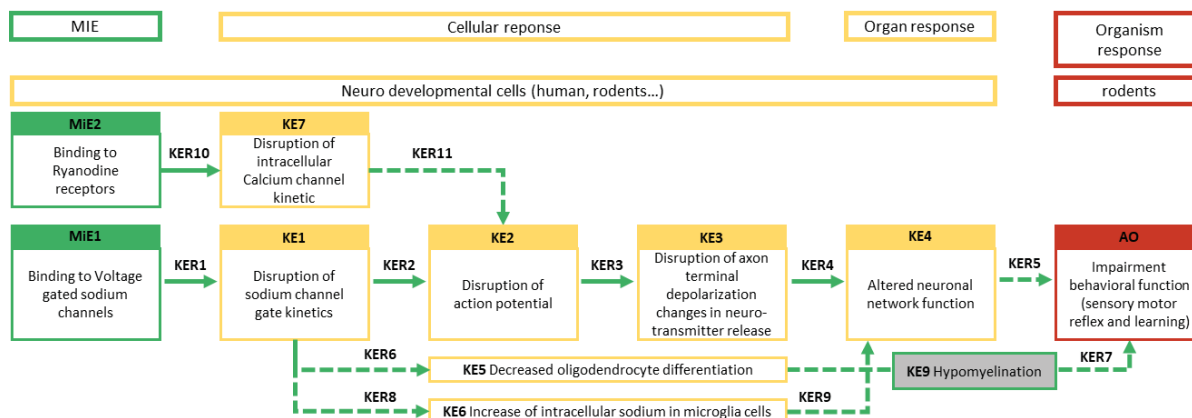
605 All of the aforementioned variations in assay setup and biology, either alone or in combination, can
606 explain the discrepancies in sensitivity between the two test methods. In the future, exposure schemes
607 of the the two NNF assays should be harmonized in order to understand the true nature of species
608 differences concerning neural network formation. This might substantially help extrapolating from rat
609 *in vivo* studies to humans using the parallelogram approach (Baumann et al. 2016).

610

611 Use of hNNF data on deltamethrin for the development of a putative AOP

612 In 2021 the EFSA developed an IATA case study with the goal of including all available *in vivo* and *in*
613 *vitro* data, among others the data generated within the DNT-IVB for DNT hazard identification for the
614 Type II pyrethroid insecticide deltamethrin (Crofton and Mundy, 2021; Hernández-Jerez et al., 2021).
615 Epidemiological studies revealed associations between childhood exposure to pyrethroids like
616 deltamethrin and neurodevelopmental disorders, e.g. attention deficit hyperactivity disorder or
617 autism spectrum disorder (Oulhote and Bouchard, 2013; Shelton et al., 2014; Wagner-Schuman et al.,
618 2015). As previously shown, deltamethrin negatively influenced 5 of 14 parameters describing network
619 function with “Number of spikes per networkburst” as the most sensitive endpoint within the hNNF
620 assay (BMC_{50} 2.7 μ M). Here, interference with voltage-gated sodium channels (VGSC) is the most
621 commonly known mode-of-action for pyrethroid insecticides like deltamethrin (Tapia et al., 2020),
622 therefore representing one of two molecular initiating (MiE) events within the AOP network (**Fig. 6**).
623 This MiE is followed by key events (KE) 1-6 and 9, describing different cellular responses, like the
624 disruption of sodium channel gate kinetics, leading to disruption of action potential and in the end
625 cumulate in an impaired behavioural function (adverse outcome). KE4 describes the alteration of
626 neural network function as shown also by data assessed in the rNNF (BMC_{50} 0.5 μ M; **Tab.2**) and hNNF
627 assay. The 5-fold higher BMC of the hNNF assay compared to the rNNF assay might be explained by
628 the different exposure paradigm and/or the different species as discussed above in more detail.
629 Compared to the current *in vivo* guideline fo DNT testing, the DNT-IVB is more cost-efficient, able to
630 screen substances in higher throughput and thus, enables the generation of large data sets for
631 chemical libraries with unknown DNT hazards. Furthermore, potential mechanisms or processes that
632 are disrupted by a chemical agent can be revealed and used for the development of adverse outcome
633 pathways (AOP) and also set a new focus for more hypothesis-driven *in-vivo* studies (Hernández-Jerez

634 et al., 2021). This case study and the inclusion of hNNF data on deltamethrin exposure showed the
 635 applicability of the hNNF assay for hazard identification and characterization, consistent with the other
 636 assays of the DNT-IVB. The 5-fold higher BMC of the hNNF assay compared to the rNNF assay might be
 637 explained by the different exposure paradigm and/or the different species as discussed above in more
 638 detail.



639
 640 **Figure 7: AOP network on deltamethrin postulated by the EFSA Panel on Plant Protection Products and their**
 641 **Residues.** Non-adjacent key events for which the biological reasonability and/or empirical evidence is less
 642 assured, are marked by dashed lines. MIE: molecular initiating event; KE: Key event; KER: key event relationship;
 643 AO: adverse outcome. Adapted from Hernández-Jerez et al., 2021.

644
 645 The presented study provides insight into the establishment of a novel new approach method,
 646 assessing alterations on neural network formation and function, using an hiPSC-derived co-culture of
 647 neurons and primary astroglia. The cell model comprises a broad variety of genes expressed exclusively
 648 in neurons and astrocytes as a prerequisite for neural network function. For example, together with
 649 the rNNF assay, it is capable of representing NMDAR expression and assessing any MoA involving
 650 NMDAR, which distinguishes these NNF assays from other assays of the DNT-IVB (Masjosthusmann et
 651 al., 2020). A proactive establishment of the assay provided already a medium readiness of the assay
 652 for use in regulatory screening approaches and the testing of 28 substances revealed the suitability of
 653 the assay for screening environmental chemicals, like pesticides. In the future, the throughput of the
 654 hNNF assay as well as its robustness and specificity will be increased by testing additional substances,
 655 thereby enlarging the chemical space, to present a suitable addition to the current DNT-IVB and close
 656 one of the identified gaps regarding network formation and function.

657
 658

659 **Funding:** This work was supported by the Danish Environmental Protection Agency (EPA) under the
660 grant number MST-667-00205.

661 **Conflict of interest:** KB, AD, SM and EF are shareholders of the company DNTOX that provides DNT-
662 IVB assay services and DH, CN, JW and PZ have been or are currently employed by NeuCyte Inc., a
663 company that commercially distributes the iN:glia co-culture described in this study and all declare no
664 potential conflicts of interest with respect to the research in this article. FB and EK have no conflict of
665 interest to declare.

666 **Availability of data:** The dataset generated during and/or analyzed during the current study is
667 available from the corresponding author upon reasonable request.

668

669

670 Aschner, M., Ceccatelli, S., Daneshian, M. et al. (2017). *Reference compounds for alternative test*
671 *methods to indicate developmental neurotoxicity (DNT) potential of chemicals: Example lists &*
672 *criteria for their selection & use.* Elsevier GmbH. <https://doi.org/10.14573/altex.1604201>.

673 Bal-Price, A., Crofton, K. M., Leist, M. et al. (2015). International STakeholder NETwork (ISTNET):
674 creating a developmental neurotoxicity (DNT) testing road map for regulatory purposes. *Arch*
675 *Toxicol* 89, 269–287. <https://doi.org/10.1007/S00204-015-1464-2>.

676 Bal-Price, A., Hogberg, H. T., Crofton, K. M. et al. (2018). Recommendation on test readiness criteria
677 for new approach methods in toxicology: Exemplified for developmental neurotoxicity. *ALTEX*
678 35, 306–352. <https://doi.org/10.14573/altex.1712081>.

679 Bartmann, K., Hartmann, J., Kapr, J. et al. (2021). Measurement of Electrical Activity of Differentiated
680 Human iPSC-Derived Neurospheres Recorded by Microelectrode Arrays (MEA). In J. Llorens and
681 M. Barenys (eds.), *Experimental Neurotoxicology Methods. Neuromethods, vol 172* (473–488).
682 New York: Humana. Available at: 10.1007/978-1-0716-1637-6_22.

683 Baumann, J., Barenys, M., Gassmann, K. et al. (2014). Comparative human and rat “neurosphere
684 assay” for developmental neurotoxicity testing. *Curr Protoc Toxicol* 1, 1–24.
685 <https://doi.org/10.1002/0471140856.tx1221s59>.

686 Baumann, J., Dach, K., Barenys, M. et al. (2015). Application of the Neurosphere Assay for DNT
687 Hazard Assessment: Challenges and Limitations. https://doi.org/10.1007/7653_2015_49.

688 Baumann, J., Gassmann, K., Masjosthusmann, S. et al. (2016). Comparative human and rat
689 neurospheres reveal species differences in chemical effects on neurodevelopmental key events.

690 *Arch Toxicol* 90, 1415–1427. <https://doi.org/10.1007/S00204-015-1568-8>.

691 Bayer, S. A., Altman, J., Russo, R. J. et al. (1993). Timetables of Neurogenesis in the Human Brain
692 Based on Experimentally Determined Patterns in the Rat. *Neurotoxicology* 14, 83–144

693 Bennett, D., Bellinger, D. C., Birnbaum, L. S. et al. (2016). Project TENDR: Targeting Environmental
694 Neuro-Developmental Risks The TENDR Consensus Statement. *Environ Health Perspect* 124,
695 A118–A122. <https://doi.org/10.1289/EHP358>.

696 Bjørling-Poulsen, M., Andersen, H. R. and Grandjean, P. (2008). Potential developmental
697 neurotoxicity of pesticides used in Europe. *Environ Heal A Glob Access Sci Source* 7.
698 <https://doi.org/10.1186/1476-069X-7-50>.

699 Brown, J. P., Hall, D., Frank, C. L. et al. (2016). Evaluation of a microelectrode array-based assay for
700 neural network ontogeny using training set chemicals. *Toxicol Sci* 154, 126–139.
701 <https://doi.org/10.1093/toxsci/kfw147>.

702 Coecke, S., Goldberg, A. M., Allen, S. et al. (2007). Workgroup Report: Incorporating In Vitro
703 Alternative Methods for Developmental Neurotoxicity into International Hazard and Risk
704 Assessment Strategies. *Environ Health Perspect* 115, 924–931.
705 <https://doi.org/10.1289/ehp.9427>.

706 Crofton, K., Fritsche, E., Ylikomi, T. et al. (2014). International STakeholder NETwork (ISTNET) for
707 creating a developmental neurotoxicity testing (DNT) roadmap for regulatory purposes. *ALTEX*
708 31, 223–224. <https://doi.org/10.14573/ALTEX.1402121>.

709 Crofton, K. M. and Mundy, W. R. (2021). External Scientific Report on the Interpretation of Data from
710 the Developmental Neurotoxicity In Vitro Testing Assays for Use in Integrated Approaches for
711 Testing and Assessment. *EFSA Support Publ* 18. <https://doi.org/10.2903/SP.EFSA.2021.EN-6924>.

712 Crofton, K. M., Mundy, W. R., Lein, P. J. et al. (2011). Developmental neurotoxicity testing:
713 Recommendations for developing alternative methods for the screening and prioritization of
714 chemicals. *ALTEX* 28, 9–15. <https://doi.org/10.14573/altex.2011.1.009>.

715 Crofton, K. M., Mundy, W. R. and Shafer, T. J. (2012). Developmental neurotoxicity testing: a path
716 forward. *Congenit Anom* 52, 140–146. <https://doi.org/10.1111/j.1741-4520.2012.00377.x>.

717 Dach, K., Bendt, F., Huebenthal, U. et al. (2017). BDE-99 impairs differentiation of human and mouse
718 NPCs into the oligodendroglial lineage by species-specific modes of action. *Sci Rep* 7.
719 <https://doi.org/10.1038/SREP44861>.

720 Das, K. P., Freudenrich, T. M. and Mundy, W. R. (2004). Assessment of PC12 cell differentiation and

721 neurite growth: a comparison of morphological and neurochemical measures. *Neurotoxicol*
722 *Teratol* 26, 397–406. <https://doi.org/10.1016/J.NTT.2004.02.006>.

723 Druwe, I., Freudenrich, T. M., Wallace, K. et al. (2016). Comparison of Human Induced Pluripotent
724 Stem Cell-Derived Neurons and Rat Primary Cortical Neurons as In Vitro Models of Neurite
725 Outgrowth. *Appl Vitro Toxicol* 2, 26–36. <https://doi.org/10.1089/aivt.2015.0025>.

726 Druwe, I., Freudenrich, T. M., Wallace, K. et al. (2015). Sensitivity of neuroprogenitor cells to
727 chemical-induced apoptosis using a multiplexed assay suitable for high-throughput screening.
728 *Toxicology* 333, 14–24. <https://doi.org/10.1016/J.TOX.2015.03.011>.

729 Dubois, J., Benders, M., Borradori-Tolsa, C. et al. (2008). Primary cortical folding in the human
730 newborn: an early marker of later functional development. *Brain* 131, 2028–2041.
731 <https://doi.org/10.1093/BRAIN/AWN137>.

732 EFSA (2013). Scientific Opinion on the developmental neurotoxicity potential of acetamiprid and
733 imidacloprid. *EFSA J* 11. <https://doi.org/10.2903/j.efsa.2013.3471>.

734 Frank, C. L., Brown, J. P., Wallace, K. et al. (2017). Developmental neurotoxicants disrupt activity in
735 cortical networks on microelectrode arrays: Results of screening 86 compounds during neural
736 network formation. *Toxicol Sci* 160, 121–135. <https://doi.org/10.1093/toxsci/kfx169>.

737 Fritsche, E. (2017). *Report on Integrated Testing Strategies for the identification and evaluation of*
738 *chemical hazards associated with the developmental neurotoxicity (DNT), to facilitate*
739 *discussions at the Joint EFSA/OECD Workshop on DNT.*
740 [https://doi.org/ENV/JM/MONO\(2017\)4/ANN1](https://doi.org/ENV/JM/MONO(2017)4/ANN1).

741 Fritsche, E., Alm, H., Baumann, J. et al. (2015). Literature review on in vitro and alternative
742 Developmental Neurotoxicity (DNT) testing methods. *EFSA Support Publ* 12, 778E.
743 <https://doi.org/10.2903/SP.EFSA.2015.EN-778>.

744 Fritsche, E., Barenys, M., Klose, J. et al. (2018). Current availability of stem cell-Based in vitro
745 methods for developmental neurotoxicity (DNT) testing. *Toxicol Sci* 165, 21–30.
746 <https://doi.org/10.1093/toxsci/kfy178>.

747 Fritsche, E., Crofton, K. M., Hernandez, A. F. et al. (2017). OECD/EFSA workshop on developmental
748 neurotoxicity (DNT): The use of non-animal test methods for regulatory purposes. *ALTEX* 34,
749 311–315. <https://doi.org/10.14573/altex.1701171s>.

750 Fritsche, E., Crofton, K. M., Hernandez, A. F. et al. (2017). OECD/EFSA workshop on developmental
751 neurotoxicity (DNT): The use of non-animal test methods for regulatory purposes. *ALTEX* -

752 *Altern to Anim Exp* 34, 311–315. <https://doi.org/10.14573/ALTEX.1701171>.

753 Fritsche, E., Grandjean, P., Crofton, K. M. et al. (2018). Consensus statement on the need for
754 innovation, transition and implementation of developmental neurotoxicity (DNT) testing for
755 regulatory purposes. *Toxicol Appl Pharmacol* 354, 3–6.
756 <https://doi.org/10.1016/j.taap.2018.02.004>.

757 Goldman, L. R. and Koduru, S. (2000). Chemicals in the environment and developmental toxicity to
758 children: a public health and policy perspective. *Environ Health Perspect* 108, 443.
759 <https://doi.org/10.1289/EHP.00108S3443>.

760 Grandjean, P. and Landrigan, P. (2006). Developmental neurotoxicity of industrial chemicals. *Lancet*
761 368, 2167–2178. [https://doi.org/10.1016/S0140-6736\(06\)69665-7](https://doi.org/10.1016/S0140-6736(06)69665-7).

762 Hama, H., Hara, C., Yamaguchi, K. et al. (2004). PKC signaling mediates global enhancement of
763 excitatory synaptogenesis in neurons triggered by local contact with astrocytes. *Neuron* 41,
764 405–415. [https://doi.org/10.1016/S0896-6273\(04\)00007-8](https://doi.org/10.1016/S0896-6273(04)00007-8).

765 Hardy, A., Benford, D., Halldorsson, T. et al. (2017). Guidance on the use of the weight of evidence
766 approach in scientific assessments. *EFSA J* 15, e04971.
767 <https://doi.org/10.2903/J.EFSA.2017.4971>.

768 Harrill, J. A., Freudenrich, T. M., Machacek, D. W. et al. (2010). Quantitative assessment of neurite
769 outgrowth in human embryonic stem cell-derived hN2 cells using automated high-content
770 image analysis. *Neurotoxicology* 31, 277–290. <https://doi.org/10.1016/J.NEURO.2010.02.003>.

771 Harrill, J. A., Freudenrich, T., Wallace, K. et al. (2018). Testing for developmental neurotoxicity using a
772 battery of in vitro assays for key cellular events in neurodevelopment. *Toxicol Appl Pharmacol*
773 354, 24–39. <https://doi.org/10.1016/J.TAAP.2018.04.001>.

774 Harrill, J. A., Robinette, B. L., Freudenrich, T. et al. (2013). Use of high content image analyses to
775 detect chemical-mediated effects on neurite sub-populations in primary rat cortical neurons.
776 *Neurotoxicology* 34, 61–73. <https://doi.org/10.1016/J.NEURO.2012.10.013>.

777 Harrill, J. A., Robinette, B. L. and Mundy, W. R. (2011). Use of high content image analysis to detect
778 chemical-induced changes in synaptogenesis in vitro. *Toxicol Vitr* 25, 368–387.
779 <https://doi.org/10.1016/j.tiv.2010.10.011>.

780 Hernández-Jerez, A., Adriaanse, P., Aldrich, A. et al. (2021). Development of Integrated Approaches
781 to Testing and Assessment (IATA) case studies on developmental neurotoxicity (DNT) risk
782 assessment. *EFSA J* 19, 63. <https://doi.org/10.2903/j.efsa.2021.6599>.

783 Hoelting, L., Klima, S., Karreman, C. et al. (2016). Stem Cell-Derived Immature Human Dorsal Root
784 Ganglia Neurons to Identify Peripheral Neurotoxicants. *Stem Cells Transl Med* 5, 476–487.
785 <https://doi.org/10.5966/SCTM.2015-0108>.

786 Hofrichter, M., Nimtz, L., Tigges, J. et al. (2017). Comparative performance analysis of human iPSC-
787 derived and primary neural progenitor cells (NPC) grown as neurospheres in vitro. *Stem Cell Res*
788 25, 72–82. <https://doi.org/10.1016/J.SCR.2017.10.013>.

789 Hyvärinen, T., Hyysalo, A., Kapucu, F. E. et al. (2019). Functional characterization of human
790 pluripotent stem cell-derived cortical networks differentiated on laminin-521 substrate:
791 comparison to rat cortical cultures. *Sci Rep* 9, 17125. [https://doi.org/10.1038/s41598-019-](https://doi.org/10.1038/s41598-019-53647-8)
792 53647-8.

793 Ishii, M. N., Yamamoto, K., Shoji, M. et al. (2017). Human induced pluripotent stem cell (hiPSC)-
794 derived neurons respond to convulsant drugs when co-cultured with hiPSC-derived astrocytes.
795 *Toxicology* 389, 130–138. <https://doi.org/10.1016/j.tox.2017.06.010>.

796 Johnston, G. A. R. (2013). Advantages of an antagonist: bicuculline and other GABA antagonists. *Br J*
797 *Pharmacol* 169, 328. <https://doi.org/10.1111/BPH.12127>.

798 Johnstone, A. F. M., Gross, G. W., Weiss, D. G. et al. (2010). Microelectrode arrays: A physiologically
799 based neurotoxicity testing platform for the 21st century. *Neurotoxicology* 31, 331–350.
800 <https://doi.org/10.1016/j.neuro.2010.04.001>.

801 Klose, J., Tigges, J., Masjosthusmann, S. et al. (2021). TBBPA targets converging key events of human
802 oligodendrocyte development resulting in two novel AOPs. *ALTEX* 38, 215–234.
803 <https://doi.org/10.14573/altex.2007201>.

804 Koch, K., Bartmann, K., Hartmann, J. et al. (2022). Scientific validation of human Neurosphere Assays
805 for developmental neurotoxicity evaluation. *Front Press O*, 1–38.
806 <https://doi.org/10.3389/FTOX.2022.816370>.

807 Kosnik, M. B., Strickland, J. D., Marvel, S. W. et al. (2020). Concentration–response evaluation of
808 ToxCast compounds for multivariate activity patterns of neural network function. *Arch Toxicol*
809 94, 469–484. <https://doi.org/10.1007/s00204-019-02636-x>.

810 Krug, A. K., Balmer, N. V., Matt, F. et al. (2013). Evaluation of a human neurite growth assay as
811 specific screen for developmental neurotoxicants. *Arch Toxicol* 87, 2215–2231.
812 <https://doi.org/10.1007/s00204-013-1072-y>.

813 Kuehn, B. M. (2010). Increased risk of ADHD associated with early exposure to pesticides, PCBs. *JAMA*

814 - *J Am Med Assoc* 304, 27–28. <https://doi.org/10.1001/JAMA.2010.860>.

815 Leist, M. and Hartung, T. (2013). Reprint: Inflammatory findings on species extrapolations: Humans
816 are definitely no 70-kg mice1. *ALTEX* 30, 227–230. <https://doi.org/10.14573/altex.2013.2.227>.

817 Little, D., Ketteler, R., Gissen, P. et al. (2019). Using stem cell–derived neurons in drug screening for
818 neurological diseases. *Neurobiol Aging* 78, 130–141.
819 <https://doi.org/10.1016/J.NEUROBIOLAGING.2019.02.008>.

820 Masjosthusmann, S., Becker, D., Petzuch, B. et al. (2018). A transcriptome comparison of time-
821 matched developing human, mouse and rat neural progenitor cells reveals human uniqueness.
822 *Toxicol Appl Pharmacol* 354, 40–55. <https://doi.org/10.1016/j.taap.2018.05.009>.

823 Masjosthusmann, S., Blum, J., Bartmann, K. et al. (2020). *Establishment of an a priori protocol for the*
824 *implementation and interpretation of an in-vitro testing battery for the assessment of*
825 *developmental neurotoxicity*. Wiley. <https://doi.org/10.2903/sp.efsa.2020.en-1938>.

826 National Research Council (2000). *Scientific Frontiers in Developmental Toxicology and Risk*
827 *Assessment*. National Academies Press. <https://doi.org/10.17226/9871>.

828 Nimtz, L., Hartmann, J., Tigges, J. et al. (2020). Characterization and application of electrically active
829 neuronal networks established from human induced pluripotent stem cell-derived neural
830 progenitor cells for neurotoxicity evaluation. *Stem Cell Res* 45, 101761.
831 <https://doi.org/10.1016/J.SCR.2020.101761>.

832 Nimtz, L., Klose, J., Masjosthusmann, S. et al. (2019). The Neurosphere Assay as an In Vitro Method
833 for Developmental Neurotoxicity (DNT) Evaluation. *Neuromethods* 145, 141–168.
834 https://doi.org/10.1007/978-1-4939-9228-7_8.

835 Nyffeler, J., Dolde, X., Krebs, A. et al. (2017). Combination of multiple neural crest migration assays to
836 identify environmental toxicants from a proof-of-concept chemical library. *Arch Toxicol* 91,
837 3613–3632. <https://doi.org/10.1007/s00204-017-1977-y>.

838 Ockleford, C., Adriaanse, P., Hougaard Bennekou, S. et al. (2018). Scientific opinion on pesticides in
839 foods for infants and young children. *EFSA J* 16. <https://doi.org/10.2903/J.EFSA.2018.5286>.

840 Odawara, A., Katoh, H., Matsuda, N. et al. (2016). Physiological maturation and drug responses of
841 human induced pluripotent stem cell-derived cortical neuronal networks in long-term culture.
842 <https://doi.org/10.1038/srep26181>.

843 Odawara, A., Matsuda, N., Ishibashi, Y. et al. (2018). Toxicological evaluation of convulsant and
844 anticonvulsant drugs in human induced pluripotent stem cell-derived cortical neuronal

845 networks using an MEA system. *Sci Rep* 8, 10416. <https://doi.org/10.1038/s41598-018-28835-7>.

846 OECD (2007). OECD guidelines for the testing of chemicals/section 4:health effects. Test No. 426:
847 developmental neurotoxicity study. Available at:
848 <http://www.oecd.org/dataoecd/20/52/37622194.pdf> [Accessed July 22, 2021].

849 Okado, N., Kakimi, S. and Kojima, T. (1979). Synaptogenesis in the cervical cord of the human
850 embryo: sequence of synapse formation in a spinal reflex pathway. *J Comp Neurol* 184, 491–
851 517. <https://doi.org/10.1002/CNE.901840305>.

852 Oulhote, Y. and Bouchard, M. F. (2013). Urinary metabolites of organophosphate and pyrethroid
853 pesticides and behavioral problems in Canadian children. *Environ Health Perspect* 121, 1378–
854 1384. <https://doi.org/10.1289/EHP.1306667>.

855 Paparella, M., Bennekou, S. H. and Bal-Price, A. (2020). An analysis of the limitations and
856 uncertainties of in vivo developmental neurotoxicity testing and assessment to identify the
857 potential for alternative approaches. *Reprod Toxicol* 96, 327–336.
858 <https://doi.org/10.1016/J.REPROTOX.2020.08.002>.

859 Pitzer, E. M., Williams, M. T. and Vorhees, C. V. (2021). Effects of pyrethroids on brain development
860 and behavior: Deltamethrin. *Neurotoxicol Teratol* 87.
861 <https://doi.org/10.1016/J.NTT.2021.106983>.

862 Radio, N. M., Breier, J. M., Shafer, T. J. et al. (2008). Assessment of chemical effects on neurite
863 outgrowth in PC12 cells using high content screening. *Toxicol Sci* 105, 106–118.
864 <https://doi.org/10.1093/TOXSCI/KFN114>.

865 Robinette, B. L., Harrill, J. A., Mundy, W. R. et al. (2011). In vitro assessment of developmental
866 neurotoxicity: Use of microelectrode arrays to measure functional changes in neuronal network
867 ontogeny. *Front Neuroeng* 0, 1–9. <https://doi.org/10.3389/FNENG.2011.00001/BIBTEX>.

868 Rodier, P. M. (1995). Developing brain as a target of toxicity. In *Environmental Health Perspectives*
869 (73–76). <https://doi.org/10.1289/ehp.95103s673>.

870 Saavedra, L., Wallace, K., Freudenrich, T. F. et al. (2021). Comparison of acute effects of neurotoxic
871 compounds on network activity in human and rodent neural cultures. *Toxicol Sci* 180, 295–312.
872 <https://doi.org/10.1093/TOXSCI/KFAB008>.

873 Sachana, M., Bal-Price, A., Crofton, K. M. et al. (2019). International Regulatory and Scientific Effort
874 for Improved Developmental Neurotoxicity Testing. *Toxicol Sci* 167, 45–57.
875 <https://doi.org/10.1093/toxsci/kfy211>.

876 Sagiv, S. K., Thurston, S. W., Bellinger, D. C. et al. (2010). Prenatal organochlorine exposure and
877 behaviors associated with attention deficit hyperactivity disorder in school-aged children. *Am J*
878 *Epidemiol* 171, 593–601. <https://doi.org/10.1093/AJE/KWP427>.

879 Schmuck, M. R., Temme, T., Dach, K. et al. (2017). Omnisphero: a high-content image analysis (HCA)
880 approach for phenotypic developmental neurotoxicity (DNT) screenings of organoid
881 neurosphere cultures in vitro. *Arch Toxicol* 91, 2017–2028. [https://doi.org/10.1007/s00204-](https://doi.org/10.1007/s00204-016-1852-2)
882 016-1852-2.

883 Shafer, T. J. (2019). Application of Microelectrode Array Approaches to Neurotoxicity Testing and
884 Screening. In (275–297). https://doi.org/10.1007/978-3-030-11135-9_12.

885 Shafer, T. J., Rijal, S. O. and Gross, G. W. (2008). Complete inhibition of spontaneous activity in
886 neuronal networks in vitro by deltamethrin and permethrin. *Neurotoxicology* 29, 203–212.
887 <https://doi.org/10.1016/j.neuro.2008.01.002>.

888 Sheets, L. P., Li, A. A., Minnema, D. J. et al. (2016). A critical review of neonicotinoid insecticides for
889 developmental neurotoxicity. *Crit Rev Toxicol* 46, 153–190.
890 <https://doi.org/10.3109/10408444.2015.1090948>.

891 Shelton, J. F., Geraghty, E. M., Tancredi, D. J. et al. (2014). Neurodevelopmental disorders and
892 prenatal residential proximity to agricultural pesticides: The charge study. *Environ Health*
893 *Perspect* 122, 1103–1109. <https://doi.org/10.1289/EHP.1307044>.

894 Smirnova, L., Hogberg, H. T., Leist, M. et al. (2014). Food for thought...: Developmental neurotoxicity
895 - Challenges in the 21st century and in vitro opportunities. *ALTEX* 31, 129–156.
896 <https://doi.org/10.14573/ALTEX.1403271>.

897 Stern, M., Gierse, A., Tan, S. et al. (2014). Human Ntera2 cells as a predictive in vitro test system for
898 developmental neurotoxicity. *Arch Toxicol* 88, 127–136. [https://doi.org/10.1007/S00204-013-](https://doi.org/10.1007/S00204-013-1098-1)
899 1098-1.

900 Takahashi, K., Tanabe, K., Ohnuki, M. et al. (2007). Induction of Pluripotent Stem Cells from Adult
901 Human Fibroblasts by Defined Factors. *Cell* 131, 861–872.
902 <https://doi.org/10.1016/j.cell.2007.11.019>.

903 Tapia, C. M., Folorunso, O., Singh, A. K. et al. (2020). Effects of Deltamethrin Acute Exposure on
904 Nav1.6 Channels and Medium Spiny Neurons of the Nucleus Accumbens. *Toxicology* 440.
905 <https://doi.org/10.1016/J.TOX.2020.152488>.

906 Terron, A. and Bennekou, S. H. (2018). Towards a regulatory use of alternative developmental

907 neurotoxicity testing (DNT). *Toxicol Appl Pharmacol* 354, 19–23.
908 <https://doi.org/10.1016/j.taap.2018.02.002>.

909 Toscano, C. D. and Guilarte, T. R. (2005). Lead neurotoxicity: From exposure to molecular effects.
910 *Brain Res Rev* 49, 529–554. <https://doi.org/10.1016/J.BRAINRESREV.2005.02.004>.

911 Tsuji, R. and Crofton, K. M. (2012). Developmental neurotoxicity guideline study: Issues with
912 methodology, evaluation and regulation*. *Congenit Anom (Kyoto)* 52, 122–128.
913 <https://doi.org/10.1111/J.1741-4520.2012.00374.X>.

914 Tukker, A. M., Bouwman, L. M. S., van Kleef, R. G. D. M. et al. (2020). Perfluorooctane sulfonate
915 (PFOS) and perfluorooctanoate (PFOA) acutely affect human $\alpha 1\beta 2\gamma 2L$ GABAA receptor and
916 spontaneous neuronal network function in vitro. *Sci Rep* 10. [https://doi.org/10.1038/s41598-](https://doi.org/10.1038/s41598-020-62152-2)
917 [020-62152-2](https://doi.org/10.1038/s41598-020-62152-2).

918 Tukker, A. M., Wijnolts, F. M. J., de Groot, A. et al. (2020). Applicability of hiPSC-derived neuronal co-
919 cultures and rodent primary cortical cultures for in vitro seizure liability assessment. *Toxicol Sci*.
920 <https://doi.org/10.1093/toxsci/kfaa136>.

921 U.S. EPA (1998). Health Effects Guidelines OPPTS 870.6300. *Dev Neurotox Study EPA* 71

922 Uhlhaas, P. and Singer, W. (2006). Neural synchrony in brain disorders: relevance for cognitive
923 dysfunctions and pathophysiology. *Neuron* 52, 155–168.
924 <https://doi.org/10.1016/J.NEURON.2006.09.020>.

925 Wagner-Schuman, M., Richardson, J. R., Auinger, P. et al. (2015). Association of pyrethroid pesticide
926 exposure with attention-deficit/hyperactivity disorder in a nationally representative sample of
927 U.S. children. *Environ Heal*. <https://doi.org/10.1186/s12940-015-0030-y>.

928 Xue, Z., Li, X., Su, Q. et al. (2013). Effect of synthetic pyrethroid pesticide exposure during pregnancy
929 on the growth and development of infants. *Asia Pac J Public Health* 25, 72S-79S.
930 <https://doi.org/10.1177/1010539513496267>.

931 Zhang, L. I. and Poo, M. M. (2001). Electrical activity and development of neural circuits. *Nat Neurosci*
932 *4 Suppl*, 1207–1214. <https://doi.org/10.1038/NN753>.

933

934

935

936

937

938 **Supplementary Material**939 **Table S1: Chemical Compounds used for toxicity testing on MEAs.**

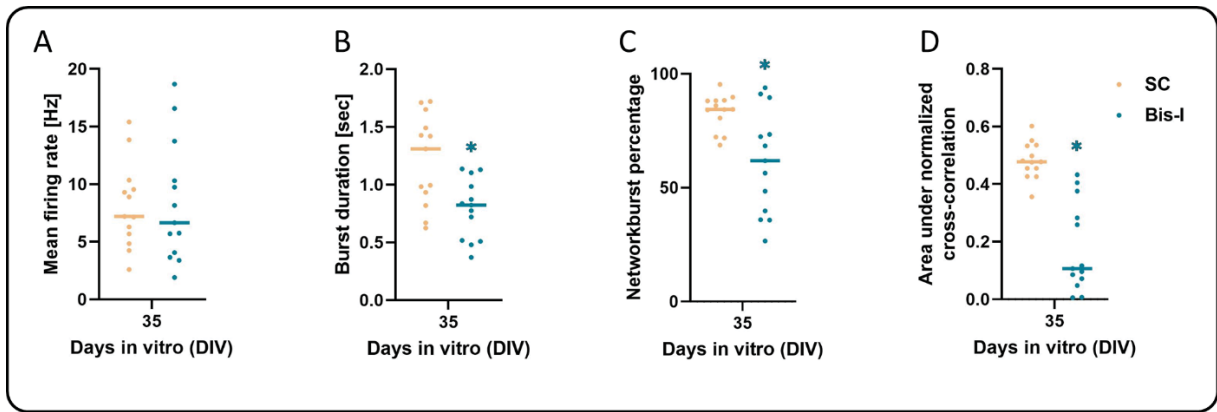
Compound	CAS No.	DTXS ID	Supplier	Start concentration [μM]	Solvent	Conducted Experiments
Acetaminophen	103-90-2	DTXSID2020006	ToxCast	20	DMSO	2
Acetamiprid	160430-64-8	DTXSID901015148	Sigma-Aldrich	20	DMSO	2
Acibenzolar-S-methyl	135158-54-2	DTXSID1032519	ToxCast	20	DMSO	2
Aldicarb	116-06-3	DTXSID0039223	Sigma-Aldrich	20	DMSO	2
Alpha-Endosulfan	959-98-8	DTXSID9037539	Sigma-Aldrich	20	DMSO	2
Beta-Cyfluthrin	182057-3-27-0	DTXSID8032330	Sigma-Aldrich	20	DMSO	3
Beta-Cypermethrin	122451-0-29-5	DTXSID6052871	LGC Standards	20	DMSO	3
Bisindolylmaleimide I	133052-90-1	DTXSID50157932	Merck	10	DMSO	1
Carbaryl	63-25-2	DTXSID9020247	Sigma-Aldrich	20	DMSO	3
Chlorpyrifos	2921-88-2	DTXSID4020458	ToxCast	20	DMSO	2
Chlorpyrifos-methyl	5598-13-0	DTXSID6032352	Sigma-Aldrich	20	DMSO	3
Clothianidin	210880-92-5	DTXSID2034465	Sigma-Aldrich	20	DMSO	2
Deltamethrin	52918-63-5	DTXSID8020381	Sigma-Aldrich	20	DMSO	3
Diazinon	333-41-5	DTXSID9020407	Sigma-Aldrich	20	DMSO	3

Dimethoate	60-51-5	DTXSID702 0479	Sigma- Aldrich	20	DMSO	2
Dinotefuran	165252 -70-0	DTXSID703 4549	Sigma- Aldrich	20	DMSO	3
Disulfoton	298-04- 4	DTXSID002 2018	ToxCast	20	DMSO	3
Etofenprox	80844- 07-1	DTXSID903 2610	ToxCast	20	DMSO	3
Fipronil	120068 -37-3	DTXSID403 4609	ToxCast	20	DMSO	3
Flufenacet	142459 -58-3	DTXSID203 2552	Sigma- Aldrich	20	DMSO	3
Imidacloprid	138261 -41-3	DTXSID503 2442	Sigma- Aldrich	20	DMSO	3
Metaflumizone	139968 -49-3	DTXSID604 0373	ToxCast	20	DMSO	3
Methamidophos	10265- 92-6	DTXSID602 4177	ToxCast	20	DMSO	3
Penthiopyrad	183675 -82-3	DTXSID605 8005	Sigma- Aldrich	20	DMSO	2
Rotenone	83-79-4	DTXSID602 1248	santa cruz	0.3	DMSO	2
Spirodiclofen	148477 -71-8	DTXSID603 4928	ToxCast	20	DMSO	3
Thiacloprid	111988 -49-9	DTXSID703 4961	Sigma- Aldrich	20	DMSO	3
Thiamethoxam	153719 -23-4	DTXSID203 4962	Sigma- Aldrich	20	DMSO	2
Tri-allate	2303- 17-5	DTXSID502 4344	ToxCast	20	DMSO	2

940

941

942



943

944 **Figure S1: Bisindolylmaleimide I (Bis-I) inhibits neural network development on 48-well microelectrode arrays**
 945 **(MEA) after 35 days of exposure, described by evaluation of specific network parameters.** Starting at DIV7
 946 networks were treated with 5 μ M Bis-I and compared to the solvent control (SC) of the respective plate. Data are
 947 represented as single experiment values (median of 3 wells each) of 13 independent experiments and merged
 948 by median (coloured bar). Statistical significance was calculated using two-tailed Student's t-tests. A p-value
 949 below 0.05 was termed significant. *significant compared to the respective SC.

950

951

952

A human iPSC-based *in vitro* neural network formation assay to investigate neurodevelopmental toxicity of pesticides

Kristina Bartmann, Farina Bendt, Arif Dönmez, Daniel Haag, Eike Keßel, Stefan Masjosthusmann, Christopher Noel, Ji Wu, Peng Zhou, Ellen Fritsche

Journal:	ALTEX
Impact factor:	6.250 (2021)
Contribution to the publication:	85 %
	Planning, performance and evaluation of all MEA experiments, writing of the manuscript
Type of authorship:	first-authorship
Status of publication:	Submitted 3 June 2022

3 Discussion

According to a study from 2020, approximately 350,000 chemicals and mixtures for global production and use are currently registered. This exploration increases the previous estimate by a factor of three and emphasizes the multitude of chemicals to which humans are potentially exposed, including agrochemicals, biocides, cosmetics, and food contact materials (Wang et al., 2020). There is evidence that exposure towards such environmental chemicals contributes to neurodevelopmental disorders in children, like autism spectrum disorder (AD), mental retardation and cerebral palsy (Mendola et al., 2002; Grandjean and Landrigan, 2006; Sagiv et al., 2010; Bennett et al., 2016), which may have pervasive consequences, both in social and economic sectors (Bellanger et al., 2013).

Human brain development is characterized by the spatiotemporal orchestration of various key neurodevelopmental processes, beginning in the third week of gestation and extending throughout late adolescence (Grandjean and Landrigan, 2014). These KNDPs, for example neural progenitor cell proliferation, migration, differentiation, synaptogenesis, myelination, apoptosis and neural network formation and function are embedded in vulnerable periods during brain development (Fig. 1; Fig. 3). The necessity for their correct spatiotemporal organization and resulting high plasticity makes the developing more sensitive towards disturbances, e.g. by chemical or physical agents, than the adult brain (Rice and Barone, 2000). Here, time, magnitude and length of exposure are critical determinations for DNT (Rice and Barone, 2000). Moreover, compared to adults, the fetus is not as well protected and therefore more vulnerable towards the chemicals' exposure. Many chemicals pass the placenta, thereby entering the fetal circulation and are also transferred through human breastmilk, as shown by the examination of a multitude of human placenta, breast milk and cord blood samples (Needham et al., 2011; Grandjean and Landrigan, 2014). Furthermore, the developmental immature blood-brain barrier does not provide complete protection of the CNS towards chemical exposure (Zheng et al., 2003).

Only 110 to 150 chemicals have been tested for their DNT potential in rodent-based DNT guideline studies so far and few are known to affect the developing brain (Makris et al., 2009; Grandjean and Landrigan, 2014; Sachana et al., 2019). The main reason for this data gap lies in the nature of these guideline studies, which are very resource-intensive with regard to animals, time and money, have high variability in their endpoint evaluations and provide a large uncertainty of extrapolation from rodents to humans (Tsuji and Crofton, 2012; Smirnova et al., 2014; Sachana et al., 2019). Therefore, regulators and scientists across the world agreed on the need for an *in vitro* testing battery, that includes various new approach methods, modelling several key

neurodevelopmental processes in a time- and cost-efficient manner without the use of animals, to allow a cheaper and faster assessment of DNT exposure, hazard and risk (EFSA, 2013; Crofton et al., 2014; Bal-Price et al., 2015; Fritsche et al., 2017; Fritsche, Grandjean, et al., 2018).

3.1 The DNT-IVB and its regulatory applications

In 2017, scientists from 15 countries across the world agreed on the development of an *in vitro* testing battery, to overcome the data gap on the DNT potential of chemicals among thousands of untested substances (Fritsche et al., 2017). To improve the international acceptance of these test methods, four research projects have been funded by the EFSA, the U.S. National Toxicology Program (NTP), the U.S. and Danish EPA (DEPA), which concentrated on the generation of additional data with the DNT-IVB (Masjosthusmann et al., 2020; Blum et al. under review - Manuscript 2.3), the testing of high priority pesticides (DEPA; Bartmann et al. under review - Manuscript 2.5), the development and validation of *in vitro* DNT methods (Bartmann et al. under review – Manuscript 2.5; Koch et al. 2022 – Manuscript 2.1), as well as the development of an effective screening strategy for specific chemical classes (Klose et al. 2021 - Manuscript 2.2; Behl et al., 2019). All assays of the battery have been reviewed and displayed a readiness that is necessary for regulatory use (Fritsche et al., 2017; Bal-Price et al., 2018; Sachana et al., 2019). In contrast to other *in vitro* batteries, like the *in vitro* batteries for detecting skin sensitization (Strickland et al., 2022) or estrogen disruption (Judson et al., 2017), the DNT-IVB with its 17 assays covers a plethora of pathways. This is owed to the fact that the KNDPs represented in the DNT-IVB, i.e. differentiation into different neural cell types, apoptosis, migration, neurite formation, synaptogenesis, and neural network formation, are each guided by complex signaling networks (Kiryushko et al., 2006; Wong et al., 2014; Bernal et al., 2015; Hevner, 2015; Lee, 2015; Ehrlich and Josselyn, 2016).

The overall goal of the DNT-IVB is the replacement of the OECD TG426 and the use of these *in vitro* methods as a data requirement for regulatory human DNT hazard assessment in the future. However, the DNT-IVB is not envisioned to be a direct replacement of the *in vivo* TG at the moment, nevertheless, it enables the use of generated *in vitro* data in different ways to inform regulatory decision-making. One use is compound hazard assessment in a targeted IATA framework. Moreover, screening for prioritization of compound classes is a second application. In addition, DNT-IVB assays can be used as a follow-up screening subsequent to identification of positive compounds by QSAR (quantitative structure-activity relationship) analyses, read-across

and other predictive computational models (Fig. 7; Sachana et al., 2021; Crofton and Mundy, 2021).

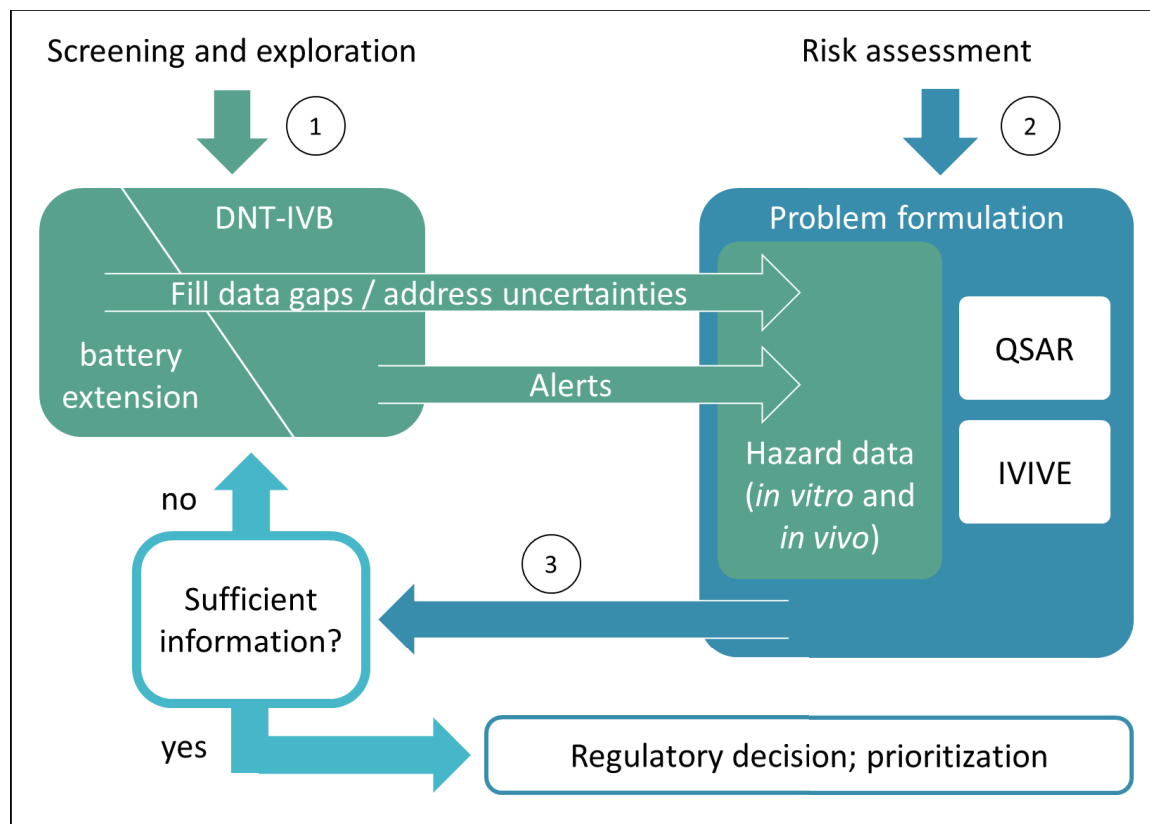


Figure 7: Application scenarios of the DNT-IVB incorporated into an IATA. The DNT-IVB will be used for screening and further exploration of compounds to generate hazard alerts (hits; (1)). The second scenario (2) described the use of the DNT-IVB in the context of risk assessment of single substances in an IATA. Starting with the problem formulation, all available data informing on hazard identification and characterization are compiled (maybe extended with data from scenario 1). QSAR (Quantitative structure activity relationships) and IVIVE (*in vitro*-to-*in vivo* extrapolation) are exemplarily presented as components of the IATA framework. If the gathered information for regulatory decision-making or prioritization of compounds is insufficient, DNT-IVB extensions are needed to fill data gaps and to reduce uncertainties (3). Adapted from Blum et al. under review (Manuscript 2.3).

Concerning the hazard assessment, the DNT-IVB data contributed to an EFSA Scientific Opinion on the DNT potential of the two pesticides Deltamethrin and Flufenacet. EFSA is now using the DNT-IVB data for Deltamethrin regulation as in contrast to the OECD426 DNT guideline study it provided positive hits for two DNT-IVB endpoints at concentrations below 1 μM and provided mechanistic information (Masjosthusmann et al., 2020; Hernández-Jerez et al., 2021; Blum et al. under review - Manuscript 2.3). For screening and prioritization, the DNT-IVB provided useful data on compounds from the compound class of flame retardants. In this work toxic, phased-out flame

retardants were compared to their novel replacements. The DNT-IVB identified identical hazards of some of the novel compared to the phased-out flame retardants (Klose et al., 2021 - Manuscript 2.2; Crofton and Mundy 2021). In addition, the DNT-IVB may address single chemical hazard assessment in case no *in vivo* data is available to specify follow-up testing and the type of guideline or targeted testing that may be needed. Furthermore, DNT-IVB data can inform on the weight of Evidence (WoE)-based assessments of chemicals, for which *in vivo* DNT data is ambiguous due to multiple studies for one compound showing divergent results, or inconclusive interpretation of data because of variability. Moreover, testing in the DNT-IVB may be consulted for *in vivo* negative compounds, that raise a concern in other novel MIE (molecular initiating event)-based assays or alternative species assays (Crofton and Mundy, 2021).

During the last years, especially since progress has been made in the field of human-derived neural cells, a plethora of *in vitro* models has been developed. In 2018, experts reviewed 17 of these methods regarding their readiness for use in a regulatory context (Bal-Price, Pistollato, et al., 2018). The readiness of each assay was assessed by a standardized scoring system that relies on four different categories, including several ranking parameters: i) initial high priority considerations, e.g. biological plausibility, reference chemicals; ii) method performance considerations, e.g. within- and between-laboratory reproducibility; iii) technical capability, e.g. test range and response characterization; and iv) other practical considerations, e.g. technological transferability and transparency of the method. These criteria were based on an OECD scoping document for validation of *in vitro* and *ex vivo* tests for thyroid-disrupting chemicals (OECD, 2014). In addition, this tool provides test method developers with a quick and clear estimation of which important criteria need to be considered during development. Assays that achieved a comparatively high score, are the assays of the 'Neurosphere Assay', NPC1-5. NPC1 (proliferation of neural progenitor cells), NPC2 (migration of radial glia), NPC3 (neuronal differentiation) and NPC5 (oligodendrocyte differentiation) scored an overall readiness of A or A-. The NPC4 assay, modelling neurite outgrowth was graded with B (Bal-Price et al., 2018).

Unlike other assays of the DNT-IVB, which mainly examine only one KNDP, the multicellular 'Neurosphere Assay' enables the parallel assessment of several KNDPs, as well as cell-cell interactions. It covers important processes, e.g. proliferation, differentiation of NPCs into neurons, astrocytes and oligodendrocytes, migration of radial glia, neurons and oligodendrocytes, and neurite outgrowth. In the last years, the 'Neurosphere Assay' has been thoroughly characterized and identified as a valuable tool for *in vitro* DNT hazard assessment. Recently, the DNT-IVB, including the 'Neurosphere Assay' was challenged with 120 chemicals, including pesticides, pharmaceuticals, industrial chemicals and flame retardants, with a structural diversity

encompassing inorganic compounds, organometals, and complex heterocycles (Masjosthusmann et al., 2020; Klose et al., 2021 - Manuscript 2.2; Blum et al., under review - Manuscript 2.3). A selection of 45 of these compounds were chosen for testing for DNT-IVB performance in the European part of the IVB (IVB-EU), which is comprised of 10 of the 17 assays of the total DNT-IVB (the NPC1-5 assays, developed at the IUF in Düsseldorf, and the UKN2, 4, 5 assays set up by the University of Konstanz) and covers 60% of the total DNT-IVB endpoints. The IVB-EU reached a performance accuracy of >80% which increased to 97% when the rat neuronal network formation assay (developed by the US-EPA) was added. Because this latter assay covers a variety of endpoints including neurite outgrowth, dendritic spine formation, and synaptogenesis, most of which are not covered in the IVB-EU, this improved performance can be easily scientifically explained (Masjosthusmann et al. 2020; Blum et al. under review – Manuscript 2.3).

3.2 Closure of identified gaps in the DNT-IVB

The development of the brain *in vivo* is a highly complex procedure uniting a plethora of KNDP. A gap analysis of the current DNT-IVB revealed that the 17 *in vitro* assays of the IVB established so far do not cover this diversity of neurodevelopmental key events. Gaps concern stem cell differentiation into NPCs, evaluation of glia-specific processes like myelination, as well as the formation, maturation, and function of human neural networks. These gaps constitute a major source of uncertainty when classifying tested compounds as negatives (Masjosthusmann et al., 2020 ; Blum et al. under review - Manuscript 2.3; Crofton and Mundy, 2021). Addressing these issues and aiming to close the identified gaps will be a major task to refine the battery, reduce uncertainty, and provide sufficient information for future regulatory action.

The formation and function of neural networks is currently modelled in an assay based on primary rat cortical cells, the rat neural network formation (rNNF) assay. These mixed rat neurons and glia cells are cultured on MEAs, which allow the evaluation of different network parameters relating to spikes, bursts, and network performance/synchronicity *in vitro* (Brown et al., 2016; Frank et al., 2017). The rNNF assay is well suited for testing large numbers of chemicals, however, it holds the issue of inter-species differences when extrapolation to humans is warranted. It has been well described in the past that the predictability of animal-based assays for human health is limited by inter-species differences (Leist and Hartung, 2013). In case of the brain, species differences between rodents and humans are obvious in their respective speed of cell maturation or the absence of gyrification leading to lissencephalic rodent, in contrast to gyrencephalic human brains (Dubois et al., 2008). In addition, human brain function is in some aspects rather species-specific,

e.g. in language, long-term planning and intellectual abilities. Due to such species differences between rodents and humans, the usage of a human-based NNF assay is advised (Crofton and Mundy, 2021).

To be included in an extended version of the DNT-IVB, an assay needs to fulfil specific inclusion criteria. Firstly, the developed test method must be a valuable addition to the DNT-IVB, regarding the defined gaps. Furthermore, the method description must be compatible to the GD211, an OECD guidance document on the documentation of *in vitro* methods (e.g. ToxTemps; Krebs et al., 2019), and the respective assay must already provide a high readiness level, which can be assessed with the help of the before mentioned readiness scoring (Bal-Price et al., 2018). Closing DNT-IVB gaps by adding more assays to the IVB is expected to improve the sensitivity of DNT predictions.

3.2.1 Establishment of a novel method for neural network formation and function

Between the fourth and fifth gestational week during the embryonic phase of brain development, neurons start to mature, connect via synapses and transmit information by electrical signaling (Okado et al., 1979). Since the developing brain requires functional networks consisting of different neuronal subtypes and glial cells, network formation and function is a crucial KNDP. Furthermore, certain brain disorders, e.g. ASD, Alzheimer's and Parkinson's disease, were linked to dysfunctional neural synchronization (Uhlhaas and Singer, 2006), linking this KNDP with human disease. In the current DNT-IVB, the rNNF assay, which is based on primary rat cortical cells, is the standard for the assessment of neural network formation and function. Because human cell-based models allow endpoint assessments without the need for extrapolation to humans, addition of the human NNF (hNNF) assay to the DNT-IVB will close an important battery gap.

Generation of hiPSCs by reprogramming adult somatic cells, e.g. fibroblasts, keratinocytes or cells in urine (Takahashi et al., 2007; Aasen et al., 2008; Zhou et al., 2012), extensively advanced the field of biomedical sciences, as hiPSC can be differentiated into almost all cell types of the human body and resemble human *in vivo* physiology without raising ethical concerns. In the last years a plethora of protocols have been developed for the differentiation of hiPSCs into tissue-specific cells of a specific lineage, e.g. brain-specific neural cell types (Aasen et al., 2008; Pang et al., 2011), also to be used for drug and chemical evaluation (Jennings, 2015; Xie and Tang, 2016; Fritsche et al., 2021). A widely applied approach for the neural induction of hiPSCs is the targeted inhibition of the TGF β /BMP-pathway by specific SMAD inhibiting agents, e.g. a combination of CHIR99021, noggin, dorsomorphin, SB431542 or LDN193189, which are added to the respective neural induction medium to direct hiPSCs into the neural lineage (Lamb et al., 1993; Moreau and Leclerc,

2003; Chambers et al., 2009; Denham and Dottori, 2011; Hofrichter et al., 2017). To study neural network formation and function *in vitro*, hiPSC-derived neural cells have been shown to be a great resource, as they can also be cultured and differentiated on MEAs (Odawara et al., 2016; Tukker et al., 2018). Since the MEA technology allows real-time recording of extracellular local field potentials on multiple electrodes (Johnstone et al., 2010), the spontaneous electrical activity of hiPSC-derived neural networks can be studied and used for addressing toxicological questions (Tukker et al., 2018; Hyvärinen et al., 2019; Nimtz et al., 2020).

The previous work of our group established a neural induction and spontaneous, non-directed differentiation protocol using hiPSC (Nimtz et al. 2020; Bartmann et al., 2021 - Manuscript 2.4). However, there were several issues with the outcome of these initial protocols that prohibited compound testing in this cell model. Although the spontaneous differentiation of hiNPC-derived NPCs into neural networks on MEAs formed synapses and exhibited electrical activity, the networks did not develop synchronicity and lacked the formation of different functional neurotransmitter systems. Furthermore, the MEA recordings of the networks resulted in a fairly high well-to-well variability between different cell differentiations (Nimtz et al., 2020). Another major issue in hiPSC-derived neural network formation is the time needed to generate functional networks. This process may take several weeks (Kuijlaars et al., 2016; Hofrichter et al., 2017; Nimtz et al., 2020) up to months (Odawara et al., 2016) and hence optimization is a lengthy process.

To overcome the variability of undirected differentiation cultures, there is also the possibility to genomically engineer hiPSCs that subsequently directly differentiate into excitatory (Frega et al., 2012) or inhibitory (Zhou et al., 2012) neurons. In a second step, these differentiated cultures can be mixed and co-cultured with astrocytes *in vitro* (Kuijlaars et al., 2016; Bartmann et al. under review – Manuscript 2.5). This procedure ensures a higher reproducibility due to a defined physiological ratio of excitatory and inhibitory neurons and hence guarantees consistent electrical activity and receptor functionality (Saavedra et al., 2021). To also overcome the issue of time efficiency, the use of commercially available cells is a convenient option to achieve a rapid, standardized and reproducible cell culture (Little et al., 2019). Some of these hiPSC-derived models have already been evaluated for their ability to form electrical active neural networks on MEAs, as well as their suitability in neurotoxicity screening approaches, e.g. iCell®Neurons/CDI iCell®Astrocytes co-cultures (Cellular Dynamics International, Madison, WI, USA); DOPA.4U® neurons (Axiogenesis, Cologne, Germany); Synfire iNs co-culture (NeuCyte, Mountain View, CA, USA) (Tukker et al., 2016, 2018; Tukker, Bouwman, et al., 2020; Saavedra et al., 2021). Despite all these achievements and progresses, there is still no human-based MEA assay available that studies the developmental alteration of neural network formation and function by chemical

exposure as the aforementioned cell systems have been solely used for testing acute neurotoxic insults.

Due to its previous excellent performance (Tukker et al., 2020b; Tukker et al., 2020a; Saavedra et al., 2021), the SynFire kit (NeuCyte, USA), was eventually chosen for the establishment of a DNT test method assessing disturbances of neural network formation, the human NNF (hNNF) assay. This test system is based on hiPSC-derived excitatory and inhibitory neurons and primary human astroglia and enables the maturation of a defined cell number and cell type ratio on MEAs (Bartmann et al. under review - Manuscript 2.5). The co-culture, consisting of 52% glutamatergic excitatory, 22% GABAergic inhibitory neurons and 26% astroglia was seeded as a 2D monolayer on each MEA well containing 16 single electrodes (Fig. 8A). This specific excitatory to inhibitory ratio of 70:30 was also recently tested and revealed the steadiest increase of spiking and coverage of electrodes over the culture period (Saavedra et al., 2021). Spontaneous electrical activity of these cells was measured weekly up to DIV35 and also medium samples were analyzed for their LDH content as a measure of cytotoxicity. To reduce the number of evaluated measurement parameters, we selected a final set of 14 network parameters, that cover the three categories “General activity”, “Bursting activity” and “Connectivity”. Furthermore, we aligned the parameter selection with the set of the rNNF assay (U.S. EPA) and thus both assays provide comparable parameters of network development to reduce uncertainty. A unique feature of the hNNF assays’ experimental design is the washout, which is conducted 24h before the weekly recording of electrical activity. This should minimize acute substance effects during MEA recordings, since there is evidence that some substances directly target synaptic receptors and thus acutely affect brain function (Fig. 8B). The heavy metal lead, for example, directly targets the NMDA receptor, leading to the inhibition of glutamatergic synapse activity (Toscano and Guilarte, 2005). Thus, the washout enables the investigation of mainly developmental alterations on the networks. The experimental procedure is explained in detail in manuscript 2.5 (Bartmann et al. under review).

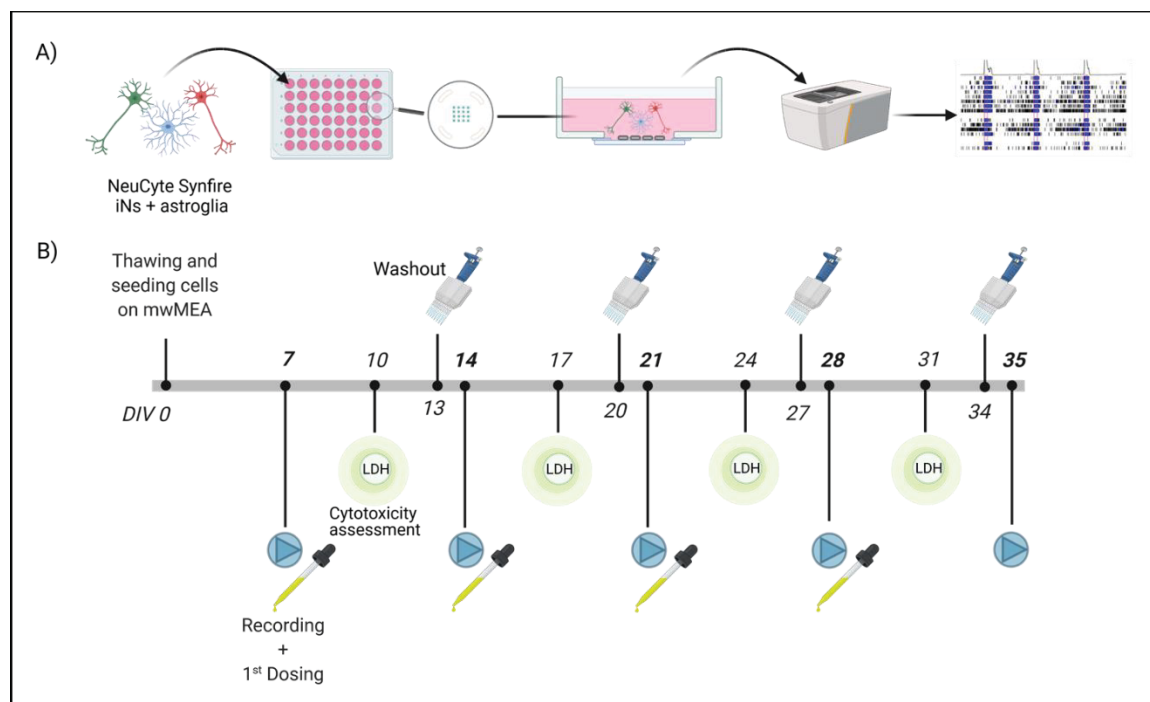


Figure 8: Experimental Setup of the human NNF assay. A co-culture of hiPSC-derived excitatory and inhibitory neurons and primary astroglia (NeuCyte, USA) was plated in a defined cell type ratio on 48-well MEA plates at DIV0. Cultures were allowed to mature for 7 days before exposure to the test compounds. 24 hours before the weekly recording of spontaneous electrical network activity on DIV7, 14, 21, 28, and 35 a washout of the respective compounds was performed. Additionally, cytotoxicity was assessed every week by the CytoTox-ONE (LDH) assay on DIV10, 17, 24, and 31 three days after dosing. Adapted from Bartmann et al. under review (Manuscript 2.5).

Considering the aim, we wanted to pursue with the establishment of the assay, namely the future embedding of the method in the DNT-IVB, we decided to follow a set of principles for *in vitro* NAM development. Crofton et al. elaborated 15 principles, which should ensure a targeted method establishment regarding endpoint-specific assay controls, precise response characterization, as well as the reasonable choice of chemicals for training and testing (Crofton et al., 2011). With respect to these principles and the before mentioned readiness scoring, the hNNF assay fulfils the majority of the requirements and can be scored a medium readiness, which is mainly due to the low number of tested chemicals, importantly known DNT positives (Aschner et al., 2017). The Manuscript 2.5 (Bartmann et al. under review) of this thesis elaborates in detail on the different principles, as well as the similarities and differences between the hNNF assay and its counterpart, the rNNF assay, based on primary rat cortical cells (Frank et al., 2017). A direct juxtaposition of BMC values for few chemicals tested in both assays reveals a lower sensitivity of the hNNF assay towards compound exposure, which may be explained by huge differences in assay set-up (washout of compound, exposure start and duration), presence and absence of serum in the

media, but also by possible species differences (Table 2 in Bartmann et al. under review – Manuscript 5.2). In the future, exposure schemes of these two NNF assays should be harmonized to gain a better understanding of the true nature of species differences, concerning the formation and function of neural networks. Moreover, the readiness of the hNNF assay will be enhanced to also meet regulatory requirements, by expanding the substance set and increasing the throughput (Bartmann et al. under review - Manuscript 2.5).

Together with the testing of 28 chemicals, mainly pesticides, the hNNF assay presents a suitable addition to the current DNT-IVB and enables the closure of one of the identified gaps regarding neural network formation and function.

3.3 Validation of new approach methods for regulatory application

A crucial issue for regulatory application of new approach methods, like the ‘Neurosphere Assay’ and other assays of the DNT-IVB, is validation (Coecke et al., 2007; Gourmelon and Delrue, 2016; Griesinger et al., 2016), which may be described as the connection between research and regulatory acceptance. The process of validation serves as a filter to assure the inclusion of only suited test methods into regulatory frameworks, e.g. OECD test guidelines, and follows defined rules (Griesinger et al., 2016). Until now, NAMs for DNT have not been formally validated. The reason for this lies mainly in lack of funding for validation studies. Especially the lab-to-lab transfer of test methods is highly resource-intensive and cannot be achieved by an academic laboratory without external funding. In 2019, PEPPER, the ‘public-private platform for the pre-validation of endocrine disruptors characterization methods’ (<https://ed-pepper.eu>) was launched. This well-funded platform is capable of validating three NAMs per year, demonstrating the huge gap in validation capacity when methods should transit from the academic lab to regulatory application. As a solution, the concept of scientific validation was proposed (Leist et al., 2014). Scientific validation, also called mechanistic validation, is based on the biological basis of the method comparative to human physiology, and hence concentrates on a mechanistic description of active and inactive pathways, that affect endpoint(s) in the NAMs. In addition, assay consistency, i.e. reproducibility of endpoint measures, is an important criterion for scientific validation, while the lab-to-lab comparison is not part of this procedure (Hartung, 2007; Leist et al., 2012; Hartung et al., 2013; Bal-Price, Hogberg, et al., 2018, Leist et al. 2014).

Recently, we scientifically validated the ‘Neurosphere Assays’, NPC1-5, which are part of the DNT-IVB, using such a mechanistic rationale approach (Koch et al., 2022 - Manuscript 2.1). We identified five criteria for our scientific validation. First, the biological plausibility of the test

methods was underlined. Fritsche et al. showed, that all endpoints assessed in the ‘Neurosphere Assay’ are important key neurodevelopmental processes and therefore indispensable (Fritsche et al., 2018). For example, the brain size is determined by the proliferation of neural progenitor cells (de Groot et al., 2005), and the differentiation into oligodendrocytes is important for forming and keeping myelin sheets around axons (Baumann and Pham-Dinh, 2001). For the ‘Neurosphere Assay’ endpoints we showed that indeed the processes NPC proliferation, migration, neuronal and oligodendrocyte differentiation and neurite outgrowth, happen in a dynamic way over time, e.g. the percentage of β (III)tubulin⁺ neurons (NPC3) and O4⁺ oligodendrocytes (NPC5) enhance over the five days of differentiation (Koch et al., 2022 - Manuscript 2.1). The developmental aspect of the assays is crucial for assessing developmental toxicity. In case of the NPC1-5 assays, like for the whole DNT-IVB it is sufficient if one of these processes is impaired for expecting an adverse outcome. The second and third criteria describe the specific cell type morphology and the expression of cell type-specific markers throughout each process. This guarantees the desired nature of the studied cells. Furthermore, the response of the diverse endpoint to the respective physiological signal stimuli during neurodevelopment was demonstrated and builds the fourth part of the scientific validation. Here the inhibition of Notch signaling regulating neurogenesis and oligodendrogenesis (Park and Appel, 2003; Borghese et al., 2010) as well as EGFR signaling regulating NPC proliferation, migration and differentiation (Ayuso-Sacido et al., 2010) during brain development were also confirmed to be functional in the respective ‘Neurosphere Assays’. Likewise, the RhoA activator narciclasine causes a specific and significant reduction of neuronal differentiation and neurite outgrowth, effects that were also described in the literature (Krug et al., 2013; Yang et al., 2016; Bogetofte et al., 2019). The last criterion of the scientific validation focused on DNT positive compounds with specific effects on the respective endpoints. Metals like cadmium or methylmercury, the pesticide deltamethrin and the flame retardant tetrabrombisphenol A specifically affected neurosphere endpoints distinguishable from cytotoxic effects. The whole scientific validation of the ‘Neurosphere Assay’ is described in detail in the manuscript 2.1 (Koch et al., 2022). In conclusion, this study stresses the validity of the ‘Neurosphere Assay’ as an integral part of the current DNT-IVB to assess important KNDPs. Moreover, it further approves that the DNT-IVB is on a steady way to regulatory acceptance (Koch et al., 2022 - Manuscript 2.1) and stresses the importance of mechanistic validation studies for NAMs in general to improve their credence.

3.4 From screen hit to DNT toxicant

The evaluation of data obtained with the DNT-IVB results in the generation of concentration-response curves. One important question is how to derive a decision from such concentration-response data leading to compound classification. In 2017 the EFSA recommended the use of the benchmark concentration (BMC) approach to derive a reference point or point of departure from curves representing concentration-effect relationships (Hardy et al., 2017). For readout of such BMCs, the benchmark response (BMR) has to be defined. This BMR effect size has to be greater than the general variability of the measured endpoint. To determine the BMRs for the different parameters of the hNNF assay, the inter-experimental standard deviations (SDs) of the solvent controls across multiple experiments were calculated for each MEA readout parameter. Here, the BMR for induction and reduction effects was defined as 1.5-fold of the SD, therefore, the BMR₅₀ (50% change from the curves starting point) was set for definition of hNNF hits (Bartmann et al. under review - Manuscript 2.5). In comparison, the variability between experiments conducted in the 'Neurosphere Assay' was lower, therefore BMR₃₀ or BMR₁₀ were applied for respective endpoints (Masjosthusmann et al., 2020; Blum et al. under review - Manuscript 2.3). The lower the variability and thus the defined BMR, the greater is the number of classified as active or positive describing the sensitivity of the assays (Crofton and Mundy, 2021).

To classify compounds tested in the DNT-IVB as active (e.g. "hit" or "positive") or inactive ("no effect" or "negative"), assay-specific classification models have to be provided. Within these decision trees, two questions have to be addressed: i) has the change of the measured endpoint passed the previously defined BMR? and ii) is the observed change selective for the endpoint ("DNT-specific-hit") or accompanied by cytotoxicity ("DNT-unspecific-hit")? In case there is no clear separation between "DNT-specific-hit" and "DNT-unspecific-hit" possible, the compound is grouped into the fourth category "borderline-hit" (Delp et al., 2018; Masjosthusmann et al., 2020; Crofton and Mundy, 2021; Blum et al. under review - Manuscript 2.3). Based on these definitions a decision model can be formulated, as shown for NPC1-5 in Masjosthusmann et al., 2020 or Manuscript 2.3 (Blum et al. under review).

In general, every observed hit in one of the DNT-IVB assays, is considered as an evidence for potential adverse effect, since the DNT-IVB presents a plethora of KNDPs at the cellular level (Lein et al., 2007; Radio and Mundy, 2008; Crofton and Mundy, 2021). Nevertheless, ranking and clustering the critical compounds by their potencies across all assays is an important tool for hazard assessment. Several methods have been proposed and also applied for the current DNT-IVB data, e.g. ranking by the most sensitive endpoint (MSE; Masjosthusmann et al., 2020; Blum et al. under review - Manuscript 2.3) or prioritization by considering also the number of positive hits

(Klose et al., 2021 - Manuscript 2.2). The MSE is defined as the most sensitive functional endpoint responding towards a compound across the DNT-IVB assays, and is considered as an important starting point for further testing. Specific hits that are located in a range of ≤ 3 -fold of the MSE, are considered to be of similar significance due to imprecision of data generation and biological relevance. This can be exemplified by testing results of the alkaloid narciclasine across the DNT-IVB assays. The MSE upon narciclasine exposure is inhibition of neuronal differentiation measured by the NPC3 assay, However, also the BMCs for the NPC1 (NPC proliferation), UKN4 and NPC4 (neurite outgrowth) as well as NPC5 (oligodendrocyte differentiation) assays lie within the 3-fold range of the MSE suggesting adverse effects on more than one KNDP. The literature describes a plethora of modes-of-actions for narciclasine including inhibition of translation at the ribosome, acting as a 'metaphase poison', activity against NO production, TNF- α antagonism, trigger of the apoptotic death receptors and activation of the Rho/Rho kinase/LIM kinase/cofilin signaling pathway (Nair et al., 2015). These pathways are involved in KNDP, cause changes during brain development or are deregulated in neurodevelopmental disorders (Petit and Isaacson, 1976; Pavlík and Teisinger, 1980; Choi and Benveniste, 2004; Schmidt-Kastner et al., 2006; Tegenge et al., 2011). Hence, the multiple hits produced by narciclasine in the DNT-IVB (Blum et al. under review – Manuscript 2.3) might reflect the multiple modes-of-action of this compound on developing brain cells. This example highlights the importance of looking not only at the MSE, but also at affected endpoints in a 3-fold range surrounding the MSE. Considering also the number of hits with prioritization methods like hierarchical clustering, chemicals based on their potency and their number of affected endpoints are ranked. Moreover, this method allows identification of chemicals with common modes-of-action due to similar effect patterns across multiple endpoints (Harrill et al., 2018; Masjosthusmann et al., 2020; Crofton and Mundy, 2021). One software tool, the open source ToxPi (Toxicological Prioritization Index; <https://toxpi.org/>) approach from the US-EPA, integrates multiple sources of evidence and clusters chemicals in compliance with their potency and assay hit patterns (Reif et al., 2010; Marvel et al., 2018). In this work, just the MSE and the MSE plus the number of endpoint hits (ToxPi) were compared across 15 banned and currently in use flame retardants as a case study. Prioritization of these flame retardants is different according to the applied method. We therefore suggested a mixture of the two methods by giving the hits at the lowest concentrations the highest priority and prioritizing secondly also the compounds with multiple endpoint hits (Klose et al. 2021 – Manuscript 2.2).

To move from pure hazard characterization to risk assessment, exposure has to be considered, because risk is defined as hazard x exposure (Fig. 9). A hazard is of no concern when exposure is lacking. Likewise, a small hazard is also not reason to large concern in case of exposure.



Figure 9: The concepts of hazard versus risk. A hazard is of no concern when there is no exposure. The risk is defined as the likelihood of hazard causing harm. Adapted from <https://www.efsa.europa.eu/de/discover/infographics/hazard-vs-risk>.

Chemical hazards identified by *in vitro* NAMs - like in this work with the DNT-IVB - are typically delivered as concentration-response curves with respective BMCs. To translate an *in vitro* hazard to an *in vivo* risk, several kinetic calculations or compound measurements have to be performed. For one, nominal *in vitro* concentrations have to be translated into cellular *in vitro* exposure. Different physicochemical properties of compounds influence their *in vitro* behavior hence affecting the relationship between the nominal medium concentration in an *in vitro* assay and the effective cellular concentration. These include protein and lipid binding, evaporation, plastic ware binding, cellular uptake and degradation (Chang et al., 2022). Secondly, the *in vivo* exposure and biokinetic behavior of the desired substance has to be estimated. Due to the lack of tissue-specific measurements for many compounds, modelling of their pharmacokinetics, i.e. their absorption, distribution, metabolism and elimination (ADME) within an organism, can be achieved by PBPK modelling allowing a concentration estimate within target tissues *in vivo* (Paini et al., 2019). To determine the minimum requirement for PBK models, e.g either data poor or data rich chemicals, different scenarios are possible and presented in Figure 10. For example, one-compartment models (only protein binding and clearance data) can be applied to data poor chemicals to support chemicals screening and prioritization. If more hazard data is available, additional compartments may be added to the PBK model (Paini et al., 2019). These PBK models help facilitating so-called quantitative *in vitro*-to-*in vivo* extrapolation (QIVIVE; Wetmore et al., 2012; Kramer et al., 2015; Bell et al., 2018; Proença et al., 2021), because it allows the extrapolation from nominal medium

concentration *in vitro* to internal exposure concentrations *in vivo*. As a proof-of-concept study, this has recently even been achieved with chemical mixtures (Valdiviezo et al., 2021).

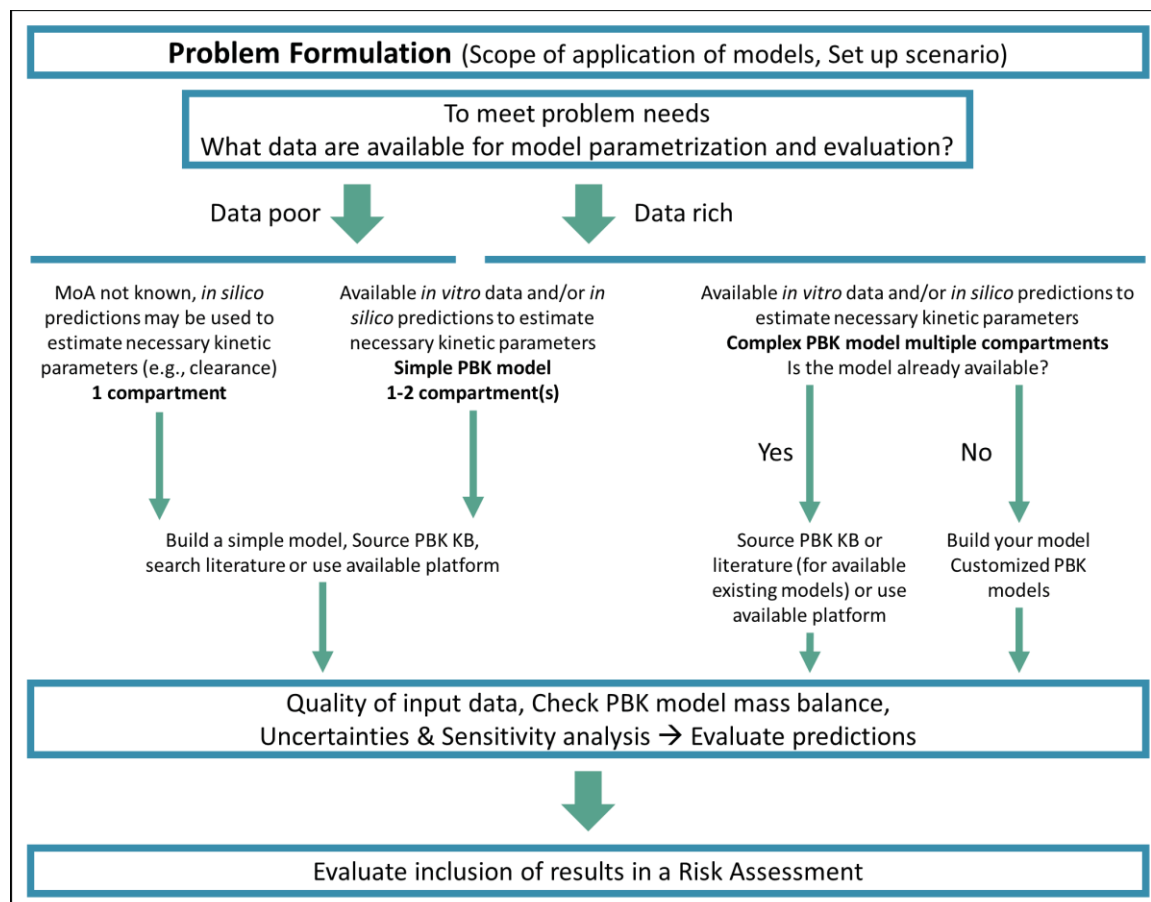


Figure 10: Schematic decision tree to determine the PBK model, based on either data-poor or data-rich chemicals and based on problem formulation. PBK=Physiologically based kinetic; MoA=Mode of action; KB=Knowledge base. Adapted from Paini et al. (2019)

Obstacles accompany acceptance and application of such next generation risk assessment methods by regulatory agencies. These result amongst others from limited experience and hence uncertainties in these novel approaches. However, each toxicological tool is accompanied by imprecisions that necessitate extrapolation. In the case of traditional animal experiments, these uncertainties are compensated for by using uncertainty / assessment factors and worst-case / precautionary approaches and thresholds. These are crude measures installed to deal with the probabilistic nature of any result. The use of probabilistic methods and Bayesian approaches seeks to characterize these uncertainties and thereby is thought to support improved risk assessment. Real-life assessments of all steps of the next generation risk assessment process uncertainties might be more realistic than worst-case scenarios. The probabilistic risk assessment concept might

therefore aid changing the paradigm of conventional risk assessment using animals towards a NAM-based next generation risk assessment (Maertens et al., 2022).

4 Abstract

Human brain development is characterized by the spatiotemporal orchestration of a plethora of key neurodevelopmental processes (KNDP), making it highly vulnerable towards chemical disruption. Up to today, only 110 to 150 chemicals have been tested for their developmental neurotoxic (DNT) potential and few are known to affect the developing brain. The main reason for this data gap lies in the current *in vivo* animal guideline studies, which are very resource-intensive and not capable of testing high number of chemicals. Therefore, regulators and scientists across the world agreed on the need for an *in vitro* testing battery (DNT-IVB) that includes various new approach methods, modelling several KNDP in a resource-efficient manner without the use of animals. One suitable model as an integral part of the DNT-IVB is the 'Neurosphere Assay', which is based on human neural progenitor cells (NPC) grown as 3D neurospheres, covering several KNDPs, like NPC proliferation, migration and differentiation into neurons and oligodendrocytes. The first manuscript (2.1) of this thesis is focused on the scientific validation of the 'Neurosphere Assay', illustrating the mechanistic validity and physiological relevance of the assay. As two case studies for DNT hazard identification, manuscript 2.2 describes application of the 'Neurosphere Assay' in a screening and prioritization study of flame retardants, and manuscript 2.3 the screening of 120 compounds of different substance classes across 10 assays of the DNT-IVB including the 'Neurosphere Assay'. Based on 45 DNT negative/positive compounds, this battery shows an accuracy of >80%. Taken together, these manuscripts provide parts of the scientific basis for the use of the DNT-IVB for regulatory application. Beside the KNDPs modelled within the 'Neurosphere Assay', the DNT-IVB also contains the assessment of neural network formation and function (NNF), an endpoint which is currently assessed in an assay based on rat primary cortical cells. Nevertheless, the use of a human cell model covering this endpoint, was identified as a gap. Manuscript 2.4 provides a protocol for the spontaneous, non-directed differentiation of human induced pluripotent stem cells (hiPSCs) into neural networks for measuring their electrical activity. These networks did not develop synchronicity and lacked the formation of functional neurotransmitter systems, hence, not suited for standardized DNT testing. Therefore, a human NNF assay based on commercially available, hiPSC-derived neurons and human astrocytes was established and challenged with 28 pesticides. These data indicate that the hNNF assay is a valuable addition to the current DNT-IVB (Manuscript 2.5).

In summary, this thesis contributed to the setup, scientific validation and compound screening of the current DNT-IVB and hence participated in the production of a data base essential for a currently prepared OECD guidance document on interpretation of the DNT-IVB and its use in regulatory contexts.

5 Zusammenfassung

Die Entwicklung des menschlichen Gehirns ist durch die räumlich-zeitliche Orchestrierung einer Vielzahl wichtiger neurologischer Entwicklungsprozesse (KNDP) gekennzeichnet, wodurch das Gehirn sehr anfällig für eine chemische Einflussnahme wird. Bis heute wurden nur 100 bis 150 Chemikalien auf ihr entwicklungsneurotoxisches (DNT) Potential getestet. Der Hauptgrund für diese Datenlücke liegt in den derzeitigen *in vivo*-Tierversuchsstudien, die sehr ressourcenintensiv und nicht in der Lage sind, eine große Anzahl von Chemikalien zu testen. Daher haben sich Regulierungsbehörden und Wissenschaftler weltweit auf die Notwendigkeit einer *in vitro*-Testbatterie (DNT-IVB) geeinigt, welche verschiedene neuartige Methoden umfasst und mehrere KNDPs auf ressourceneffiziente Weise und tierversuchsfrei modelliert. Ein geeignetes Modell als integraler Bestandteil der DNT-IVB, ist der Neurosphärenassay, der auf menschlichen neuronalen Vorläuferzellen (NPC) basiert, und so mehrere KNDPs abdeckt. Das erste Manuskript (2.1) dieser Arbeit befasst sich mit der wissenschaftlichen Validierung des Neurosphärenassays und veranschaulicht die mechanistische Validität und physiologische Relevanz des Assays. Manuskript 2.2 beschreibt die Anwendung des Neurosphärenassays in einer Screening- und Priorisierungsstudie von Flammschutzmitteln und Manuskript 2.3 das Screening von 120 Substanzen verschiedener Klassen in 10 Assays der DNT-IVB einschließlich des Neurosphärenassays, wobei die Batterie hierbei eine Genauigkeit von >80% aufzeigt. Zusammengefasst liefern diese Manuskripte einen Teil der wissenschaftlichen Grundlage für den Einsatz der DNT-IVB für regulatorische Anwendungen. Neben den KNDPs, die im Neurosphärenassay modelliert werden, untersucht die DNT-IVB auch die Bildung und Funktion neuraler Netzwerke (NNF), ein Endpunkt, der derzeit basierend auf primären kortikalen Rattenzellen erfasst wird. Die Verwendung eines menschlichen Zellmodells, das diesen Endpunkt abdeckt, wurde jedoch als Lücke der Batterie erkannt. Manuskript 2.4 beschreibt ein Protokoll für die spontane, ungerichtete Differenzierung menschlicher induzierter pluripotenter Stammzellen (hiPSC) in neuronale Netzwerke zur Messung ihrer elektrischen Aktivität. Diese Netzwerke entwickelten jedoch keine Synchronität oder funktionale Neurotransmittersysteme aus, sodass sie für standardisierte DNT-Tests nicht geeignet waren. Daher wurde ein humaner NNF-Test auf der Grundlage einer kommerziell erhältlichen, hiPSC-basierten Ko-Kultur entwickelt und mit 27 Pestiziden getestet. Diese Daten deuten darauf hin, dass der hNNF-Assay eine wertvolle Ergänzung der aktuellen DNT-IVB darstellt (Manuskript 2.5). Zusammenfassend lässt sich sagen, dass diese Arbeit einen Beitrag zum Aufbau, zur wissenschaftlichen Validierung und zum Substanzscreening der aktuellen DNT-IVB geleistet hat und somit an der Erstellung einer Datenbasis beteiligt war, die für ein derzeit in Vorbereitung befindliches OECD-Leitliniendokument zur Verwendung und Interpretation der DNT-IVB für regulatorische Anwendungen von wesentlicher Bedeutung ist.

Abbreviations

2D	Two-dimensional
3D	Three-dimensional
AC	Astrocyte
AD	Autism spectrum disorder
ADHD	Attention deficit hyperactivity disorder
ADME	Absorption, distribution, metabolism, elimination
AI	Artificial intelligence
ANOVA	Analysis of variance
AO	Adverse outcome
AOP	Adverse outcome pathway
Asc	Ascorbic acid
BBOEP	Bis-(2-butoxyethyl) phosphate
BDE-47	2,2',4,4'-tetrabromodiphenylether
BDE-99	2,2',4,4',5-pentabromodiphenylether
BDNF	Brain-derived neurotrophic factor
Bis-I	Bisindolylmaleimide 1
BMC	Benchmark concentration
BMCL	Lower limit of the BMC
BMCU	Upper limit of the BMC
BMP	Bone morphogenic protein
BMR	Benchmark response
BrdU	Bromodeoxyuridine
Ca	Calcium
CAS	Chemical Abstracts Service

Abbreviations

CBR	Carbaryl
cDNA	Complementary DNA
CEFIC	European Chemical Industry Council
<i>C. elegans</i>	<i>Caenorhabditis elegans</i>
CI	Confidence intervals
Cl	Chloride
cMINC/UKN2	Neural crest migration assay
CNN	Convolutional neural network
CNS	Central nervous system
CNQX	Cyanquixalin
CTB	CellTiter-Blue
d	Day
DAPT	n-[n-(3,5-difluorophenacetyl)-L-alanyl]-S-phenylglycine t-butyl ester
DIV	Day <i>in vitro</i>
DMEM	Dulbecco's modified Eagle's medium
DMSO	Dimethyl sulfoxide
DNA	Deoxyribonucleic acid
DNT	Developmental neurotoxicity
DNT-IVB	DNT- <i>in vitro</i> testing battery
ED	Endocrine disruption
EDC	Endocrine disrupting chemical
EFSA	European food safety authority
e.g.	<i>Exempli gratia</i>
EGF	Epidermal growth factor
EGFR	Epidermal growth factor receptor

EU	European Union
EPA	Environmental protection agency
FDR	False discovery rate
FGF	Fibroblast growth factor
FN	False negative
FP	False positive
FR	Flame retardant
GABA	γ -aminobutyric acid
GALC	Galactosylceramidase
GD	Guidance document
GFAP	Glial fibrillary acidic protein
GIVIMP	Good <i>In Vitro</i> Method Practices
GS	Goat serum
GW	Gestational week
h	Hour
HCA	High Content Analysis
hiNPC	Human induced pluripotent stem cell-derived NPCs
hiPSC	Human induced pluripotent stem cell
hNNF	human neural network formation
hNPC	Human neural progenitor cells
IATA	Integrated approach to testing and assessment
ICC	Immunocytochemistry
iNPC	Induced neural progenitor cell
IQ	Intelligence Quotient
IUF	Leibniz Research Institute for Environmental Medicine

Abbreviations

IVB	<i>In vitro</i> battery
IVB-EU	IVB based on methods available in European laboratories
IVIVE	<i>In vitro-to-in vivo</i> extrapolation
KE	Key event
KER	Key event relationship
KNDP	Key neurodevelopmental process
LDH	Lactate dehydrogenase
LUHMES	Lund human mesencephalic cells
MBP	Myelin basic protein
MEA	Microelectrode array
MeHg	Methylmercury
MG	Microglia
MoA	Mode-of-action
mRNA	Messenger ribonucleic acid
MSE	Most sensitive endpoint
Na	Sodium
NAM	New approach methodology
NCC	Neural crest cell
NeuriTox/UKN4	Neurite outgrowth of CNS (LUHMES) neurons test
NMDA	N-methyl-D-aspartate
NNF	Neural network formation
NPC	Neural progenitor cell
NPC1a	Primary hNPC Proliferation Assay by Area
NPC1b	Primary hNPC Proliferation Assay by BrdU
NPC2a	Primary hNPC Migration Assay

NPC2b	Primary hNPC Neuronal Migration Assay
NPC2c	Primary hNPC Oligodendrocyte Migration Assay
NPC3	Primary hNPC Neuronal Differentiation Assay
NPC4a	Primary hNPC Neuronal Morphology (neurite length) Assay
NPC4b	Primary hNPC Neuronal Morphology (neurite area) Assay
NPC5	Primary hNPC Oligodendrocyte Differentiation Assay
NPC6	Primary hNPC Oligodendrocyte Maturation Assay
NRC	National research council
NTP	National toxicology program
O4	Oligodendrocyte marker
OECD	Organisation for Economic Co-operation and Development
OL	Myelinating oligodendrocyte
OPC	Oligodendrocytes precursor cell
PBDEs	Polybrominated diphenyl ethers
PBPK	Physiologically based pharmacokinetic
PBS	Phosphate buffered saline
PCR	Polymerase chain reaction
PDGFRA	Platelet-derived growth factor alpha
PDL	Poly-D-lysine
PeriTox/UKN5	Neurite outgrowth of peripheral (hiPSC) neurons test
PFA	Paraformaldehyde
PKC	Protein kinase C
PLP1	Proteolipid protein 1
PND	Postnatal day
PPV	Positive predictive value

Abbreviations

PVL	Periventricular leukomalacia
QM	Maturation quotient
qRT-PCR	Quantitative real-time polymerase chain reactions
QSAR	Quantitative structure-activity relationship
RASAR	Read-across structure-activity relationship
RFU	Relative fluorescent unit
RG	Radial glia
RNA	Ribonucleic acid
RNAseq	Ribonucleic acid sequencing
rNNF	Rat neural network formation
ROCK	Rho-associated protein kinase
ROS	Reactive oxygen species
SC	Solvent control
SD	Standard deviation
SEM	Standard error of mean
SOX2	SRY-box 2
T3	L-triiodothyronine
TBBPA	Tetrabromobisphenol A
TG	Testing guideline
TH	Thyroid hormone
TN	True negative
ToxPi	Toxicological prioritization index
TP	True positive
TUBB3	neuronal marker (β -III-tubulin)
U	Unit

UKN	University Konstanz
US	United States
US EPA	United States Environmental Protection Agency
VGSC	Voltage-gated sodium channels
vs	Versus
v:v	Volume per volume
w/o	Without
WoE	Weight of evidence

References

- Aasen, T., Raya, A., Barrero, M. J. et al. (2008). Efficient and rapid generation of induced pluripotent stem cells from human keratinocytes. *Nat Biotechnol* 26, 1276–1284. <https://doi.org/10.1038/NBT.1503>.
- Adhya, D., Annuario, E., Lancaster, M. A. et al. (2018). Understanding the role of steroids in typical and atypical brain development: Advantages of using a “brain in a dish” approach. *J Neuroendocrinol* 30, e12547. <https://doi.org/10.1111/JNE.12547>.
- Allen, N. J. (2014). Astrocyte regulation of synaptic behavior. *Annu Rev Cell Dev Biol* 30, 439–463. <https://doi.org/10.1146/ANNUREV-CELLBIO-100913-013053>.
- Aschner, M., Ceccatelli, S., Daneshian, M. et al. (2017). *Reference compounds for alternative test methods to indicate developmental neurotoxicity (DNT) potential of chemicals: Example lists & criteria for their selection & use*. Elsevier GmbH. <https://doi.org/10.14573/altex.1604201>.
- Ayuso-Sacido, A., Moliterno, J. A., Kratovac, S. et al. (2010). Activated EGFR signaling increases proliferation, survival, and migration and blocks neuronal differentiation in post-natal neural stem cells. *J Neurooncol* 97, 323–337. <https://doi.org/10.1007/S11060-009-0035-X>.
- Bal-Price, A., Crofton, K. M., Leist, M. et al. (2015). International STakeholder NETwork (ISTNET): creating a developmental neurotoxicity (DNT) testing road map for regulatory purposes. *Arch Toxicol* 89, 269–287. <https://doi.org/10.1007/S00204-015-1464-2>.
- Bal-Price, A., Hogberg, H. T., Crofton, K. M. et al. (2018). Recommendation on test readiness criteria for new approach methods in toxicology: Exemplified for developmental neurotoxicity. *ALTEX* 35, 306–352. <https://doi.org/10.14573/altex.1712081>.
- Bal-Price, A. K., Coecke, S., Costa, L. et al. (2012). Advancing the science of developmental neurotoxicity (DNT): testing for better safety evaluation. *ALTEX* 29, 202–15. <https://doi.org/10.14573/altex.2012.2.202>.
- Bal-Price, A., Pistollato, F., Sachana, M. et al. (2018). Strategies to improve the regulatory assessment of developmental neurotoxicity (DNT) using in vitro methods. *Toxicol Appl Pharmacol* 354, 7–18. <https://doi.org/10.1016/j.taap.2018.02.008>.
- Balmer, N. V., Weng, M. K., Zimmer, B. et al. (2012). Epigenetic changes and disturbed neural development in a human embryonic stem cell-based model relating to the fetal valproate syndrome. *Hum Mol Genet* 21, 4104–4114. <https://doi.org/10.1093/HMG/DDS239>.

References

- Bartmann, K., Hartmann, J., Kapr, J. et al. (2021). Measurement of Electrical Activity of Differentiated Human iPSC-Derived Neurospheres Recorded by Microelectrode Arrays (MEA). In J. Llorens and M. Barenys (eds.), *Experimental Neurotoxicology Methods. Neuromethods, vol 172* (473–488). New York: Humana. Available at: [10.1007/978-1-0716-1637-6_22](https://doi.org/10.1007/978-1-0716-1637-6_22).
- Baumann, J., Barenys, M., Gassmann, K. et al. (2014). Comparative human and rat “neurosphere assay” for developmental neurotoxicity testing. *Curr Protoc Toxicol* 1. <https://doi.org/10.1002/0471140856.TX1221S59>.
- Baumann, J., Dach, K., Barenys, M. et al. (2015). Application of the Neurosphere Assay for DNT Hazard Assessment: Challenges and Limitations. In *Methods in Pharmacology and Toxicology* (29). Totowa, NJ: Humana Press. https://doi.org/10.1007/7653_2015_49.
- Baumann, J., Gassmann, K., Masjosthusmann, S. et al. (2016). Comparative human and rat neurospheres reveal species differences in chemical effects on neurodevelopmental key events. *Arch Toxicol* 90, 1415–1427. <https://doi.org/10.1007/S00204-015-1568-8>.
- Baumann, N. and Pham-Dinh, D. (2001). Biology of oligodendrocyte and myelin in the mammalian central nervous system. *Physiol Rev* 81, 871–927. <https://doi.org/10.1152/PHYSREV.2001.81.2.871>/ASSET/IMAGES/LARGE/9J0210133008.JPG.
- Bean, B. P. (2007). The action potential in mammalian central neurons. *Nat Rev Neurosci* 8, 451–465. <https://doi.org/10.1038/NRN2148>.
- Behl, M., Ryan, K., Hsieh, J. H. et al. (2019). Screening for Developmental Neurotoxicity at the National Toxicology Program: The Future Is Here. *Toxicol Sci* 167, 6–14. <https://doi.org/10.1093/TOXSCI/KFY278>.
- Bell, S. M., Chang, X., Wambaugh, J. F. et al. (2018). In vitro to in vivo extrapolation for high throughput prioritization and decision making HHS Public Access. *Toxicol Vitr* 47, 213–227. <https://doi.org/10.1016/j.tiv.2017.11.016>.
- Bellanger, M., Pichery, C., Aerts, D. et al. (2013). Economic benefits of methylmercury exposure control in Europe: Monetary value of neurotoxicity prevention. *Environ Heal A Glob Access Sci Source* 12, 1–10. <https://doi.org/10.1186/1476-069X-12-3/TABLES/3>.
- Bennett, D., Bellinger, D. C., Birnbaum, L. S. et al. (2016). Project TENDR: Targeting Environmental Neuro-Developmental Risks The TENDR Consensus Statement. *Environ Health Perspect* 124,

- A118–A122. <https://doi.org/10.1289/EHP358>.
- Bernal, J. (2022). Thyroid Hormones in Brain Development and Function. *Endotext*. Available at: <https://www.ncbi.nlm.nih.gov/books/NBK285549/> [Accessed June 13, 2022].
- Bernal, J., Guadaño-Ferraz, A. and Morte, B. (2015). Thyroid hormone transporters--functions and clinical implications. *Nat Rev Endocrinol* 11, 406–417. <https://doi.org/10.1038/NREND0.2015.66>.
- Bogetofte, H., Jensen, P., Okarmus, J. et al. (2019). Perturbations in RhoA signalling cause altered migration and impaired neuritogenesis in human iPSC-derived neural cells with PARK2 mutation. *Neurobiol Dis* 132. <https://doi.org/10.1016/J.NBD.2019.104581>.
- Borghese, L., Dolezalova, D., Opitz, T. et al. (2010). Inhibition of Notch Signaling in Human Embryonic Stem Cell-Derived Neural Stem Cells Delays G1/S Phase Transition and Accelerates Neuronal Differentiation In Vitro and In Vivo. *Stem Cells* 28, 955–964. <https://doi.org/10.1002/stem.408>.
- Borrell, V. and Götz, M. (2014). Role of radial glial cells in cerebral cortex folding. *Curr Opin Neurobiol* 27, 39–46. <https://doi.org/10.1016/j.conb.2014.02.007>.
- Brown, J. P., Hall, D., Frank, C. L. et al. (2016). Evaluation of a microelectrode array-based assay for neural network ontogeny using training set chemicals. *Toxicol Sci* 154, 126–139. <https://doi.org/10.1093/toxsci/kfw147>.
- Buc-Caron, M.-H. (1995). Neuroepithelial progenitor cells explanted from human fetal brain proliferate and differentiate in vitro. *Neurobiol Dis* 2, 37–47. <https://doi.org/10.1006/nbdi.1995.0004>.
- Buzsáki, G., Anastassiou, C. A. and Koch, C. (2012). The origin of extracellular fields and currents--EEG, ECoG, LFP and spikes. *Nat Rev Neurosci* 13, 407–420. <https://doi.org/10.1038/NRN3241>.
- Chambers, S. M., Fasano, C. A., Papapetrou, E. P. et al. (2009). Highly efficient neural conversion of human ES and iPS cells by dual inhibition of SMAD signaling. *Nat Biotechnol* 27, 275–280. <https://doi.org/10.1038/nbt.1529>.
- Chang, X., Tan, Y. M., Allen, D. G. et al. (2022). IVIVE: Facilitating the Use of In Vitro Toxicity Data in Risk Assessment and Decision Making. *Toxics* 10. <https://doi.org/10.3390/TOXICS10050232>.

References

- Choi, C. and Benveniste, E. N. (2004). Fas ligand/Fas system in the brain: Regulator of immune and apoptotic responses. *Brain Res Rev* 44, 65–81. <https://doi.org/10.1016/J.BRAINRESREV.2003.08.007>.
- Coecke, S., Goldberg, A. M., Allen, S. et al. (2007). Workgroup Report: Incorporating In Vitro Alternative Methods for Developmental Neurotoxicity into International Hazard and Risk Assessment Strategies. *Environ Health Perspect* 115, 924–931. <https://doi.org/10.1289/ehp.9427>.
- Collins, F. S., Gray, G. M. and Bucher, J. R. (2008). Transforming Environmental Health Protection. *Science* 319, 906. <https://doi.org/10.1126/SCIENCE.1154619>.
- Copp, A. J., Greene, N. D. E. and Murdoch, J. N. (2003). The genetic basis of mammalian neurulation. *Nat Rev Genet* 4, 784–793. <https://doi.org/10.1038/nrg1181>.
- Crofton, K., Fritsche, E., Ylikomi, T. et al. (2014). International STakeholder NETwork (ISTNET) for creating a developmental neurotoxicity testing (DNT) roadmap for regulatory purposes. *ALTEX* 31, 223–224. <https://doi.org/10.14573/ALTEX.1402121>.
- Crofton, K. M. and Mundy, W. R. (2021). External Scientific Report on the Interpretation of Data from the Developmental Neurotoxicity In Vitro Testing Assays for Use in Integrated Approaches for Testing and Assessment. *EFSA Support Publ* 18. <https://doi.org/10.2903/SP.EFSA.2021.EN-6924>.
- Crofton, K. M., Mundy, W. R., Lein, P. J. et al. (2011). Developmental neurotoxicity testing: Recommendations for developing alternative methods for the screening and prioritization of chemicals. *ALTEX* 28, 9–15. <https://doi.org/10.14573/altex.2011.1.009>.
- Crofton, K. M., Mundy, W. R. and Shafer, T. J. (2012). Developmental neurotoxicity testing: A path forward. *Congenit Anom (Kyoto)* 52, 140–146. <https://doi.org/10.1111/j.1741-4520.2012.00377.x>.
- Dach, K., Bendt, F., Huebenthal, U. et al. (2017). BDE-99 impairs differentiation of human and mouse NPCs into the oligodendroglial lineage by species-specific modes of action. *Sci Rep* 7. <https://doi.org/10.1038/srep44861>.
- Delp, J., Gutbier, S., Klima, S. et al. (2018). A high-throughput approach to identify specific neurotoxicants/ developmental toxicants in human neuronal cell function assays. *ALTEX* 35, 235–253. <https://doi.org/10.14573/altex.1712182>.
- Denham, M. and Dottori, M. (2011). Neural differentiation of induced pluripotent stem cells.

-
- Methods Mol Biol* 793, 99–110. https://doi.org/10.1007/978-1-61779-328-8_7/COVER/.
- Dubois, J., Benders, M., Borradori-Tolsa, C. et al. (2008). Primary cortical folding in the human newborn: an early marker of later functional development. *Brain* 131, 2028–2041. <https://doi.org/10.1093/BRAIN/AWN137>.
- EFSA (2013). Scientific Opinion on the developmental neurotoxicity potential of acetamiprid and imidacloprid. *EFSA J* 11. <https://doi.org/10.2903/j.efsa.2013.3471>.
- Egert, U. and Hämmerle, H. (2002). Application of the microelectrode-array (MEA) technology in pharmaceutical drug research. *Sensoren im Fokus neuer Anwendungen w.e.b Univ Dresden*, 51–54
- Ehrlich, D. E. and Josselyn, S. A. (2016). Plasticity-related genes in brain development and amygdala-dependent learning. *Genes Brain Behav* 15, 125–143. <https://doi.org/10.1111/GBB.12255>.
- Fernández, V., Llinares-Benadero, C. and Borrell, V. (2016). Cerebral cortex expansion and folding: what have we learned? *EMBO J* 35, 1021–1044. <https://doi.org/10.15252/EMBJ.201593701>.
- Fields, R. D. (2008). White matter in learning, cognition and psychiatric disorders. *Trends Neurosci* 31, 361–370. <https://doi.org/10.1016/J.TINS.2008.04.001>.
- Fonnum, F. (1984). Glutamate: A Neurotransmitter in Mammalian Brain. *J Neurochem* 42, 1–11. <https://doi.org/10.1111/J.1471-4159.1984.TB09689.X>.
- Förster, N., Butke, J., Keßel, E. H. et al. (2021). Reliable Identification and Quantification of Neural Cells in Microscopic Images of Neurospheres. *Cytom Part A*. <https://doi.org/10.1002/cyto.a.24514>.
- Frank, C. L., Brown, J. P., Wallace, K. et al. (2017). Developmental neurotoxicants disrupt activity in cortical networks on microelectrode arrays: Results of screening 86 compounds during neural network formation. *Toxicol Sci* 160, 121–135. <https://doi.org/10.1093/toxsci/kfx169>.
- Frega, M., Pasquale, V., Tedesco, M. et al. (2012). Cortical cultures coupled to Micro-Electrode Arrays: A novel approach to perform in vitro excitotoxicity testing. *Neurotoxicol Teratol* 34, 116–127. <https://doi.org/10.1016/j.ntt.2011.08.001>.
- Fritsche, E., Barenys, M., Klose, J. et al. (2018). Current availability of stem cell-Based in vitro methods for developmental neurotoxicity (DNT) testing. *Toxicol Sci* 165, 21–30. <https://doi.org/10.1093/toxsci/kfy178>.

- Fritsche, E., Crofton, K. M., Hernandez, A. F. et al. (2017). OECD/EFSA workshop on developmental neurotoxicity (DNT): The use of non-animal test methods for regulatory purposes. *ALTEX - Altern to Anim Exp* 34, 311–315. <https://doi.org/10.14573/ALTEX.1701171>.
- Fritsche, E., Grandjean, P., Crofton, K. M. et al. (2018). Consensus statement on the need for innovation, transition and implementation of developmental neurotoxicity (DNT) testing for regulatory purposes. *Toxicol Appl Pharmacol* 354, 3–6. <https://doi.org/10.1016/J.TAAP.2018.02.004>.
- Fritsche, E., Haarmann-Stemmann, T., Kapr, J. et al. (2021). Stem Cells for Next Level Toxicity Testing in the 21st Century. *Small* 17, 1–31. <https://doi.org/10.1002/sml.202006252>.
- Gibb, S. (2008). Toxicity testing in the 21st century: A vision and a strategy. *Reprod Toxicol* 25, 136–138. <https://doi.org/10.1016/J.REPROTOX.2007.10.013>.
- Giordano, G. and Costa, L. G. (2012). Developmental Neurotoxicity: Some Old and New Issues. *ISRN Toxicol* 2012, 1–12. <https://doi.org/10.5402/2012/814795>.
- Gourmelon, A. and Delrue, N. (2016). Validation in support of internationally harmonised OECD test guidelines for assessing the safety of chemicals. In C. Eskes and M. Whelan (eds.), *Validation of Alternative Methods for Toxicity Testing* (9–32). Springer. https://doi.org/10.1007/978-3-319-33826-2_2.
- Grandjean, P. and Landrigan, P. (2006). Developmental neurotoxicity of industrial chemicals. *Lancet* 368, 2167–2178. [https://doi.org/10.1016/S0140-6736\(06\)69665-7](https://doi.org/10.1016/S0140-6736(06)69665-7).
- Grandjean, P. and Landrigan, P. J. (2014). Neurobehavioural effects of developmental toxicity. *Lancet Neurol* 13, 330–338. [https://doi.org/10.1016/S1474-4422\(13\)70278-3](https://doi.org/10.1016/S1474-4422(13)70278-3).
- Griesinger, C., Desprez, B., Coecke, S. et al. (2016). Validation of alternative methods for toxicity testing: Concepts, Challenges, Processes and Tools. In C. Eskes and M. Whelan (eds.), *Validation of Alternative Methods for Toxicity Testing* (65–132). Springer. <https://doi.org/10.1007/978-3-319-33826-2>.
- de Groot, D. M. G., Hartgring, S., van de Horst, L. et al. (2005). 2D and 3D assessment of neuropathology in rat brain after prenatal exposure to methylazoxymethanol, a model for developmental neurotoxicity. *Reprod Toxicol* 20, 417–432. <https://doi.org/10.1016/j.reprotox.2005.04.006>.
- Hardy, A., Benford, D., Halldorsson, T. et al. (2017). Guidance on the use of the weight of evidence approach in scientific assessments. *EFSA J* 15, e04971.

- <https://doi.org/10.2903/J.EFSA.2017.4971>.
- Harrill, J. A., Freudenrich, T., Wallace, K. et al. (2018). Testing for developmental neurotoxicity using a battery of in vitro assays for key cellular events in neurodevelopment. *Toxicol Appl Pharmacol* 354, 24–39. <https://doi.org/10.1016/J.TAAP.2018.04.001>.
- Hartung, T. (2007). Food for thought ... on validation. *ALTEX* 24, 67–73. <https://doi.org/10.14573/ALTEX.2007.2.67>.
- Hartung, T., Hoffmann, S. and Stephens, M. (2013). Food for Thought ... Mechanistic Validation. *ALTEX* 30, 119–130. <https://doi.org/10.14573/ALTEX.2013.2.119>.
- Hernández-Jerez, A., Adriaanse, P., Aldrich, A. et al. (2021). Development of Integrated Approaches to Testing and Assessment (IATA) case studies on developmental neurotoxicity (DNT) risk assessment. *EFSA J* 19, 63. <https://doi.org/10.2903/j.efsa.2021.6599>.
- Hevner, R. F. (2015). Brain overgrowth in disorders of RTK–PI3K–AKT signaling: A mosaic of malformations. *Semin Perinatol* 39, 36–43. <https://doi.org/10.1053/J.SEMPERI.2014.10.006>.
- Hofrichter, M., Nimtz, L., Tigges, J. et al. (2017). Comparative performance analysis of human iPSC-derived and primary neural progenitor cells (NPC) grown as neurospheres in vitro. *Stem Cell Res* 25, 72–82. <https://doi.org/10.1016/J.SCR.2017.10.013>.
- Howard, B. M., Mo, Z., Filipovic, R. et al. (2008). Radial glia cells in the developing human brain. *Neuroscientist* 14, 459–473. <https://doi.org/10.1177/1073858407313512>.
- de Hoz, L. and Simons, M. (2015). The emerging functions of oligodendrocytes in regulating neuronal network behaviour. *BioEssays* 37, 60–69. <https://doi.org/10.1002/BIES.201400127>.
- Hyman, S. E. (2005). Neurotransmitters. *Curr Biol* 15. <https://doi.org/10.1016/J.CUB.2005.02.037>.
- Hyvärinen, T., Hysalo, A., Kapucu, F. E. et al. (2019). Functional characterization of human pluripotent stem cell-derived cortical networks differentiated on laminin-521 substrate: comparison to rat cortical cultures. *Sci Rep* 9, 17125. <https://doi.org/10.1038/s41598-019-53647-8>.
- Jakovcevski, I., Filipovic, R., Mo, Z. et al. (2009). Oligodendrocyte Development and the Onset of Myelination in the Human Fetal Brain. *Front Neuroanat* 3. <https://doi.org/10.3389/NEURO.05.005.2009>.
- Jennings, P. (2015). “The future of in vitro toxicology.” *Toxicol Vitro* 29, 1217–1221.

- <https://doi.org/10.1016/J.TIV.2014.08.011>.
- Johnstone, A. F. M., Gross, G. W., Weiss, D. G. et al. (2010). Microelectrode arrays: A physiologically based neurotoxicity testing platform for the 21st century. *Neurotoxicology* 31, 331–350. <https://doi.org/10.1016/j.neuro.2010.04.001>.
- Judson, R. S., Houck, K. A., Watt, E. D. et al. (2017). On selecting a minimal set of in vitro assays to reliably determine estrogen agonist activity. *Regul Toxicol Pharmacol* 91, 39–49. <https://doi.org/10.1016/J.YRTPH.2017.09.022>.
- Kadereit, S., Zimmer, B., Van Thriel, C. et al. (2012). Compound selection for in vitro modeling of developmental neurotoxicity. *Front Biosci (Landmark Ed)* 17, 2442–2460. <https://doi.org/10.2741/4064>.
- Kapucu, F. E., A Tanskanen, J. M., Mikkonen, J. E. et al. (2012). Burst analysis tool for developing neuronal networks exhibiting highly varying action potential dynamics. <https://doi.org/10.3389/fncom.2012.00038>.
- Kavlock, R. J., Bahadori, T., Barton-Maclaren, T. S. et al. (2018). Accelerating the Pace of Chemical Risk Assessment. *Chem Res Toxicol* 31, 287–290. <https://doi.org/10.1021/ACS.CHEMRESTOX.7B00339>.
- Kiryushko, D., Korshunova, I., Berezin, V. et al. (2006). Neural Cell Adhesion Molecule Induces Intracellular Signaling via Multiple Mechanisms of Ca²⁺ Homeostasis. *Mol Biol Cell* 17, 2278. <https://doi.org/10.1091/MBC.E05-10-0987>.
- Klose, J., Pahl, M., Bartmann, K. et al. (2021). Neurodevelopmental toxicity assessment of flame retardants using a human DNT in vitro testing battery. *Cell Biol Toxicol*, 1–27. <https://doi.org/10.1007/s10565-021-09603-2>.
- Klose, J., Tigges, J., Masjosthusmann, S. et al. (2021). TBBPA targets converging key events of human oligodendrocyte development resulting in two novel AOPs. *ALTEX* 38, 215–234. <https://doi.org/10.14573/altex.2007201>.
- Knuesel, I., Chicha, L., Britschgi, M. et al. (2014). Maternal immune activation and abnormal brain development across CNS disorders. *Nat Rev Neurol* 10, 643–660. <https://doi.org/10.1038/NRNEUROL.2014.187>.
- Koch, K., Bartmann, K., Hartmann, J. et al. (2022). Scientific validation of human Neurosphere Assays for developmental neurotoxicity evaluation. *Front Press* 0, 1–38. <https://doi.org/10.3389/FTOX.2022.816370>.

-
- Kramer, N. I., Di Consiglio, E., Blaauboer, B. J. et al. (2015). Biokinetics in repeated-dosing in vitro drug toxicity studies. *Toxicol Vitr* 30, 217–224. <https://doi.org/10.1016/J.TIV.2015.09.005>.
- Krebs, A., Waldmann, T., Wilks, M. F. et al. (2019). Template for the description of cell-based toxicological test methods to allow evaluation and regulatory use of the data. *ALTEX - Altern to Anim Exp* 36, 682–699. <https://doi.org/10.14573/ALTEX.1909271>.
- Krewski, D., Andersen, M. E., Tyshenko, M. G. et al. (2019). Toxicity testing in the 21st century: progress in the past decade and future perspectives. *Arch Toxicol* 94. <https://doi.org/10.1007/s00204-019-02613-4>.
- Kriegstein, A. and Alvarez-Buylla, A. (2009). The Glial Nature of Embryonic and Adult Neural Stem Cells. *Annu Rev Neurosci* 32, 149. <https://doi.org/10.1146/ANNUREV.NEURO.051508.135600>.
- Krug, A. K., Balmer, N. V., Matt, F. et al. (2013). Evaluation of a human neurite growth assay as specific screen for developmental neurotoxicants. *Arch Toxicol* 87, 2215–2231. <https://doi.org/10.1007/s00204-013-1072-y>.
- Kuijlaars, J., Oyelami, T., Diels, A. et al. (2016). Sustained synchronized neuronal network activity in a human astrocyte co-culture system. *Sci Reports* 2016 61 6, 1–14. <https://doi.org/10.1038/srep36529>.
- Lamb, T. M., Knecht, A. K., Smith, W. C. et al. (1993). Neural Induction by the Secreted Polypeptide Noggin. *Science (80-)* 262, 713–718. <https://doi.org/10.1126/SCIENCE.8235591>.
- Lee, D. Y. (2015). Roles of mTOR Signaling in Brain Development. *Exp Neurobiol* 24, 177–185. <https://doi.org/10.5607/EN.2015.24.3.177>.
- Lein, P., Locke, P. and Goldberg, A. (2007). Meeting Report: Alternatives for Developmental Neurotoxicity Testing. *Environ Health Perspect* 115, 764–768. <https://doi.org/10.1289/ehp.9841>.
- Leist, M. and Hartung, T. (2013). Inflammatory findings on species extrapolations: humans are definitely no 70-kg mice. *Arch Toxicol* 87, 563–567. <https://doi.org/10.1007/S00204-013-1038-0>.
- Leist, M., Hasiwa, N., Daneshian, M. et al. (2012). Validation and quality control of replacement alternatives - current status and future challenges. *Toxicol Res (Camb)* 1, 8–22. <https://doi.org/10.1039/c2tx20011b>.

References

- Leist, M., Hasiwa, N., Rovida, C. et al. (2014). Consensus report on the future of animal-free systemic toxicity testing. *ALTEX* 31, 341–356. <https://doi.org/10.14573/altex.1406091>.
- Little, D., Ketteler, R., Gissen, P. et al. (2019). Using stem cell–derived neurons in drug screening for neurological diseases. *Neurobiol Aging* 78, 130–141. <https://doi.org/10.1016/J.NEUROBIOLAGING.2019.02.008>.
- Lupu, D., Andersson, P., Bornehag, C.-G. et al. (2020). The ENDpoiNTs Project: Novel Testing Strategies for Endocrine Disruptors Linked to Developmental Neurotoxicity. *Int J Mol Sci* 21. <https://doi.org/10.3390/IJMS21113978>.
- Maertens, A., Golden, E., Luechtefeld, T. H. et al. (2022). Probabilistic risk assessment - the keystone for the future of toxicology. *ALTEX* 39, 3–29. <https://doi.org/10.14573/ALTEX.2201081>.
- Makris, S. L., Raffaele, K., Allen, S. et al. (2009). A retrospective performance assessment of the developmental neurotoxicity study in support of OECD test guideline 426. *Environ Health Perspect* 117, 17–25. <https://doi.org/10.1289/EHP.11447>.
- Marvel, S. W., To, K., Grimm, F. A. et al. (2018). ToxPi Graphical User Interface 2.0: Dynamic exploration, visualization, and sharing of integrated data models. *BMC Bioinformatics* 19, 1–7. <https://doi.org/10.1186/S12859-018-2089-2/FIGURES/3>.
- Masjosthusmann, S., Becker, D., Petzuch, B. et al. (2018). A transcriptome comparison of time-matched developing human, mouse and rat neural progenitor cells reveals human uniqueness. *Toxicol Appl Pharmacol* 354, 40–55. <https://doi.org/10.1016/j.taap.2018.05.009>.
- Masjosthusmann, S., Blum, J., Bartmann, K. et al. (2020). *Establishment of an a priori protocol for the implementation and interpretation of an in-vitro testing battery for the assessment of developmental neurotoxicity*. Wiley. <https://doi.org/10.2903/sp.efsa.2020.en-1938>.
- Mendola, P., Selevan, S. G., Gutter, S. et al. (2002). Environmental factors associated with a spectrum of neurodevelopmental deficits. *Ment Retard Dev Disabil Res Rev* 8, 188–197. <https://doi.org/10.1002/MRDD.10033>.
- Miller, M. D., Crofton, K. M., Rice, D. C. et al. (2009). Thyroid-disrupting chemicals: interpreting upstream biomarkers of adverse outcomes. *Environ Health Perspect* 117, 1033–1041. <https://doi.org/10.1289/EHP.0800247>.
- Moors, M., Cline, J. E., Abel, J. et al. (2007). ERK-dependent and -independent pathways trigger

- human neural progenitor cell migration. *Toxicol Appl Pharmacol* 221, 57–67. <https://doi.org/10.1016/j.taap.2007.02.018>.
- Moors, M., Rockel, T. D., Abel, J. et al. (2009). Human Neurospheres as Three-Dimensional Cellular Systems for Developmental Neurotoxicity Testing. *Environ Health Perspect* 117, 1131–1138. <https://doi.org/10.1289/EHP.0800207>.
- Moreau, M. and Leclerc, C. (2003). The choice between epidermal and neural fate: a matter of calcium. *Int J Dev Biol* 48, 75–84. <https://doi.org/10.1387/IJDB.15272372>.
- Nair, J. J., Rárová, L., Strnad, M. et al. (2015). Mechanistic insights to the cytotoxicity of amaryllidaceae alkaloids. *Nat Prod Commun* 10, 171–182. <https://doi.org/10.1177/1934578X1501000138>.
- National Research Council (2006). Toxicity Testing for Assessment of Environmental Agents: Interim Report. *Toxic Test Assess Environ Agents Interim Rep*, 1–244. <https://doi.org/10.17226/11523>.
- National Research Council (2007). Toxicity Testing in the 21st Century: A Vision and a Strategy. *Toxic Test 21st Century A Vis a Strateg*, 1–196. <https://doi.org/10.17226/11970>.
- Needham, L. L., Grandjean, P., Heinzow, B. et al. (2011). Partition of environmental chemicals between maternal and fetal blood and tissues. *Environ Sci Technol* 45, 1121–1126. <https://doi.org/10.1021/ES1019614>.
- Nimtz, L., Hartmann, J., Tigges, J. et al. (2020). Characterization and application of electrically active neuronal networks established from human induced pluripotent stem cell-derived neural progenitor cells for neurotoxicity evaluation. *Stem Cell Res* 45, 101761. <https://doi.org/10.1016/J.SCR.2020.101761>.
- Odawara, A., Katoh, H., Matsuda, N. et al. (2016). Physiological maturation and drug responses of human induced pluripotent stem cell-derived cortical neuronal networks in long-term culture. <https://doi.org/10.1038/srep26181>.
- OECD (2016). Guidance document on the reporting of defined approaches to be used within integrated approaches to testing and assessment. *OECD Environ Heal Saf Publ*
- OECD (2021). Guideline No. 497 Guideline on Defined Approaches for Skin Sensitisation. *Section 4*. Available at: <http://www.oecd.org/termsandconditions/>. [Accessed July 8, 2022].
- OECD (2014). New Scoping Document on In Vitro and Ex Vivo Assays for the Identification of

- Modulators of Thyroid Hormone Signalling. ENV/JM/MONO(2014)23. *OECD Publ Series on*
- OECD (2018). *Oecd/Ocde 443 Oecd Guideline for the Testing of Chemicals*. Available at: <http://www.oecd.org/termsandconditions/>. [Accessed May 27, 2022].
- OECD (2007). *OECD guidelines for the testing of chemicals/section 4:health effects. Test No. 426: developmental neurotoxicity study*. Available at: <http://www.oecd.org/dataoecd/20/52/37622194.pdf> [Accessed July 22, 2021].
- OECD (2020). *Overview of Concepts and Available Guidance related to Integrated Approaches to Testing and Assessment (IATA)*. *Environ Heal Safety, Environ Dir OECD*
- OECD (2008). *Series on Testing and Assessment No. 89 - Retrospective Performance Assessment of the Test Guideline 426 on Developmental Neurotoxicity*. *ENV/JM/MON*
- Okado, N., Kakimi, S. and Kojima, T. (1979). *Synaptogenesis in the cervical cord of the human embryo: sequence of synapse formation in a spinal reflex pathway*. *J Comp Neurol* 184, 491–517. <https://doi.org/10.1002/CNE.901840305>.
- Paini, A., Leonard, J. A., Joossens, E. et al. (2019). *Next generation physiologically based kinetic (NG-PBK) models in support of regulatory decision making*. *Comput Toxicol* 9, 61–72. <https://doi.org/10.1016/J.COMTOX.2018.11.002>.
- Pang, Z. P., Yang, N., Vierbuchen, T. et al. (2011). *Induction of human neuronal cells by defined transcription factors*. *Nature* 476, 220. <https://doi.org/10.1038/NATURE10202>.
- Paparella, M., Bennekou, S. H. and Bal-Price, A. (2020). *An analysis of the limitations and uncertainties of in vivo developmental neurotoxicity testing and assessment to identify the potential for alternative approaches*. *Reprod Toxicol* 96, 327–336. <https://doi.org/10.1016/J.REPROTOX.2020.08.002>.
- Park, H. C. and Appel, B. (2003). *Delta-Notch signaling regulates oligodendrocyte specification*. *Development* 130, 3747–3755. <https://doi.org/10.1242/DEV.00576>.
- Pavlík, A. and Teisinger, J. (1980). *Effect of cycloheximide administered to rats in early postnatal life: Prolonged inhibition of DNA synthesis in the developing brain*. *Brain Res* 192, 531–541. [https://doi.org/10.1016/0006-8993\(80\)90903-8](https://doi.org/10.1016/0006-8993(80)90903-8).
- Petit, T. L. and Isaacson, R. L. (1976). *Anatomical and behavioral effects of colchicine administration to rats late in utero*. *Dev Psychobiol* 9, 119–129. <https://doi.org/10.1002/DEV.420090204>.

-
- Piper, D. R., Mujtaba, T., Keyoung, H. et al. (2001). Identification and characterization of neuronal precursors and their progeny from human fetal tissue. *J Neurosci Res* 66, 356–368. <https://doi.org/10.1002/JNR.1228>.
- Pistollato, F., Madia, F., Corvi, R. et al. (2021). Current EU regulatory requirements for the assessment of chemicals and cosmetic products: challenges and opportunities for introducing new approach methodologies. *Arch Toxicol* 95, 1867–1897. <https://doi.org/10.1007/S00204-021-03034-Y>.
- Proença, S., Escher, B. I., Fischer, F. C. et al. (2021). Effective exposure of chemicals in in vitro cell systems: A review of chemical distribution models. *Toxicol Vitr* 73. <https://doi.org/10.1016/J.TIV.2021.105133>.
- Purves, D. and Lichtman, J. W. (1980). Elimination of synapses in the developing nervous system. *Science* 210, 153–7. Available at: <http://www.ncbi.nlm.nih.gov/pubmed/7414326> [Accessed October 13, 2018].
- Radio, N. M. and Mundy, W. R. (2008). Developmental neurotoxicity testing in vitro: Models for assessing chemical effects on neurite outgrowth. *Neurotoxicology* 29, 361–376. <https://doi.org/10.1016/J.NEURO.2008.02.011>.
- Reif, D. M., Martin, M. T., Tan, S. W. et al. (2010). Endocrine profiling and prioritization of environmental chemicals using ToxCast data. *Env Heal Perspect* 118, 1714–1720. <https://doi.org/10.1289/ehp.1002180>.
- Reubinoff, B. E., Itsykson, P., Turetsky, T. et al. (2001). Neural progenitors from human embryonic stem cells. *Nat Biotechnol* 19, 1134–1140. <https://doi.org/10.1038/NBT1201-1134>.
- Reynolds, B. A., Tetzlaff, W. and Weiss, S. (1992). A multipotent EGF-responsive striatal embryonic progenitor cell produces neurons and astrocytes. *J Neurosci* 12, 4565–4574. <https://doi.org/10.1523/JNEUROSCI.12-11-04565.1992>.
- Rice, D. and Barone, S. (2000). Critical periods of vulnerability for the developing nervous system: Evidence from humans and animal models. *Environ Health Perspect* 108, 511–533. <https://doi.org/10.1289/ehp.00108s3511>.
- Roberts, E. and Frankel, S. (1950). γ -Aminobutyric acid in brain: Its formation from glutamic acid. *J Biol Chem* 187, 55–63
- Saavedra, L., Wallace, K., Freudenrich, T. F. et al. (2021). Comparison of acute effects of neurotoxic compounds on network activity in human and rodent neural cultures. *Toxicol Sci* 180, 295–

312. <https://doi.org/10.1093/TOXSCI/KFAB008>.
- Sachana, M., Bal-Price, A., Crofton, K. M. et al. (2019). International Regulatory and Scientific Effort for Improved Developmental Neurotoxicity Testing. *Toxicol Sci* 167, 45–57. <https://doi.org/10.1093/toxsci/kfy211>.
- Sagiv, S. K., Thurston, S. W., Bellinger, D. C. et al. (2010). Prenatal organochlorine exposure and behaviors associated with attention deficit hyperactivity disorder in school-aged children. *Am J Epidemiol* 171, 593–601. <https://doi.org/10.1093/AJE/KWP427>.
- Schmidt-Kastner, R., van Os, J., W.M. Steinbusch, H. et al. (2006). Gene regulation by hypoxia and the neurodevelopmental origin of schizophrenia. *Schizophr Res* 84, 253–271. <https://doi.org/10.1016/J.SCHRES.2006.02.022>.
- Schmidt, C. W. (2013). Beyond Uncertainty Factors: Protecting the Tails of the Bell Curve. *Environ Health Perspect* 121, a26. <https://doi.org/10.1289/EHP.121-A26>.
- Schmuck, M. R., Temme, T., Dach, K. et al. (2017). Omnisphero: a high-content image analysis (HCA) approach for phenotypic developmental neurotoxicity (DNT) screenings of organoid neurosphere cultures in vitro. *Arch Toxicol* 91, 2017–2028. <https://doi.org/10.1007/s00204-016-1852-2>.
- Silbereis, J. C., Pochareddy, S., Zhu, Y. et al. (2016). The Cellular and Molecular Landscapes of the Developing Human Central Nervous System. *Neuron* 89, 248–68. <https://doi.org/10.1016/j.neuron.2015.12.008>.
- Smirnova, L., Hogberg, H. T., Leist, M. et al. (2014). Food for thought...: Developmental neurotoxicity - Challenges in the 21st century and in vitro opportunities. *ALTEX* 31, 129–156. <https://doi.org/10.14573/ALTEX.1403271>.
- Spear, L. P. (2013). Adolescent Neurodevelopment. *J Adolesc Health* 52, S7. <https://doi.org/10.1016/J.JADOHEALTH.2012.05.006>.
- Stiles, J. and Jernigan, T. L. (2010). The Basics of Brain Development. *Neuropsychol Rev* 20, 327–348. <https://doi.org/10.1007/s11065-010-9148-4>.
- Strickland, J., Truax, J., Corvaro, M. et al. (2022). Application of Defined Approaches for Skin Sensitization to Agrochemical Products. *Front Toxicol* 0, 46. <https://doi.org/10.3389/FTOX.2022.852856>.
- Svendsen, C. N., Fawcett, J. W., Bentlage, C. et al. (1995). Increased survival of rat EGF-generated

- CNS precursor cells using B27 supplemented medium. *Exp Brain Res* 102. <https://doi.org/10.1007/BF00230645>.
- Takahashi, K., Tanabe, K., Ohnuki, M. et al. (2007). Induction of Pluripotent Stem Cells from Adult Human Fibroblasts by Defined Factors. *Cell* 131, 861–872. <https://doi.org/10.1016/j.cell.2007.11.019>.
- Tau, G. Z. and Peterson, B. S. (2010). Normal Development of Brain Circuits. *Neuropsychopharmacology* 35, 147. <https://doi.org/10.1038/NPP.2009.115>.
- Tegenge, M. A., Rockel, T. D., Fritsche, E. et al. (2011). Nitric oxide stimulates human neural progenitor cell migration via cGMP-mediated signal transduction. *Cell Mol Life Sci* 68, 2089–2099. <https://doi.org/10.1007/S00018-010-0554-9>.
- Terron, A. and Bennekou, S. H. (2018). Towards a regulatory use of alternative developmental neurotoxicity testing (DNT). *Toxicol Appl Pharmacol* 354, 19–23. <https://doi.org/10.1016/J.TAAP.2018.02.002>.
- Toscano, C. D. and Guilarte, T. R. (2005). Lead neurotoxicity: From exposure to molecular effects. *Brain Res Rev* 49, 529–554. <https://doi.org/10.1016/J.BRAINRESREV.2005.02.004>.
- Trasande, L., Landrigan, P. J. and Schechter, C. (2005). Public Health and Economic Consequences of Methyl Mercury Toxicity to the Developing Brain. *Environ Health Perspect* 113, 590. <https://doi.org/10.1289/EHP.7743>.
- Tsuji, R. and Crofton, K. M. (2012). Developmental neurotoxicity guideline study: Issues with methodology, evaluation and regulation*. *Congenit Anom (Kyoto)* 52, 122–128. <https://doi.org/10.1111/J.1741-4520.2012.00374.X>.
- Tukker, A. M., Bouwman, L. M. S., van Kleef, R. G. D. M. et al. (2020). Perfluorooctane sulfonate (PFOS) and perfluorooctanoate (PFOA) acutely affect human $\alpha 1\beta 2\gamma 2L$ GABAA receptor and spontaneous neuronal network function in vitro. *Sci Rep* 10. <https://doi.org/10.1038/s41598-020-62152-2>.
- Tukker, A. M., De Groot, M. W. G. D. M., Wijnolts, F. M. J. et al. (2016). Research article is the time right for in vitro neurotoxicity testing using human iPSC-derived neurons? *ALTEX* 33, 261–271. <https://doi.org/10.14573/altex.1510091>.
- Tukker, A. M., van Kleef, R. G. D. M., Wijnolts, F. M. J. et al. (2020). Towards animal-free neurotoxicity screening: Applicability of hiPSC-derived neuronal models for in vitro seizure liability assessment. *ALTEX* 37, 121–135. <https://doi.org/10.14573/altex.1907121>.

References

- Tukker, A. M., Wijnolts, F. M. J., de Groot, A. et al. (2018). Human iPSC-derived neuronal models for in vitro neurotoxicity assessment. *Neurotoxicology* 67, 215–225. <https://doi.org/10.1016/j.neuro.2018.06.007>.
- U.S. EPA (1998). Health Effects Guidelines OPPTS 870.6300. *Dev Neurotox Study EPA 71*
- Uhlhaas, P. and Singer, W. (2006). Neural synchrony in brain disorders: relevance for cognitive dysfunctions and pathophysiology. *Neuron* 52, 155–168. <https://doi.org/10.1016/J.NEURON.2006.09.020>.
- Valdiviezo, A., Luo, Y. S., Chen, Z. et al. (2021). Quantitative In Vitro-to-In Vivo Extrapolation for Mixtures: A Case Study of Superfund Priority List Pesticides. *Toxicol Sci* 183, 60–69. <https://doi.org/10.1093/TOXSCI/KFAB076>.
- Wang, Z., Walker, G. W., Muir, D. C. G. et al. (2020). Toward a Global Understanding of Chemical Pollution: A First Comprehensive Analysis of National and Regional Chemical Inventories. *Environ Sci Technol* 54, 2575–2584. https://doi.org/10.1021/ACS.EST.9B06379/ASSET/IMAGES/LARGE/ES9B06379_0002.JPEG.
- Weiss, B. (1988). Neurobehavioral toxicity as a basis for risk assessment. *Trends Pharmacol Sci* 9, 59–62. [https://doi.org/10.1016/0165-6147\(88\)90118-6](https://doi.org/10.1016/0165-6147(88)90118-6).
- Wetmore, B. A., Wambaugh, J. F., Ferguson, S. S. et al. (2012). Integration of dosimetry, exposure, and high-throughput screening data in chemical toxicity assessment. *Toxicol Sci* 125, 157–174. <https://doi.org/10.1093/TOXSCI/KFR254>.
- Wong, C. T., Ahmad, E., Li, H. et al. (2014). Prostaglandin E2 alters Wnt-dependent migration and proliferation in neuroectodermal stem cells: implications for autism spectrum disorders. *Cell Commun Signal* 12, 19. <https://doi.org/10.1186/1478-811X-12-19>.
- Xie, N. and Tang, B. (2016). The Application of Human iPSCs in Neurological Diseases: From Bench to Bedside. <https://doi.org/10.1155/2016/6484713>.
- Yang, J., Wu, C., Stefanescu, I. et al. (2016). RhoA inhibits neural differentiation in murine stem cells through multiple mechanisms. *Sci Signal* 9. <https://doi.org/10.1126/scisignal.aaf0791>.
- Zheng, W., Aschner, M. and Ghersi-Egea, J. F. (2003). Brain barrier systems: a new frontier in metal neurotoxicological research. *Toxicol Appl Pharmacol* 192, 1–11. [https://doi.org/10.1016/S0041-008X\(03\)00251-5](https://doi.org/10.1016/S0041-008X(03)00251-5).
- Zhou, T., Benda, C., Dunzinger, S. et al. (2012). Generation of human induced pluripotent stem

cells from urine samples. *Nat Protoc* 7, 2080–2089.
<https://doi.org/10.1038/NPROT.2012.115>.

Danksagung

An dieser Stelle möchte ich mich bei allen Personen bedanken, die meine Promotion ermöglicht und mich in den letzten Jahren ununterbrochen unterstützt haben:

Ein besonderer Dank gilt Frau Prof. Dr. Ellen Fritsche, für die Aufnahme in ihre Arbeitsgruppe und die Bereitstellung des sowohl sehr interessanten als auch zukunftsversierten Themas. In den letzten Jahren konnte ich mich durch ihre Unterstützung, die umfassende Betreuung und Förderung, sowie das entgegengebrachte Vertrauen, beruflich und persönlich sehr weiterentwickeln.

Bei Herrn Prof. Dr. Rüdiger Simon bedanke ich mich für die fakultätsübergreifende Betreuung und Übernahme der Mentorenschaft bedanken, durch die meine Promotion erst möglich wurde.

Herrn Dr. Stefan Masjosthusmann danke ich besonders für die Betreuung während meiner Promotion und für die stetigen Hilfestellungen bei Planung, Durchführung und Auswertung meiner vielen, komplexen Versuche.

Ein großer Dank gilt allen ehemaligen und derzeitigen Arbeitskollegen der AG Fritsche. Danke für all eure Hilfe und Unterstützung, auf die ich jederzeit zählen konnte. Ihr habt immer für die notwendige Abwechslung zwischen all den Stunden im IUF gesorgt, auch durch die kulinarische Vielfalt am Dönerstag!

Danke für all die tollen Erlebnisse in den letzten Jahren, wie beispielsweise die Konferenzen in Hannover, Düsseldorf, Helsinki und Brüssel, die vor allem durch unsere abendlichen Unternehmungen unvergesslich wurden. Danke für die feuchtfröhlichen Weihnachtsfeiern (mit Feuerspuckern und Suppe), Grillabende und die anschließenden fulminanten Nächte in der Altstadt.

Ein weiterer Dank gilt dem Team von DNTOX. Danke für die spannenden, arbeits- und lehrreichen letzten 1,5 Jahre, eure Unterstützung und all die tollen Erlebnisse.

Ganz besonders möchte ich mich bei Jördis, Etta und Farina bedanken, die auch außerhalb der Arbeit immer ein offenes Ohr für mich hatten, danke für all die schönen Unternehmungen nach der Arbeit. Jördis und Etta danke ich außerdem für die schnelle und gründliche Korrektur meiner Arbeit.

Ein riesengroßer Dank gilt meinen Eltern und meinem Bruder! Danke für eure unermüdliche Unterstützung, eure motivierenden Worte und all die Gespräche, die mich immer wieder aufgebaut haben. Zuletzt möchte ich mich vor allem bei Basti, für all die Unterstützung und

Danksagung

Motivation an jedem einzelnen Tag in den letzten Jahren bedanken. Danke, dass du mir immer den nötigen Rückhalt gibst.

Vielen, vielen Dank für alles!

Eidesstattliche Erklärung/Declaration

Hiermit versichere ich an Eides statt, dass die vorliegende Dissertation „Entwicklung und Validierung von Stammzell-basierten Testmethoden im Rahmen einer humanen *in vitro*-Batterie zur regulatorischen Testung auf Entwicklungsneurotoxizität“ von mir selbständig und ohne unzulässige fremde Hilfe unter Beachtung der „Grundsätze zur Sicherung guter wissenschaftlicher Praxis and der Heinrich-Heine-Universität Düsseldorf“ erstellt worden ist. Die Dissertation wurde in der vorgelegten oder einer ähnlichen Form noch bei keiner anderen Institution eingereicht. Ich habe bisher keine erfolglosen Promotionsversuche unternommen.

I declare that I have developed and written the enclosed thesis ‘Development and validation of stem cell-based test methods contributing to a human *in vitro* battery for regulatory developmental neurotoxicity evaluation’ completely by myself, and have not used sources or means without declaration in the text. Any thoughts from others or literal quotations are clearly marked. The thesis was prepared in compliance with the principles of ‘Good Scientific Practice at the Heinrich-Heine-University Dusseldorf’. The thesis was not used in the same or in a similar version to achieve an academic grading elsewhere.

Düsseldorf, den 28.07.2022



Kristina Eva Bartmann